

**APPLICABILITY OF THE NLOS MODEL FOR PREDICTIONS OF
SOIL WATER MOVEMENT AND NITROGEN TRANSPORT IN AN
AGRICULTURAL SOIL, AGASSIZ, BC**

By

Heather R. Hirsch

Accepted in Partial Completion

of the Requirements for the Degree

Master of Science

Moheb A. Ghali, Dean of the Graduate School

ADVISORY COMMITTEE

Chair, Dr. Robert J. Mitchell

Dr. Shabtai Bittman

Dr. Peter Homann

Mr. Derek Hunt

Dr. R. Scott Babcock

MASTER'S THESIS

In presenting this thesis in partial fulfillment of the requirements for a master's degree at Western Washington University, I agree that the Library shall make its copies freely available for inspection. I further agree that copying of this thesis in whole or in part is allowable only for scholarly purposes. It is understood however, that any copying or publication of this thesis for commercial purposes, or financial gain, shall not be allowed without my written permission.

Signature _____

Date _____

**APPLICABILITY OF THE NLOS MODEL FOR PREDICTIONS OF
SOIL WATER MOVEMENT AND NITROGEN TRANSPORT IN AN
AGRICULTURAL SOIL, AGASSIZ, BC**

A Thesis
Presented to
The Faculty of
Western Washington University

In Partial Fulfillment
Of the Requirements for the Degree
Master of Science

by
Heather R. Hirsch
April 2007

ABSTRACT

The Abbotsford-Sumas aquifer is a shallow, unconfined aquifer in northern Whatcom County, WA and southern British Columbia, Canada that is contaminated with nitrates due to agricultural land use. Currently, conservation managers rely on Post-Harvest Soil Nitrate Tests (PHSNTs) to predict nitrate leaching potential to the aquifer. However, these tests have limitations as an assessment tool because of their inaccuracy. Therefore, US and Canadian government agencies are considering the NLEAP on STELLA (NLOS) leaching model as an additional tool for assessing nutrient management strategies. NLOS is an adaptation of the Nitrogen Leaching and Economic Analysis Package (NLEAP) model. I examined the applicability of the model by calibrating it to an agricultural field plot in southern British Columbia. NLOS was calibrated to an agricultural field in Agassiz, BC for this study, but I expect it will perform similarly in the Abbotsford-Sumas aquifer due to similar soil types and climatic conditions.

NLOS incorporates fertilizer application events, climatic data, and soil properties, to simulate one-dimensional water flow and nitrogen fate and transport. Field data from a trial of silage corn located at the Pacific Agri-Foods Research Centre in Agassiz, BC (PARC Agassiz) was used to calibrate the model. Monthly sampling included soil, soil pore water, nitrous oxide emissions, and groundwater chemistry parameters. The field soil (a silt loam) was subjected to a nutrient loading and crop management scenario comparable to regional farming practices.

The ability of NLOS to predict water and nitrate transport during seasonal precipitation events was examined by comparing simulations to monthly field data. NLOS was found to be

useful for predictions of soil nitrate and ammonium in the upper 12 inches of the soil profile, and nitrate leaching from the 36-inch depth. Model predictions accounted for 84% of the observed variability in nitrate leached from 24 to 36 inches deep. Simulated soil nitrate and ammonium in the upper 12 inches of the soil profile accounted for 84% and 87%, respectively, of the variability in the observed values. NLOS also produced adequate predictions of nitrate leaching from 12 to 24 inches deep ($R^2 = 0.63$), and soil water from 0 to 36 inches deep (average R^2 for all layers = 0.52). Field observations and model simulations indicate that nutrients in the soil and soil pore water fluctuated in direct response to fertilizer applications, crop events, and precipitation. Although the model performed reasonably well, more frequent field data collection is recommended for further model calibration and validation.

The calibrated model was also used to assess various nutrient-loading scenarios and to recommend the timing of the PHSNT. Hypothetical scenarios suggest that timing fertilizer application to rainfall events is the most effective way to reduce nitrate leaching. Field observations and model simulations also indicate that conducting the PHSNT concurrent with crop harvesting would provide the most accurate assessment of nitrate leaching potential.

ACKNOWLEDGEMENTS

This thesis would not have been possible without the support of the Pacific Agri-Foods Research Centre in Agassiz, BC (PARC Agassiz). In addition to providing two invaluable members of my thesis committee, Dr. Shabtai Bittman and Mr. Derek Hunt, PARC Agassiz staff assisted with field investigations, performed laboratory analyses, and provided the location and facilities to conduct my field research. Without their technical, analytical, and computational expertise and assistance, this project would not have been as comprehensive in scope or as successful. Therefore, thanks are due to the following PARC Agassiz staff:

Frederic Bounaix, Anthony Friesen, Maureen Schaber, and Andrew Bradley. I would also like to provide special thanks to Dr. Shabtai Bittman for making my collaboration with PARC Agassiz possible and for his enthusiasm and inspiration, which helped to pique my scientific curiosity and to motivate me through the more difficult times of this project.

Equally important to the success of this thesis was the combined expertise of my thesis committee. In addition to Shabtai Bittman, whose agricultural, soil, and crop knowledge was necessary to make this project work, Mr. Derek Hunt provided assistance with modeling tasks, Dr. Peter Homann was an excellent resource for experimental design, statistical, and soil information as well as careful editing, and Dr. Scott Babcock provided analytical and editorial assistance. Most important to the inception and completion of this thesis was the committee chair, Dr. Robert Mitchell. Bob provided a perfect blend of freedom and guidance throughout this thesis. His coordination of ideas and resources provided the backbone of this project and made collaborative work a possibility. Bob had an uncanny ability to put me in the right place at the right time and to implant ideas without pressure so that I could take

ownership of my work. His careful and dedicated teaching efforts and hydrogeological expertise gave me the skills and guidance needed to tackle this work.

Thanks are also due to the Institute for Watershed Studies (IWS) at Western Washington University (WWU). IWS provided laboratory facilities and supplies in addition to analytical support from Joan Vandersypen, Mike Hilles, and staff. Joan also provided additional knowledge on procedures and techniques for presenting quality control data. Dr. Robin Matthews, the director of IWS, not only facilitated my collaboration with IWS, but also provided consultation on experimental design and statistical analyses.

I would also like to recognize my funding sources and field assistants. The WWU Geology Department provided funding for field research and the WWU Office of Research and Sponsored Programs and the American Association of Petroleum Geologists Grants-In-Aid Foundation provided funding for field and analytical work. The following individuals braved inclement weather and bears to assist me in the field: Michelle Malone, Shawn Divitt, David Hirsch, Ben Clawson, Erica Martell, John Gillaspay, Amy Flurette, Robert Mitchell, Brendon Johnsen, and Stephen Bond.

And last, but not least, I would like to publicly acknowledge the essential roles that my wonderful husband Dr. David Hirsch fulfilled throughout this thesis. In addition to being a confidante and an emotional rock, David was always willing to listen to and digest problems that I was tackling. Not only was his role as sounding board useful in parsing difficult problems, but he also provided technical and computational assistance on a number of occasions. Most notably, David's assistance made the automation of the 2,000 Monte Carlo runs a possibility. His love and support led me to pursue an advanced degree in the first place and his partnership throughout this process made my endeavor a success.

TABLE OF CONTENTS

ABSTRACT	iv
ACKNOWLEDGEMENTS.....	vi
LIST OF TABLES	x
LIST OF FIGURES	xi
LIST OF APPENDICES	xv
1.0 INTRODUCTION.....	1
2.0 BACKGROUND.....	4
2.1 Nitrogen Cycle	4
2.2 NLEAP On STELLA (NLOS).....	6
2.3 Steady-state vs. Transient Flow and Transport.....	7
2.4 NLOS vs. Other Nitrate Leaching Models	9
2.5 Site Description	12
2.5.1 Topography	12
2.5.2 Hydrology.....	12
2.5.3 Climate	13
2.5.4 Soil.....	13
2.5.5 Site History.....	14
3.0 RESEARCH OBJECTIVES	15
4.0 METHODOLOGY	17
4.1 Experimental Design	17
4.1.1 Field Set-Up	17
4.1.2 Field Data Collection	19
4.1.3 Additional Data Required as Model Inputs.....	20
4.2 Bulk Density Determination and Usage	20
4.3 Field Methods.....	22
4.3.1 Soil Sampling	22
4.3.2 Water Sampling	22
4.3.3 Nitrous Oxide Sampling.....	23
4.3.4 Soil Moisture Measurements.....	24
4.3.5 Depth to Water Measurements	25
4.4 Groundwater Flow Direction Determination	25

4.5	Analytical Methods	26
4.5.1	Soil Analyses	27
4.5.2	Water Analyses	30
4.5.3	Nitrous Oxide Analysis	30
4.5.4	Crop Analyses	31
4.6	Statistical Methods	31
4.7	Modeling Methods	33
4.7.1	NLOS Model Set-Up	34
4.7.2	Sensitivity Analysis	39
4.7.3	Uncertainty Analysis	41
4.7.4	Model Calibration	43
5.0	RESULTS and DISCUSSION	45
5.1	Field Observations	45
5.1.1	Weather	46
5.1.2	Soil	47
5.1.3	Soil pore water	48
5.1.4	Groundwater	52
5.1.5	Nitrous oxide	54
5.2	Statistical Results	55
5.3	Sensitivity Results	56
5.4	Uncertainty Results	59
5.5	Calibration Results	61
5.6	Model Simulations	66
5.6.1	Nitrogen flux	66
5.6.2	Water flux	71
5.6.3	Steady-state vs. transient flow	74
5.6.4	Post-Harvest Soil Nitrate Test (PHSNT)	76
5.6.5	Hypothetical scenarios	77
6.0	CONCLUSIONS	80
7.0	RECOMMENDATIONS	84
8.0	REFERENCES	86

LIST OF TABLES

Table 1. Hydraulic gradient calculation parameters	92
Table 2. Required model inputs: descriptions and sources	93
Table 3. Crop management and sample collection events	101
Table 4. Bulk density depth ranges and average values by soil layer.....	102
Table 5. Summary statistics for the initial soil data collected on March 24, 2004.....	103
Table 6. Soil water sub-model sensitivity analysis inputs and data.....	104
Table 7. Nitrogen dynamics sub-model sensitivity analysis inputs and data	105
Table 8. Soil water sub-model sensitivity analysis ranks.....	106
Table 9. Nitrogen dynamics sub-model sensitivity analysis ranks	107
Table 10. Uncertainty analysis inputs	108
Table 11. Model calibration efficiency coefficients	109
Table 12. Soil water sub-model calibration parameters.....	110
Table 13. Nitrogen sub-model calibration parameters.....	111
Table 14. Balanced nitrogen budget from the calibrated model simulation	112
Table 15. Kruskal Wallis confirmatory test results	113
Table 16. Pairwise Wilcoxon Rank Sums Test results	114
Table 17. Balanced water budget from the calibrated model simulation.....	115
Table 18. Summary statistics for the simulated values of nitrate leached for uncertainty analysis	116
Table 19. Porosity and percent saturation at maximum observed soil water content.....	117
Table 20. Model calibration efficiency coefficients for the wet vs. dry months.....	118
Table 21. Linear regression coefficients from the correlation analysis of the simulated and observed values	119
Table 22. Soil hydraulic characteristics	120
Table 23. Hypothetical scenario descriptions.....	121
Table 24. Hypothetical scenario balanced nitrogen budgets	122
Table A1. Sample container, storage, and holding times.....	193
Table A2. Analytical methods, detection limits, and precision.....	194

LIST OF FIGURES

Figure 1. Field site location relative to the Abbotsford-Sumas aquifer study areas.....	123
Figure 2. Nitrogen gains, losses, and transformations occurring in agricultural soils.....	124
Figure 3. Aerial photo (1995) of the Pacific Agri-Foods Research Centre, Agassiz BC	125
Figure 4. Field layout used for the swine manure study conducted on the study site from 1998-2001	126
Figure 5. Field site set-up.....	127
Figure 6. A push-probe soil core sampler used in this study.....	128
Figure 7. Ceramic cup lysimeter set-up	129
Figure 8. A non-flow-through chamber for nitrous oxide sample collection.....	130
Figure 9. Gravimetric soil moisture vs. Diviner 2000 soil conductance probe soil moisture measurements.....	131
Figure 10. Notched boxplots of initial soil data collected on March 24, 2004 by depth	132
Figure 11. Notched boxplots of initial soil data collected on March 24, 2004 by replicate .	133
Figure 12. Notched boxplots of initial soil data collected on March 24, 2004 by plot.....	134
Figure 13. Notched boxplots of initial soil data collected on March 24, 2004 by splashplate	135
Figure 14. Scatterplots of initial soil ammonium data collected on March 24, 2004 by plot, replicate, depth, and splashplate.....	136
Figure 15. Scatterplots of initial soil nitrate data collected on March 24, 2004 by plot, replicate, depth, and splashplate.....	137
Figure 16. Scatterplots of initial soil carbon to nitrogen ratio data collected on March 24, 2004 by plot, replicate, depth, and splashplate	138
Figure 17. Scatterplots of initial soil coarse fragment percentage data collected on March 24, 2004 by replicate and depth	139
Figure 18. Scatterplots of initial soil organic matter content data collected on March 24, 2004 by plot, replicate, depth, and splashplate.....	140
Figure 19. Scatterplots of initial soil moisture data collected on March 24, 2004 by plot, replicate, depth, and splashplate.....	141
Figure 20. Mean monthly precipitation totals for the study period vs. the 30-year average mean monthly totals	142

Figure 21. Mean monthly minimum temperature for the study period vs. the 30-year average	143
Figure 22. Mean monthly maximum temperature for the study period vs. the 30-year average	144
Figure 23. Mean daily values of evapotranspiration by month for the study period vs. the long-term mean monthly values.....	145
Figure 24. Observed soil nitrate for soil layers 1 to 3, cumulative net water, and precipitation	146
Figure 25. Observed soil ammonium for soil layers 1 to 3, cumulative net water, and precipitation	147
Figure 26. Observed depth to water in relation to the sampling depths, cumulative net water, and precipitation.....	148
Figure 27. Observed soil water for soil layers 1 -3, cumulative net water, and precipitation	149
Figure 28. Observed nitrate concentration in soil water and groundwater, cumulative net water, and precipitation	150
Figure 29. Observed ammonium concentration in soil water, cumulative net water, and precipitation	151
Figure 30. Observed daily nitrous oxide emissions and precipitation	152
Figure 31. Observed daily nitrous oxide emissions, soil moisture in soil layer 1, and maximum daily air temperature	153
Figure 32. Observed daily nitrous oxide emissions and soil nitrate and ammonium in soil layer 1	154
Figure 33. Histogram of the 2,000 simulated values of nitrate leached from the uncertainty analysis	155
Figure 34. Cumulative probability of obtaining the simulated values of nitrate leached generated during the uncertainty analysis.....	156
Figure 35. Observed vs. the uncalibrated and calibrated simulations of nitrate leached from soil layer 2.....	157
Figure 36. Observed vs. the uncalibrated and calibrated simulations of nitrate leached from soil layer 3.....	158
Figure 37. Observed vs. the uncalibrated and calibrated simulations of soil nitrate in layer 1	159

Figure 38. Observed vs. the uncalibrated and calibrated simulations of soil nitrate in layer 2	160
Figure 39. Observed vs. the uncalibrated and calibrated simulations of soil nitrate in layer 3	161
Figure 40. Observed vs. the uncalibrated and calibrated simulations of soil ammonium in layer 1	162
Figure 41. Observed vs. the uncalibrated and calibrated simulations of nitrous oxide emissions.....	163
Figure 42. Observed vs. the uncalibrated and calibrated simulations of soil water in layer 1	164
Figure 43. Observed vs. the uncalibrated and calibrated simulations of soil water in layer 2	165
Figure 44. Observed vs. the uncalibrated and calibrated simulations of soil water in layer 3	166
Figure 45. Observed vs. the calibrated simulation of nitrate leached from soil layer 2.....	167
Figure 46. Observed vs. the calibrated simulation of nitrate leached from soil layer 3.....	168
Figure 47. Observed vs. the calibrated simulation of soil nitrate in layer 1.....	169
Figure 48. Observed vs. the calibrated simulation of soil nitrate in layer 2.....	170
Figure 49. Observed vs. the calibrated simulation of soil nitrate in layer 3.....	171
Figure 50. Observed vs. the calibrated simulation of soil ammonium in layer 1	172
Figure 51. Observed vs. the calibrated simulation of nitrous oxide emissions	173
Figure 52. Simulated soil nitrate for layers 1 and 2 and crop nitrate uptake.....	174
Figure 53. Simulated soil ammonium for soil layer 1 and crop ammonium uptake.....	175
Figure 54. Simulated nitrate leached from soil layers 1 and 2 and crop nitrate uptake.....	176
Figure 55. Simulated nitrate leached from soil layers 1 – 3, cumulative net water, and precipitation	177
Figure 56. Simulated nitrous oxide emissions, cumulative net water, and precipitation.....	178
Figure 57. Simulated nitrous oxide emissions and soil nitrate and ammonium in layer 1....	179
Figure 58. Simulated nitrous oxide emissions, soil water in layer 1, and maximum daily air temperature	180
Figure 59. Simulated cumulative nitrous oxide emissions from nitrification and denitrification in the surface layer and soil layer 1	181
Figure 60. Observed vs. the calibrated simulation of soil water in layer 1	182
Figure 61. Observed vs. the calibrated simulation of soil water in layer 2.....	183

Figure 62. Observed vs. the calibrated simulation of soil water in layer 3	184
Figure 63. Simulated soil water in layers 1 – 3, precipitation, and net water	185
Figure 64. Simulated nitrate leached from the bottom of the soil profile	186
Figure 65. Simulated nitrate leached from soil layers 1 – 3, precipitation, and net water	187
Figure 66. Simulated soil nitrate in layers 1 – 3, precipitation, and net water	188
Figure A1. Nitrate laboratory duplicates	195
Figure A2. Ammonium laboratory duplicates	196
Figure A3. Nitrate field duplicates	197
Figure A4. Ammonium field duplicates	198
Figure A5. Nitrate check standards	199
Figure A6. Ammonium check standards	200
Figure A7. Nitrate spike recoveries	201
Figure A8. Ammonium spike recoveries control chart	202

LIST OF APPENDICES

Appendix A. Quality Control	189
Appendix B. Changes Made to NLOS.....	203
Appendix C. Data CD	211

1.0 INTRODUCTION

From a public health standpoint, the protection of groundwater quality has become an important concern for many communities. More than half of the US uses groundwater for drinking water (Solley et al., 1993); and some rural communities use groundwater as their sole drinking water source (Hii et al., 1999). In 1990, Washington State withdrew between 200 and 500 million gallons of groundwater per day for public water supplies (<http://water.usgs.gov>). Nitrate is the most common nutrient in groundwater (Nolan and Stoner, 2000) and is the most ubiquitous groundwater contaminant in the world (Spalding and Exner, 1993). Nitrate poses a serious threat to public drinking water supplies because of the health risks related to nitrate consumption. Once ingested, nitrates are converted to nitrites that can react with hemoglobin in the blood, which decreases the capacity of the blood to transport oxygen (<http://www.epa.gov/OGWDW/dwh/c-ioc/nitrates.html>). This potentially fatal condition, termed methemoglobinemia, is particularly acute in infants (<http://www.emedicine.com/EMERG/topic313.htm>). Long-term exposure to nitrate has the potential to cause diuresis, increased starchy deposits and hemorrhaging of the spleen in adults (<http://www.epa.gov/OGWDW/dwh/c-ioc/nitrates.html>) and also has been implicated as a carcinogen. The US Environmental Protection Agency (USEPA) has established a maximum contaminant level (MCL) of 10 mg nitrate as nitrogen per liter (mg NO₃-N/L). Nitrate exceeded the MCL in 12 out of 25 residential drinking water wells during the 2002-2004 monitoring study conducted in the Abbotsford-Sumas aquifer located in northwestern Whatcom County (Mitchell et al., 2005).

Despite the implementation of Best Management Practices (BMPs) over the last two decades, nitrate levels continue to persist at levels exceeding the USEPA's MCL in surface and groundwater in northwestern Washington (Mitchell et al., 2005). Shallow groundwater beneath

agricultural land has the highest median nitrate concentration (Mitchell et al., 2005). The Abbotsford-Sumas aquifer is located in the lower Fraser and Nooksack River Valleys (Figure 1), a region dominated by intense agricultural activity. The high precipitation and irrigation in the area combined with the well-drained, thin soils (<6 feet), high aquifer permeability, and dense agricultural activity create a situation where surface contaminants readily interact with groundwater (Tesoriero and Voss, 1997). In addition, land use in southwestern British Columbia is also impacting water quality in the aquifer because groundwater flows to the south. This is problematic because the aquifer serves as a drinking water supply for rural residents and communities in both the US and Canada (Hii et al., 1999). In an effort to improve water quality, the State of Washington passed the Dairy Nutrient Management Act in 1998 requiring all dairy farms to develop and implement Dairy Nutrient Management Plans (DNMPs) by December 2003.

The identification of two possible sources of groundwater nitrate in northwestern Washington has made the assessment and implementation of management plans difficult. The highest nitrate levels (>20 NO₃-N/L) occur in shallow wells (<25 ft) and lower nitrate levels, but still greater than the EPA MCL (>10 mg NO₃-N/L), occur in deeper wells (>25 ft; Mitchell et al., 2003; Mitchell et al., 2005). Agricultural sources in northwestern Washington were linked to nitrate in the shallow wells whereas agricultural sources in Canada were linked to the deep wells (Mitchell et al., 2003). This suggests that there is a nitrate overprint due to US sources on background levels of nitrate flowing south in the aquifer from Canada. Numerous studies conducted in the British Columbian portion of the Abbotsford-Sumas aquifer have reported nitrate concentrations exceeding the 10 mg NO₃-N/L MCL (Hii et al., 1999; Liebscher et al., 1992; Wassenaar, 1995; Zebarth et al., 1998). In order to effectively manage agronomic loading

in northwestern Washington, it is important that the proportions of nitrate entering the aquifer from Canadian and US sources are distinguishable.

Numerous models have been developed to aid regulatory agencies and agricultural professionals with on-farm nutrient management with the goal of minimizing excessive nutrient loading. NLEAP is a one-dimensional (1-D) deterministic-numerical model that simulates nitrogen fate and transport in an agricultural soil. Most recently, the model has been translated from the original FORTRAN code to the STELLA environment and renamed NLEAP on STELLA (NLOS). NLOS employs the same mechanisms for nitrogen dynamics, crop growth, and water flux as the original NLEAP. The US Department of Agriculture Natural Resources Conservation Service (USDA NRCS), Whatcom Conservation District (WCD), and Agriculture Canada are considering NLOS as a tool that will assist in the distinction of nitrate sources entering the Abbotsford-Sumas aquifer.

There are no published studies utilizing nitrate leaching models in this region. The majority of existing knowledge about the fate of nitrogen in agricultural soils comes from studies conducted in the southern, midwestern, and eastern US (Hermanson et al., 2000). Neither NLEAP nor NLOS has ever been tested for the climate, soil conditions, and cropping systems that are specific to the Pacific Northwest. Whether or not NLOS may provide useful predictions of soil nitrogen movement in this region needs to be evaluated. Of particular concern is the steady-state, tipping-bucket approach to soil water flux that NLOS utilizes, which may poorly simulate nitrate leaching under transient conditions. Soil water flux under transient conditions is typified by variable soil moisture, conductivity, and matric suction with time and depth in the soil. The variable intensity precipitation events that occur in this region induce non-steady soil moisture conditions in the field. A transient flow nitrate leaching model may better simulate nitrate leaching in this environment. In addition, the regional climate is typified by winter rainfall

and relatively cool night-time temperatures, both of which have an effect on the nitrogen cycle (Hermanson et al., 2000).

The goal for this project was to calibrate NLOS to local conditions and then use the calibrated model to characterize the movement of water and nitrogen through the shallow vadose zone in response to precipitation events and agricultural nutrient loading and management. NLOS was also used to simulate predictions of nitrogen and water flux for a number of hypothetical scenarios and to recommend the optimal time for the post-harvest soil nitrate test. Finally, this study will provide a comprehensive data set, of which there are few, including many aspects of the nitrogen cycle (crop-N uptake, leaching, nitrous oxide emissions, and soil-N). Previous researchers have only focused on one or a few aspects of the nitrogen cycle (Hermanson et al., 2000).

2.0 BACKGROUND

2.1 Nitrogen Cycle

The nitrogen pathways that are modeled by NLOS are detailed in this section. This discussion describes only the nitrogen gains, losses, or transformations that occur in upland, agricultural soils, and that are included in the model. Nitrogen enters the soil from natural sources, crop residues, amendments, irrigation, precipitation, run-on, and fertilizer or manure applications. Nitrogen on the soil surface is removed by denitrification, ammonium volatilization, runoff, or erosion. Once nitrogen infiltrates the soil, it is subject to leaching and crop uptake or one of the transformation processes described below (Shaffer and Ma, 2001). The nitrogen cycle is depicted in Figure 2 (taken from <http://www.mda.state.mn.us>). This figure depicts the nitrogen processes that are in the model with the exception of nitrogen fixation, which is shown but not included in the model.

Mineralization or ammonification

In the mineralization (ammonification) process, aerobic and anaerobic microbes decompose nitrogen-containing residues from crops and soil amendments and soil organic matter to form ammonium and more stable forms of soil organic matter. Carbon dioxide gas is the primary by-product, although, methane may be produced instead of carbon dioxide if anaerobic conditions exist.

Immobilization

Immobilization occurs when there is insufficient nitrogen in residues to meet the biomass growth needs of soil microbes. Under these conditions, the microbes temporarily resort to consumption of mineral soil nitrate and ammonium resulting in a net uptake, or immobilization, of these forms of nitrogen. This is the converse of the mineralization process. Immobilized nitrogen is not available for uptake by crops. When the microbes die and are recycled, the nitrogen is released back into the soil.

Nitrification

Nitrification is the microbially mediated conversion of ammonium to nitrate. This is a two-stage process where the ammonium is first converted to nitrite and then nitrite is converted to nitrate. The first stage is controlled by Nitrosomonas, and the second stage by Nitrobacter, both of which are aerobic autotrophic organisms. The conversion of nitrite to nitrous oxide and NO_x greenhouse gases can occur as a by-product of this reaction.

Denitrification

Denitrification is the microbially mediated conversion of nitrate and nitrite to di-nitrogen gas, nitrous oxide, and NO_x . Facultative anaerobic bacteria primarily mediate this process.

Denitrification is enhanced by the following conditions: a large nitrate source, a fresh carbon

source, Mn or Fe rich soils, warm temperatures, precipitation or irrigation, and temporary flooding.

2.2 *NLEAP On STELLA (NLOS)*

Dr. Shabtai Bittman and Derek Hunt (Research Technician) at PARC Agassiz are developing NLOS. Derek Hunt translated NLEAP from the original FORTRAN language using the icon-based model building and simulation tool STELLA and renamed it NLOS. NLOS simulates the fate and transport of nitrogen in the soil profile, plant growth, and soil water movement at a field scale, at a daily time step for one calendar year. The core of the model simulates the flow of nitrate in three soil layers, organic decomposition and denitrification of nitrate, inputs and outputs, irrigation, and application of crop residues. There are also a series of sub-models that function as separate entities and focus on soil, crops and residues, manure, amendment and fertilizers, and other topics. Trials have been conducted with NLEAP data sets that show a good correlation between simulations produced with the NLEAP and NLOS (Shaffer et al., 2001).

NLOS was designed as a tool for farmers, extension agencies, and regulatory agencies to use in making estimates of nitrate leaching potential under agricultural crops and the resulting effect on groundwater (Shaffer et al., 1991). In order to fully develop NLOS as a tool for regulatory purposes, the model must be calibrated to local conditions. NLEAP was developed and tested in the midwestern states where soils are typically poor to moderately well developed (e.g., Entisols and Mollisols) and annual precipitation is low (e.g., Chichester, 1977; Delgado, 1998; Delgado et al., 1998a; Delgado et al., 1998b; Delgado et al., 2005; Follett et al., 1994; Shaffer et al., 1991; Shaffer et al., 1994). These conditions are very different from northwest Washington, where soils are more developed (e.g., Spodosols and Alfisols) and annual precipitation is moderate to heavy. The seasonality of precipitation also differs in these regions, with the Midwest receiving most of its precipitation in the spring and early summer and the Pacific Northwest receiving most of its

precipitation during the late fall and winter months. Steady-state unsaturated flow ignores all complexities related to soil hydraulic properties, soil heterogeneities, preferential flow, surface ponding, upward water migration, lateral flow, and hysteresis. Calibrated testing of the model for local field conditions is necessary to determine whether or not this highly simplified approach is acceptable for determining nitrate available for leaching.

NLOS has many qualities that have made it more appealing and tractable for regional development and implementation. Many modelers protect their source code by making it unavailable to the public. The NLEAP developer, M.J. Shaffer, freely shared his source code and his expertise with Dr. Bittman and Derek Hunt of Agriculture Canada. Access to the original FORTRAN code and to the model developer made it possible for Bittman and Hunt to recreate the model with STELLA. The graphical interface of the STELLA platform provides an innovative alternative to the “black box” approach by allowing users who are unfamiliar with programming languages to view or adapt the model structure. This makes the model flexible and user friendly. With STELLA, model developers may choose to modify and enhance existing models, thereby building on previous work and knowledge without “reinventing the wheel.” Bittman et al. (2001) cited these reasons as the impetus for choosing NLEAP and STELLA.

2.3 Steady-state vs. Transient Flow and Transport

Water flow close to the surface is a highly complex process due to the spatial heterogeneity of soil characteristics and soil moisture. Modeling the transient process of water flow and solute transport in field soils under natural conditions requires excessive input parameters and computational rigor. Assumptions are usually made to simplify the modeling process. It is debatable what simplifications are acceptable for various flow conditions.

Vadose zone flow is, by definition, unsaturated and dominantly vertically downward. Therefore, I will present the 1-dimensional (vertically downward where z is elevation measured

positively downward) flow equation for transient, unsaturated conditions. The following assumptions apply to this flow scenario: homogeneous, isotropic, incompressible fluid, non-deformable media, and air does not restrict water from filling void space. Under these conditions, Richards's equation describes unsaturated transient flow:

$$\frac{\partial \theta}{\partial t} = \frac{\partial}{\partial z} \left[K(\psi) \frac{\partial \psi}{\partial z} \right] \quad (1)$$

where θ is water content, z is elevation, K is unsaturated hydraulic conductivity, and ψ is matric suction. Under transient conditions, the rate of change in water content, or water flow, varies with time and space according to the divergence of the flux due to the variation in matric suction and conductivity, which varies as a function of matric suction, with depth. Under steady-state unsaturated flow for the same scenario, matric suction and conductivity are uniform with depth; therefore, unsaturated water flow is constant. In areas with frequent rainfall, such as the winter months in the Pacific Northwest, constant wetting may produce nearly uniform saturation throughout the soil column. Under these conditions, a steady-state unsaturated flow equation may produce the best approximation of vadose zone flow.

Numerous studies have been conducted to evaluate the effect of moisture content on transport parameters. These studies have shown dispersivity values, apparent distribution coefficients, and dispersion coefficients to increase, decrease, or remain unchanged with varying soil moisture contents (e.g., Corey et al., 1963; DeSmedt and Wierenga, 1984; Gamedainger et al., 2001; Jardine et al., 1993; Maraqa et al., 1997; Maraqa et al., 1999; Seyfried and Rao, 1987). Hammel and Roth (1998) found that analytical approximations of asymptotic dispersivity are highly dependent on the degree of saturation. Many researchers have focused on processes occurring under saturated conditions or have used steady-state flow assumptions to simplify solute transport in the unsaturated zone (e.g., Bresler and Dagan, 1981; Butters and Jury, 1989;

Destouni and Cvetkovic, 1991; Jury, 1982; Small and Mular, 1987; van Genuchten and Wierenga, 1976). Studies comparing model results with and without these simplifying assumptions have led to contradictory conclusions about whether or not ignoring transient flow is justified. Wierenga (1977) found that predictions of solute transport based on transient flow were comparable to those based on steady-state flow if the breakthrough curve is presented as a function of cumulative drainage. Bresler and Dagan (1983) found that solute movement may be faster under transient conditions than under steady-state conditions for relatively homogeneous fields. A study by Russo et al. (1989) found contrasting results indicating solute movement may be faster with a steady-state flow model. Vanderborght et al. (2000) found that transient flow in a sandy loam could be approximated by a steady-state flow transport process when a solute penetration depth coordinate was used, but this process produced inconsistent results in a loam soil due to bypass flow and transport through macropores. Therefore, there is a need to determine whether or not a steady-state solute transport approach is applicable for the climatic conditions and soil types characteristic of this region.

2.4 NLOS vs. Other Nitrate Leaching Models

NLOS uses a simplified steady-state algorithm (tipping-bucket approach) to simulate water flow under saturated and unsaturated conditions. This approach uses even more simplifying assumptions than the steady-state flow equation described above and therefore deserves further scrutiny than a model employing the Richards' equation for flow.

NLOS uses an exponential expression involving the movement of water and various soil properties to simulate solute transport. These processes are implemented in the soil water sub-model of NLOS. The following text, modified from "NLOS Documentation" by Derek Hunt, Shabtai Bittman, Lucy De Pieri, and Marvin J. Shaffer, details the concepts and algorithms involved in the soil water sub-model.

The soil water sub-model simulates the details of water movement affecting the overall nitrogen cycle. Water movement is simulated on a field scale with a daily time step by a simple set of mass balance equations computed for the water in each soil layer. The inputs and outputs in these mass balance equations are represented by a number of subroutines.

Water enters the system through the first soil layer (L1) according to the following equation:

$$\text{Water in L1} = \text{Precipitation} + \text{Irrigation} + \text{Snowmelt} + \text{Storage} - \text{Runoff} \quad (2)$$

It is assumed that there is no resistance to the water flowing into L1. At this time there is no inclusion of a waterlogged soil with high water table that is restricting flow into L1. In frozen conditions ($T \leq 32^\circ F$) there is no flow from the surface to layer 1.

The water flowing out of the bottom of L1 (DP1) is expressed as:

$$\begin{aligned} \text{Water out L1 (DP1)} = & \text{Water in L1} - \text{Evaporation} - \text{Transpiration} - \text{WHC} - \\ & \text{Bound water} \end{aligned} \quad (3)$$

where DP1 is used to represent the water flowing from L1 to L2, WHC is the water holding capacity and bound water is the irreducible water content of L1. WHC is a misnomer as this parameter is actually representing the plant available water or plant available water holding capacity (Plant AWHC), which is the difference between the field capacity and the permanent wilting point and is considered to be the water available for use by plants (Dingman, 2002). Plant AWHC is a user-entered value and WHC is calculated as the product of the Plant AWHC and the soil layer thickness; therefore, WHC, as defined by this model, is the Plant AWHC converted to inches of water in the soil layer. Bound water is also a misnomer, as this term does not refer to the irreducible water content according to the traditional definition of water that cannot be removed with any decrease in capillary pressure, but rather it refers to the permanent wilting point (PWP). The PWP is the water content at which transpiration ceases and plants begin to wilt

(Dingman, 2002). PWP is a user-entered value. Bound water, as defined by this model, is the product of the PWP and the soil layer thickness.

The water flowing into L2 is expressed as:

$$\text{Water in L2} = \text{Water out L1 (DP1)} + \text{Initial water in L2} \quad (4)$$

The water flowing out of the bottom of L2 (DP2):

$$\text{Water out L2 (DP2)} = \text{Water in L2} - \text{Transpiration} - \text{WHC} - \text{Bound water} \quad (5)$$

Note that evaporation is assumed not to occur in L2. The expression for water flowing into L3 is similar to that for L2.

The water flowing out of the bottom of L3 (DP3):

$$\text{Water out L3 (DP3)} = \text{Water in L3} - \text{WHC} - \text{Bound water} \quad (6)$$

Note that both evaporation and transpiration do not occur in L3. The water exiting the soil is termed Water Leached and is equal to Water out L3. In the absence of a third layer, the water leached is equal to the water out of L2.

There are a number of nitrate leaching models that incorporate a more rigorous approach to soil water flow and solute transport. The Root Zone Water Quality Model (RZWQM) uses the Green-Ampt equation to simulate water movement during infiltration and the Richards equation during redistribution (Ahuja et al., 2000). Nitrogen, Tillage, and crop-Residue Management (NTRM) uses the Richards equation for water movement (Shaffer and Gupta, 1987) and the diffusion equation for solute transport (Shaffer, 1985). Crop Estimation Through Resource and Environment Synthesis (CERES) uses a relatively simple water balance similar to RZWQM where water redistribution is dependent upon water holding capacity and soil runoff is estimated using the USDA Soil Conservation Service (SCS) curve number (Ritchie, 1998). Additionally, the Erosion/Productivity Impact Calculator (EPIC; Williams, 1995), Groundwater Loading Effects of Agricultural Management Systems (GLEAMS; Leonard et al., 1987), CENTURY

(Parton et al., 1994), and NCSOIL (Molina et al., 1983) models primarily use water flow components based on draining excess water above field capacity, but some also include upward flow (EPIC & NCSOIL).

2.5 *Site Description*

The study site for this research is a 0.59-hectare plot at the Pacific Agri-Foods Research Centre located in Agassiz, B.C (about 60 miles east of Vancouver, BC). The field site is located on the northwest corner of the research centre at the base of Bear Mountain and is known as the Swine Plot or Field 19 (Figure 3). There are other experimental fields located to the northwest and southwest of Field 19.

2.5.1 TOPOGRAPHY

The research centre occupies a topographically flat valley bounded by Bear Mountain to the northeast, the Fraser River along the east and southern extent, and Mount Agassiz to the west (Figure 3). Gentle ridge-and-swale topography is evident upon visual inspection at the site and is consistent with the alluvial parent material.

2.5.2 HYDROLOGY

An irrigation ditch runs along the northwest side of the field and an overgrown creek runs along the southeast side. The site is underlain by a continuous unconfined aquifer that is comprised of Fraser River alluvial permeable sands and gravel. One piezometer is installed at approximately 73 inches deep along the middle of each edge of the field. Groundwater levels were recorded with auto-recorders in the piezometers from November 1998 through March 2001. Using the piezometer locations and elevations I measured during this study, the groundwater flow direction averaged 167° from north during that time (Table 1). This suggests that the groundwater is generally flowing into the creek from the northwest (Figure 3).

2.5.3 CLIMATE

The inshore maritime climate is predominantly cool and humid, characterized by mild winters and annual precipitation ranging from 39 to 67 inches (Patni et al., 2000). About two-thirds of the yearly precipitation occurs during the winter months of October through March, which can lead to drainage problems. The region receives about 3 feet of snow per year (Luttmerding and Sprout, 1967). The water table can range anywhere from 0 to greater than 73 inches below the surface. There are no data below about 73 inches because this is the maximum depth of the piezometers existing at the site. The depth to the water table was recorded at a minimum of about 20 inches below the surface in December 1998 and flooding is known to occur at the site (Patni et al., 2000). Conversely, soil moisture deficiencies may occur during the summer months when rainfall is minimal (Luttmerding and Sprout, 1967). Rapid water table fluctuations of up to 39 inches/week were observed in response to high precipitation from November 1998 to March 1999 (Patni et al., 2000). After March, water table movement is influenced by rises in the nearby Fraser and Harrison Rivers, which tend to peak in May/June in response to spring snowmelt off the mountains (Patni et al., 2000). The coldest and warmest mean monthly temperatures recorded from 1974-2004 at the Agassiz CS weather station, located about 1500 ft from the study site, range from 32 to 42°F in January and 55 to 75°F in July as determined from Environment Canada's National Climate Archive (<http://www.climate.weatheroffice.ec.gc.ca/>).

2.5.4 SOIL

The field is situated on a silt loam of the Monroe series, which has been described as an Eluviated Eutric Brunisol (Canadian Soil Classification System) or a Eutrochrept (US Soil Classification System) of moderate to good drainage, derived from medium textured stone-free Fraser River deposits (Bittman et al., 1999; Kowalenko, 1991). The Canadian Soil Classification System does not quantify its soil drainage classes, but the USDA SCS definition of moderate

permeability is 0.59 to 2.0 in/hr (SCS, 1992). Eutric Brunisols are typified by no Ah or a thin Ah (<2 in), a Bm horizon with 100% base saturation (NaCl), and pH < 5.5 (http://sis.agr.gc.ca/cansis/glossary/eutric_brunisol.html).

2.5.5 SITE HISTORY

Previous field research was conducted on Field 19. The field was planted with tall fescue and treated with hog manure for 3 years (1997-1999), which was applied with a variety of methods. During the hog manure study, the field was apportioned into forty test strips 10 to 16 feet wide by 112 feet long (Figure 4). These test strips were grouped into four replicates comprising ten test strips each. Within a replicate, each test strip was treated with a different fertilizer application method: Splashplate (2x rate), Splashplate (3x rate), Sleighfoot (2x rate), Fertilizer (3x), and a control. The field was left as bare ground from 1999 to May 2004 and was not tilled. The ground around the field was tilled and planted with grass in March 2004. Two of the test strips within each replicate from the previous study were chosen for use in this study. Initial soil data were analyzed to determine if there were any lasting effects from the previous treatments.

Porous ceramic suction cup lysimeters were installed in 1998 at 24- and 36-inch depths in five of the test strips in each replicate. Water that is held in the soil pores at matric suctions less than the applied vacuum is drawn through the pores of the suction cup at the bottom end of the lysimeter and collects inside the hollow tubing. The lysimeters existing in the test strips chosen for this study were used to collect soil pore water.

Soil pore water sampling conducted from November 1998 through September 1999 found a low potential for nitrate leaching in perennial forage fields with moderate to high annual rates of manure application (Patni et al., 2000). Patni et al. (2000) suggested that high precipitation and rapid water table movement diluted solute concentrations resulting in moderately low values of

nitrate nitrogen and that ammonium nitrogen is being immobilized or nitrified in the soil resulting in consistently low values (always < 0.1 mg $\text{NO}_3\text{-N/L}$). Higher concentrations of nitrate nitrogen were measured in November-December (mostly < 10 mg $\text{NO}_3\text{-N/L}$), directly following a flooding event, and in samples from the shallower lysimeters (24-inch depth).

3.0 RESEARCH OBJECTIVES

The impetus for this research is the need to determine nitrate leaching to groundwater in agricultural regions of Whatcom County. The underlying assumption is that the soil and climate conditions are similar enough throughout the Fraser Valley that the model will perform similarly in both Agassiz, BC, with a silt loam field soil, and in a silt loam in Whatcom County. The unique nature of the soils and variable intensity rainfall that commonly occurs in the Fraser Valley may create transient flow conditions in the vadose zone. Transient flow is typified by hysteretic infiltration, redistribution, and the shallow, highly fluctuating water table all of which create conditions unfavorable to steady-state flow simplifications. These factors become more important in the summer and early fall. In late fall and winter, when most leaching is thought to occur, heavy rainfall may saturate soils. For late fall and winter conditions, a simplistic steady-state flow model may produce leaching concentrations closely matched to field conditions. Therefore, there is a definite need to better understand the nature of water flow in the vadose zone throughout the year in this region and to relate flow conditions to fertilizer application timing so that an appropriate model structure can be applied for predictions of nitrate leaching to the water table. This research attempted to add to the understanding of water flow and nitrate flux in the vadose zone below an agricultural field through the completion of the following research tasks.

Research Tasks:

- Perform field investigations involving the combined monitoring of the sources, fate, and transport of nitrogen and water;
- Test the sensitivity of nitrate-leached and water-leached predictions to variations in the input parameters and internal model parameters involved in the soil water sub-model algorithms;
- Perform Monte Carlo simulations to determine the uncertainty in nitrate-leaching predictions;
- Calibrate NLOS to local climatic conditions and a local agricultural soil (a silt loam belonging to the Monroe Series) under a nutrient loading and crop management scenario comparable to local farming practices;
- Examine the ability of the soil water sub-model of NLOS to predict soil water and nitrogen fluxes during seasonal precipitation events by comparing model simulations to field observations;
- Characterize the distribution, concentrations, and temporal patterns of water and nitrate leaching in response to precipitation, fertilizer application, and cropping events using model simulations and field observations;
- Assess the impact of the steady-state model assumptions on nitrate and water transport simulations by comparing model simulations to field observations during both transient and steady-state flow conditions;
- Determine the optimal time to perform the Post-Harvest Soil Nitrate Test (PHSNT);
- Use the calibrated model to simulate nitrate leaching under various hypothetical fertilizer-application and cropping scenarios;

- Make recommendations about the applicability of NLOS in its current state of development for local predictions of nitrate transport through the vadose zone;
- Recommend improvements to NLOS if model predictions poorly fit the observed data.

4.0 METHODOLOGY

4.1 Experimental Design

This study was designed to measure and monitor the physical and chemical parameters required as inputs or delivered as outputs by NLOS (see Table 2 for a list of the required model inputs).

Note that all data presented for this study are in English units, but the inputs required by the model use a mix of English and metric units. Designing the field study to match the model outputs allowed for direct comparison of field measurements to model simulations. It is impossible to measure all parameters, but this study attempted to quantify nitrogen concentrations at each stage of the nitrogen cycle incorporated in NLOS (Figure 2) and to track the flow of nitrogen and water through the upper four feet of the soil profile. Field data collection began on March 24, 2004 and ceased on April 26, 2005.

4.1.1 FIELD SET-UP

The field site set-up is shown in Figure 5. I chose to locate the sampling equipment in two adjacent test strips in each replicate. Each test strip includes two pairs of lysimeters at 24- and 36-inch depths, installed in 1998, and was treated with either the Splashplate (2x rate) or Splashplate (3x rate) during the previous study. “Splashplate” is another term for the broadcast application of manure and the rate refers to the amount of swine manure that was being applied. From now on, I will refer to the chosen test strips as Plot 1 or Plot 2. Each plot, 1 or 2, may have received either the Splashplate (2x rate) or the Splashplate (3x rate) treatment. Each of the four

replicates has a Plot 1 and a Plot 2; therefore, there are a total of 8 plots and 16 lysimeters being used in this study. The lysimeters were used to sample soil pore water for nitrogen analyses.

One piezometer had been installed in the middle of each perimeter side of the field in October 1998 at the following depths (in): S-1 at 67.0, S-2 at 57.0, S-3 at 72.5, and S-4 at 56.5. The piezometers were used to sample groundwater for nitrogen analyses and to measure the depth to the groundwater table. Soil pore water and groundwater nitrogen concentrations were used to examine nitrogen flux and for comparison to simulated values of nitrate leached.

On May 20, 2004, eight 28 in x 28 in x 6-in deep aluminum collars with lids, or chambers, were installed adjacent to the lysimeters. The chambers were used to collect gaseous emissions from the soil surface for analysis of nitrous oxide flux and for comparison to simulated values of nitrification to nitrous oxide.

Composite soil samples were collected from random locations throughout the plots. Soil samples were analyzed for moisture and nitrogen as well as a number of physical and chemical soil properties required as model inputs. Soil nitrogen concentrations were used to examine nitrogen flux and transformations and for comparison to simulated values of soil nitrate and ammonium.

During August 2004, one PVC tube was installed to a 39-in depth in each replicate for collection of soil moisture data with a soil conductance probe (described later). These data were not used for reasons discussed in the soil moisture measurements section. Tensiometers were installed in May 2004 in order to measure soil suction- a proxy for soil moisture. The tensiometers were removed during the study due to irreparable damage from bears and coyotes and the data were unused. Only the soil moisture data collected from the composite soil samples were used to examine soil water flux and for comparison to simulated values of soil water.

The field was planted with silage corn using a no-till method in May 2004 and side-dressed with triple superphosphate (0-45-0). Two commercial fertilizers, 18-18-18 (Triple 18) and ammonium nitrate, were uniformly applied throughout the field at 495 lbs/acre and 259 lbs/acre, respectively, for a total of 178 lbs-N/acre (see Table 3 for details of all crop events). Triple 18 contains 18% each of nitrogen (from organic and inorganic sources), phosphorus, and potassium and ammonium nitrate contains 34.5% nitrogen. Agriculture Canada staff determined all fertilizer applications and crop management decisions in accordance with local farming practices. The field did not receive any water as irrigation during the previous study, nor did it throughout the duration of the study.

4.1.2 FIELD DATA COLLECTION

In this section I describe the frequency and type of field data collected. The sampling and analysis methods are described in detail in the following sections. I collected initial soil and soil pore water samples in March 2004 in order to determine background conditions before any fertilizer was applied and before the corn was planted. These initial soil samples were analyzed for moisture, nitrate, ammonium, cation exchange capacity (CEC), organic matter content, the C:N ratio of the organic matter, and coarse fragment percentage. The soil pore water samples were analyzed for nitrate and ammonium. Monthly sampling began in May 2004 and continued through April 2005. Two or three consecutive days were required each month for the collection of all field samples and measurements and the upkeep of field equipment. Monthly soil samples were analyzed for nitrate, ammonium, and moisture; monthly soil pore water samples were analyzed for nitrate, ammonium, and pH. Nitrous oxide sampling began on May 20, 2004, the day after the application of the fertilizers. In May, nitrous oxide sampling was conducted for 2 consecutive days per week for 3 weeks directly following fertilizer application. After that initial period, sampling was conducted twice a day for 2 consecutive days each month. Depth to water

measurements were performed and groundwater samples were collected from the piezometers once a month, when water was available. Tensiometers were installed in May 2004 and sampled monthly through September 2004. Soil moisture measurements were collected using the Diviner 2000 soil conductance probe at least once each sampling day, when weather conditions were favorable, from August 2004 through April 2005. The Agricultural Research Centre collected nitrogen concentration, moisture, and dry matter yield data for the corn crop.

4.1.3 ADDITIONAL DATA REQUIRED AS MODEL INPUTS

Daily temperature and precipitation data from the Agassiz CS weather station (located at lat: 49.25, long: -121.77, elevation: 49 feet), which is located on the Pacific Agri-Foods Research Centre about 1500 feet from the study site, were downloaded from Environment Canada's National Climate Archive (<http://www.climate.weatheroffice.ec.gc.ca/>). Hourly temperature and humidity data were also accessed from the above source for use in nitrous oxide emission determinations (discussed below). Evapotranspiration data from the same station were unavailable from Environment Canada, but accessed instead from www.farmwest.com, which uses the Penman-Monteith model for evapotranspiration.

The following data were obtained from the Agassiz soil survey for a Monroe series soil (Luttmerding and Sprout, 1967): soil drainage classification, percent slope, and landscape position (see Table 2 for a description of all model input values). The plant available water holding capacity and permanent wilting point are average values for a silt loam according to Brady (1974).

4.2 Bulk Density Determination and Usage

Methods to measure bulk density are labor intensive and time-consuming; therefore, existing bulk density values from a previous investigation conducted at PARC Agassiz were obtained

from Derek Hunt. Bulk density values collected in May and July 1997 from a field site adjacent to mine, were used to determine average bulk density values for each user-defined model soil layer. The bulk density values from the depths that overlapped with or were closest to the predetermined soil layer depth ranges were averaged and assigned to that soil layer. These depths and the average bulk density values for each soil layer are shown in Table 4.

Soil bulk density measurements are required as inputs for the NLOS model. The model first adjusts the bulk density (BD) to account for the bulk density of soil excluding the coarse fragments (Coarse_Frag_%). BD is then used to determine the porosity of the soil layer (POR), excluding the coarse fragments, in inches of water using an assumed particle density of 2.65 g/cm³. Note that the user may alter all algorithms within NLOS. The particle density used in the following equation changed during the calibration process.

$$BD = \text{Bulk_Density} * (1 - (\text{Coarse_Frag_}/100)) \quad (7)$$

$$POR = (1 - (BD/2.65)) * \text{Soil_Thickness} \quad (8)$$

I used the soil bulk density to convert the gravimetric soil moisture measurements obtained from the oven-dried soil to volumetric soil moisture according to the following equation:

$$\text{Vol. moisture} = \text{Grav. Moisture} * \text{Bulk density} \quad (9)$$

which was then used to determine soil water in inches:

$$\text{Vol. moisture} * \text{Soil Thickness (inches)} = \text{Soil Water (inches)} \quad (10)$$

Finally, bulk density was used to convert measurements of soil nitrate and ammonium from µg/L to lbs/acre according to the equation 16 detailed in the Unit Conversion Equations section.

4.3 Field Methods

4.3.1 SOIL SAMPLING

Soil cores were collected using a push-probe soil core sampler to the following depth ranges: 0-6, 6-12, 12-24, 24-36, and 36-45 inches. When fully extended, the sampler could only access soil to the 45-inch depth. The push-probe soil core sampler is a 1-inch diameter extendable hollow metal tube connected to a t-bar handle with foot pedals on each side (Figure 6). The sampler is pushed into the soil by stepping on the pedals and then retracted by pulling up on the handle. The sample cavity is 12 inches long; therefore, multiple cores were extracted from the same hole in 12-inch increments up to a 45-in depth. Soil samples from two randomly selected locations within each plot were combined into composite samples for each depth. No soil cores were collected within an approximately 5-foot radius of the lysimeters to avoid creating preferential flow pathways to the lysimeter cups. The 5-foot radius was estimated to be a sufficient distance based on the placement on the lysimeters in the unsaturated zone where flow is dominantly vertical. No measurements were made to confirm this estimate. Loose composite samples were collected in plastic bags and transported on ice.

4.3.2 WATER SAMPLING

Combined groundwater and soil pore water samples for nitrate and ammonium were collected in 125-ml 2N hydrochloric acid-washed Nalgene bottles and transported to the laboratory on ice (see Table A1 for sample container, storage, and holding times). Sub-samples were taken from the regular monthly shallow lysimeter samples for pH on November 17, 2004. Soil pH is a required model input and is used to determine the volatilization rate. Measurements of soil water pH from lysimeter samples are an acceptable substitute to measuring the pH of soil extract.

I used a peristaltic pump to collect groundwater from the piezometers and a hand pump to apply a vacuum and to collect soil pore water from the lysimeters. A diagram of the lysimeter

set-up is shown in Figure 7. The piezometers were sampled simply by inserting the peristaltic pump tubing below the water surface inside the piezometer and pumping water up to the surface for collection. A vacuum of approximately 60 psi was applied to the lysimeters. They were left in this primed state overnight and then sampled the next day. The e-flask used for sample collection was rinsed 3 times with deionized water between each sample collected. Due to the low volumes of water available in the lysimeters, the tubing and e-flask were only rinsed once with water suctioned from the lysimeters before the sample was collected. The set-up was rinsed three times with water suctioned from the piezometers before the sample was collected. Water samples were collected from the lysimeters and piezometers once a month, when water was available.

The lysimeters were inspected at the start of each sampling session for tampering by animals. A number of times the rubber stoppers had been removed or the plastic tubing chewed. When the lysimeters were left open to the elements, soil, insects, and other debris accumulated inside the lysimeter. When this occurred, the lysimeters were flushed multiple times with deionized water and scrubbed with a bottle brush on a long handle. The peristaltic pump was used to extract all the debris and rinse water and new tubing and stoppers were installed as necessary. No similar problems were encountered with the piezometers.

4.3.3 NITROUS OXIDE SAMPLING

Air samples were collected from non-steady-state, non-flow-through, about 2050 in³ in total volume, vented chambers for determination of nitrous oxide emission rates (Figure 8). A water seal was used to get an airtight connection between the vented, insulated covers and the aluminum collars. Ten-milliliter air samples were collected from the chambers at 0, 15, 30, and 45 minutes using pre-evacuated tubes with two-way needle valves. The chamber volume was measured three times during the study period; the average volume for each chamber was then used in the nitrous oxide flux calculation.

Chamber performance and gas emission rates can be affected by a number of factors including soil and air temperatures and moisture and soil nutrient concentrations. Therefore, hourly temperature and humidity data were retrieved from the Agassiz CS weather station for the sampling periods, soil temperature was measured, and soil nutrient and moisture samples were collected concurrently with nitrous oxide sampling. Prior to collecting the first sample of the 45-minute cycle, soil temperature was measured at a 6-in depth at three randomly distributed points adjacent to each chamber. Soil samples for moisture and nitrogen analysis were also collected every day that nitrous oxide sampling occurred. If the nitrous oxide sampling coincided with the regular monthly soil sampling, no additional soil samples were collected. Otherwise, composite samples of four 0-6 inch deep cores were collected adjacent to, but no closer than a foot away from, the nitrous oxide chambers.

4.3.4 SOIL MOISTURE MEASUREMENTS

In addition to the soil samples collected for gravimetric soil moisture, volumetric soil moisture was also measured in situ using a Diviner 2000 (Sentek Environmental Technologies, Stepney, South Australia) soil conductance probe. Soil moisture measurements were made on each sampling day as weather and time permitted, but at least once per month. Measurements were not performed during heavy rainfall, as water entering the tubing would cause measurement errors. The probe was calibrated to ambient air moisture in the laboratory on each sampling day. On October 27, 2004 soil samples for gravimetric moisture analysis were collected from the soil conductance sampling depths for comparison to the Diviner 2000 soil moisture measurements. Soil samples were collected within a few feet of the probe sampling well. A comparison of the moisture values determined from the two methods is shown in Figure 9. Soil moisture measurements from the two methods are poorly matched and show no discernable trend with depth or by method. The maximum absolute difference between volumetric moisture estimates at

one depth was 9.9% and the average absolute difference was 4.3%. Considering this difference and that the probe was never calibrated to the field soil, the conductance probe moisture data were considered inaccurate and were not used in the model calibration.

At the beginning of each sampling day, conductance readings were collected in the laboratory in a dry, sealed, normalization tube. These measurements were performed in order to normalize the sensor to ambient air. These normalization readings allow one to standardize the sensor readings. Prior to sampling in the field, each tube was inspected for any standing water or condensation. To collect soil moisture data, the soil conductance probe was inserted into the 39-inch deep PVC tubing that was installed in the field for this purpose, and slowly withdrawn as data points were collected every 4 inches. This procedure was repeated three times consecutively and the three measurements were averaged for that site and day. The measurement depths were corrected during data post-processing if the instrument probe zero depth measuring point did not match up with the ground surface when the probe was inserted in the tubing.

4.3.5 DEPTH TO WATER MEASUREMENTS

Depth to water measurements were performed in the piezometers when water was available. An electrical sounding tape was used to measure the distance from the top of the PVC tubing to the water surface. The length of the PVC tubing protruding from the ground surface was then subtracted from the depth to water measurements to determine the depth to water below the ground surface.

4.4 Groundwater Flow Direction Determination

At the outset of this study, I measured the locations (WGS84 UTM) and elevations (meters AMSL) to the measuring point (the top lip of the PVC tubing) of each piezometer using a handheld Magellan GPS unit. Note that the error associated with handheld GPS measurements can be

on the order of 150-650 feet; therefore, absolute elevations were not used in this study. I compared the relative elevation measurements made at each piezometer in the hydraulic gradient calculation. When water was available in the piezometers, I measured the depth to water from the measuring point. Depth to water measurements were recorded in all piezometers on only 6 sampling days. I also calculated the average water level elevations recorded during the previous study on the field site from 1998-2001. Using the depth to water (DTW) measurements and the measured elevations to the measuring points (MP), I calculated the water surface elevation, or head (all values are in feet) using the following equation:

$$\text{MP elevation} - \text{DTW} = \text{Water Surface elevation} \quad (11)$$

Using the northings and eastings and the calculated water surface elevation for each of the four piezometers, I calculated a groundwater flow gradient and flow direction using the EPA on-line tool for calculating gradients by fitting a plane to up to as many as fifteen points (<http://www.epa.gov/Athens/learn2model/part-two/onsite/gradient4plus-ns.htm>). The groundwater flow direction was used to determine which piezometers were located up-gradient vs. down-gradient. This information was used to distinguish nitrogen loading from the field site from background levels.

4.5 Analytical Methods

In this section I detail only the sample preparation, laboratory analyses, and calculations that I performed. Details of the analyses conducted by other institutions will not be provided. The quality control measures used for sample analysis are detailed in Appendix A.

4.5.1 SOIL ANALYSES

Gravimetric moisture

The monthly composite soil samples were well mixed and then a sub-sample was removed for soil moisture. Soil samples that could not be weighed and dried immediately were refrigerated. The sample was then weighed, dried for at least 16 hours at 105°C, and then reweighed to determine the percent moisture content (ASTM, 1995). The moisture content was calculated as follows:

$$\text{Moisture Content, \%} = [(A-B) \times 100] / A \quad (12)$$

where A is the fresh weight (g) and B is the oven-dried weight (g).

Soil nutrient extractions

The monthly composite soil samples were well mixed and then a sub-sample was removed for soil nutrients. Soil samples that could not be weighed and dried immediately were refrigerated. Soil samples for nutrient analysis were not refrigerated for greater than 24 hours. The sample was then weighed and then set out to air dry for at least two weeks, or until a dry state (based on the criteria described below) was achieved, in a humidity controlled (<10% relative humidity) soil drying room located at PARC Agassiz.

Ideally, soil samples for inorganic nitrogen analysis should be analyzed immediately, but that was not logistically possible for this study. Air-drying can lead to small, but significant increases in NH_4^+ -N (Nelson and Bremner, 1972). The air-drying procedure employed by PARC Agassiz takes the following precautions to reduce the impact of samples storage on ammonium values: stored in a NH_3 -free atmosphere, samples are enclosed in a room specifically for soil drying and then bagged in plastic before being transported or shelved for long-term storage, soil is not dried at an elevated temperature (the drying room is kept at room temperature), and the drying room is humidity controlled. No specific procedure exists for air-drying soil samples, but known

precautions were observed. The drying time was arbitrarily chosen based on the prior knowledge of the time required (Hunt, D.E., personal communication), under the conditions present in the laboratory soil drying room, to dry the soil types collected from the test fields on the research centre. Since the condition of being dry for a soil is an arbitrarily determined state (Black et al., 1965), for the purposes of this research completely air-dried soil is defined as a soil that appears dry to the touch and easily disaggregates or crumbles when ground. Two weeks of air-drying time was sufficient to reach this state.

Once the nutrient samples had completely air-dried, PARC Agassiz staff then reweighed and bagged each sample. These dried and weighed samples were temporarily stored at the research centre until I was ready to analyze them for nitrate and ammonium. At that point, I transported the samples to Western Washington University (WWU) where I ground the samples with a rolling pin and sieved them through a 2.0 mm sieve in preparation for KCl extraction. KCl extractions were performed according to the methodology described on page 648-649 of *Methods of Soil Analysis* (Page et al., 1982). The KCl extract was then filtered through 0.45-micron 2 N hydrochloric acid- soaked filter and preserved with sulfuric acid to a pH of 2. Nitrate and ammonium were then analyzed at the Institute for Watershed Studies (IWS) laboratory (a Washington State Department of Ecology Accredited laboratory, Accreditation #A006). IWS follows standard operating procedures adapted from APHA (1998) for all analytical work (see Table A2).

Organic matter

A sub-sample of the initial composite soil samples collected in March 2004 from the 0-6 and 6-12 inch depths were analyzed to determine the C:N ratio of the organic matter. Sample preparation for C:N ratio analysis included weighing, air-drying, roller-grinding, and sieving to separate the fine fraction (<2 mm diameter). The fine fraction of the samples was then

transported to the University of Washington Analytical Center where they were analyzed for percent carbon and percent nitrogen using a Perkin Elmer CHN Analyzer 2400 Model. These data were then used to calculate the C:N ratio of the organic matter:

$$\text{C:N ratio} = \%C/\%N \quad (13)$$

An additional sub-sample of the initial composite soil samples from the 0-6 and 6-12 inch depths were analyzed for organic matter content. The organic matter samples were weighed, oven-dried at 105° C, and analyzed in the WWU Geology Geomorphology Laboratory. The ash content was determined by burning the oven-dried samples in a muffle furnace at 440°C until a constant mass was achieved (ASTM, 1995). The ash content was then used to calculate the amount of organic matter, as follows:

$$\text{Organic matter, \%} = 100.0 - \text{ash content, \%} \quad (14)$$

Coarse fragment percentage

Sub-samples from the initial composite soil samples from all depths were analyzed for soil coarse fragment percentage. Oven-dried samples were weighed, roller-ground and sieved through a 2.0 mm diameter sieve. The sample portion >2.0 mm was then weighed and the coarse fragment percentage calculated as follows:

$$\text{Coarse fragment, \%} = [(A/B) \times 100] \quad (15)$$

where A is the weight of the sample portion >2.0 mm (g) and B is the weight of the total sample (g).

Cation exchange capacity

One large composite soil sample was created by mixing sub-samples of the oven-dried initial composite soil samples from all depths for cation exchange capacity (CEC) analysis. Avocet

Environmental Laboratories in Bellingham then analyzed the composite sample for CEC using EPA method 9081 (sodium acetate).

4.5.2 WATER ANALYSES

Combined water samples were collected for nitrate and ammonium analysis. After collection, the samples were filtered the same day at the IWS Water Quality Laboratory with a 0.45-micron 2 N hydrochloric acid- soaked filter and preserved with sulfuric acid to a pH of 2. The samples were then refrigerated until analysis. See Table A1 for sample handling and storage procedures. Sub-samples were taken from the combined water samples, before filtration and preservation, for pH measurements. These measurements were performed immediately after arriving in the laboratory from the field. All water samples were analyzed at the IWS laboratory (see Table A2). The IWS laboratory historically has obtained more accurate pH results from its laboratory meter than from the available field meters; therefore, the laboratory meter was used in this study.

4.5.3 NITROUS OXIDE ANALYSIS

Nitrous oxide was analyzed at the PARC Agassiz laboratories. Samples were analyzed using a Varian Gas Chromatograph equipped with a ⁶³Ni electron capture detector. The slope of increasing nitrous oxide with time was calculated from the successive samples that were collected from the closed chamber at 0, 15, 30, and 45 minutes. The Ideal Gas Law was then used to calculate a flux using the calculated slope, the ambient air temperature and pressure, and the average volume of the chamber. This process determines the nitrous oxide emission rate in g-N₂O-N/ha/day.

4.5.4 CROP ANALYSES

Crop moisture, crop yield, and crop nitrogen % were analyzed at the PARC Agassiz laboratories. Derek Hunt summarized and averaged the data to determine the precise input values needed for the model.

4.6 *Statistical Methods*

Statistical analyses were performed on the data from the initial soil and water samples collected in March 2004. The initial data set consists of values of nitrate and ammonium in soil, soil pore water, and groundwater, and the following soil conditions: moisture, organic matter, coarse fragment percentage, and carbon to nitrogen ratio. These data were collected before the initiation of any agricultural activity on the field for this project. The purpose of the statistical analysis was to determine whether or not there were significant differences in any of the above-mentioned values with depth in the soil profile, location in the field, or due to the potentially lasting effects of differing manure treatment methods employed during the previous study conducted on the field site. The statistical results were used to determine how and if the initial model input values should be segregated based on depth, location, or previous treatment method.

Exploratory statistical analyses were performed first to examine trends in the data and to visually assess relationships between variables that might warrant further analysis with confirmatory statistical methods. The statistical software R was used to generate summary statistics, which consist of the maximum, minimum, mean, and median, for each parameter in the data set. Summary statistics are provided in Table 5. R was then used to generate a number of notched boxplots and scatterplots in order to visually examine the relationships between each parameter and depth, location, or previous treatment method (i.e., Splashplate (2x) or Splashplate (3x), which are represented as 2 and 3 on the figures; Figures 10-19). R was also used to conduct the confirmatory and pairwise tests described below.

The exploratory statistics results indicated which confirmatory analyses were appropriate. Where the notched boxplots showed no overlap in the group means for multiple depths, locations, or previous treatment methods, a Kruskal Wallis Rank Sums Test was used in order to determine if the population distributions were significantly different. The Kruskal Wallis Rank Sums Test is a non-parametric generalization of the two-sample Student T-Test applicable to multiple populations. Non-parametric tests allow you to avoid issues of normality and homogeneity (<http://mathworld.wolfram.com/>). The Kruskal Wallis Ranks Sums Test is an Analysis of Variance (ANOVA) significance test that determines differences between population distributions for k populations. The null hypothesis is that the k population distributions are identical. The null hypothesis of no difference between populations is rejected for p-values less than 0.05. At this acceptance level, the probability of a Type I error (erroneously rejecting the null hypothesis) is only 5%. If the null hypothesis is rejected, the alternative hypothesis that at least two populations differ is accepted. The following assumptions, taken from <http://www.statsdirect.com>, must be met for the Kruskal Wallis Rank Sums Test:

- random samples from populations
- independence within each sample
- mutual independence among samples
- measurement scale is at least ordinal
- either k population distribution functions are identical, or else some of the populations tend to yield larger group means than other populations

The non-parametric Kruskal Wallis Rank Sums Test was used since the sample sizes were small and the data met the assumptions listed above.

Rejection of the null hypothesis for the Kruskal Wallis Rank Sums Test indicates that there were differences between at least two of the population distributions. Pairwise testing indicates

which population distributions differed. The Pairwise Wilcoxon Rank Sums Test is a non-parametric generalization of the Paired Student T-Test applicable to multiple populations. The Holm adjustment was used to expand the test to multiple populations. The test assumes that there are n paired observations of the form (X_i, Y_i) . The null hypothesis is that the population distributions for the X 's and Y 's are identical. The null hypothesis of no difference between X 's and Y 's is accepted for p -values less than 0.05. If the null hypothesis is rejected, the alternative hypothesis that the two populations differ in location is accepted. The following assumptions, taken from <http://www.statsdirect.com>, must be met for the Pairwise Wilcoxon Rank Sums Test (D_i are the ranks of the positive, non-zero differences between a pair of samples):

- distribution of each D_i is symmetrical
- all D_i are mutually independent
- all D_i have the same median
- measurement scale of D_i is at least interval

The non-parametric Pairwise Wilcoxon Rank Sums Test was used since the data met the assumptions listed above and the Wilcoxon Rank Sums Test indicated significant differences between data populations.

4.7 Modeling Methods

Once the field samples were collected and analyzed, I determined the base model inputs and began simulations for the sensitivity analysis. The sensitivity analysis results focused the calibration on the input parameters that had the largest impact on water and nitrate leached predictions. The model was calibrated to the field measurements of nitrate and ammonium in soil and soil pore water, nitrous oxide, and soil water. The calibrated model was then used to determine the fate of nitrogen and water during various hypothetical scenarios and to recommend the optimal time for performing the post-harvest soil nitrate test (PHSNT).

4.7.1 NLOS MODEL SET-UP

All simulations were conducted over a 399-day period from March 24, 2004, when the initial samples were collected, to the last sampling day on April 26, 2005. The model uses Julian dates; therefore, to maintain a continuous simulation period, January 1, 2004 was designated as day one and days 84 (March 24, 2004) through day 482 (April 26, 2005) were designated as the simulation period.

Model inputs were derived from the field data, historical data collected on a nearby field, the Agassiz soil survey (Luttmerding and Sprout, 1967), and from published sources of typical values for silt loams (see Table 2 for all model inputs and the sources). The model allows the user to specify soil layer thicknesses, for up to four soil layers (one surface layer and up to three sub-surface layers), with certain restrictions. I collected soil, soil pore water, and soil moisture at varying depths within the field. Using the depths at which I had collected samples and a number of other factors as a guide, I designated three soil layers, in addition to a 1-inch surface layer (LS), for which the model considers separate processes but includes in the total thickness of soil layer 1. See the next section for a description of the soil layer determination. Soil layer 1 (L1) spans 0-12 inches, L2 from 12-36, and L3 from 36-45. Once the soil layer thicknesses for modeling purposes were determined, I averaged the initial and daily field data from the five soil layers sampled into three soil layers. The data for these three layers was then averaged for the two plots within each replicate and then for the four replicates to obtain average values for the entire study area. Supporting evidence for the data averaging methods is provided in the Statistical Results section.

The final step was to prepare the field data for comparison to the model simulations by converting the field data measurement units to match the units used by the model. Ammonium and nitrate concentrations from lysimeter samples and soil extractions had to be converted from

$\mu\text{g-N/L}$ to lbs-N/acre ; the gravimetric soil moisture fractions had to be converted first to volumetric fractions, and then all the volumetric fractions to inches of water by soil layer. The unit conversion equations are shown in the Unit Conversion Equations section.

Soil Layer Determination

The depths in the soil column at which I was able to collect soil and soil water solution samples were constrained by the available soil sampling equipment and existing lysimeter depths: 24 and 36 inches. The depth at which I could collect soil samples was flexible from 0-45 inches. I chose to sample soil at the depths suggested by existing Pacific Agri-Foods Research Centre sampling protocol: 6, 12, 24, 36, and 45 inches. The Diviner 2000 soil conductance probe likewise had some flexibility in the increments of measure up to the maximum depth of 39 inches. I sampled in the smallest increment provided by the instrument: 4 inches. The strategy behind these sampling depths was that the resolution of the samples could always be reduced later by averaging data for multiple soil depths. That is what I eventually did when I decided on where to make the breaks for the user-defined soil layers used in the model.

All depths were first converted to inches and then the overlaps between the sampling depths for the multiple sample types were determined. Using a combination of the model default depth for soil layer 1 (12 inches), the maximum crop rooting depth of 24 inches (Hunt, D.E., personal communication), and the maximum sampling depth (45 inches), I defined three soil layers with the following depths: soil layer 1, 0-12 inches, soil layer 2, 12-24 inches, and soil layer 3, 24-45 inches. Note that with these soil layer designations, the leached nitrate values measured in soil solution samples from the 24-inch lysimeter are more accurately compared to the model simulated values of nitrate leached from L2, L2 terminates at the 24-inch depth, than the comparison of nitrate leached from L3 (45 inches) to the 36-inch lysimeter samples. There was no direct comparison for the 36-inch lysimeter samples. Soil layer 3 was originally determined to

terminate as close as possible to the piezometer sampling depths. After the soil layer determination was made, I decided not to include the piezometer data in the analysis. In retrospect, 36 inches would have been a better termination depth for L3 for better comparison to the 36-inch deep lysimeter, but there was too much work built into the original soil layer determinations to change the layer thicknesses once the decision was made not to use the piezometer data.

Unit Conversion Equations

The model simulates all nitrogen pools in lbs-N/acre. In order to compare the observed values of nitrate and ammonium in the soil extracts and lysimeter samples to simulated values of nitrate and ammonium in the soil and leachate, the observed data were converted. The measured concentrations of nitrate and ammonium in the extract and lysimeter water were converted from $\mu\text{g-N/L}$ to lbs-N/acre. I was unable to locate any equations for converting from $\mu\text{g/L}$ to lbs/acre that did not make oversimplifying assumptions for bulk density or soil thickness; therefore, I derived conversion equations specific to the analytic work and field samples. Observed gravimetric soil moisture was also converted for comparison to simulated soil water in inches. Equations 9 and 10, presented in the Bulk Density Determination and Usage Section, were used to convert gravimetric to volumetric soil moisture and the volumetric moisture fractions to soil water in inches.

Soil Extract Conversion

Soil samples were collected across the depth of each soil layer of known thickness, for example a sample from L1 consists of soil from 0-12 inches deep. The soil samples were then ground and a sub-sample was extracted from the total ground sample and weighed (this is the soil weight used below). The soil sub-sample was then mixed with 50 mL of KCl solution and agitated. The soil-

KCl solution was then filtered and the KCl extract was analyzed for NO₃-N and NH₄-N. The resulting lbs-N/acre is the total soil N and is considered to be uniform across the soil layer thickness. See the Soil Analysis section for a more detailed description.

To convert from µg/L of NO₃-N or NH₄-N in the soil extract solution to lbs_N/acre-in_{soil} for a designated soil layer:

$$\frac{lbs_N}{acre - in_{soil}} = \left(\frac{X \text{ } \mu\text{g}_N}{1 L_{KCl}} \right) \left(\frac{1 \text{ g}_N}{10^6 \text{ } \mu\text{g}_N} \right) \left(\frac{0.00220462262 \text{ lbs}_N}{1 \text{ g}_N} \right) \left(\frac{1 L_{KCl}}{1000 \text{ mL}_{KCl}} \right) \left(\frac{50 \text{ mL}_{KCl}}{Y \text{ g}_{air-dried soil}} \right) \left(\frac{\rho_b \text{ g}_{oven-dried soil}}{1 \text{ cc}_{soil}} \right) \left(\frac{10^6 \text{ cc}_{soil}}{1 \text{ m}^3_{soil}} \right) \left(\frac{1233.48184 \text{ m}^3_{soil}}{1 \text{ acre} - \text{foot}_{soil}} \right) \left(\frac{1 \text{ acre} - \text{foot}_{soil}}{12 \text{ acre} - in_{soil}} \right) \quad (16)$$

where,

X = concentration of NO₃-N or NH₄⁺-N measured in soil extract solution (µg_N/L_{KCl});

Y = soil weight used in 50-ml KCl soil extraction (g_{soil});

ρ_b = average bulk density for that soil layer (g_{soil}/cm³_{soil}).

Note that both oven-dried and air-dried soil weights are used in the equation above. The assumption is that the air-dried weight and the oven-dried weight are comparable (no additional water remaining in the air-dried sample to increase its weight over an oven-dried sample of the same soil). This assumption is based on an analysis of the difference between the air-dried soil moisture and the oven-dried soil moisture for samples collected in the same replicate and at the same depth on the same day. The soil moisture values from the two methods varied 3% on average. Since this difference is small, there will be a very small error from using both in the conversion equation. This equation condenses down to:

$$\frac{lbs_N}{acre - in_{soil}} = \frac{X \cdot \rho_b \cdot 0.011}{Y} \quad (17)$$

The following equation was then used to convert to lbs_N/acre for the entire designated soil layer:

$$\left(\frac{lbs_N}{acre}\right)_{soil\ layer} = \left(\frac{lbs_N}{acre - in_{soil}}\right) \left(\frac{in_{soil}}{soil\ layer}\right) \quad (18)$$

Lysimeter Water Conversion

Water samples were collected from lysimeters located at 24- and 36-inch depths. The porous cup is 2 inches thick, but I assumed that the collected water is from those depths, ignoring the span of the cup and the vertical and radial influence of the lysimeter suction. I also assumed that the lysimeter is collecting percolating water only.

The concentration of simulated nitrate leaching from L2 to L3 is uniform throughout L2. Therefore, the concentration of nitrate in the water collected from the lysimeter located at the 24-inch depth was compared to the amount of nitrate leaching out of the bottom of L2 (12-24 in). The concentration of nitrate in the 36-inch deep lysimeter was compared to the nitrate leaching from L3 (24-45 in). In the model simulation, the amount of nitrate leached is related to the amount of water moving from L2 to L3.

To convert the nitrate concentrations measured in the lysimeter water (μg NO₃-N/L) to nitrate leached values (lbs NO₃-N/acre), I derived the following conversion equation:

$$\frac{lbs_N}{acre - in_{water}} = \left(\frac{\mu g_N}{L_{water}}\right) \left(\frac{1\ lb_N}{453592370\ \mu g_N}\right) \left(\frac{0.016387064\ L_{water}}{1\ in^3_{water}}\right) \left(\frac{6272640\ in^2_{water} \cdot x\ in_{percolating\ water}}{1\ acre - in_{water}}\right) \quad (19)$$

where, x ($in_{percolating\ water}$) is the total water in the designated soil layer (in) from the daily soil moisture measurements minus the plant AWHC and the PWP. Simulated nitrate leached is derived from the amount of nitrate in L2 (NO₃_L2) as provided by soil tests, but for the lysimeter samples, it is referring to the amount of nitrate in water, “nitrate leached”; therefore,

the units of $\text{lbs}/\text{acre}_{\text{soil}}$ are assumed to be interchangeable with $\text{lbs}/\text{acre}_{\text{water}}$. This equation condenses down to:

$$\frac{\text{lbs}_N}{\text{acre} - \text{in}_{\text{water}}} = \left(\frac{\mu\text{g}_N}{L_{\text{water}}} \right) \left(x \text{ in}_{\text{percolating water}} \right) (0.00022661) \quad (20)$$

The following equation was then used to convert to lbs_N/acre for the entire designated soil layer:

$$\frac{\text{lbs}_N}{\text{acre}_{\text{water}}} = \left(\frac{\text{lbs}_N}{\text{acre} - \text{in}_{\text{water}}} \right) \left(\frac{\text{in}_{\text{soil}}}{\text{soil layer}} \right) \quad (21)$$

4.7.2 SENSITIVITY ANALYSIS

A sensitive input is hereby defined according to D.M. Hamby (1994) as: (a) a parameter whose variability or uncertainty is propagated throughout the model resulting in a large contribution to the overall output variability, and (b) a parameter that is highly correlated with the model result so that small changes in the parameter result in significant changes in the output. A detailed sensitivity analysis was performed to determine the sensitivity of nitrate and water leached to variations in input parameters affecting the water budget. The model calibration process focused on the input parameters that caused the most significant response in simulations of nitrate or water leached.

A set of base values was determined as initial model inputs. These base values were determined from either the initial soil data averaged for the entire study area or from literature values (Table 2). The input parameters affecting the soil water sub-model were identified and only those parameters were tested during the sensitivity analysis with the exception of the internal model parameter $K_N2O_Leakage$. The $K_N2O_Leakage$ is the fraction representing the maximum leakage of nitrous oxide from the nitrification process. During the model calibration, simulations of nitrous oxide emissions were found to be extremely poor. In order to improve the calibration, this parameter was added to the sensitivity analysis and the calibration.

The model's sensitivity to any other inputs that did not affect the water budget was not examined since the water sub-model was the focus for the overall model calibration. Although the study was concentrated on only those parameters affecting the water budget, those parameters constitute a majority of the model inputs (Tables 2, 6, & 7). There are only a few untested parameters, which may have improved the overall calibration. Model sensitivity to initial soil nitrate and ammonium was untested and these parameters may have had an impact on total nitrate leached. However, initial soil nitrate and ammonium only accounted for 0.17% and 0.22%, respectively, of the initial and added nitrogen; therefore, the impact on nitrate leached would be small. Sensitivity to the user-defined soil layer thicknesses was also not tested due to time constraints.

The sensitivity analysis was performed using the "one-at-a-time" or "local" method where a sensitivity ranking is obtained by increasing or decreasing each input value by a given percentage (60% in this study) while leaving all others constant, and quantifying the change in the model output. Two sensitivity analyses were conducted. The first used the outputs of nitrate available for leaching, termed "nitrate leached," and the second used the outputs of total water leached. Using the base values as inputs, starting nitrate and water leached outputs were recorded. The interval of variation of 60% for the test parameters is consistent with the sensitivity analysis of a nitrogen transport and transformation model by Garnier et al. (2001). Every input value in the base data set for each climate parameter was increased or decreased all at once, not as increases or decreases in individual daily values.

The resulting model output was recorded for each increase or decrease in each individually varied parameter (Tables 6 & 7). The percent change from the base output of either nitrate or water leached was calculated for each increase or decrease in the varied parameters. The average percent change was then calculated and the parameters ranked by decreasing influence (Tables 8

& 9). The input parameters that effected the greatest change in outputs of nitrate or water leached were focused on during the nitrogen sub-model and water sub-model calibrations, respectively.

4.7.3 UNCERTAINTY ANALYSIS

The goal of the uncertainty analysis was to objectively identify the amount of error associated with simulated values of nitrate leached due to the uncertainty in the input values. The maximum and minimum values possible for the field site were determined for a sub-set of the model inputs. The model inputs chosen for uncertainty analysis were the same set of parameters used in the sensitivity analysis, excluding the internal model parameters, climate inputs, and K_N2O_Leakage (Table 10). Uncertainty analysis considers the effect of the inherent uncertainty in model input data on the model output. In contrast, sensitivity analysis makes no use of information concerning the sources or ranges of uncertainty in model input data (Beck, 1987).

The uncertainty in the model's prediction of nitrate leached was determined using the Monte Carlo Method. The Monte Carlo Method involves randomly sampling from assumed or known distributions for each input variable in order to create a new set of input values from the population of observed field values. Therefore, the Monte Carlo analysis results generated many possible model simulations.

A Monte Carlo simulator was incorporated into NLOS as a new sub-model. The simulator uses the random number generator function in STELLA to produce random values for each input parameter within specified, user-entered maximum and minimum ranges assuming uniform distributions (see Table 10 for all input ranges). Random values were generated for all the same inputs used in the sensitivity analysis, excluding the climate parameters and internal model parameters. A new STELLA list input device was created for each model input used in the

Monte Carlo simulations. This list input device allows the user to either enter a value for each parameter or turn on the Monte Carlo equation for a randomly generated input value.

The Monte Carlo simulator was built into the Soil Characteristics model sector. This was just a matter of convenience as many of the user-entered values used in the Monte Carlo simulations were available in this sector. When the equation option in the list input device is selected for a parameter, then the following algorithm is used to select the input value for that parameter (I will run through an example using PWP_1, but this could be substituted by any other parameter in the Monte Carlo list):

```
if TIME > 84 THEN Random_Reservoir[PWP_1_] else
Var_Init_Defaults[PWP_1_] (22)
```

The algorithm is computed on the first time-step (for the model simulations, the initial time step was set to 84, March 24, 2004). The above equation tells the model to use the randomly generated value for PWP_1 for all simulation days following March 24, 2004 or else to use the initial default value entered for that variable (Var_Init_Defaults[PWP_1_]). The initial default values are entered as an array in the Var_Init_Defaults converter.

The random value is generated using the random number generator built into STELLA that randomly selects a number from a uniform distribution bound by user-entered maxima and minima. These maximum and minimum values are drawn from arrays in the Rand_Low[PWP_1] and Rand_High[PWP_1] converters. To compute the random value, NLOS draws from the Infinite_Reservoir and uses the Random_Transfer flow to convert to a random input that is stored in the Random_Reservoir. The reservoirs and flow are detailed below.

Infinite_Reservoir[Variable_Inputs]

Stock (Reservoir)

(Variable type: 1-D array over Variable_Inputs)

10000000000000000

Random_Transfer[Variable_Inputs]

Flow (Uniflow)

if TIME=84 then RANDOM(Rand_Low[Variable_Inputs,

Rand_High[Variable_Inputs]) else 0 (23)

Random_Reservoir[Variable_Inputs]

Stock (Reservoir)

(Variable type: 1-D array over Variable_Inputs)

0

An Apple Script was written to initiate each model run and then store the resulting simulated nitrate-leached values in a text file. Using this automation technique, 2,000 Monte Carlo simulations were conducted. Each simulation was generated using a unique, random set of input values. The uncertainty in the nitrate-leached prediction from the 2,000 simulations was examined using summary statistics and graphical techniques (see the Uncertainty Analysis section).

4.7.4 MODEL CALIBRATION

The goal of the model calibration was to produce simulations that best fit the field data. By tuning the model to best predict the field data, the model may become a better predictive tool, if conditions similar to those present in the calibration data set are maintained. In order to test the robustness of the calibration, it is necessary to also validate the calibrated model using a new data set. The model was not validated as part of this study due to the unavailability of an appropriate data set. To remove subjectivity in fitting the model to the field data, I used an

automatic optimization technique as described by Nash and Sutcliffe (1970). The parameters chosen for use in the calibration are those that were identified as most sensitive by the sensitivity analysis.

To compare model simulations to field data, I calculated the model efficiency coefficient (E_f) by comparing each individual field measurement to the corresponding simulated value on the same day. The efficiency coefficient is defined as

$$E_f = \frac{\sum_{i=1}^n (m_i - \bar{m})^2 - \sum_{i=1}^n (s_i - m_i)^2}{\sum_{i=1}^n (m_i - \bar{m})^2} \quad (24)$$

where m_i and s_i are the measured and simulated results, and \bar{m} is the mean of the n measured results (Nash and Sutcliffe, 1970). The efficiency coefficient is defined as the proportion of the initial variance accounted for by the model. The maximum model efficiency possible is 1, which indicates perfect agreement between the simulated and observed values, but there is no lower limit. Negative efficiencies may be obtained when the relative difference between the simulated and observed values is greater than the difference between the observed value and the mean of the observed values. Only parameters for which both the model produces an output and for which field data were collected were used in the overall model efficiency calculation (see Table 11).

The model inputs chosen for the initial calibration were those identified by the sensitivity analysis as effecting a measurable change on water leached predictions and at least a 5% change on nitrate leached predictions, excluding climate inputs (Tables 12 & 13). For each sensitive input identified for calibration, successive model runs were performed with either an increase or a decrease in the input's base value while holding all other inputs constant to their base values. For each simulation, the average efficiency for the overall model was calculated. In the

calibration process, each input was varied multiple times in successively smaller increments down to the smallest increment of 0.1 or 0.01 units to achieve the maximum efficiency for the overall model. The parameters were not varied outside pre-determined ranges, which were identified for each variable at the outset from either published ranges or from the field data. The sources for the pre-determined ranges for each variable are listed in Tables 12 & 13. Once the maximum efficiency for the overall model was achieved for an input, that input was considered calibrated. The calibrated value was then used as the new base value for that input when the next most sensitive variable was calibrated. I performed two iterations of parameter calibration. For each iteration, the soil water sub-model was calibrated first, followed by the nitrogen dynamics sub-model. The soil water sub-model was calibrated by using the parameters that produced a measurable effect on water leached predictions in the sensitivity analysis. The nitrogen dynamics sub-model was calibrated by using the parameters that produced at least a 5% change on nitrate leached predictions.

5.0 RESULTS and DISCUSSION

5.1 *Field Observations*

In addition to model inputs and calibration, field data were also used to characterize the distributions, concentrations, and temporal patterns of nitrate leaching to the water table in response to soil water movement and fertilizer application for the study site. Note that the observed nitrate and ammonium data from the lysimeter samples are presented in the unconverted, original measurement units ($\mu\text{g-N/L}$). The values were left in the original units for comparison to nitrate and ammonium concentrations in groundwater. The groundwater data could not be converted because the leachate volumes needed for the conversion are unknown. Also, soil moisture is presented as a moisture fraction when compared to the calibrated values for

the PWP, Plant AWHC, and porosity since these values are commonly expressed as fractions. Elsewhere, the soil moisture data have been converted to soil water in inches by soil layer.

5.1.1 WEATHER

In order to assess whether or not the data represent typical field conditions, I compared monthly averages of weather data from the study period to 30-year climate normals (Figures 20-23). All weather data were measured at the Agassiz CS weather station. The monthly average evapotranspiration data are compared to the monthly averages from 1991 – 2004 since a 30-year history was unavailable. Mean total monthly precipitation during this study was lower than the 30-year normal in February, April, June, and July, and higher in August, September, and November. The mean total yearly precipitation average over the 30-year normal and this study period are 68.5 and 65.5 inches, respectively. Although this study spanned longer than one year, the weather data analyzed were for one calendar year from April 2004 to March 2005. The relative scarcity of water during the warmer months may have inhibited both microbial activity and crop growth.

Excluding January and September, the mean monthly maximum and minimum temperatures were slightly higher for the study period. The 30-year mean minimum temperature was higher for some months causing evapotranspiration to be higher during the study period, excluding May and September.

Weather during the study period may have influenced the nitrogen cycle. Since microbes and crop uptake are important parts of the nitrogen cycle, the relative scarcity of water during the warmer months may have had consequences for nutrient flux during the study period. Since temperature and evapotranspiration increases were fairly consistent throughout the study period, these increases may not have effected any change on the normal cycles of microbial or plant growth, but instead affected the magnitude of these processes. Another possible scenario is that

the increased air temperature raised the soil temperature above the threshold required to initial soil microbial activity, thereby extending the amount of time that microbes were active in the soil. Increased microbial activity could greatly affect soil nutrient levels.

5.1.2 SOIL

Soil nitrate and ammonium concentrations in soil layer 1 (0-12 inches deep) spiked immediately following fertilizer application (Figures 24 & 25). There was a progressively longer delay before peak nitrate concentrations were met in soil layers 2 and then 3. These delayed peaks in the deeper layers are attributed to the slow leaching of nitrate in soil pore water. There was a slight increase in soil nitrate and ammonium in soil layers 2 and 3 directly following fertilizer application, but such a rapid response is unexpected considering the time required for solute transport from the surface to deeper soil layers as evidenced by the soil pore water data; therefore, this initial immediate spike in ammonium is attributed to contamination of the soil samples. Preferential flow could also account for a rapid response time, but this seems unlikely since there was no corresponding spike in the soil pore water data. If preferential flow occurred, the effect would also be evident in the soil pore water nitrate and ammonium data. Sample contamination is a more likely cause considering the nature of the sample collection. The deeper samples are extracted from one boring by removing successively deeper soil cores. During this process, the hole is open to soil falling in from the surface and the deeper samples come into contact with the soil probe that was just in contact with the shallow samples. The soil was brushed from the probe between samples, but it was not cleaned. Since ammonium concentrations at depth never exceeded the level of that initial spike, which is attributed to contamination, ammonium from the fertilizer applied at the surface did not ever reach the deeper soil layers. The ammonium at the surface is lost to volatilization and nitrification before it has a chance to leach downward.

Soil layer 3 was saturated from below due to the rising water table on a few sampling days between December and February (Figure 26) and all the soil layers were saturated on January 20, 2005. Ammonium had already returned to background conditions before the soil became saturated. Soil ammonium shows no change in concentration on the sampling days when soil layer 3 was water logged (Figures 25 & 26). On January 20, 2005, slush, snow, and pooled water were observed at the surface while the water table was very shallow, above the bottom depth of L1. Although I did not sample all soil layers on that day, I assumed all layers were saturated. Soil samples were collected from the upper six inches for only soil moisture analysis. Nitrate in L1 and L2 had returned to background conditions by December 13, 2004 and there was no evidence for dilution when sampling resumed on February 23, 2005 (Figure 24). Soil layer 3 was also water logged on November 17 and December 13, 2004. There is a slight rise in nitrate in L3 on those sampling days, but nitrate concentrations started to rise on October 20, 2004, before the soil became water logged. Soil layer 2 also showed a rise on October 20 when it was not saturated. Nitrate concentrations would decrease due to dilution, not increase. Therefore, the slight rise in nitrate in L2 and L3 that began on October 20 may be a result of the crop harvesting, which took place on September 28. There were large fluctuations in nitrate concentration at the top of the peak in L1 with dips on July 8 and August 10. The cause for these dips in nitrate, as opposed to a gradual decline from a peak value, is unknown. The most likely cause is sample contamination or measurement error.

5.1.3 SOIL PORE WATER

The temporal resolution of the soil water data is coarse, which makes it difficult to attribute a direct response in increased soil moisture to net water (precipitation – evapotranspiration) or precipitation (Figure 27). Net water is more appropriate for comparison to soil water at depth since water is removed from the surface soil by evaporation and removed mostly from L1 and L2

by crop uptake (transpiration). The precipitation minus these withdrawals (net water) is the water that is actually entering or percolating through the soil. There is an overall rise in soil water levels following the onset of increased precipitation and rising net water on about August 20 (Figure 27). Soil water levels begin to taper off after about December 13 (L3) to January 21 (L1 & L2). There is a spike in the soil water content in L1 on January 20 and 21 directly following a period of increased precipitation beginning on about January 16 (Figure 27). The soil samples on January 20 and 21 were collected on the day when slush, snow, and ponded water were observed on the soil surface. I assumed these samples were saturated due to the aforementioned field observations. The soil moisture content is slightly below the calibrated porosity though, which suggests that the porosity is slightly too high. Soil water measurements made on a few consecutive days in L1 show some discrepancies. The most dramatic of these are the soil water measurements for L1 on June 3 and 4, which vary considerably (1.4 and 3.1 inches, respectively) despite the fact that there was no recorded precipitation on either of those days. The differences in these data are possibly due to measurement errors, heterogeneities in the hydraulic properties of the soil, or the upward migration of soil water due to capillary suction.

Soil pore water sampling from shallow (24 in) and deep (36 in) lysimeters began prior to fertilization and crop planting; therefore, the initial soil pore water nitrate and ammonium concentrations are assumed to be due to background concentrations for that time of year (see Table 14 for the initial amounts by soil layer and Figures 28 & 29). Soil pore water nitrate concentrations do not show an appreciable rise until September 23, just five days prior to crop harvesting (Figure 28). The first peak nitrate concentrations appear after a period of heavier, more frequent rainfall events from August 21 to September 18. The delay is due to the time required for infiltrated water to percolate down to the respective layers, leaching nitrate and ammonium, discussed below, as it flows. These peaks also occur after net water begins to rise.

There is a delay between the peak nitrate concentrations measure in L2 and L3. This is evidence of nitrate leaching with percolating water, which takes longer to reach the lower soil layer.

Nitrate concentrations above the EPA MCL of 10 mg NO₃-N/L were observed in L2 from September 23 to November 17 and in L3 from October 20 to November 17. The depth to the groundwater table during that time is unknown, but is somewhere below the depth of the piezometers (~73 inches deep). Since most nitrate reduction is known to occur in the upper soil horizon where microbial activity is predominant, the nitrate concentration observed at 36 inches deep most likely persisted as the water percolated down to the water table. Dilution would occur as the percolating water mixed with groundwater, but it is likely that soil pore water with nitrate >10 mg NO₃-N/L is mixing with groundwater.

The late-season peaks in soil pore water nitrate concentrations are attributed to the downward migration of surface-applied fertilizer and mineralized nitrogen from soil organic matter. Soil water increases in all layers on about August 23 and soil nitrate declines rapidly from August 21 to September 22 in response to a period of heavier, more frequent rainfall events from August 21 to September 18, and the corresponding rise in net water (Figures 24 & 27). These data provide evidence for soil storage of nutrients during drier times of the year with rapid leaching in response to the onset of increased precipitation. These data show a return to pre-fertilization background conditions about 153-208 days after the application of fertilizer and only about 61-116 days after the onset of increased precipitation.

There is an immediate rise in ammonium concentration in the deeper lysimeter directly following fertilization, but the first spike in ammonium concentration at both depths on September 23 occurs after a period of heavier, more frequent rainfall events from August 21 to September 18 (Figure 29). This spike also occurs after net water begins to rise. There was most likely a higher peak ammonium concentration for L3 some time after the peak observed in L2

that would have been observed with more frequent sample collection. This is supported by the observed arrival of the peak nitrate concentration in L3, which was delayed after the peak in L2. This evidence further supports the relationship between downward water movement and leaching. Ammonium concentrations return to pre-fertilization background levels on October 20 and nitrate on January 21 and remain at those low levels for the duration of the study.

The initial spike in soil water ammonium directly following fertilization is likely due to frequent tampering by animals, which resulted in incredibly high ammonium values from one lysimeter as well as the presence of a potent musky smell and black bear fur. The lysimeter caps were removed and/or damaged by this tampering leaving the lysimeter open to the air and therefore open to contamination. Data from samples that were clearly contaminated were not used in this study, although data from samples that may have experienced some contamination without the obvious indicators may have been retained and may account for this ammonium spike. Preferential flow of fertilizer along the lysimeter casing is not suspected as a cause for this spike in ammonium since there was no corresponding spike in nitrate.

On December 14 and January 21, the water table level was above the depths of the lysimeter porous cups during sampling (Figure 26); therefore, the water collected was a mixture of groundwater and soil pore water. Mixing of the lower nutrient concentration groundwater with the soil pore water should decrease the nutrient concentration in the lysimeter samples. Soil pore water ammonium had already returned to background conditions before this mixing occurred and hence there is no drop in ammonium concentrations on those days or thereafter. However, soil pore water nitrate concentrations had not returned to background conditions before December 14. With the available data, it is impossible to conclude whether the rising water table diluted soil pore water nitrate or it had already returned to background levels when this mixing occurred.

5.1.4 GROUNDWATER

Water was available from all four piezometers only on six sampling days and from one or two piezometers on three more additional days during the study. Depth to water measurements were performed on all days when water was available and samples were collected from all piezometers on three sampling days and from just one piezometer on two days. The rest of the time, the piezometers were dry. There are too little data from these few sampling days to analyze annual trends in groundwater concentrations of nitrate and ammonium. The average concentration of nitrate in groundwater averaged for the study site was noticeably less than the concentrations in the deep lysimeter (Figure 28). This suggests that high concentration of nitrate in leachate will be diluted when mixed with groundwater. Groundwater ammonium was about the same as the ammonium concentrations measured in L2 and L3, except on January 21 (Figure 29). The low ammonium concentrations coincide with background conditions. On January 21, the water table was just inches below the soil surface in some areas and above the surface, as evidenced by the observed ponding, in other areas. The increase in groundwater ammonium on that day is attributed to mixing with a higher ammonium source near the soil surface.

There was a slight shift in groundwater flow direction from the previous study (1998-2001) and gradient magnitudes were slightly higher, but overall there is good agreement between historical measurements and DTW measurements made during this study. Depth to water measurements recorded during this study coincide with the groundwater flow estimate produced with the historical depth to water data. Water level data suggest groundwater was flowing at an average of 167° east of north (Table 1; Figures 3 & 5). The calculated gradient magnitudes, directions, and regression coefficients for the fitting of the plane are shown in Table 1.

The average groundwater flow direction was used to determine whether piezometers were located approximately up- or down-gradient. Piezometers S-1 and S-4 were up-gradient and S-2

and S-3 were down-gradient (Figure 5). I expected to see higher nitrate concentrations in groundwater from down-gradient piezometers due to mixing with higher nitrate concentration soil pore water. Nitrate and ammonium concentrations were higher in the up-gradient piezometers on all days when water was available in both up- and down-gradient piezometers: November 17, December 14, and January 21. The differences in nitrate and ammonium ($\mu\text{g-N/L}$), respectively, between the up-gradient and the down-gradient piezometers on those days were -1886 and -3.3 on November 17, -629 and -39 on December 14, and -1706 and -165 on January 21. Agricultural activity on the adjacent, up-gradient field site may have increased groundwater nutrient concentrations in the up-gradient piezometers. More and deeper piezometers are needed to quantify the addition of nitrate and ammonium in leachate from the study site to groundwater.

The water table rose above the maximum soil sampling depth and above the depths of the lysimeter porous cups on a number of sampling days (Figure 26). Although these data are uncorrected for variations in surface elevation, they are fairly close since there is little change in elevation across the field. On sampling days when no water was available in the piezometers, the water table depth was greater than 6 feet, the depth of the deepest piezometer. Depth to water measurements were recorded on two consecutive days per month whenever water was present in the piezometers. Out of all the days when water was observed in the piezometers, only 4 days showed depths to water above the deepest sampling depth: December 13 and 14, January 20 and 21 (Figure 26). Dilution of the sampling column by a rising water table occurred between November 17 and February 23. Water was below the greatest sampling depth on both of these days and above on the four sampling days in between (Figure 26). It is unlikely that water table elevations rose above the deepest sampling depth outside of this date range on days when sampling was not conducted, since the precipitation data show that the heaviest precipitation

events occurred during that date range (Figure 26). Therefore, the time period during which the sampling column may have been saturated by the rising water table, thereby diluting solute concentrations, is from November 17 to February 23.

5.1.5 NITROUS OXIDE

Nitrous oxide emissions spiked twice during the study period. The first spike occurs on May 28-June 4 following the fertilizer application on May 19 (Figure 30). There is a small rise on September 23 and 24 after a period of heavier, more frequent rainfall events from August 21 to September 18 (Figure 30). The second spike occurs on January 24 may be a response to a sequence of heavy rainfall days, which occurred from January 12 to 22, or due to a freeze-thaw event. This spike coincides with a spike in soil moisture in L1 measured on January 20 (Figure 31). There was also a dramatic rise in the maximum daily air temperature from below-freezing (25°F) to above-freezing (56°F) temperatures from January 14 to 21 (Figure 31).

Nitrous oxide is the by-product of the microbially-mediated denitrification and nitrification reactions; therefore, nitrous oxide emissions are dependent upon nitrate or ammonium availability in the soil. The initial peak in nitrous oxide emissions coincides with the initial peaks in nitrate and ammonium in L1 (Figure 32). The later peaks in nitrous oxide emissions do not coincide with rises in nitrate or ammonium. There was some nitrate and ammonium, although relatively low levels, available in the soil when the later peaks in nitrous oxide occurred, but they are attributed to precipitation and temperature as discussed above. These field data agree with the typical behavior of emissions due to denitrification, which are usually small during much of the year with spikes following rainfall events or irrigation (Hermanson et al., 2000).

5.2 *Statistical Results*

Statistics and related plots were generated using the statistical software R. The R code and input data sets are provided on the data CD. Summary statistics, scatterplots, and boxplots, revealed small, non-normal, heteroskedastic sample distributions for the field soil parameters (Table 5, Figures 10-19). Note that in all the statistical results tables and figures, soil sampling depth is represented by 1 to 5 (1=0-6", 2=6-12", 3=12-24", 4=24-36", and 5=36-45"), which are the original sampling depths as opposed to the soil layer averages. Splashplate method is represented by either 2 or 3, which correspond to the Splashplate (2x) and Splashplate (3x) methods, respectively. Soil ammonium and nitrate are presented in the original, unconverted sample concentrations ($\mu\text{g/L}$) and soil moisture is presented in the unconverted gravimetric form (g/g).

I proceeded with non-parametric inference testing given the small sample sizes and the non-normality of the data. Notched boxplots showed significant group mean overlap in most cases (Figures 10-13). Overlapping notches suggest no significant differences in population distributions. Where overlap was unclear or non-existent, I employed a Kruskal Wallis Rank Sums Test. P-values less than 0.05 were obtained for the following pairings: soil ammonium by depth, soil moisture by plot, and soil coarse fragments and moisture by replicate. The null hypothesis of no difference between groups was rejected for these data populations (Table 15). The alternative hypothesis that at least two populations differed in location was accepted. I proceeded with pairwise testing using the Pairwise Wilcoxon Rank Sums Test. P-values of less than 0.05 indicated differences in population distributions for the following initial field measurements: soil ammonium differed for all soil depths except 1 and 2, soil coarse fragments differed between replicates 1 and 2, and soil moisture differed between replicate 1 and all other replicates, (Table 16). For a number of data group pairs, there were too few observations to

perform the test. In this instance, the comparison between groups is indicated by “no significance.”

The previous treatment method did not account for any significant differences in the initial field data. The only significant difference between locations was for coarse fragments between replicates 1 and 2 and soil moisture between replicate 1 and all other replicates. The difference in replicate 1 was determined not to be widespread enough, i.e., it did not affect all soil parameters, to segregate replicate 1 data from the study site averages. The differences in soil ammonium for all depths except 1 and 2 did not affect the soil layer determination. The lack of difference between soil ammonium for depths 1 and 2 supports the decision to lump these layers into the user-defined L1 for modeling purposes. Depths 4 and 5 were lumped into L3 despite the significant difference in soil ammonium between these depths. Model input values were calculated by averaging the initial soil data as follows. Data from soil depths 1 and 2 were averaged into L1, depth 3 became L2, and depths 4 and 5 were averaged into L3. See the Soil Layer Determination section for a complete discussion of the soil layer determination methods. Previous treatment method was ignored in the averaging. Once the data were averaged by depth, the two plots within each replicate were averaged, and finally data from the four replicates were averaged to obtain values for the entire study area.

5.3 Sensitivity Results

The average % changes in nitrate or water leached with $\pm 60\%$ of each input are listed in Tables 8 & 9. The model inputs are ranked from highest to lowest average % change on the model output of nitrate or water leached. Nitrate and water leached predictions are most sensitive to the highest ranked parameters.

Nitrate leached is most sensitive to the Plant AWHC of L3 (AWHC 3), bulk density in L1, the particle densities of all soil layers, and organic matter in L1 (Soil OrgM % C L1 and Soil

OrgM % L1; Table 9). The Plant AWHC of L3 is used to determine the WHC (the product of the AWHC 3 and soil thickness), which restricts water flow out of L3 (DP3) according to equation 6. Particle density is an internal model parameter that is used in the calculation of porosity by soil layer, along with bulk density, according to the following equation for porosity in L1:

$$\text{POR1} = (1 - \text{Bulk Density} / \text{Particle Density}) * \text{Soil thickness} \quad (25)$$

where POR1 is the porosity of L1 in inches, bulk density is given in g/cm^3 , the particle density is given in g/cm^3 , and soil thickness in inches, which was kept constant. The standard range of particle densities used for calculating porosity is 2.60-2.65 g/cm^3 . Many soils contain an abundance of quartz, which has a particle density of 2.65 g/cm^3 . Porosity is converted from its usual format, a unitless fraction, to inches by multiplying the fraction by the soil layer thickness in inches (as shown in equation 25 above). All water variables are modeled in inches by NLOS. NLOS uses porosity and water flow (DP1 in the equation below, but this equation is also applicable to L3) to calculate soil nitrate and fertilizer nitrate leached from one soil layer to the next. The following equation calculates soil nitrate leached from L1 to L2:

$$\text{NO3_Leach_L1} = \text{NO3_L1} * (1 - \text{EXP}(((1 * k1) * (\text{DP1})) / \text{POR1})) \quad (26)$$

where POR1 is the porosity of L1 in inches, DP1 is the movement of water from L1 to L2 in inches, NO3_L1 is the amount of $\text{NO}_3\text{-N}$ in L1, k1 is a coefficient for nitrate leaching calculated as

$$k1 = 7.6 - (64 * \text{PWP_1}) \quad (27)$$

where PWP_1 is the permanent wilting point of L1. The permanent wilting point is the soil water content at which water is no longer available for plant uptake, which is identified as the soil water content at 15 bars of soil suction. Nitrate leached was also very sensitive to PWP 1 and PWP 2 (Table 9). Fertilizer nitrate leached from L1 to L2:

$$\text{Fert_NO3_Leach_L1} = \text{FERT_NO3_L1} * (1 - \text{EXP}(((1 * k1) * (\text{DP1})) / \text{POR1})) \quad (28)$$

where POR1 is the porosity of soil L1 in inches, DP1 is the movement of water from L1 to L2 in inches, FERT_NO3_L1 is the amount of fertilizer NO₃-N in L1, k1 is a coefficient for nitrate leaching. Nitrate losses due to leaching accounted for the highest percentage of nitrate removed in the final calibrated model simulation (Table 14).

Nitrate leached is also very sensitive to the percentage of soil organic matter carbon in L1. This value is used to calculate the % nitrogen in soil organic matter (Soil_OrgM_%_M_L1) according to the following equation:

$$\text{Soil_OrgM_}\%_N_L1 = \text{Soil_OrgM_}\%_C_L1 / \text{Soil_OrgM_CN_L1} \quad (29)$$

where Soil_OrgM_%_C_L1 is the % carbon in soil organic matter in L1 and Soil_OrgM_CN_L1 is the carbon to nitrogen ratio of soil organic matter in L1. Nitrate leached predictions are sensitive to the % nitrogen in soil organic matter because the soil organic matter pool of nitrogen constitutes by far the greatest percentage of the initial and current (i.e., final) nitrogen at 99% and 90% of the respective budgets (Table 14).

Nitrate leached was sixth most sensitive to the initial soil organic matter percent in L1 (Soil OrgM % L1; Table 9). The initial soil organic matter in L1 is used to determine the first order denitrification rate constant. Denitrification accounts for only 3.5% of the total nitrogen removed from the system (Table 14). This is a small percentage of the total nitrogen removed relative to large sinks such as crop uptake and leaching. The parameters affecting crop uptake were not tested in the sensitivity analysis; therefore denitrification is the largest sink after leaching. Any significant reductions in the nitrate available for leaching will affect the final nitrate leached values.

A sensitivity analysis of the original NLEAP conducted by Follett et al. (1994) found the model to be particularly sensitive to soil water content at the permanent wilting point, referred to as permanent wilting point (PWP) in NLEAP, and the nitrogen uptake index (NUI). NUI is the

total crop N uptake per unit of crop yield and is analogous to value of Crop A Target N Yield in NLOS, which is calculated from user-entered values of Crop yield and Crop N%. These parameters were not tested in the sensitivity analysis. The entire list of input parameters that were tested for sensitivity by Follett et al. (1994) was not specified; therefore, it is not possible to directly compare results.

As expected, water leached is by far most sensitive to user-entered rainfall, which constituted the greatest percentage (81%) of the initial pool of water (Tables 8 & 17). This is the only source of water to the system aside from the relatively small initial amounts present in the soil layers. Water leached was also sensitive to the runoff adjust factor, evapotranspiration, and initial water, Plant AWHC, and PWP for all soil layers (Table 8). The runoff adjust factor is a user-entered fraction (0 to 1) that can be varied to adjust the amount of runoff specific to the modeler's field conditions. For the sensitivity analysis, the runoff adjust factor was varied between the maximum and minimum of this range, as opposed to $\pm 60\%$. The base value of the runoff adjust factor was set to zero to reflect the nearly level field and highly permeable soils, but the final calibrated value was 0.20 (Tables 12 & 13). Runoff accounted for 4.6% of the total water removed from the system (Table 17). Evapotranspiration is entered as daily values by the user and constituted 27% of the water removed from the system (Table 17). The Plant AWHC and PWP, after being converted to WHC and Bound Water, are used to calculate the amount of water flowing from one layer to the next according to equations 3, 5, and 6.

5.4 *Uncertainty Results*

Using the Monte Carlo simulator that I built into the model and the automation technique for recording predicted nitrate leached from each model run, 2,000 model runs were conducted for uncertainty analysis. For each model run, only the total nitrate leached value was recorded. Using these 2,000 values, I used the histogram tool in the Data Analysis package of Excel to

create a histogram and related summary statistics for the simulated values (Figure 33 and Table 18). The histogram uses a bin size of 5 units from 40 to 195 lbs NO₃-N/acre in order to capture the entire range of simulated values. Finally, the probability of occurrence for each bin value was calculated (probability = frequency/total number of observations) and the cumulative probability for each bin size plotted (Figure 34).

Each model run was performed using a new set of randomly generated inputs. The input data sets were not recorded. Analysis of the nitrate-leached values from the uncertainty runs shows that uncertainty is large, varying between 43 and 195 lbs/acre of NO₃-N leached (Figure 33 and Table 18). The distribution appears normal, there do not appear to be any outliers, and data appear to be unimodal. The histogram is very slightly skewed (non-normal) right (skew is 0.045) and is slightly sharper than a normal distribution (kurtosis is 0.019; Table 18). The skew of the data to the right suggests a tendency towards a lower bound on the data. A good typical value for a skewed distribution is described by the median (130 lbs NO₃-N/acre) or the mean (131 lbs NO₃-N/acre). The standard error of the simulated distribution is 0.49. The lower and upper 95% bounds on the data are 90 and 175 lbs NO₃-N/acre, respectively. This suggests that given the uncertainty in each tested input parameter, nitrate leached values will fall between 90 and 175 lbs NO₃-N/acre 95% of the time. The random values used to produce this result were all drawn from uniform distributions since this was the only option available in STELLA. The actual data distributions were not determined. The input parameters may not be uniformly distributed or may have a central tendency, which, if accounted for in the random number generator, could produce a much smaller uncertainty in nitrate leached predictions. The final uncertainty analysis result is that nitrate leached predictions will fall between 90 and 175 lbs NO₃-N/acre 95% of the time under the following conditions: a silt loam, slightly drier and warmer climatic conditions than the 30-year average at the Agassiz CS weather station, a no-till, non-irrigated silage corn crop

fertilized with commercial fertilizers, and the chosen uncertainty ranges associated with the input parameters that affect only the soil water sub-model varied along a uniform distribution.

5.5 Calibration Results

Sensitivity rank was used to determine which inputs to adjust in the model calibration and the order in which they were calibrated. Despite the sensitivity of water and nitrate leached to climate inputs, they were not calibrated. Tables 12 and 13 list the parameters used in the model calibration listed in order of decreasing sensitivity based on the sensitivity results. At the start of calibration, the model settings and base inputs were set to those listed in Table 2 with one exception: K_N2O_Leakage. As discussed in the Sensitivity Analysis section, K_N2O_Leakage was added to the sensitivity analysis due to the very poor match between simulated and observed nitrous oxide emission values. K_N2O_Leakage was set to the value (0.01) determined from previous model calibration efforts at the start of the calibration, but it was recalibrated for the new calibration. Since water and nitrate leached were insensitive to K_N2O_Leakage, it was calibrated last.

All parameters were varied within their pre-determined allowable ranges during the calibration (Tables 12 & 13). Each parameter was calibrated to obtain the best efficiency for the model overall. For each iteration, I calibrated the soil water sub-model parameters first (Table 12), i.e., the parameters to which water leached was most sensitive (Table 13), and the nitrogen dynamics sub-model parameters second, i.e., the parameters to which nitrate leached was most sensitive. Some of the parameters used in the soil water sub-model calibration were also used in the nitrogen dynamics sub-model calibration. If there was a change from the previous calibration for a repeated parameter, it was set to the new calibrated value. The calibrated values listed in Tables 12 and 13 are the final calibrated values achieved after the two iterations. The calibration was ceased after the second iteration because there was very little change in any of the values.

Particle densities and bulk densities were varied within their pre-determined ranges to obtain porosities (as determined by equation 25) as close as possible to the range of 0.435 for a sandy loam to 0.485 for a silt loam (Brady, 1974) while also maximizing model efficiency. The calibrated porosities are shown in Table 19. The porosities for L1 and L2 are outside the allowable range, but limiting bulk density and particle density to values that returned porosities within the range sacrificed model efficiency too greatly. The calibrated porosity for L2 (0.489) is very close to the average porosity for a silt loam (0.485). The calibrated porosity for L1 (0.574) is quite a bit higher than the porosity for a silt loam, but cracks in the soil surface, burrows, roots, and soil disruption from agricultural activities could all increase soil porosity in the shallow soil; therefore, this calibrated porosity was determined to be acceptable. Field observations on January 20 suggested that L1 was saturated on that day. The soil moisture content on January 20 (0.56) is nearly equal to the calibrated porosity. The soil moisture content of a fully saturated soil would equal the porosity. These data suggest that the calibrated porosity of 0.574 for L2 closely represent the actual field conditions.

Comparisons of both calibrated and uncalibrated model outputs to field data are shown in Figures 35-44. The final calibrated model is considered calibrated only for the climate, soil, crop, agricultural management, and fertilizer conditions tested at this study site. The average efficiency of the overall model increased from -2.19 to -0.17, the average soil water sub-model efficiency increased from -1.82 to -0.63, and the average nitrogen dynamics sub-model efficiency increased from -2.34 to 0.02 (Table 11). A model efficiency coefficient less than one suggests that there are deficiencies in the model or that there are errors in the observed data due to sampling and/or measurement. The best model efficiency possible is 1, which indicates perfect agreement between the simulated and measured values.

An overall model efficiency of -0.17 appears to be low. Garnier, et al. (2001) used the same model efficiency calculation to evaluate the nitrogen transport model CANTIS (Carbon and Nitrogen Transformations in Soil) for a year-long field trial. Efficiency coefficients were specified for each modeled parameter at multiple simulation depths. The average coefficients for all depths were compared to the results from the current study. The researches found the following efficiency coefficients for the CANTIS model: 0.50 for predictions of soil water content, -0.61 for nitrate in soil, and 0.74 for nitrate in leachate collected in suction cup lysimeters. For comparison, the following average efficiency coefficients were obtained with the calibrated NLOS model: -0.63 for soil water content, -0.02 for nitrate in soil, and -0.38 for nitrate in leachate. The best efficiency was obtained for predictions of nitrate in soil with NLOS, with considerably less efficiency for soil water and nitrate leached predictions.

The model efficiency values for individual parameters indicate that the model is best at predicting soil nitrate in L1 ($E_f = 0.71$) and worst at predicting soil water in L1 ($E_f = -0.63$; Table 11). The greatest increase in efficiency was obtained for total nitrous oxide emissions (-16.08 to 0.31). This great change was in large part due to the adjustment of the rate constant for leakage of nitrous oxide from the nitrification process ($K_{N_2O_Leakage}$).

The efficiency of the calibrated model was calculated for both wet and dry periods (Table 20). The wet period was designated as October – April and the dry period as April - October (Figure 20). The efficiency of the overall model was -5.13 for the wet months and -0.53 for the dry months. For the wet months, the largest gains in efficiency were made in predictions of soil nitrate in L2 and L3 whereas the greatest losses were made in the prediction efficiency for soil nitrate and ammonium in L1 (Tables 11 & 20). For the dry months, the only gains in efficiency were for predictions of soil water L2 and total nitrous oxide emissions whereas the greatest loss was made in the prediction efficiency for nitrate leached from L3 (Tables 11 & 20). Better model

efficiency was expected for the wet months since the model uses steady-state flow assumptions and steady-state conditions are approximated by uniform soil wetting, which would occur during the wet months. Contrary to the expected result, better efficiency was obtained for the dry months. Leaching was greatest during the wet months. Accumulative error from the higher concentrations of leached nitrate and ammonium may account for the poor efficiency during the wet months.

The model efficiency was also averaged by individual soil layer using the observed and simulated values from the calibrated model that were associated with that soil layer. L1: soil nitrate, soil ammonium, and soil water; L2 and L3: nitrate leached, soil nitrate, and soil water. The model was most efficient at predicting nitrate, ammonium, and water in L1 ($E_f = 0.17$) and less efficient at predicting nitrate leached, nitrate, and water in L2 ($E_f = -0.37$) and L3 ($E_f = -0.48$). Since the downward migration of nitrate is dependent upon water flux (see equation 26), the decreasing efficiency in soil nitrate predictions with depth could be attributed to problems with the soil water sub-model or with the nitrogen withdrawals from each soil layer, which would then compound with depth.

The algorithms used to calculate leaching do not change with depth, i.e., the equation for nitrate leaching from L1 to L2 is the same equation used for nitrate leaching from L2 to L3. Water movement (DP1) and soil nitrate (NO3_L1) are the only factors that vary with time in the leaching equation. For L2, these variables would be DP2 and NO3_L2, etc. Leaching and crop uptake are the only processes that deplete nitrate from L2 (NO3_L2) and leaching is the only process that depletes nitrate from L3 (NO3_L3). Crop uptake from L2 accounts for only 8.1% of the total budget of removed nitrogen from L2 whereas leaching accounts for the rest of the fluctuation in L2 soil nitrate. Leaching from L3 is completely dependent on variations in water movement (DP3). The algorithms for water movement, on the other hand, vary with depth, i.e.,

the algorithm for calculating DP1 is different than for DP2 and DP3 (see equations 3 to 6). Errors in predictions of the amount of water flowing from L1 to L2 would increase or decrease the amount of water available for flow from L2 to L3. Since DP1 – DP3 are dependent on the water in each layer (Water_L1, etc.), inaccurate prediction of water flow from L1 to L2 would lead to an inaccurate prediction of flow from L2 to L3 and so on. Therefore, the decreasing efficiency in soil nitrate predictions with depth could be attributed to the propagation of errors in soil water flow predictions.

Overall, the model efficiency results were satisfactory for the intended purpose, which was to guide model calibration. Garnier et al. (2001) found their simulations of nitrate transport and transformation with the CANTIS model to be satisfactory and suggested that the model efficiency calculated from nitrate content data was not a good criterion for proper evaluation of the model. Also, the model calibration is only as good as the data used to calibrate the model. Whitmore (1995) attributed model inefficiencies to problems in obtaining accurate field-measured values of nitrogen. There is a large degree of variance in the initial soil data collected for the current study. This is exhibited by the long whiskers, a number of outliers, and the length of the boxes in the notched boxplots produced for the statistical analysis of the initial soil data (Figures 10-13). Boxplots were not produced for all the field data after those initial samples, but similar variances for the rest of the study period are expected due to the inherent heterogeneity of soil. Considering the variance of the field data and the scarcity of data points that were available for use in the model efficiency calculations, the model efficiency is not an accurate measure of the fitness of the model. The efficiency coefficient was not used to evaluate the fitness of the model; visual assessments and linear regression were used. The model efficiency, though, was useful for calibration and for identifying potential problem areas of the model.

5.6 *Model Simulations*

The calibrated model was used to track the flow of nitrogen and water through the vadose zone for the duration of the study period. The STELLA environment allows the user to create tables and graphs within the model to track specified model outputs; therefore, there are countless options of how to display and examine model results. This discussion provides the model results pertinent to the following goals: assess the ability of the model to reproduce the field data, specifically soil water fluxes following precipitation events; investigate the impact of transient vs. steady-state field conditions and model assumptions on simulations of water flow and nitrate transport; examine temporal patterns of nitrate leaching to the water table in response to soil water movement and fertilizer application; and determine the optimal time to perform the Post-Harvest Soil Nitrate Test (PHSNT). Model simulations were then conducted using model inputs for various hypothetical field, fertilizer, and climate conditions scenarios, within the calibrated range of the model, to examine the fate of nitrogen. Finally, I recommended uses for the calibrated NLOS model and proposed any changes to the model that might improve those predictions.

5.6.1 NITROGEN FLUX

Linear regression analysis was used to examine the ability of the model to predict the observed data. The trend lines on Figures 45-51 represent the actual fit between the observed and the simulated values, determined by linear regression. Perfect agreement between the simulated and observed values would fall directly on a 1:1 line. The corresponding equations and regression coefficients (R^2) are shown on the figures. The actual fit to the field data may be better than the R^2 values indicate due to timing shifts in the simulated and observed data. For example, the peak value of observed nitrate leached from L2 (9.15 lbs $\text{NO}_3\text{-N/acre}$) matches the simulated peak value (8.52 lbs $\text{NO}_3\text{-N/acre}$) very well, but the simulated value occurs on October 10 whereas the

observed value was measured on October 20. The simulated and observed values that occurred on the same day were compared for the linear regression analysis; therefore, the peak observed value of nitrate leached from L2 on October 20 was compared instead to the simulated value for that same day (1.95 lbs NO₃-N/acre), which indicates a much worse fit. The regression analysis results alone are not an appropriate sole indicator of model fitness. They can aid in the model evaluation though, in conjunction with visual inspection of the plots of simulated and observed values.

Calibrated simulations of nitrogen along various pathways were compared to the observed values. Observations of soil pore water nitrate, as measured in both shallow and deep lysimeters, and soil nitrate and ammonium in L1 correlate well with the simulated values (Figures 45-47 & 50; Table 21). The regression coefficients for the equations determined for soil pore water nitrate in the shallow and deep lysimeters and soil nitrate and ammonium in L1 are 0.63, 0.84, 0.84, and 0.87, respectively. The simulated peaks and magnitudes correlate well with the observed data for these variables. The model is less efficient at predicting soil nitrate in layers 2 and 3 and nitrous oxide emissions (Figures 48, 49, & 51); the regression coefficients for the equations determined from these parameters were too low ($R^2 = 0.011, 0.0092, \text{ and } 0.33$, respectively). A poor fit between simulations and the field data could be the result of either insufficiencies in the model or difficulties or problems in obtaining accurate field measurements for those variables. Also, it is likely that the conversion of nitrate and ammonium concentrations in lysimeter water and soil extract ($\mu\text{g-N/L}$) to lbs-N/acre had at least a 3% error due to the use air-dried soil weights, instead oven-dried weights, in the conversion. This was discussed in the Unit Conversion Equations section.

A three-year study evaluated NLEAP for predictions of residual soil nitrate with irrigated and non-irrigated corn on a sandy soil near Oakes, ND (Follett et al., 1994). The researchers found

that NLEAP accounted for 85% of the variability in the mass of residual soil nitrate (RSN) for the calibrated site, but only 46% for the validation site by regression analysis. They concluded that NLEAP was valuable as a decision-making tool for the tested climate, treatments, and soil types, but that further testing would be required for other soils, N-sources, and climatic conditions. Lysimeter leachate data from a five-year study of a corn field in Coshocton, OH, were used as a validation data set to test NLEAP. NLEAP was found to account for 86% of the variability in the mass of nitrate leached as measured monthly with lysimeters (Shaffer et al., 1991). The results for the soil pore water nitrate and nitrate and ammonium in L1 produced for the current study are as good or better than these published results, although predictions of soil nitrate in L2 and L3 are much worse. I did not find any published studies comparing observed to predicted values of nitrous oxide emissions with the original NLEAP.

Predictions of soil nitrate and ammonium in L1 were the most efficient predictions of soil nutrients according to correlation analyses (Table 21). For L1, the magnitudes and timing of variations in nitrate and ammonium are fairly well matched to model simulations upon visual inspection (Figures 37 & 40), although there are unexplained dips in peak nitrate on July 7 and 8 and August 9 that are not present in the simulated values. The model does not simulate nitrate in L2 and L3 as efficiently. The model completely misses the first peaks in nitrate for both soil layers (Figures 38 & 39). This suggests that the simulated response to precipitation events, in the form of eventual leaching of nitrate from the surface to the deeper soil layers, is slower than the actual response.

Nitrate and ammonium in the soil respond immediately to fertilization with large spikes occurring within 1-2 days of application (Figures 52 & 53). The model does not track crop growth specifically, but crop nitrogen uptake is based on crop growth. As nitrogen becomes available for growth, the growing crop progressively increases its nitrogen uptake. The nitrogen

uptake then diminishes as the crop matures, and there is no uptake after harvest. As the crop demand for nitrate in L1 diminishes, more nitrate accumulates in soil and becomes available for leaching (Figure 52). The first large rise in leaching from L1 to L2 occurred on August 25 (Figure 54) and the first large increase in soil nitrate in L2 started on about August 29 (Figure 52). Thereafter, nitrate in L1 was depleted and nitrate levels in L2 and L3 increased predominantly due to leaching. Only about 20% of the total crop root density extends into L2. Correspondingly, crop nitrogen uptake from L2 was only 27 lbs-N/acre compared to 136 lbs-N/acre in L1 (Table 14). The user-defined model settings did not allow the roots to extend into L3.

Ammonium in L1 spiked to its maximum value five days after fertilizer application (May 23; Figure 53). The crop ammonium uptake rate showed a first response as a small peak 3 days later (May 26), a slight decrease, and then it peaks at its maximum value on June 4. Soil ammonium showed a sharp decline from its initial peak as it is removed by volatilization, crop uptake, nitrification, and mineralization. Simulation results from NLOS predict the loss of 6.0 lbs $\text{NH}_4\text{-N}$ to volatilization from a starting pool of 11 lbs $\text{NH}_4\text{-N}$ and the release of 1.5 lbs-N/acre as nitrous oxide, the by-product of nitrification, to the atmosphere (Table 14). Ammonium volatilization typically accounts for 0 to 25% of the applied N for a soil of $\text{pH} < 7$ (Hermanson et al., 2000) and about 5% of ammonium nitrate (S. Bittman, personal communication). Simulated ammonium volatilization accounted for 1.5% of the applied ammonium-N, which falls within the expected range.

Nitrate leached does not show a direct correlation with crop growth, crop harvesting, or fertilization (Figure 54). The first spike in nitrate leaching occurred on May 31 and then again on August 25. Both peaks occurred following stretches of increased precipitation from May 21 to

June 14 and August 21 to September 18 (Figure 55). Both peaks also correspond to a slight increase in net water from May 25 to June 1 and a more dramatic increase from August 20 to 29.

The correlation analysis results show that the model was inefficient at predicting nitrous oxide emissions (Table 21). This is also evident in the comparison of simulated nitrous oxide emissions to field data (Figure 51). Nitrous oxide is produced by the nitrification of ammonium by aerobic microbes and the denitrification of nitrate by anaerobic microbes. Microbial activity is a function of soil water content, air temperature, and soil nitrate and ammonium. The factors that control nitrous oxide emissions are poorly understood (Robertson, 1993); therefore, a deterministic model of nitrous oxide production based on a poor understanding of the processes involved would be expected to produce unsatisfactory predictions. Also, it is difficult to measure nitrous oxide emissions from soil.

Nitrous oxide emissions increase rapidly following fertilization, level off once crop growth begins, and increases dramatically again after a period of more frequent, heavier rainfall (Figure 56). The last peak in nitrous oxide emissions occurs before nitrate in L1 decreases to background conditions (Figure 57). The observed data and the model simulations for nitrous oxide both exhibit the same character of sharp peaks with an immediate return to little or no nitrous oxide being emitted. This character is attributed to the reliance on air temperature and soil water data, which both exhibit jagged peaks (Figure 58).

NLOS under-predicted soil water in all layers (Figures 42-44). Denitrification occurs under anaerobic conditions. If simulated soil moisture was consistently low, anaerobic conditions may have been simulated more frequently than they actually occurred leading to an erroneous increase in nitrous oxide emissions from denitrification. This may account for some of the simulated peaks in nitrous oxide emissions that were not observed in the field (Figure 41). More

nitrous oxide was produced from denitrification (5.2 lbs-N/acre) than nitrification (1.5 lbs-N/acre; Table 14 and Figure 59).

Simulated nitrous oxide completely misses the peak in observed values on January 25 (Figure 41). This peak was attributed to either a freeze-thaw event or to a stretch of increased precipitation events (see the Nitrous Oxide section within Field Observations). Currently, NLOS is not able to simulate a nitrous oxide response to freeze-thaw. Although NLOS is inefficient at predicting nitrous oxide emissions, this does not have a large effect on leaching predictions since it constitutes such a small percentage of the overall nitrogen budget (0.18% and 1.8% of removed N in LS and L1, respectively, from both denitrification and nitrification; Table 14). Further research into the factors controlling nitrous oxide emissions is currently being conducted at the Pacific Agri-Foods Research Centre and may some day become useful for improving NLOS.

5.6.2 WATER FLUX

Examination of the linear regression plots of observed and simulated soil water values shows that NLOS is systematically under-predicting soil water (Figures 60-62). This may be due to the calibrated values of PWP and Plant AWHC (Table 12). These values were not varied outside the range for a loam to a clay loam as given by Brady (1974). If higher values for PWP and Plant AWHC were used, the simulated soil water would shift upwards accordingly.

Comparisons of monthly averages of soil water may produce a better fit than daily values, especially considering the erratic behavior of the daily measured values, but monthly averaging is not feasible since there are data for at most one or two days each month. The erratic nature of the soil water simulations is attributed to the daily time step and the tipping bucket approach to modeling soil water flux. The monthly soil water observations show a much smoother trend.

Simulation of soil water in L2 was fairly close to observed values ($R^2 = 0.58$; Figure 61). Regression coefficients from the linear regression correlation between simulated and observed values for L1 and L3 were lower (0.53 and 0.45, respectively; Table 21). This is due to the fact that the calibrated model efficiency was greater for L2 (Table 11). The simulated and observed soil water values in L1 are more erratic than in L2 and L3 and model processes become more complex and harder to calibrate deeper in the model, accounting for the poorer calibration to L1 and L3. The result is a higher efficiency for L2 and a better fit between the observed and simulated values for L2.

Previous studies using the original NLEAP model focused mainly on nutrient flux. Monthly leachate volumes collected in a five-year study in Coshocton, OH were used as a validation data set for NLEAP. NLEAP accounted for 91% of the variability in the observed data (Shaffer et al., 1991). An evaluation of the performance of NLEAP for predictions of soil water content in a silty clay and a clay loam soil under a wheat crop in Saskatchewan, Canada found that NLEAP estimated soil nitrate better than soil water and that it under-predicted soil water in the silty clay soil and over-predicted soil water values in the clay loam (Beckie et al., 1995). Beckie et al. (1995) used NLEAP for event-based simulations and Shaffer et al. (1991) made comparisons to monthly field measurements, whereas the simulation period for this study spanned the study year using a daily time step.

Soil water is removed from L1 by downward flow, evaporation, and transpiration; from L2 by downward flow and transpiration; and from L3 by downward flow only. The evaporation depth is defined by the user-entered value of consolidated evaporation depth for either a heavy or a light textured soil. A permanent wilting point for L1 greater than 0.22 is classified as a heavy textured soil and less than or equal to 0.22 as a light textured soil. The calibrated PWP for L1 is 0.13; therefore, the soil is light textured and the consolidated evaporation depth is 4.0 inches.

This is the default model value. Transpiration does not occur from L3 because the maximum rooting depth was defined as 2 feet. The maximum rooting depth determines the thickness of L2.

The water budget indicates that the highest percentage of water removed from the system is from leaching, followed by evapotranspiration and runoff (Table 17). Since water leaching accounts for the highest percentage of water removed, inaccuracies with the water flow algorithm will have a large effect on soil water predictions. Downward flow is limited by the water holding capacity (WHC) and the bound water (equations 3-6). Water holding capacity is the product of the user-entered plant available water holding capacity (AWHC) and the soil thickness, and bound water is the product of the user-entered permanent wilting point (PWP) and the soil thickness (Table 22). The soil water content must be greater than the sum of the WHC and bound water in order for any water to be removed from a soil layer by downward flow. Water may not be removed below the value of the bound water by evaporation or transpiration. Therefore, in the simulation results there is a straight line at these boundaries if no additional water is being added or removed (for the upper boundary only) by evaporation or transpiration. What this means for L1 is that all the simulated soil water loss below 3.12 inches was due to evaporation and transpiration, not downward flow; in L2, values below 3.48 inches of soil water are due to water being removed by transpiration only; and no evaporation or transpiration is occurring in L3, therefore there are no simulated values less than 6.09 inches (Figures 42-44). Soil water in L2 did not drop below the no-flow boundary after the crop was harvested on September 28 since transpiration is no longer occurring (Figure 43).

When transpiration was no longer occurring, after the corn harvest on September 28, the peaks in simulated soil water match daily peaks in rainfall (Figure 63). There is some deviation from this in L1 where evaporation was still occurring, but all the peaks match the peaks in daily rainfall. There is a delay after the rainfall event before the corresponding soil water peak appears

in L1, a further delay until it appears in L2, and an even longer delay until it appears in L3. In the simpler post-harvest case where there is no transpiration, the magnitude of the rainfall peak is diminished by evaporation before it arrives in L1. This entire slug of water is then moved the next day, to the next soil layer, and on until the water is leached from the system. Field soil moisture data were not collected frequently enough to characterize the soil water response to a precipitation event for comparison to these simulations.

5.6.3 STEADY-STATE VS. TRANSIENT FLOW

The soil water sub-model uses a simplified unidirectional, steady-state flow algorithm. With frequent rainfall, nearly uniform soil moisture may be achieved with depth within each soil layer. Under these conditions, a steady-state flow algorithm may provide the best approximation of flow. Soil moisture sampling was not conducted at multiple depths within each soil layer, so the data do not exist to determine if soil moisture content was uniform with depth within each layer. A comparison of the average soil moisture fraction for each soil layer by sampling day shows overlapping moisture fractions for each soil layer on a majority of sampling days (Figure 27). These data can be extrapolated to suggest that the soil moisture fraction within each layer was also uniform, but this is only speculative.

Steady-state conditions may also be approximated if the entire soil column is fully saturated. If and when saturated conditions were reached in the field soil was determined by computing the percent saturation of each soil layer for the maximum soil moisture measured during the study. Complete saturation is defined by soil water content equal to the porosity. Porosity was not directly measured in the field; it was calibrated through the calibration of the bulk and particle densities. I used equation 25, which is the equation used by NLOS, to calculate an approximate porosity for each soil layer. The calibrated bulk and particle densities were used in the calculation. To calculate percent saturation, I used the following equation:

$$\% \text{ Saturation} = (\text{Soil Water} / \text{Porosity}) * 100 \quad (30)$$

where soil water and porosity are in inches. Only L1 ever achieved 100% saturation, but L2 and L3 were very nearly fully saturated (96% and 97% saturation, respectively; Table 19). Figure 27 shows that the observed soil water was well below the calibrated porosity on most sampling days for all layers. These data suggest that the field soils are dominated by predominantly unsaturated flow conditions. Uniform moisture concentrations with depth may still occur, leading to nearly steady-state conditions, despite the fact that the soils were never fully saturated. Soil sampling did not occur during heavy rainfall, but sampling did occur within a day of heavy rainfall in some instances. For example, 0.7 inches of precipitation fell on November 15 and soil sampling was conducted on November 16 (Figure 27). The nearly one-month delay in peak leached nitrate from L2 to L3 suggests that water is moving fairly slowly through the soil (Figure 28); therefore, sampling did not have to occur simultaneous with a precipitation event in order to capture the soil water response except for in soil very close to the surface.

The simplified tipping-bucket approach to soil water flow modeling best represents steady-state flow conditions; therefore, I would expect to see better model simulations for the wetter months when precipitation events were more frequent. As described in the calibration results section, model efficiencies for the calibrated model were calculated for the wet and dry months separately. Contrary to what I would expect, the model efficiency coefficients from these two scenarios show that the soil water sub-model produced a better fit overall to the dry months than to the wet months (Table 20). The regression coefficients for the correlation analysis of the simulated vs. observed soil water data for the wet and dry months were also calculated, although the figures are not provided. The average R^2 value for all three soil layers for the wet months (0.34) was also less than for the dry months (0.38). This may be due to the fact that the original NLEAP was developed in the Midwest where soils are typically much drier.

The observed data indicate that unsaturated flow conditions existed in the field. Steady-state conditions are hypothesized to have been predominant most of the year based on the moisture fraction data by soil layer, but more sampling at various depths within each soil layer would have to be conducted to confirm this hypothesis. The current steady-state flow algorithm used by NLOS produced fairly good simulations. A better fit between observed and simulated values could be achieved with further calibration of the model, calibration to a data set spanning longer than one year, and a better field data set obtained by longer, more frequent sampling and sampling for some of the input parameters that were determined from previous studies or from published values for a silt loam. I do not recommend implementing a transient flow algorithm at this time since the simulations were fairly good for such a limited study period.

5.6.4 POST-HARVEST SOIL NITRATE TEST (PHSNT)

Soil tests are conducted after the final harvest in the late summer or early fall with the aim of identifying excess nitrate accumulation in the upper 12 inches of soil at the end of the growing season. A sampling depth of 0-12 inches is recommended, which corresponds to L1. Post-Harvest Soil Nitrate Tests (PHSNTs) can return variable results depending on the timing of sample collection. As discussed above, soil nitrate levels are predominantly dependent upon leaching in response to rainfall events, followed by denitrification, which is influenced by temperature and rainfall, and crop uptake; therefore, the results of the post-harvest soil test will be impacted most by the timing in relation to the onset of increased precipitation. The current guidelines for conducting the test, as discussed in a pamphlet distributed by the Oregon State University Extension Service, suggest sampling as soon as possible post-harvest and before any heavy rainfall events (Sullivan and Cogger, 2003). During this study period, increased rainfall began on about August 21, before the crop was harvested on September 28; therefore, excess nitrate had already begun to leach before the crop was harvested. Figure 64 shows that the first

peak in nitrate leached was on May 31. Post-harvest, soil nitrate levels remained steady until about October 24. At this point, nitrate began leaching from L1 downward and leaching continued from L2 and L3 until soil nitrate was depleted to background levels (Figure 65). The initiation of the post-harvest leaching occurred directly following the first post-harvest precipitation event (Figure 65). Excess soil nitrate was at peak post-harvest levels only until a rainstorm occurred. From that point onward, soil nitrate was continually depleted mainly due to leaching (Figure 66). Also, nitrate depletion post-harvest due to leaching removed nitrate from the soil; the first post-harvest rainfall event leached 16.1 lbs NO₃-N/acre of nitrate from L1. Based on these findings, I concur that the PHSNT be performed as soon as possible post-harvest, and especially before any heavy rainstorm events. Any delay in sampling will return lower nitrate levels as nitrate will be immediately lost to leaching with a rainstorm. These data also indicate that reliance on the PHSNT alone will provide an inaccurate measure of nitrate available for leaching since some leaching is already occurring pre-harvest. Additional testing, such as a pre-sidedress nitrate test (PSNT), which is typically conducted when the corn is at the four- to six-leaf stage, and soil nitrate testing in spring or early summer are also suggested for nitrogen management in corn (Sullivan and Cogger, 2003). The results correspond with these recommendations.

5.6.5 HYPOTHETICAL SCENARIOS

Using the calibrated model, a number of simulations were conducted using various sets of hypothetical inputs in order to predict the fate of nitrogen under a variety of field, fertilizer, and climate conditions. For each simulation, the output parameters associated with only the nitrogen budget were recorded. Descriptions of the changes made to the model inputs with each hypothetical scenario are listed in Table 23. The resulting balanced nitrogen budgets from each simulation are shown in Table 24.

In order to quantify the amount of nitrate leaching due to natural field conditions as opposed to the impacts of the cultivation and fertilization that occurred, in scenario 1 the calibrated model was run with no fertilizer and no crop (fallow). In this scenario, 145 lbs/acre of NO₃-N were leached as opposed to 140 lbs/acre leached with the calibrated model. Nitrate lost to denitrification was reduced from 12 to 8.9 lbs NO₃-N/acre, volatilization decreased from 6.0 to 0 lbs-N/acre, and nitrification and runoff were slightly reduced (Table 24). There was also a reduction in the final amounts of soil organic matter N in the slow pool (4671 to 4663 lbs-N/acre). The increase in nitrate leached and the decrease in soil organic matter N was caused by increased mineralization of organic matter to ammonium, which was then nitrified and leached. The amount of mineralization that occurred can be determined from the nitrogen budgets by subtracting the total initial soil organic matter from the total current soil organic matter in all pools. In scenario 1, the total amount of mineralization was 175 lbs-N/acre compared to 167 lbs-N/acre in every other scenario. The crop nitrogen uptake and greater denitrification that occurred in the calibrated scenario removed all additional nitrogen from fertilizer applications in addition to a greater amount of organic nitrogen than in scenario 1. Scenario 1 suggests that there is more leaching under fallow conditions due to the high amounts of soil organic nitrogen and due to the lack of nitrogen uptake by a crop. This scenario also suggests that the amount of soil organic nitrogen will decrease with time as it is slowly mineralized, denitrified, and leached as nitrate.

In order to gain an understanding of the time span required to remove the initial soil organic nitrogen by mineralization, denitrification, and eventual leaching, the model was run for 1500 simulation days (the maximum allowed by the model; equivalent to just over 4 years) under fallow conditions with no fertilizer applied (scenario 5). The base climate data were repeated for the simulation years after the study period. In the four-year simulation period, 577 lbs of NO₃-N/acre were leached and soil organic matter nitrogen only decreased by about 12 percent (Table

24). Total nitrate leached during each of the four simulation years was about equal to the amount leached in scenario 1. This suggests an average reduction in soil organic matter of 3% each year; therefore, approximately 33 years would be required to deplete the soil organic matter nitrogen storage and finally decrease nitrate leaching below the 145 lbs NO₃-N/acre observed in scenario 1.

A number of hypothetical scenarios were tested with the aim of reducing nitrate leaching. The total amount of fertilizer applied was unchanged in these scenarios in order to maintain realistic conditions for the calibrated maximum crop yield input. In scenario 2 the fertilizer was applied on July 30. This day was chosen because crop nitrogen uptake peaked on this day in the calibrated simulation. I expected total crop nitrogen uptake would increase if the fertilizer were applied to coincide with peak crop growth. Crop nitrogen uptake decreased from 163 to 121 lbs-N/acre. Ammonium volatilization, denitrification, and nitrate leaching increased by 14, 19, and 19 lbs NO₃-N/acre, respectively. Increased volatilization and denitrification will lead to increased greenhouse gas emissions (NH₃, N₂O, and N₂). In this scenario, air quality and groundwater quality were degraded.

In scenario 3, the fertilizer was applied on June 18 as opposed to May 19. June 18 is the first day of a long stretch of low-precipitation days during the growing season (Figure 63). I expected to see a decrease in nitrate leached and in fact, there was a 2-lb-N/acre decrease. Ammonium volatilization increased from 6 to 22 lbs-N/acre. The decrease in nitrate leached is attributed to increased volatilization, which would make less ammonium available for mineralization and then nitrification, since all other factors affecting nitrate would lead to increased leaching, i.e., decreased crop nitrate uptake, decreased denitrification, and increased nitrification in LS. The peak crop nitrogen uptake had already passed on June 18; therefore the crop removed less nitrogen. To minimize leaching, an ideal scenario would consist of fertilizer being applied just

before maximum crop growth and just after substantial rainfall and before a dry stretch, so that the soil is saturated, but no further precipitation leaches any excess nitrate from the system before it has the chance to be taken up by the crop or denitrified.

Gascho and Hook (1991) recommended applying 25% of the fertilizer at planting and the remainder at two later growth stages (V6 and V8) since there is a time lapse after planting before significant N uptake occurs. The Department of Ecology also recommends multiple N applications for silage corn grown in western Washington due to frequent precipitation, which may impede N uptake by the crop (Hermanson et al., 2000). For scenario 4, the fertilizer applications were split into three even events of 251 lbs/acre on May 19, July 2, and August 15 (these last two days were chosen as one-third and two-thirds of the way through the crop growing season). Contrary to the published recommendations, this produced an 15-lb increase in nitrate leached. The increase is attributed to the last application of the fertilizer, which was applied only 6 days before a rainfall event, decreased ammonium volatilization, which left more ammonium available to potentially be mineralized, nitrified, and then leached, and decreased denitrification. The decrease in volatilization and denitrification accounted for 5.4 lbs-N/acre, assigning a 9.6-lb NO₃-N/acre increase to leaching. This scenario suggests that timing fertilizer application to rainfall events is more important than evenly spacing the applications throughout the growing period.

6.0 CONCLUSIONS

The central objective of this project was to evaluate the applicability of the NLOS model for use by regulatory agencies to make local predictions of nitrate leaching under agricultural soils. Due to time and monetary constraints, I was not able to evaluate all aspects of the NLOS model. This research focused on the soil water sub-model and its affect on simulations of water and nitrate

flux. In consideration of the fact that this study was not a comprehensive evaluation of the model, I can only make recommendations about specific portions of the model. In its current form, NLOS makes satisfactory predictions of nitrate and ammonium in the upper 12 inches of the soil profile and nitrate leaching from a 36-in depth, according to linear regression analysis (R^2 values greater than or equal to 0.84). As discussed, timing shifts may have resulted in very low R^2 values whereas visual inspection reveals a good fit between simulated and observed values. Based on visual inspection of the plots of observed vs. the calibrated simulation values, NLOS matches trends in nitrate leaching from the 24-in soil depth, late season, i.e., post-harvest, trends in soil nitrate from 24 to 36 inches, and trends in soil water from 0-36 inches. Restrictions on the depth of soil and water sampling prohibited any observations of processes occurring deeper than the maximum depths the soil and water sampling equipment would allow (45 inches for soil nutrients and soil moisture, about 73 inches for groundwater, and 36 inches for soil pore water). The newly calibrated NLOS model should not be relied on for predictions of nitrous oxide emissions as the field data showed evidence of nitrous oxide release in response to freeze-thaw, which is not modeled. Nitrous oxide simulations also show large peaks that occurred in late August and September, which were not observed in the field. However, more frequent field sampling may have captured these peak emission events.

Model simulations may have an improved fit to the field data if all aspects of the model, as opposed to only those parameters associated with the soil water sub-model, were included in the sensitivity analysis and calibration and if field data collection was improved. I would expect to only see a slight improvement in model predictions from the inclusion of a more expansive set of parameters in the sensitivity analysis and calibration. There are very few input parameters that were not included in the original calibration since almost every model process is tied to the soil water sub-model. Implementing changes to the model algorithms is the only remaining route to

an improved model efficiency using the available observed data and without expanding the focus of the calibration. This may effect great changes on the model results though. For instance, the adjustment of the soil particle densities and the nitrous oxide emission rate constant (K_N2O_Leakage) effected dramatic changes on the simulated results. Tuning rate constants and standard values embedded in the soil nitrogen dynamics sub-model may lead to dramatic improvements in nitrogen flux simulations. I would not expect to see any increases in the efficiency of water predictions without changes to the basic model structure as this sub-model was thoroughly tested.

More frequent field data collection may improve the calibration and the fit between the simulated and observed values. There were very few data points to use in the model efficiency calculations, and therefore, the calibration. There were many simulation days where water was flowing and there was a simulated value of nitrate leaching, but there was no field data for that day for comparison. If field sampling had occurred during the time that the peak nitrous oxide emissions were simulated, a similar peak in the field data may have been observed thereby increasing the fit between the observed and simulated values. An increase in the frequency and number of field observations would provide more points for comparison and also would produce a more detailed and accurate picture of field conditions.

Improvements to the soil water sub-model may improve model predictions. NLOS does not simulate water flow or solute movement at low soil water contents. Instead, water would accumulate in a layer and then flow; resulting in zero values on a number of simulation days. On days when water was accumulating and not flowing, the model did not simulate any leaching between layers. When field observations happened to coincide with these no flow days, there was no simulated value for comparison thereby decreasing the model efficiency. If NLOS were

altered in order to simulate water flux at low soil water contents, then the model efficiency may be improved.

Leaching of excess soil nitrate occurs directly following fertilizer application and before crop nitrate N increases and continues until heavy fall rains have leached away excess nitrate and the soil is returned to background conditions. Since nitrate is made available for leaching immediately following fertilizer application, a soil nitrate test conducted post-harvest alone is not an accurate measure of nitrate leaching potential in response to agricultural activities. Soil nitrate tests conducted prior to harvest in addition to the PHSNT would more accurately indicate the amount of leaching that has already occurred, as long as the amount of nitrogen applied and crop N uptake is known. Use of the PHSNT to indicate leaching potential after harvest has already missed substantial amounts of nitrate leached. Also, the PHSNT would have to be conducted before the first heavy post-harvest rainfall event in order to catch any significant amount of available nitrate before it is leached away; therefore, I recommend performing the test concurrent with harvesting and not relying on the PHSNT alone.

In addition to the above discussion, the major conclusions of this study as revealed through evaluation of field observations and model simulations are as follows:

- Simulated and observed nitrate in the soil and leachate showed an immediate response to rainfall events;
- Peak simulated and observed nitrate in the soil and leachate and ammonium in the soil occurred directly following fertilization;
- Attenuation of nitrate solute curves was evident in the field data as nitrogen losses occurred with the downward migration of nitrate in percolating water;
- Excess nitrate was leached out of the system and background conditions were restored during the study year;

- Nitrous oxide emissions increased in response to temperature increases and rainfall events;
- The study period experienced a drier spring, a wetter fall, and higher air temperatures than the 30-year averages;
- Location, depth, and treatment history were not significantly related to the observed parameters;
- Water leached predictions are by far most sensitive to user-entered rainfall amounts;
- Nitrate leached predictions are most sensitive to the Plant AWHC for L3, which is used in the equation for water movement;
- NLOS prediction efficiency was greater from April to October than from October to April;
- NLOS prediction efficiency decreased with increasing depth in the soil column;
- NLOS predictions of nitrate leached will fall within 90-175 lbs NO₃-N/acre 95% of the time if uniform uncertainty within the defined ranges is assumed for model inputs associated with the soil water sub-model, and the climate, soil, crop management, and fertilizer conditions are consistent with the study:
- Hypothetical scenarios suggest that timing fertilizer application to rainfall events is the most effective way to reduce nitrate leaching when all other conditions are constant.

7.0 RECOMMENDATIONS

The icon-based modeling used in STELLA is an ideal environment for model development. Considering the success many researchers have achieved with the original NLEAP model and the user-friendly STELLA environment, continued research with NLOS would be ideal for

future student projects. Ideas for future projects, stemming from this research, are enumerated below.

1. Further calibration and sensitivity analysis to include all aspects of the model, as opposed to focusing on the soil water sub-model. In addition, more frequent field data collection or event-based field data collection and modeling may improve the calibration.
2. Once a calibrated model is attained, validate the model to another field data set for conditions similar to those of the calibration data set.
3. Install deeper wells both up-gradient and down-gradient of the field site to compare background groundwater nitrate concentrations to groundwater with nitrate leached from the study area in order to quantify nitrate leached to the water table.
4. Compare water flux simulations from NLOS to a model using a transient, unsaturated flow algorithm in the soil water sub-model.
5. Install wick or zero-tension pan lysimeters in order to quantify leachate volumes at multiple depths.
6. Measure values for the model inputs that were obtained from existing field sites or from published studies in order to more accurately represent field conditions.
7. Evaluate recent studies on the factors controlling nitrous oxide emissions for possible model improvements.
8. Use NLOS to perform monthly simulations or event-based simulations of nitrogen and water flux in relation to cropping events.
9. Update NLOS to simulate ammonium leaching, since it was observed in the field.

8.0 REFERENCES

- Ahuja, L.R., D.E. Johnsen, and K.W. Roja. 2000. Water and chemical transport in soil matrix and macropores., p. 13-50, *In* L. R. Ajuha, et al., eds. Root Zone Water Quality Model: Modeling Management Effects on Water Quality and Crop Production. Water Resources Publication, LLC, Highlands Ranch, CO.
- APHA. 1998. Standard Methods for the Examination of Water and Wastewater, 20th Edition. American Public Health Association, Washington, DC.
- ASTM. 1995. Standard test methods for moisture, ash and organic matter of peat and other organic soils. ASTM D 2974-87.
- Beck, M.B. 1987. Water quality modeling: A review of the analysis of uncertainty. *Water Resources Research* 23:1393-1442.
- Beckie, H.J., A.P. Moulin, C.A. Campbell, and S.A. Brandt. 1995. Testing the effectiveness of four simulation models for estimating nitrates and water in two soils. *Canadian Journal of Soil Science* 75:135-143.
- Bittman, S., D.E. Hunt, and M.J. Shaffer. 2001. NLOS (NLEAP On STELLA)- A nitrogen cycling model with a graphical interface: Implications for model developers and users., *In* M. J. Shaffer, et al., eds. Modeling carbon and nitrogen dynamics for soil management. Lewis Publishers.
- Bittman, S., C.G. Kowalenko, D.E. Hunt, and O. Schmidt. 1999. Surface-banded and broadcast dairy manure effects on tall fescue yield and nitrogen uptake. *Agronomy Journal* 91:826-833.
- Black, C.A., D.D. Evans, L.E. Ensminger, J.L. White, and F.E. Clark, (eds.) 1965. Methods of soil analysis part 1- physical and mineralogical properties, including statistics of measurement and sampling., Vol. 9. American Society of Agronomy, Inc., Madison, Wisconsin USA.
- Brady, N.C. 1974. The Nature and Properties of Soils. 8th ed. Macmillan Publishing Co., Inc., New York.
- Bresler, E., and G. Dagan. 1981. Convective and pore scale dispersive solute transport in unsaturated heterogeneous fields. *Water Resources Research* 17:1683-1693.
- Bresler, E., and G. Dagan. 1983. Unsaturated flow in spatially variable fields, 3, Solute transport models and their application to two fields. *Water Resources Research* 19:429-435.
- Butters, G.L., and W.A. Jury. 1989. Field scale transport of bromide in an unsaturated soil, 2, Dispersion modeling. *Water Resources Research* 25:1583-1589.

- Chichester, F.W. 1977. Effects of increased fertilizer rates on nitrogen content of runoff and percolate from monolith lysimeters. *Journal of Environmental Quality* 6:211-217.
- Corey, J.C., D.R. Nielsen, and J.W. Biggar. 1963. Miscible displacement in saturated and unsaturated sandstone. *Soil Science Society of America Journal* 27:258-262.
- Delgado, J.A. 1998. Sequential NLEAP simulations to examine the effect of early and late planned winter cover crops on nitrogen dynamics. *Journal of Soil and Water Conservation* 53:241-244.
- Delgado, J.A., M.J. Shaffer, and M.K. Brodahl. 1998a. New NLEAP for shallow and deep rooted rotations. *Journal of Soil and Water Conservation* 53:338-340.
- Delgado, J.A., R.F. Follett, J.L. Sharkoff, M.K. Brodahl, and M.J. Shaffer. 1998b. NLEAP facts about nitrogen management. *Journal of Soil and Water Conservation* 53.
- Delgado, J.A., R. Khosla, W.C. Bausch, D.G. Westfall, and D.J. Inman. 2005. Nitrogen fertilizer management based on site-specific management zones reduces potential for nitrate leaching. *Journal of Soil and Water Conservation* 60.
- DeSmedt, F., and P.J. Wierenga. 1984. Solute transfer through columns of glass beads. *Water Resources Research* 20:225-232.
- Destouni, G., and V. Cvetkovic. 1991. Field scale mass arrival of sorptive solute into the groundwater. *Water Resources Research* 27:1315-1325.
- Dingman, S.L. 2002. *Physical Hydrology*. 2nd ed. Prentice-Hall, Inc., Upper Saddle River, New Jersey.
- Follett, R.F., M.J. Shaffer, M.K. Brodahl, and G.A. Reichman. 1994. NLEAP Simulation of residual soil nitrate for irrigated and nonirrigated corn. *Journal of Soil and Water Conservation* 49:375-382.
- Gamerding, A.P., D.I. Kaplan, D.M. Wellman, and R.J. Serne. 2001. Two-region flow and decreased sorption of uranium (VI) during transport in Hanford groundwater and unsaturated sands. *Water Resources Research* 37:3155-3162.
- Garnier, P., C. Néel, B. Mary, and F. Lafolie. 2001. Evaluation of a nitrogen transport and transformation model in a bare soil. *European Journal of Soil Science* 52:253-268.
- Gascho, G.J., and J.E. Hook. 1991. Development of a fertigation program for sprinkler-irrigated corn. *J. Prod. Agric.* 4:306-312.
- Hamby, D.M. 1994. A review of techniques for parameter sensitivity analysis of environmental models. *Environmental Monitoring and Assessment* 32:135-154.
- Hammel, K., and K. Roth. 1998. Approximation of asymptotic dispersivity of conservative solute in unsaturated heterogeneous media with steady state flow. *Water Resources Research* 34:709-715.

- Hermanson, R., W. Pan, C. Perillo, R. Stevens, and C. Stockle. 2000. Nitrogen Use by Crops and the Fate of Nitrogen in the Soil and Vadose Zone: A Literature Search Publication No. 00-10-015. Washington State University and Washington Department of Ecology.
- Hii, B., H. Liebscher, M. Mazalek, and T. Tuominen. 1999. Ground water quality and flow rates in the Abbotsford aquifer, British Columbia. Aquatic and Atmospheric Science Division, Environmental Conservation Branch, Environment Canada, Pacific and Yukon Region, Vancouver, BC.
- Jardine, P.M., G.K. Jacobs, and G.V. Wilson. 1993. Unsaturated transport processes in undistrubed heterogeneous porous media. I. Inorganic contaminants. *Soil Science Society of America Journal*:363-368.
- Jury, W.A. 1982. Simulation of solute transport with a transfer function model. *Water Resources Research* 18:363-368.
- Kowalenko, C.G. 1991. Fall vs. spring soil sampling for calibrating nutrient applications on individual fields. *Journal of Production Agriculture*:322-329.
- Leonard, R.A., W.G. Knisel, and D.S. Still. 1987. GLEAMS: Groundwater Loading Effects of Agricultural Management Systems. *ASAE* 30:1403-1418.
- Liebscher, H., B. Hii, and D. McNaughton. 1992. Nitrates and pesticides in the Abbotsford aquifer, southwestern British Columbia. Inland Waters Directorate, Environment Canada, North Vancouver, BC.
- Luttmerding, H.A., and P.N. Sprout. 1967. Soil survey of Agassiz area. Preliminary Report No. 8 of the Lower Fraser Valley Soil Survey. British Columbia Department of Agriculture, Kelowna, BC.
- Maraq, M.A., R.B. Wallace, and T.C. Voice. 1997. Effects of degree of water saturation on dispersivity and immobile water in sandy soil columns. *Journal of Contaminant Hydrology* 25:199-218.
- Maraq, M.A., R.B. Wallace, and T.C. Voice. 1999. Effect of water saturation on retardation of ground-water contaminants. *Journal of Environmental Engineering* 125:697-704.
- Mitchell, R.J., R.S. Babcock, S. Gelinas, L. Nanus, and D.E. Stasney. 2003. Nitrate distributions and source identification in the Abbotsford-Sumas aquifer, northwestern Washington State. *Journal of Environmental Quality* 32:789-800.
- Mitchell, R.J., R.S. Babcock, H.R. Hirsch, L. McKee, R.A. Matthews, and J. Vandersypen. 2005. *Water Quality: Abbotsford-Sumas Final Report*. Western Washington University, Bellingham, Washington.
- Molina, J.A.E., C.E. Clapp, M.J. Shaffer, F.W. Chichester, and W.E. Larson. 1983. NCSOIL, A model of nitrogen and carbon transformations in soil: description, calibration, and behavior. *Soil Science Society of America Journal*:85-91.

- Nash, J.E., and J.V. Sutcliffe. 1970. River flow forecasting through conceptual models part I- A discussion of principles. *Journal of Hydrology* 10:282-290.
- Nelson, D.W., and J.M. Bremner. 1972. Preservation of soil samples for inorganic nitrogen analysis. *Agronomy Journal*:196-199.
- Nolan, B.T., and J.D. Stoner. 2000. Nutrients in groundwaters of the coterminous United States, 1992-1995. *Environmental Science and Technology* 34:1156-1165.
- Page, A.L., R.H. Miller, and D.R. Keeney, (eds.) 1982. *Methods of soil analysis part 2- chemical and microbiological properties.*, Vol. 9. American Society of Agronomy, Inc., Madison, Wisconsin USA.
- Parton, W.J., D.S. Ojima, C.V. Cole, and D.S. Schimel. 1994. A general model for soil organic matter dynamics: sensitivity to litter chemistry, texture and management, *Quantitative Modeling of Soil Forming Processes.*, p. 147-167 SSSA Spec. Pub., Madison, WI.
- Patni, N.K., S. Bittman, and L. vanVliet. 2000. Effect of swine manure application on subsurface water quality in forage grass fields. Technical Report #158. Pacific Agri-Foods Research Centre, Agassiz, BC.
- Ritchie, J.T. 1998. Soil water balance and plant water stress, p. 41-54, *In* G. Y. Tsuji, et al., eds. *Understanding Options for Agricultural Production*. Kluwer Academic, Boston, MA.
- Robertson, G.P. 1993. Fluxes of nitrous oxide and other nitrogen trace gases from intensively managed landscapes: A global perspective., p. 95-108, *In* L. A. Harper, et al., eds. *Agricultural Ecosystem Effects on Trace Gases and Global Climate Change*, Vol. Special Publication 55. Amer. Soc. Agronomy, Madison, WI.
- Russo, D., W.A. Jury, and G.L. Butters. 1989. Numerical analysis of solute transport during transient irrigation, 1, The effect of hysteresis and profile heterogeneity. *Water Resources Research* 25:2109-2118.
- SCS, U.a. 1992. *Soil Survey of Whatcom County Area, Washington*. US Department of Agriculture and Soil Conservation Service.
- Seyfried, M.S., and P.S.C. Rao. 1987. Solute transport in undisturbed columns of an aggregated tropical soil: Preferential flow effects. *Soil Science Society of America Journal* 51:1434-1444.
- Shaffer, M.J. 1985. Simulation model for soil erosion-productivity relationships. *Journal of Environmental Quality*:144-150.
- Shaffer, M.J., and S.C. Gupta. 1987. Unsaturated flow submodel., p. 51-56, *In* M. J. Shaffer and W. E. Larson, eds. *NTRM, A Soil-Crop Simulation Model for Nitrogen, Tillage, and Crop-Residue Management*. U.S. Department of Agriculture.

- Shaffer, M.J., and L. Ma. 2001. Carbon and nitrogen dynamics in upland soils, *In* M. J. Shaffer, et al., eds. Modeling carbon and nitrogen dynamics for soil management. Lewis Publishers, Boca Raton, Florida.
- Shaffer, M.J., A.D. Halvorson, and F.J. Pierce. 1991. Nitrate Leaching and Economic Analysis Package (NLEAP): Model Description and Application, p. 285-322 *Managing Nitrogen for Groundwater Quality and Farm Profitability*. Soil Science Society of America, Madison, WI.
- Shaffer, M.J., B.K. Wylie, and M.K. Brodahl. 1994. NLEAP as a predictive tool for regional nitrate leaching in Colorado, pp. 197-202 *Great Plains Soil Fertility Conference*, Denver, Colorado.
- Shaffer, M.J., L. Ma, and S. Hansen, (eds.) 2001. Modeling carbon and nitrogen dynamics for soil management. Lewis Publishers.
- Small, M.J., and J.R. Mular. 1987. Long-term pollutant degradation in the unsaturated zone with stochastic rainfall infiltration. *Water Resources Research*:2246-2256.
- Solley, W.B., R.R. Pierce, and H.A. Perlman. 1993. Estimated use of water in the United States in 1990. Circular 1081. U.S. Geological Survey, Reston, VA.
- Spalding, R.F., and M.E. Exner. 1993. Occurrence of nitrate in ground water- A review. *Journal of Environmental Quality*:392-402.
- Sullivan, D.M., and C.G. Cogger. 2003. Post-harvest soil nitrate testing for manured cropping systems west of the Cascades. Oregon State University Extension Service.
- Tesoriero, A.J., and F.D. Voss. 1997. Predicting the probability of elevated nitrate concentrations in the Puget Sound Basin: Implications for aquifer susceptibility and vulnerability. *Ground Water*:1029-1039.
- van Genuchten, M.T., and P.J. Wierenga. 1976. Mass transfer studies in sorbing porous media, I, Analytical solutions. *Soil Science Society of America Journal* 40:473-480.
- Vanderborght, J., A. Timmerman, and J. Feyen. 2000. Solute transport for steady-state and transient flow in soils with and without macropores. *Soil Science Society of America Journal* 64:1305-1317.
- Wassenaar, L. 1995. Evaluation of the origin and fate of nitrate in the Abbotsford aquifer using the isotopes of ^{15}N and ^{18}O in $\text{NO}_3\text{-N}$. *Applied Geochemistry* 10:391-405.
- Whitmore, A.P. 1995. Modeling the mineralization and leaching of nitrogen from crop residues during three successive growing seasons. *Ecol. Modeling* 81:233-241.
- Wierenga, P.J. 1977. Solute distribution profiles computed with steady-state and transient water movement models. *Soil Science Society of America Journal* 41:1050-1055.
- Williams, J.R. 1995. The EPIC model., p. 909-1000, *In* V. P. Singh, ed. *Computer Models of Watershed Hydrology*. Water Resources Publications, Highlands Ranch, CO.

Zebarth, B.J., B. Hii, H. Liebscher, K. Chipperfield, J.W. Paul, G. Grove, and S.Y. Szeto. 1998. Agricultural land use practices and nitrate contamination in the Abbotsford aquifer, British Columbia, Canada. *Agriculture, Ecosystems & Environment* 69:99-112.

Table 1. Hydraulic gradient calculation parameters.

Date	Points used in calculation	Max difference b/t head values (ft)	Gradient Magnitude (i)	Flow direction (degrees from north)	Coefficient of Determination (R²)
1998-2001	4	4.8	0.38	164.9	0.91
11/16/04	4	5.3	0.42	166.4	0.97
11/17/04	4	5.3	0.42	166.4	0.97
12/13/04	4	5.3	0.42	166.4	0.97
12/14/04	4	5.4	0.43	166.4	0.98
1/20/05	4	5.6	0.44	167.5	0.97
1/21/05	4	5.5	0.43	166.8	0.98
Average from study period:			0.43	166.7	

Table 2. Required model inputs: descriptions and sources.

Soil Data

General Information	Description	Units	Base input	Data source
Province	code for Canadian province or territory; not used anywhere in the model	unitless	2	2 = British Columbia
Municipality	code for municipality (geographical level of government smaller than a province); not used anywhere in the model	unitless	2	2 = Chilliwack
Soil ID	a means to identify a soil in a given location; not used anywhere in the model	unitless	NA	NA
Field	a means to identify the field where the soil samples were taken; not used anywhere in the model	unitless	1	1 = Field 9717
Soil Survey	code to identify a soil survey; not used anywhere in the model	unitless	NA	NA
Soil Classification	a switch to identify a soil as heavy textured (assigned a value of 1) or light textured (2); a soil is heavy textured if the PWP is >0.22 in/in and light textured if the PWP is <0.22 in/in	unitless	equation on	NA
Hydrologic Group	code to indicate the hydrologic group	unitless	2	ASS
Soil drainage classification	code to classify the soil type in terms of its drainage characteristics	unitless	8	ASS: 8= moderately well
Impermeable layer classification	code to indicate the presence or absence of a compacted soil layer that is very slowly permeable and located below the plow depth but above 4 feet deep	unitless	0	HRH
Percent slope	percent slope of the field being simulated	unitless	4.5	ASS (avg of 0-9% slopes = 4.5)
Landscape position	code indicating the general landscape position of the field	unitless	4	ASS

Continued on next page...

Soil depth information

Soil Thickness LS	surface layer; approx. 1 inch; characterized by litter decomposition and the application of fertilizers, manure, and soil amendments; soil microbial activity	inches	1	default, also this was the amount scraped off the surface before soil samples were collected
Soil Thickness L1	soil microbial activity, incorporation of fertilizers, manure and soil amendment, and root growth	inches	12	default value; also concurs w/ sampling depths; ~80% of roots in the upper 12 inches of soil (Derek Hunt, personal communication)
Profile Depth	depth of the three soil layers (L1, L2, and L3); max depth of 60 inches	inches	45	this is the the max depth to which soil samples were collected; soil transitions to coarse sand and cobbles below this depth (Shabtai Bittman & Derek Hunt, personal communication)
Depth to Root Restriction	defines the depth at which roots may encounter a restriction, such as an impermeable layer or rocks, that will reduce the rate of their growth; reduces the thickness of L2	feet	0	no restrictions observed in soil samples collected within the root zone (HRH)
Depth to H2O Restriction	defines the presence and depth of a water restriction layer; reduces the thickness of L2	feet	0	no water restrictions observed in soil samples (HRH)
consol evap depth heavy	the depth at which evaporation occurs in a heavy textured soil; default is 2.0 inches	inches	2	default value
consol evap depth light	the depth at which evaporation occurs in a light textured soil; default is 4.0 inches	inches	4	default value
Root depth max for simulation	root depth max for simulation is normally calculated within the model from crop rooting depth information. However, the internal calculation may be frozen (equation off) and a user-entered value used instead; reduces the thickness of L2	feet	2	80% rooting in the top 12 inches, 20 % from 12 to 24 inches (Derek Hunt, personal communication)

Continued on next page...

Soil physical characteristics

Bulk Density LS	bulk density for LS	g/cm3	1.12	Agassiz data from field 9419- all treatments (first 3" meas)
Bulk Density L1	bulk density for L1	g/cm3	1.13	Agassiz data from field 9419- all treatments (avg of 3-12" meas)
Bulk Density L2	bulk density for L2	g/cm3	1.15	Agassiz data from field 9419- all treatments (avg of 13-19" meas)
Bulk Density L3	bulk density for L3	g/cm3	1.15	Agassiz data from field 9419- all treatments (avg of 13-19" meas)
CEC 1	cation exchange capacity (CEC) for L1	meq/100g	14.9	Avocet lab results run on a composite sample from depth 2- multiple dates and reps
Clay L1	percent clay in L1 (% of soil volume); not used anywhere in the model	unitless	0	NA
Clay L2	percent clay in L2 (% of soil volume); not used anywhere in the model	unitless	0	NA
Coarse Frag % L1	coarse fragment (fragments >2.0mm in diameter) % in L1 (% of soil volume)	unitless	0.36	HRH (sieve analysis data)
Coarse Frag % L2	coarse fragment (fragments >2.0mm in diameter) % in L2 (% of soil volume)	unitless	0.17	HRH (sieve analysis data)
Permeability L1	permeability of L1; not used anywhere in the model	inches/hour	0	NA
Permeability L2	permeability of L2; not used anywhere in the model	inches/hour	0	NA
Plant AWHC L1	plant available water holding capacity (AWHC) for L1 (inches/inches)	unitless	0.13	Typical value for a silt loam from Norton & Silvertooth, 1998
Plant AWHC L2	plant available water holding capacity (AWHC) for L2 (inches/inches)	unitless	0.13	Typical value for a silt loam from Norton & Silvertooth, 1998
PWP 1	permanent wilting point (PWP) for L1 (soil water content @ 15 bars; inch/inch)	unitless	0.13	Typical value for a silt loam from Norton & Silvertooth, 1998
PWP 2	permanent wilting point (PWP) for L2 (soil water content @ 15 bars; inch/inch)	unitless	0.13	Typical value for a silt loam from Norton & Silvertooth, 1998

Continued on next page...

Salinity L1	salinity of L1; not used anywhere in the model	??	0	NA
Salinity L2	salinity of L2; not used anywhere in the model	??	0	NA
Soil pH L1	soil pH for L1	pH units	5.96	HRH (avg lysimeter water pH from all depth 2 lysimeters)
Soil pH L2	soil pH for L2; not used anywhere in the model	pH units	0	NA
AWHC L3	plant available water holding capacity (AWHC) for L3 (inches/inches)	unitless	0.13	Typical value for a silt loam from Norton & Silvertooth, 1998
Coarse Frag % L3	coarse fragment (fragments >2.0mm in diameter) % in L3 (% of soil volume)	unitless	0.30	HRH (sieve analysis data)
Coarse Frag % LS	coarse fragment (fragments >2.0mm in diameter) % in LS (% of soil volume)	unitless	0.39	HRH (sieve analysis data)
PWP 3	permanent wilting point (PWP) for L2 (soil water content @ 15 bars; inch/inch)	unitless	0.13	Typical value for a silt loam from Norton & Silvertooth, 1998
<u>Soil OM characteristics</u>				
Soil OrgM % LS	initial soil organic matter % for LS; will vary depending on the soil type in the simulation run	unitless	8.03	HRH (avg OM% for depth 1 from Muffle Furnace test)
Soil OrgM % L1	initial soil organic matter % for L1; will vary depending on the soil type in the simulation run	unitless	7.68	HRH (avg OM% for depths 1&2 from Muffle Furnace test)
Soil OrgM CN LS	C:N ratio of the initial soil organic matter in LS (default=10)	unitless	12.0	HRH (avg C:N ratio for depth 1 from UW analysis)
Soil OrgM CN L1	C:N ratio of the initial soil organic matter in L1 (default=10)	unitless	12.2	HRH (avg C:N ratio for depths 1&2 from UW analysis)
Soil OrgM % C LS	percent carbon of the initial soil organic matter in LS (default=58)	unitless	28.5	HRH (avg C:N ratio for depth 1 from UW analysis)
Soil OrgM % C L1	percent carbon of the initial soil organic matter in L1 (default=58)	unitless	28.3	HRH (avg C:N ratio for depths 1&2 from UW analysis)
<u>Soil Management</u>				
Use nitrif inhibitor	a switch to indicate if a nitrification inhibitor has been used	unitless	0	HRH observation
Tillage classification	code to indicate the type of tillage applied	unitless	3	HRH observation
Planted & tilled on Contour	code to indicate whether the field is planted on contour or not	unitless	0	HRH observation

Continued on next page...

Terraced Field	code to indicate whether the field is terraced or not	unitless	0	HRH observation
Tile drainage classification	code to indicate the presence or absence of tile drainage	unitless	0	HRH observation
<u>Initial soil water and nitrogen</u>				
Initial H2O LS	initial soil water for LS	inches/inches	0.38	HRH (avg by soil layer; converted gravimetric soil moist to volumetric by multiplying by the bulk density; samples collected on 3/24/04, the start date)
Initial H2O L1	initial soil water for L1	inches/inches	0.38	HRH (avg by soil layer; converted gravimetric soil moist to volumetric by multiplying by the bulk density; samples collected on 3/24/04, the start date)
Initial H2O L2	initial soil water for L2	inches/inches	0.37	HRH (avg by soil layer; converted gravimetric soil moist to volumetric by multiplying by the bulk density; samples collected on 3/24/04, the start date)
Initial H2O L3	initial soil water for L3	inches/inches	0.36	HRH (avg by soil layer; converted gravimetric soil moist to volumetric by multiplying by the bulk density; samples collected on 3/24/04, the start date)
Initial NH4 LS	initial soil ammonium (NH4-N) in LS	lbs/acre	0.85	HRH (soil extract analysis; avg by soil layer; samples collected on 3/24/04, the start date)
Initial NH4 L1	initial soil ammonium (NH4-N) in L1	lbs/acre	10.2	HRH (soil extract analysis; avg by soil layer; samples collected on 3/24/04, the start date)

Continued on next page...

Initial NO3 LS	initial soil nitrate (NO3-N) for LS	lbs/acre	0.33	HRH (soil extract analysis; avg by soil layer; samples collected on 3/24/04, the start date)
Initial NO3 L1	initial soil nitrate (NO3-N) for L1	lbs/acre	4.0	HRH (soil extract analysis; avg by soil layer; samples collected on 3/24/04, the start date)
Initial NO3 L2	initial soil nitrate (NO3-N) for L2	lbs/acre	3.7	HRH (soil extract analysis; avg by soil layer; samples collected on 3/24/04, the start date)
Initial NO3 L3	initial soil nitrate (NO3-N) for L3	lbs/acre	6.1	HRH (soil extract analysis; avg by soil layer; samples collected on 3/24/04, the start date)

Crop Manager

Crop Type	type of crop (annual, perennial, or fallow)	unitless	1	Derek Hunt, personal communication
-----------	---	----------	---	------------------------------------

Annual Crop Manager

Select Crop Ann[1]	type of crop	unitless	9	Derek Hunt, personal communication
--------------------	--------------	----------	---	------------------------------------

Planting Dates

Select Crop AnnPD[1]	planting date for crop 1 in julian dates	unitless	140	Frederic Bounaix, personal communication
----------------------	--	----------	-----	--

Crop harvest dates

Select Crop annHD[1]	harvest date for crop 1 in julian dates	unitless	272	Frederic Bounaix, personal communication
----------------------	---	----------	-----	--

Crop N%

Select Crop Ann N%[1]	concentration of N (N%) in the harvested crop as a percentage	unitless	1.15	Agri-Foods (Avg. whole plant (wp) Leco N%)
-----------------------	---	----------	------	--

Crop moisture fraction (%)

Select Crop Ann H2Ofrac[1]	not used anywhere in the model; moisture content in the total harvested annual crop as a fraction	unitless	0.659	Agri-Foods (Avg. sub-sample moisture from corn collected on harvest date (8/19/04))
----------------------------	---	----------	-------	---

Continued on next page...

Crop yield
(tons/acre)

Selet Crop Ann MaxYld[1]	dry matter yield of the annual crop maximum harvest	tons/acre	7.44	Agri-Foods (Avg. dry matter yield from corn collected on harvest date (8/19/04))
-----------------------------	--	-----------	------	---

Fertilizer
Manager

Fertilizer type

Select fert type[Applic 1]	code for the type of commercially available fertilizer or a custom blend	unitless	4	Frederic Bounaix, personal communication
Select fert type[Applic 2]	code for the type of commercially available fertilizer or a custom blend	unitless	1	Frederic Bounaix, personal communication
Select fert type[Applic 3]	code for the type of commercially available fertilizer or a custom blend	unitless	7	Frederic Bounaix, personal communication

Fertilizer method

Select fert applic method[Applic 1]	code for the fertilizer application method	unitless	2	Frederic Bounaix, personal communication
Select fert applic method[Applic 2]	code for the fertilizer application method	unitless	2	Frederic Bounaix, personal communication
Select fert applic method[Applic 3]	code for the fertilizer application method	unitless	2	Frederic Bounaix, personal communication

Fertilizer amount

Select fert amount[Applic 1]	amount of fertilizer applied	lbs/acre	260	Frederic Bounaix, personal communication
Select fert amount[Applic 2]	amount of fertilizer applied	lbs/acre	130	Frederic Bounaix, personal communication
Select fert amount[Applic 3]	amount of fertilizer applied	lbs/acre	250	Frederic Bounaix, personal communication

Fertilization date

Select fert date[Applic 1]	application date in julian dates	unitless	140	Frederic Bounaix, personal communication
Select fert date[Applic 2]	application date in julian dates	unitless	140	Frederic Bounaix, personal communication
Select fert date[Applic 3]	application date in julian dates	unitless	140	Frederic Bounaix, personal communication

Continued on next page...

Tillage

Manager

Tillage type code

Select Tillage Type[Tillage 1]	code for the type of tillage	unitless	2	HRH observation
--------------------------------	------------------------------	----------	---	-----------------

Date of tillage

Select Tillage Date[Tillage 1]	date of tillage in julian dates	unitless	0	HRH observation
--------------------------------	---------------------------------	----------	---	-----------------

Tillage depth

Tillage Depth[No Till]	depth of tillage can be entered here if it varies from the default	inches	0	HRH observation
------------------------	--	--------	---	-----------------

Climate Data

T Max	maximum daily temperature	degrees C	data cd	http://www.climate.weatheroffice.ec.gc.ca & some missing points from http://historical.farmzone.com
T Min	minimum daily temperature	degrees C	data cd	http://www.climate.weatheroffice.ec.gc.ca
Rainfall in mm	daily total amount of precipitation	mm	data cd	http://www.climate.weatheroffice.ec.gc.ca & some missing points from http://historical.farmzone.com
ET in mm	estimation of evapotranspiration	mm	data cd	www.farmwest.com

Select Internal Model Parameters

Effective Precip	the effective precipitation amount below which certain activities, like runoff and counting the day as a wet day for denitrification, do not occur	unitless	0.21	default value
CCFAC A	a crop correction factor for crop yields less than the crop maximum; calculated as a ratio of yield goal / crop maximum yield	unitless	0.87	default value
Particle density LS	used in the equation for calculating the porosity of the surface layer (POR_LS)	g/cm ³	2.65	default value
Particle density L1	used in the equation for calculating the porosity of the surface layer (POR1)	g/cm ³	2.65	default value
Particle density L2	used in the equation for calculating the porosity of the surface layer (POR2)	g/cm ³	2.65	default value
Particle density L3	used in the equation for calculating the porosity of the surface layer (POR3)	g/cm ³	2.65	default value
Runoff adjust factor	an adjustment factor for runoff; can be changed by the user to reflect local conditions	unitless	0	default value
K N2O Leakage	a fraction representing the maximum leakage of N ₂ O from the nitrification process	unitless	0.065	default value

Table 3. Crop management and sample collection events.

Calendar Date	Julian Date	Action	Notes
4/6/04	97	Herbicide applied	Roundup applied.
5/19/04	140	Seeded	No-till planting of silage corn. The areas around the lysimeters (~15-20 ft in each direction) were hand-seeded to avoid damage by equipment.
5/19/04	140	Fertilization	Side-dressed 489 lbs of superphosphate (P ₂ O ₅ ; 45% phosphorus (0-45-0)) at same time as seeding (missed rows 1&2) using John Deere Model 7200 4-row corn planter. Hand-applied superphosphate to the 2 rows on either side of the N ₂ O chambers. Surface broadcast Triple 18 (NH ₃ , P ₂ O ₅ , K ₂ O @ 18% each) at 495 lbs/acre (89 lbs-N/acre). Surface broadcast 34.5% Ammonium-nitrate @ 259 lbs/acre (89 lbs-N/acre).
8/19/04	232	Crop sample collection	Samples collected in a 2-row x 8-foot area (40 ft ²) for dry matter yield and crop moisture.
9/28/04	272	Crop harvest and sample collection	Samples collected in a 2-row x 12-foot area (60 ft ²) for dry matter yield, crop moisture, and crop N%.

Table 4. Bulk density depth ranges and average values by soil layer.

Soil layer	Defined soil layer depths (in)	<u>Bulk density values</u>		Average bulk density by soil layer (g/cm ³)
		<u>depth range (in)</u>	Min.	
LS	0-1	3	3	1.12
L1	0-12	3	4	1.13
L2	12-24	13	19	1.15
L3	24-45	13	19	1.15

Table 5. Summary statistics for the initial soil data collected on March 24, 2004.

<u>Summary Statistic</u>	<u>cn</u>	<u>coarsefrag</u>	<u>om</u>	<u>moist</u>	<u>soil.nh4</u>	<u>soil.no3</u>
Minimum	11.06	0.01	6.01	0.26	89.52	71.24
1st Quadrant	11.84	0.03	7.20	0.30	123.28	101.79
Median	12.25	0.08	7.81	0.32	188.11	115.79
Mean	12.24	0.30	7.68	0.32	219.88	123.57
3rd Quadrant	12.62	0.24	7.94	0.35	328.04	135.46
Maximum	13.50	1.72	9.39	0.38	417.49	208.92

cn = carbon to nitrogen ratio of organic matter (unitless)

coarsefrag = coarse fragment percentage (g/g)

om = organic matter content (% of dry weight)

moist = soil moisture (g/g)

soil.nh4 = soil ammonium ($\mu\text{g NH}_4\text{-N/L}$)

soil.no3 = soil nitrate ($\mu\text{g NO}_3\text{-N/L}$)

Table 6. Soil water sub-model sensitivity analysis inputs and data.

Base output of water leached (inches): 57.6

Input parameter	Base input	Units	+60% input	-60% input	+60% output	-60% output	% change w/ +60% input	% change w/ - 60% input	Avg. % change
AWHC L3	0.13	in/in	0.21	0.052	55.9	59.2	2.9	2.8	2.9
Bulk Density L1	1.13	g/cm ³	1.81	0.45	57.6	57.6	0.0	0.0	0.0
Bulk Density L2	1.15	g/cm ³	1.84	0.46	57.6	57.6	0.0	0.0	0.0
Bulk Density L3	1.15	g/cm ³	1.84	0.46	57.6	57.6	0.0	0.0	0.0
Bulk Density LS	1.12	g/cm ³	1.792	0.448	57.6	57.6	0.0	0.0	0.0
CEC 1	14.9	meq/100g	23.84	5.96	57.6	57.6	0.0	0.0	0.0
Coarse Frag % L1	0.36	g/g	0.576	0.144	57.6	57.6	0.0	0.0	0.0
Coarse Frag % L2	0.17	g/g	0.272	0.068	57.6	57.6	0.0	0.0	0.0
Coarse Frag % L3	0.30	g/g	0.48	0.12	57.6	57.6	0.0	0.0	0.0
Coarse Frag % LS	0.39	g/g	0.624	0.156	57.6	57.6	0.0	0.0	0.0
consol evap depth heavy	2	in	3.2	0.8	57.6	57.6	0.0	0.0	0.0
consol evap depth light	4	in	6.4	1.6	57.6	57.6	0.0	0.0	0.0
Initial H2O L1	0.38	in/in	0.608	0.152	60.3	54.9	4.8	4.7	4.7
Initial H2O L2	0.37	in/in	0.592	0.148	60.2	54.9	4.6	4.6	4.6
Initial H2O L3	0.36	in/in	0.576	0.144	62.1	53.0	7.9	7.9	7.9
Initial H2O LS	0.38	in/in	0.608	0.152	57.6	57.6	0.0	0.0	0.0
Initial NH4 L1	10.20	in/in	16.32	4.08	57.6	57.6	0.0	0.0	0.0
Initial NH4 LS	0.85	in/in	1.36	0.34	57.6	57.6	0.0	0.0	0.0
Initial NO3 L1	4.00	lbs/acre	6.4	1.6	57.6	57.6	0.0	0.0	0.0
Initial NO3 L2	3.70	lbs/acre	5.92	1.48	57.6	57.6	0.0	0.0	0.0
Initial NO3 L3	6.10	lbs/acre	9.76	2.44	57.6	57.6	0.0	0.0	0.0
Initial NO3 LS	0.33	lbs/acre	0.528	0.132	57.6	57.6	0.0	0.0	0.0
Percent slope	4.5	unitless	7.2	1.8	57.6	57.6	0.0	0.0	0.0
Plant AWHC L1	0.13	in/in	0.208	0.052	54.7	63.0	5.0	9.5	7.2
Plant AWHC L2	0.13	in/in	0.208	0.052	56.6	59.5	1.8	3.3	2.5
PWP 1	0.13	in/in	0.208	0.052	56.6	58.5	1.6	1.6	1.6
PWP 2	0.13	in/in	0.208	0.052	56.6	58.5	1.6	1.6	1.6
PWP 3	0.13	in/in	0.208	0.052	55.9	59.2	2.8	2.8	2.8
Select Crop Ann H2Ofrac[1]	0.659	unitless	1.05	0.26	57.6	57.6	0.0	0.0	0.0
Soil OrgM % C L1	28.3	unitless	45.3	11.3	57.6	57.6	0.0	0.0	0.0
Soil OrgM % C LS	28.5	unitless	45.6	11.4	57.6	57.6	0.0	0.0	0.0
Soil OrgM % L1	7.68	unitless	12.3	3.1	57.6	57.6	0.0	0.0	0.0
Soil OrgM % LS	8.03	unitless	12.8	3.2	57.6	57.6	0.0	0.0	0.0
Soil OrgM CN L1	12.2	unitless	19.5	4.9	57.6	57.6	0.0	0.0	0.0
Soil OrgM CN LS	12.0	unitless	19.2	4.8	57.6	57.6	0.0	0.0	0.0
Soil pH L1	5.96	pH units	9.54	2.38	57.6	57.6	0.0	0.0	0.0
ET	*	mm	*	*	52.2	66.7	9.3	16	13
Rainfall	*	mm	*	*	99.6	17.9	73	69	71
T Min	*	deg. C	*	*	57.6	57.6	0.034	0.048	0.041
T Max	*	deg. C	*	*	57.5	57.6	0.17	0.0	0.085
Internal model parameter									
Effective precipitation	0.21	unitless	0.336	0.084	57.6	57.6	0.0	0.0	0.0
Runoff Adjust Factor	0.0	unitless	1	0	36.9	57.6	35.8	0.0	18
CCFAC A	0.87	unitless	1.4	0.35	57.2	58.5	0.7	1.7	1.2
particle density LS	2.65	g/cm ³	4.24	1.06	57.6	57.6	0.0	0.0	0.0
particle density L1	2.65	g/cm ³	4.24	1.06	57.6	57.6	0.0	0.0	0.0
particle density L2	2.65	g/cm ³	4.24	1.06	57.6	57.6	0.0	0.0	0.0
particle density L3	2.65	g/cm ³	4.24	1.06	57.6	57.6	0.0	0.0	0.0
K N2O Leakage	0.065	unitless	0.104	0.026	58	58	0.0	0.0	0.0

*See climate data table for climate inputs

Table 7. Nitrogen dynamics sub-model sensitivity inputs and data.

Base output of nitrate leached (lbs NO ₃ -N/acre):			132						
Input parameter	Base input	Units	+60% input	-60% input	+60% output	-60% output	% change w/ +60% input	% change w/ 60% input	Avg. % change
AWHC L3	0.13	in/in	0.21	0.052	132	312	0.0	136	68
Bulk Density L1	1.13	g/cm ³	1.81	0.45	222	47	68	65	66
Bulk Density L2	1.15	g/cm ³	1.84	0.46	140	126	5.5	4.5	5.0
Bulk Density L3	1.15	g/cm ³	1.84	0.46	140	124	5.8	6.7	6.3
Bulk Density LS	1.12	g/cm ³	1.792	0.448	133	133	0.52	0.50	0.51
CEC 1	14.9	meq/100g	23.84	5.96	132	129	0.0	2.5	1.2
Coarse Frag % L1	0.36	g/g	0.576	0.144	132	134	0.74	0.96	0.85
Coarse Frag % L2	0.17	g/g	0.272	0.068	132	133	0.0	0.0	0.0
Coarse Frag % L3	0.30	g/g	0.48	0.12	132	133	0.0	0.0	0.0
Coarse Frag % LS	0.39	g/g	0.624	0.156	133	132	0.59	0.28	0.44
consol evap depth heavy	2	in	3.2	0.8	132	132	0.0	0.0	0.0
consol evap depth light	4	in	6.4	1.6	132	132	0.0	0.0	0.0
Initial H2O L1	0.38	in/in	0.608	0.152	133	133	0.48	0.09	0.28
Initial H2O L2	0.37	in/in	0.592	0.148	133	131	0.43	0.78	0.60
Initial H2O L3	0.36	in/in	0.576	0.144	133	132	0.0	0.0	0.0
Initial H2O LS	0.38	in/in	0.608	0.152	132	132	0.0	0.0	0.0
Initial NH4 L1	10.20	in/in	16.32	4.08	136	129	2.7	2.6	2.7
Initial NH4 LS	0.85	in/in	1.36	0.34	133	132	0.23	0.27	0.25
Initial NO3 L1	4.00	lbs/acre	6.4	1.6	134	131	0.92	0.92	0.92
Initial NO3 L2	3.70	lbs/acre	5.92	1.48	134	131	1.0	1.0	1.0
Initial NO3 L3	6.10	lbs/acre	9.76	2.44	136	129	2.7	2.7	2.7
Initial NO3 LS	0.33	lbs/acre	0.528	0.132	133	132	0.08	0.08	0.08
Percent slope	4.5	unitless	7.2	1.8	132	132	0.0	0.0	0.0
Plant AWHC L1	0.13	in/in	0.208	0.052	168	104	26.8	21.4	24.1
Plant AWHC L2	0.13	in/in	0.208	0.052	132	133	0.21	0.20	0.20
PWP 1	0.13	in/in	0.208	0.052	186	92	41	31	36
PWP 2	0.13	in/in	0.208	0.052	132	146	0.21	10	5.3
PWP 3	0.13	in/in	0.208	0.052	132	132	0.0	0.0	0.0
Select Crop Ann H2Ofrac[1]	0.659	unitless	1.05	0.26	132	132	0.0	0.0	0.0
Soil OrgM % C L1	28.3	unitless	45.3	11.3	203	61	54	54	54
Soil OrgM % C LS	28.5	unitless	45.6	11.4	133	133	0.51	0.39	0.45
Soil OrgM % L1	7.68	unitless	12.3	3.1	204	67	54	50	52
Soil OrgM % LS	8.03	unitless	12.8	3.2	133	133	0.28	0.29	0.28
Soil OrgM CN L1	12.2	unitless	19.5	4.9	132	135	0.71	1.6	1.1
Soil OrgM CN LS	12.0	unitless	19.2	4.8	132	133	0.08	0.06	0.07
Soil pH L1	5.96	pH units	9.54	2.38	128	132	3.6	0.0	1.8
ET in mm	*	mm	*	*	126	157	5.0	18	12
Rainfall in mm	*	mm	*	*	151	48	14	64	39
T Min	*	deg. C	*	*	146	120	10	9.7	9.9
T Max	*	deg. C	*	*	164	105	24	20	22
Internal model parameter									
Effective precipitation	0.21	unitless	0.336	0.084	140	113	5.4	15	10
Runoff Adjust Factor	0.0	unitless	1	0	91	132	31	0.0	16
CCFAC A	0.87	unitless	1.4	0.35	131	133	1.4	0.34	0.86
particle density LS	2.65	g/cm ³	4.24	1.06	132	132	0.0	0.0	0.0
particle density L1	2.65	g/cm ³	4.24	1.06	99	8.2	25	94	59
particle density L2	2.65	g/cm ³	4.24	1.06	129	6.1	2.9	95	49
particle density L3	2.65	g/cm ³	4.24	1.06	127	0.0	4.1	100	52
K N2O Leakage	0.065	unitless	0.104	0.026	130	134	1.9	1.5	1.7

*See climate data table for climate inputs

Table 8. Soil water sub-model sensitivity analysis ranks.

Rank	Input	Avg. % Change
1	Rainfall in mm	71
2	Runoff Adjust Factor*	18
3	ET in mm	13
4	Initial H2O L3*	7.9
5	Plant AWHC L1*	7.2
6	Initial H2O L1*	4.7
7	Initial H2O L2*	4.6
8	AWHC L3*	2.9
9	PWP 3*	2.8
10	Plant AWHC L2*	2.5
11	PWP 1*	1.6
12	PWP 2*	1.6
13	CCFAC A*	1.2
14	T Max	0.085
15	T Min	0.041
16	Bulk Density L1	0.0
17	Bulk Density L2	0.0
18	Bulk Density L3	0.0
19	Bulk Density LS	0.0
20	CEC 1	0.0
21	Coarse Frag % L1	0.0
22	Coarse Frag % L2	0.0
23	Coarse Frag % L3	0.0
24	Coarse Frag % LS	0.0
25	consol evap depth heavy	0.0
26	consol evap depth light	0.0
27	Initial H2O LS	0.0
28	Initial NH4 L1	0.0
29	Initial NH4 LS	0.0
30	Initial NO3 L1	0.0
31	Initial NO3 L2	0.0
32	Initial NO3 L3	0.0
33	Initial NO3 LS	0.0
34	Percent slope	0.0
35	Select Crop Ann H2Ofrac[1]	0.0
36	Soil OrgM % C L1	0.0
37	Soil OrgM % C LS	0.0
38	Soil OrgM % L1	0.0
39	Soil OrgM % LS	0.0
40	Soil OrgM CN L1	0.0
41	Soil OrgM CN LS	0.0
42	Soil pH L1	0.0
43	Effective precipitation	0.0
44	particle density LS	0.0
45	particle density L1	0.0
46	particle density L2	0.0
47	particle density L3	0.0
48	K N2O Leakage	0.0

*Inputs used in the water sub-model calibration. Excludes climate inputs.

Table 9. Nitrogen dynamics sub-model sensitivity analysis ranks.

Rank	Input	Avg. % Change
1	AWHC L3*	68
2	Bulk Density L1*	66
3	particle density L1*	59
4	Soil OrgM % C L1*	54
5	particle density L3*	52
6	Soil OrgM % L1*	52
7	particle density L2*	49
8	Rainfall in mm	39
9	PWP 1*	36
10	Plant AWHC L1*	24
11	T Max	22
12	Runoff Adjust Factor*	16
13	ET in mm	12
14	Effective precipitation*	10
15	T Min	9.9
16	Bulk Density L3*	6.3
17	PWP 2*	5.3
18	Bulk Density L2*	5.0
19	Initial NO3 L3	2.7
20	Initial NH4 L1	2.7
21	Soil pH L1	1.8
22	K N2O Leakage	1.7
23	CEC 1	1.2
24	Soil OrgM CN L1	1.1
25	Initial NO3 L2	0.98
26	Initial NO3 L1	0.92
27	CCFAC A	0.86
28	Coarse Frag % L1	0.85
29	Initial H2O L2	0.60
30	Bulk Density LS	0.51
31	Soil OrgM % C LS	0.45
32	Coarse Frag % LS	0.44
33	Soil OrgM % LS	0.28
34	Initial H2O L1	0.28
35	Initial NH4 LS	0.25
36	Plant AWHC L2	0.20
37	Initial NO3 LS	0.08
38	Soil OrgM CN LS	0.07
39	Coarse Frag % L3	0.02
40	Coarse Frag % L2	0.01
41	Initial H2O L3	0.01
42	PWP 3	0.0023
43	consol evap depth heavy	0.0
44	consol evap depth light	0.0
45	Initial H2O LS	0.0
46	Percent slope	0.0
47	Select Crop Ann H2Offrac[1]	0.0
48	particle density LS	0.0

*Inputs used in the nitrogen sub-model calibration. Effected at least a 5% change on the nitrate leached output. Excludes climate inputs.

Table 10. Uncertainty analysis inputs.

Input parameter	Base Value	Minimum Value	Maximum Value	Units	Data source
Bulk Density L1	1.13	1.02	1.26	g/cm ³	max/min measured values for specified soil layer depth from 1997 study on field 9420
Bulk Density L2	1.15	0.99	1.30	g/cm ³	max/min measured values for specified soil layer depth from 1997 study on field 9421
Bulk Density L3	1.15	0.99	1.30	g/cm ³	max/min measured values for specified soil layer depth from 1997 study on field 9422
Bulk Density LS	1.12	1.02	1.18	g/cm ³	max/min measured values for specified soil layer depth from 1997 study on field 9419
CEC 1	14.9	10.9	17.0	meq/100g	min/max for a Monroe silt loam from the Agassiz soil survey
Coarse Frag % L1	0.36	0.03	1.34	unitless	min/max of all measurements by soil layer
Coarse Frag % L2	0.17	0.01	0.52	unitless	min/max of all measurements by soil layer
Coarse Frag % L3	0.30	0.02	1.72	unitless	min/max of all measurements by soil layer
Coarse Frag % LS	0.39	0.06	1.34	unitless	min/max of all measurements by soil layer
consol evap depth heavy	2	1	3	inches	min is the default minus 1/3 and max is the default plus 1/3
consol evap depth light	4	3	5	inches	min is the default minus 1/3 and max is the default plus 1/3
Initial H2O L1	0.38	0.32	0.43	inch/inch	min/max of initial gravimetric soil moisture data by soil layer
Initial H2O L2	0.37	0.30	0.44	inch/inch	min/max of initial gravimetric soil moisture data by soil layer
Initial H2O L3	0.36	0.33	0.39	inch/inch	min/max of initial gravimetric soil moisture data by soil layer
Initial H2O LS	0.38	0.32	0.43	inch/inch	min/max of initial gravimetric soil moisture data by soil layer
Initial NH4 L1	10.2	7.7	12.4	lbs NH ₄ -N/acre	min/max of initial soil extract nutrient data by soil layer
Initial NH4 LS	0.85	0.64	1.0	lbs NH ₄ -N/acre	min/max of initial soil extract nutrient data by soil layer
Initial NO3 L1	4.0	2.9	6.2	lbs NO ₃ -N/acre	min/max of initial soil extract nutrient data by soil layer
Initial NO3 L2	3.7	2.2	5.5	lbs NO ₃ -N/acre	min/max of initial soil extract nutrient data by soil layer
Initial NO3 L3	6.1	4.6	9.5	lbs NO ₃ -N/acre	min/max of initial soil extract nutrient data by soil layer
Initial NO3 LS	0.33	0.25	0.52	lbs NO ₃ -N/acre	min/max of initial soil extract nutrient data by soil layer
Percent slope	4.5	0	9	unitless	range of percent slope values from Agassiz Soil Survey
Plant AWHC L1	0.13	0.11	0.13	in/in	min is the Plant AWHC for a loam from Brady (1974) and the initial value and the maximum value are the Plant AWHC was for a silt loam
Plant AWHC L2	0.13	0.11	0.13	in/in	min is the Plant AWHC for a loam from Brady (1974) and the initial value and the maximum value are the Plant AWHC was for a silt loam
Plant AWHC L3	0.13	0.11	0.13	in/in	min is the Plant AWHC for a loam from Brady (1974) and the initial value and the maximum value are the Plant AWHC was for a silt loam
PWP 1	0.13	0.11	0.16	in/in	min is the PWP for a loam and max is the PWP for a clay loam from Brady (1974)
PWP 2	0.13	0.11	0.16	in/in	min is the PWP for a loam and max is the PWP for a clay loam from Brady (1974)
PWP 3	0.13	0.11	0.16	in/in	min is the PWP for a loam and max is the PWP for a clay loam from Brady (1974)
Select Crop Ann H2Ofrac[1]	0.659	0.650	0.673	unitless	min/max final corn harvest moisture fractions
Select Crop Ann MaxYld[1]	7.44	6.88	8.35	tons/acre	min/max final corn harvest yield measurements
Select Crop Ann N%[1]	1.15	0.93	1.34	unitless	min/max of final corn harvest Leco N% measurements
Soil OrgM % C L1	28.3	23.6	29.7	unitless	min/max of all measurements by soil layer
Soil OrgM % C LS	28.5	21.1	29.7	unitless	min/max of all measurements by soil layer
Soil OrgM % L1	7.68	6.01	9.39	unitless	min/max of all measurements by soil layer
Soil OrgM % LS	8.03	7.26	9.39	unitless	min/max of all measurements by soil layer
Soil OrgM CN L1	12.2	11.1	13.5	unitless	min/max of all measurements by soil layer
Soil OrgM CN LS	12.0	11.1	12.9	unitless	min/max of all measurements by soil layer
Soil pH L1	5.96	5.31	6.39	pH units	min/max of all measured values in depth 2 lysimeter samples

Table 11. Model calibration efficiency coefficients (E_f).

Model output	Number of observations	Uncalibrated E_f	Calibrated E_f
Overall model average		-2.19	-0.17
Overall soil water sub-model average		-1.82	-0.63
SOIL WATER L1	28	-0.84	-0.86
SOIL WATER L2	10	-1.80	-0.38
SOIL WATER L3	10	-2.84	-0.64
Overall nitrogen sub-model average		-2.34	0.02
LYS NO3 L2	10	-0.39	-0.32
LYS NO3 L3	10	-0.50	-0.43
SOIL NO3 L1	26	0.76	0.71
SOIL NO3 L2	13	-0.44	-0.42
SOIL NO3 L3	12	-0.39	-0.36
SOIL NH4 L1	26	0.65	0.64
N2O	28	-16.08	0.31

Table 12. Soil-water sub-model calibration parameters.

Soil Water Sub-Model Calibration

Model parameter	Units	Base value	Calibrated value	Allowable Min.	Allowable Max.	Min./Max. Data Source
Runoff Adjust Factor	unitless	0	0.20	0	1	limits defined by NLOS
Initial H2O L3	in/in	0.36	0.36	0.33	0.39	min/max of initial gravimetric soil moisture data by soil layer
Plant AWHC L1	in/in	0.13	0.13	0.11	0.13	min/max are the Plant AWHCs for a loam and silt loam, respectively, from Brady (1974)
Initial H2O L1	in/in	0.38	0.38	0.32	0.43	min/max of initial gravimetric soil moisture data by soil layer
Initial H2O L2	in/in	0.37	0.37	0.3	0.44	min/max of initial gravimetric soil moisture data by soil layer
AWHC L3	in/in	0.13	0.13	0.11	0.13	min/max are the Plant AWHCs for a loam and silt loam, respectively, from Brady (1974)
PWP 3	in/in	0.13	0.16	0.11	0.16	min/max are the PWPs for a loam a clay loam, respectively, from Brady (1974)
Plant AWHC L2	in/in	0.13	0.13	0.11	0.13	min/max are the Plant AWHCs for a loam and silt loam, respectively, from Brady (1974)
PWP 1	in/in	0.13	0.13	0.11	0.16	min/max are the PWPs for a loam a clay loam, respectively, from Brady (1974)
PWP 2	in/in	0.13	0.16	0.11	0.16	min/max are the PWPs for a loam a clay loam, respectively, from Brady (1974)
CCFAC A	unitless	0.87	0.87	0	1	limits defined by NLOS

Table 13. Nitrogen sub-model calibration parameters.

Nitrogen Sub-Model Calibration

<u>Model parameter</u>	<u>Units</u>	<u>Base value</u>	<u>Calibrated value</u>	<u>Allowable Min.</u>	<u>Allowable Max.</u>	<u>Min./Max. Data Source</u>
AWHC L3	in/in	0.13	0.13	0.11	0.13	min/max are the Plant AWHCs for a loam and silt loam, respectively, from Brady (1974)
Bulk Density L1	g/cm ³	1.13	1.13	1.02	1.26	min/max of measured values by soil layer from 1997 study on field 9420
particle density L1	g/cm ³	2.65	2.65	2.33	2.7	min is for a no-till, silt loam, agricultural soil treated with beef cattle manure from Blanco-Canqui et al. (2006); max is the high-end of the standard range of particle densities used for computing porosity
Soil OrgM % C L1	unitless	28.3	25.1	23.6	29.7	min/max of all measurements by soil layer
particle density L3	g/cm ³	2.65	2.33	2.33	2.7	min is for a no-till, silt loam, agricultural soil treated with beef cattle manure from Blanco-Canqui et al. (2006); max is the high-end of the standard range of particle densities used for computing porosity
Soil OrgM % L1	unitless	7.68	7.68	6.01	9.39	min/max of all measurements by soil layer
particle density L2	g/cm ³	2.65	2.35	2.33	2.7	min is for a no-till, silt loam, agricultural soil treated with beef cattle manure from Blanco-Canqui et al. (2006); max is the high-end of the standard range of particle densities used for computing porosity
PWP 1	in/in	0.13	0.13	0.11	0.16	min/max are the PWPs for a loam a clay loam, respectively, from Brady (1974)
Plant AWHC L1	in/in	0.13	0.13	0.11	0.13	min/max are the Plant AWHCs for a loam and silt loam, respectively, from Brady (1974)
Runoff Adjust Factor	unitless	0	0.2	0	1	limits defined by NLOS
Effective precipitation	unitless	0.21	0.8	0	1	limits defined by NLOS

Table 14. Balanced nitrogen budget from the calibrated model simulation.

Initial N	lbs N/acre	% of Total Initial N	Description
NH4 START ALL	11	0.21	Initial user-entered ammonium in all soil layers
NO3 START ALL	14	0.26	Initial user-entered nitrate in all soil layers
INITIAL SOIL ORGM N LS	482	9.0	Initial user-entered soil organic matter in the surface layer
INITIAL SOIL ORGM N L1	4838	91	Initial user-entered soil organic matter in soil layer 1
Total	5345		
N Additions	lbs N/acre	% of Total Added N	
ACCUM FERT APPLIC NH4 LS[APPLIC 1]	45	25	Accumulation of ammonium in the surface layer from fertilizer application 1
ACCUM FERT APPLIC NH4 LS[APPLIC 2]	60	34	Accumulation of ammonium in the surface layer from fertilizer application 2
ACCUM FERT APPLIC NH4 LS[APPLIC 3]	28	16	Accumulation of ammonium in the surface layer from fertilizer application 3
ACCUM FERT APPLIC NO3 LS[APPLIC 1]	45	25	Accumulation of nitrate in the surface layer from fertilizer application 1
ACCUM FERT APPLIC NO3 LS[APPLIC 2]	0.0	0.0	Accumulation of nitrate in the surface layer from fertilizer application 2
ACCUM FERT APPLIC NO3 LS[APPLIC 3]	0.0	0.0	Accumulation of nitrate in the surface layer from fertilizer application 3
Total	177		
N Removed	lbs N/acre	% of Total Removed N	
NH4 VOLAT	6.0	1.8	Ammonium volatilized from the surface layer
NO3 LEACHED	140	42	Nitrate leached out of soil layer 3
TOTAL NO3 DENITR TO N2 OR N LS	-0.050	-0.015	Nitrate denitrified from the surface layer and released as either dinitrogen or nitrogen gas
TOTAL NO3 DENITR TO N2 OR N L1	6.4	1.9	Nitrate denitrified from soil layer 1 and released as either dinitrogen or nitrogen gas
TOTAL NO3 DENITR TO N20 LS	0.050	0.015	Nitrous oxide emissions from the soil surface produced as a by-product of the denitrification of nitrate
TOTAL NO3 DENITR TO N20 L1	5.1	1.5	Nitrous oxide emissions from soil layer 1 produced as a by-product of the denitrification of nitrate
N20 NITRIF LS	0.58	0.17	Ammonium nitrification to nitrous oxide for the soil layer
N20 NITRIF L1	0.90	0.27	Ammonium nitrification to nitrous oxide for soil layer 1
TOTAL NH4 A CROP L1	3.9	1.2	Annual crop uptake of ammonium from soil layer 1
TOTAL NO3 A CROP L1	136	41	Annual crop uptake of nitrate from soil layer 1
TOTAL NO3 A CROP L2	27	8.1	Annual crop uptake of nitrate from soil layer 2
TOTAL NH4 IMMOB LS	0.0	0.0	Ammonium immobilized from the surface layer
TOTAL NH4 IMMOB L1	0.0	0.0	Ammonium immobilized from soil layer 1
TOTAL NO3 IMMOB LS	0.0	0.0	Nitrate immobilized from the surface layer
TOTAL NO3 IMMOB L1	0.0	0.0	Nitrate immobilized from soil layer 1
TOTAL NH4 RUNOFF	0.0	0.0	Runoff of ammonium
TOTAL NO3 RUNOFF LS	0.0	0.0	Runoff of nitrate from the surface layer
TOTAL NO3 RUNOFF L1	6.1	1.8	Runoff of nitrate from soil layer 1
TOTAL NH4 ERODED	0.0	0.0	Total ammonium erosion (currently not simulated)
TOTAL NO3 ERODED LS	0.0	0.0	Total nitrate erosion from the soil surface (currently not simulated)
TOTAL NO3 ERODED L1	0.0	0.0	Total nitrate erosion from soil layer 1 (currently not simulated)
Total	332		
Current N	lbs N/acre	% of Total Current N	
NH4 END ALL	0.0	0.0	Final ammonium in all soil layers
NO3 END ALL	37	0.72	Final nitrate in all soil layers
SOIL OM N FAST LS	24	0.45	Final soil organic matter nitrogen in the fast pool of the surface layer
SOIL OM N SLOW LS	458	8.8	Final soil organic matter nitrogen in the slow pool of the surface layer
SOIL OM N FAST L1	0.0	0.0	Final soil organic matter nitrogen in the fast pool of soil layer 1
SOIL OM N SLOW L1	4671	90	Final soil organic matter nitrogen in the slow pool of soil layer 1
Total	5190		
INPUTS + ADDITIONS	5522.07		
REMOVED + CURRENT	5522.08		
DIFFERENCE	-0.01		

Table 15. Kruskal Wallis confirmatory test results.

P-values

<u>variable</u>	<u>depth</u>	<u>plot</u>	<u>replicate</u>	<u>splashplate</u>
cn	0.93	0.075	0.11	0.074
coarsefrag	0.93	NA	0.014	NA
om	0.14	0.088	0.078	0.12
moist	0.88	0.025	0.0038	0.28
soil.nh4	4.6E-07	0.99	0.75	0.94
soil.no3	0.14	0.42	0.55	0.14

Accept (A) or Reject (R) H₀

<u>variable</u>	<u>depth</u>	<u>plot</u>	<u>replicate</u>	<u>splashplate</u>
cn	A	A	A	A
coarsefrag	A	NA	R	NA
om	A	A	A	A
moist	A	R	R	A
soil.nh4	R	A	A	A
soil.no3	A	A	A	A

cn = carbon to nitrogen ratio of organic matter (unitless)

coarsefrag = coarse fragment percentage (g/g)

om = organic matter content (% of dry weight)

moist = soil moisture (g/g)

soil.nh4 = soil ammonium ($\mu\text{g NH}_4\text{-N/L}$)

soil.no3 = soil nitrate ($\mu\text{g NO}_3\text{-N/L}$)

Table 16. Pairwise Wilcoxon Rank Sums Test results.

P-values

soil.nh4 by depth

	1	2	3	4
2	0.1304	NA	NA	NA
3	0.0016	0.0016	NA	NA
4	0.0016	0.0016	0.0019	NA
5	0.0016	0.0016	0.0016	0.0140

Accept (A) or Reject (R) H₀

soil.nh4 by depth

	1	2	3	4
2	A	NA	NA	NA
3	R	R	NA	NA
4	R	R	R	NA
5	R	R	R	R

moist by plot

	103	104	223	224	311	312	331
104	1.00	NA	NA	NA	NA	NA	NA
223	0.76	0.43	NA	NA	NA	NA	NA
224	1.00	0.76	1.00	NA	NA	NA	NA
311	1.00	0.76	1.00	1.00	NA	NA	NA
312	0.46	0.22	1.00	1.00	1.00	NA	NA
331	1.00	1.00	1.00	1.00	1.00	1.00	NA
332	1.00	1.00	1.00	1.00	1.00	1.00	1.00

moist by plot

	103	104	223	224	311	312	331
104	no sig.	NA	NA	NA	NA	NA	NA
223	A	A	NA	NA	NA	NA	NA
224	no sig.	A	no sig.	NA	NA	NA	NA
311	no sig.	A	no sig.	no sig.	NA	NA	NA
312	A	A	no sig.	no sig.	no sig.	NA	NA
331	no sig.	NA					
332	no sig.						

coarsefrag by rep

	1	2	3
2	0.048	NA	NA
3	0.159	0.452	NA
4	0.159	0.452	1.000

coarsefrag by rep

	1	2	3
2	R	NA	NA
3	A	A	NA
4	A	A	no sig.

moist by rep

	1	2	3
2	0.0068	NA	NA
3	0.0101	1.0000	NA
4	0.0446	1.0000	1.0000

moist by rep

	1	2	3
2	R	NA	NA
3	R	no sig.	NA
4	R	no sig.	no sig.

H₀ = null hypothesis
 coarsefrag = coarse fragment percentage (g/g)
 moist = soil moisture (g/g)
 soil.nh4 = soil ammonium (µg NH₄-N/L)
 soil.no3 = soil nitrate (µg NO₃-N/L)
 no sig. = no significance

Table 17. Balanced water budget from the calibrated model simulation.

INPUTS	Inches of Water	% of Total Inputs	Description
WATER START L1	4.6	5.1	Initial user-entered water in soil layer 1
WATER START L2	4.4	5.0	Initial user-entered water in soil layer 2
WATER START L3	7.6	8.4	Initial user-entered water in soil layer 3
WATER PRECIP	73	81	Total user-entered water as precipitation
TOTAL	90		
OUTPUTS	Inches of Water	% of Total Outputs	
WATER RUNOFF	3.5	4.6	Runoff of water
WATER LEACHED	53	68	Total water leached out of soil layer 3
TOTAL ACTUAL EVAPOTRANSPIRATION	21	27	The potential evapotranspiration from the user-entered climate data adjusted to account for water deficits
TOTAL	78		
CURRENT	Inches of Water	% of Total Current	
WATER L1	2.4	20	Final water in soil layer 1
WATER L2	3.5	29	Final water in soil layer 2
WATER L3	6.1	51	Final water in soil layer 3
TOTAL	12		
INPUTS	89.50		
OUTPUTS + CURRENT	89.48		
DIFFERENCE	0.02		

Table 18. Summary statistics for the simulation values of nitrate leached for uncertainty analysis.

Summary Statistics	
Minimum	43
Maximum	195
Median	130
Mean	131
Standard Deviation	22
Sample Size	2000
Skewness	0.045
Kurtosis	0.019
Standard Error	0.49
95% Lower Bound	90
95% Upper Bound	175

Table 19. Porosity and percent saturation at maximum observed soil water content.

Soil Layer	Soil Thickness (in)	Porosity (in/in)	Porosity (in)	Max. Observed Soil Water Content (in/in)	Max. Observed Soil Water Content (in)	Saturation (%); cannot exceed 100%
L1	12	0.574	6.9	0.66	7.9	100
L2	12	0.489	5.9	0.47	5.6	96
L3	21	0.485	10.2	0.47	9.9	97

Table 20. Model calibration efficiency coefficients (E_f) for the wet vs. dry months.

Model output	E_f		E_f	
	October-April	$n_{\text{wet months}}^*$	April-October	$n_{\text{dry months}}^*$
Overall model average	-5.13		-0.53	
Overall soil water sub-model average	-5.24		-0.76	
SOIL WATER L1	-4.25	14	-1.14	14
SOIL WATER L2	-8.68	5	0.02	5
SOIL WATER L3	-2.79	5	-1.17	5
Overall nitrogen sub-model average	-5.08		-0.43	
LYS NO3 L2	-0.65	5	-0.93	5
LYS NO3 L3	-0.87	5	-1.95	5
SOIL NO3 L1	-18.32	10	0.59	16
SOIL NO3 L2	0.72	6	-1.03	7
SOIL NO3 L3	0.67	6	-0.57	6
SOIL NH4 L1	-17.22	10	0.58	16
N2O	0.09	14	0.32	14

* n = the number of observations

Table 21. Linear regression coefficients (R^2) from the correlation analysis of the simulated and observed values.

Model output	Regression coefficients (R^2)	
	Uncalibrated Model	Calibrated Model
Nitrate Leached L2	0.63	0.63
Nitrate Leached L3	0.80	0.84
Soil Nitrate L1	0.84	0.84
Soil Nitrate L2	0.0031	0.011
Soil Nitrate L3	0.0019	0.0092
Soil Ammonium L1	0.87	0.87
Nitrous Oxide Emissions	0.27	0.33
Soil Water L1	0.54	0.53
Soil Water L2	0.50	0.58
Soil Water L3	0.43	0.45
Average R^2	0.49	0.51

Table 22. Soil hydraulic characteristics.

	Soil layer Soil layer thickness (in)	Plant AWHC (in/in)	PWP (in/in)	WHC (in)	Bound Water (in)	WHC + Bound Water (in)
L1	12	0.13	0.13	1.56	1.56	3.12
L2	12	0.13	0.16	1.56	1.92	3.48
L3	21	0.13	0.16	2.73	3.36	6.09

Table 23. Hypothetical scenario descriptions.

Hypothetical Scenario	Description
1	No fertilizer and no crop for comparison to background soil nutrient and water conditions
2	Fertilizer applied on day 212 (7/30/04), the peak of crop growth according to the crop nitrate uptake curve from the calibrated simulation
3	Fertilizer applied on day 170 (6/18/04), the first day of a long stretch of low precipitation days
4	Fertilizer applied as a user-defined blend (24% N, 75% of N as NH ₄ , 25% of N as NO ₃) on 3 days: 140 (5/19/04), 184 (7/2/04), and 228 (8/15/04), which represent crop planting, 1/3, 2/3 through crop growth, at 1/3 the total application amount each time (251 lbs/acre)
5	No fertilizer and no crop run with study period weather data repeated for a total of 1500 simulation days (the maximum allowed by the model; equivalent to just over 4 years)

Table 24. Hypothetical scenario balanced nitrogen budgets.

	Calibrated Output	Hypothetical Scenarios				
		1	2	3	4	5
	lbs N/acre	lbs N/acre	lbs N/acre	lbs N/acre	lbs N/acre	lbs N/acre
Initial N						
NH4 START ALL	11	11	11	11	11	11
NO3 START ALL	14	14	14	14	14	14
INITIAL SOIL ORGM N LS	482	482	482	482	482	482
INITIAL SOIL ORGM N L1	4838	4838	4838	4838	4838	4838
Total	5345	5345	5345	5345	5345	5345
Additions						
ACCUM FERT APPLIC NH4 LS[APPLIC 1]	45	0.0	45	45	45	0
ACCUM FERT APPLIC NH4 LS[APPLIC 2]	60	0.0	60	60	45	0
ACCUM FERT APPLIC NH4 LS[APPLIC 3]	28	0.0	28	28	45	0
ACCUM FERT APPLIC NO3 LS[APPLIC 1]	45	0.0	45	45	15	0
ACCUM FERT APPLIC NO3 LS[APPLIC 2]	0.0	0.0	0.0	0.0	15	0
ACCUM FERT APPLIC NO3 LS[APPLIC 3]	0.0	0.0	0.0	0.0	15	0
Total	177	0.0	177	177	181	0
N Removed						
NH4 VOLAT	6.0	0.0	20	22	1.3	0.0
NO3 LEACHED	140	145	159	138	155	577
TOTAL NO3 DENITR LS	0.0	0.0	0.050	0.010	0.050	0.0
TOTAL NO3 DENITR L1	12	8.9	11	11	11	34
TOTAL NH4 A CROP L1	3.9	0.0	14	1.9	3.4	0.0
TOTAL NO3 A CROP L1	136	0.0	106	137	136	0.0
TOTAL NO3 A CROP L2	27	0.0	15	15	21	0.0
TOTAL NH4 IMMOB LS	0.0	0.0	0.0	0.0	0.0	0.0
TOTAL NH4 IMMOB L1	0.0	0.0	0.0	0.0	0.0	0.0
TOTAL NO3 IMMOB LS	0.0	0.0	0.0	0.0	0.0	0.0
TOTAL NO3 IMMOB L1	0.0	0.0	0.0	0.0	0.0	0.0
N2O NITRIF LS	0.58	0.59	0.58	0.65	0.60	2.2
N2O NITRIF L1	0.90	0.86	0.88	0.84	0.89	3.5
TOTAL NH4 RUNOFF	0.0	0.0	0.020	0.0	0.020	0.0
TOTAL NO3 RUNOFF LS	0.0	0.0	0.0	0.0	0.0	0.0
TOTAL NO3 RUNOFF L1	6.1	7.6	6.7	6.1	6.5	28
TOTAL NH4 ERODED	0.0	0.0	0.0	0.0	0.0	0.0
TOTAL NO3 ERODED LS	0.0	0.0	0.0	0.0	0.0	0.0
TOTAL NO3 ERODED L1	0.0	0.0	0.0	0.0	0.0	0.0
Total	332	163	332	332	336	644
Current N						
NH4 END ALL	0.0	0.46	0.0	0.0	0.0	0.48
NO3 END ALL	37	37	38	37	38	37
SOIL OM N FAST LS	24	24	24	24	24	22
SOIL OM N SLOW LS	458	458	458	458	458	458
SOIL OM N FAST L1	0.0	0.0	0.0	0.0	0.0	0.0
SOIL OM N SLOW L1	4671	4663	4671	4671	4671	4184
Total	5190	5182	5190	5190	5190	4701
INPUTS + ADDITIONS	5522.07	5345.07	5522.07	5522.07	5525.79	5345.07
REMOVED + CURRENT	5522.08	5345.07	5522.07	5522.08	5525.81	5345.09
DIFFERENCE	-0.01	0.00	0.00	-0.01	-0.02	-0.02

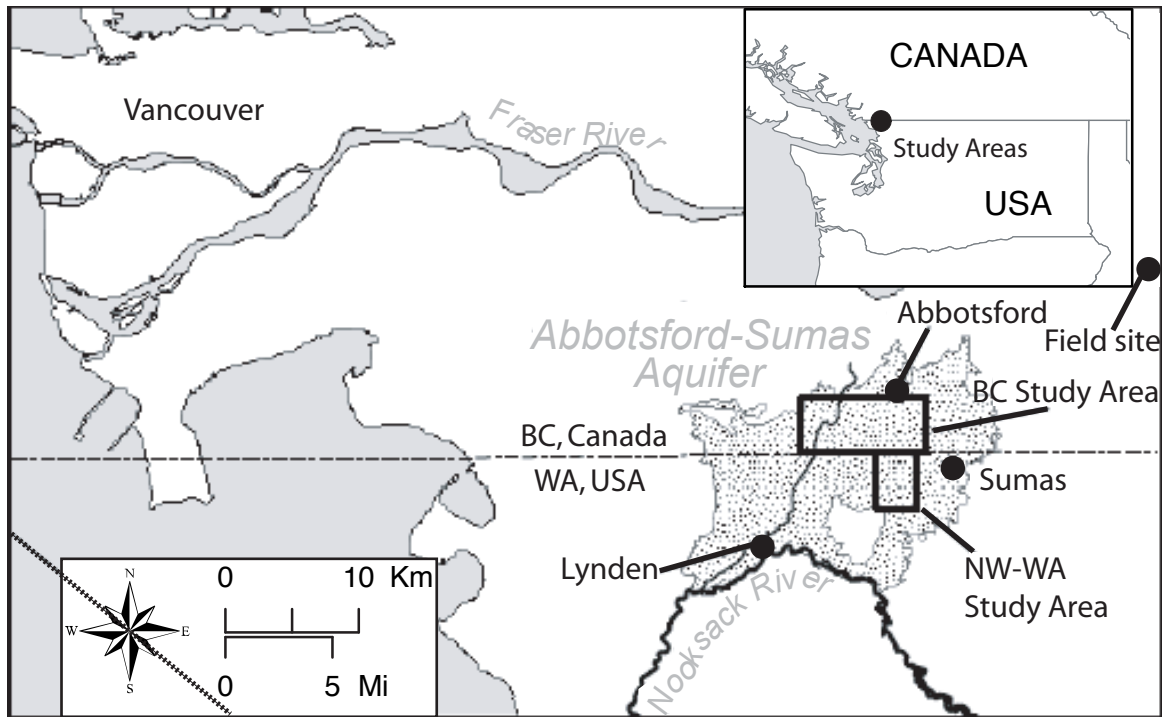


Figure 1. Field site location relative to the Abbotsford-Sumas aquifer study areas.

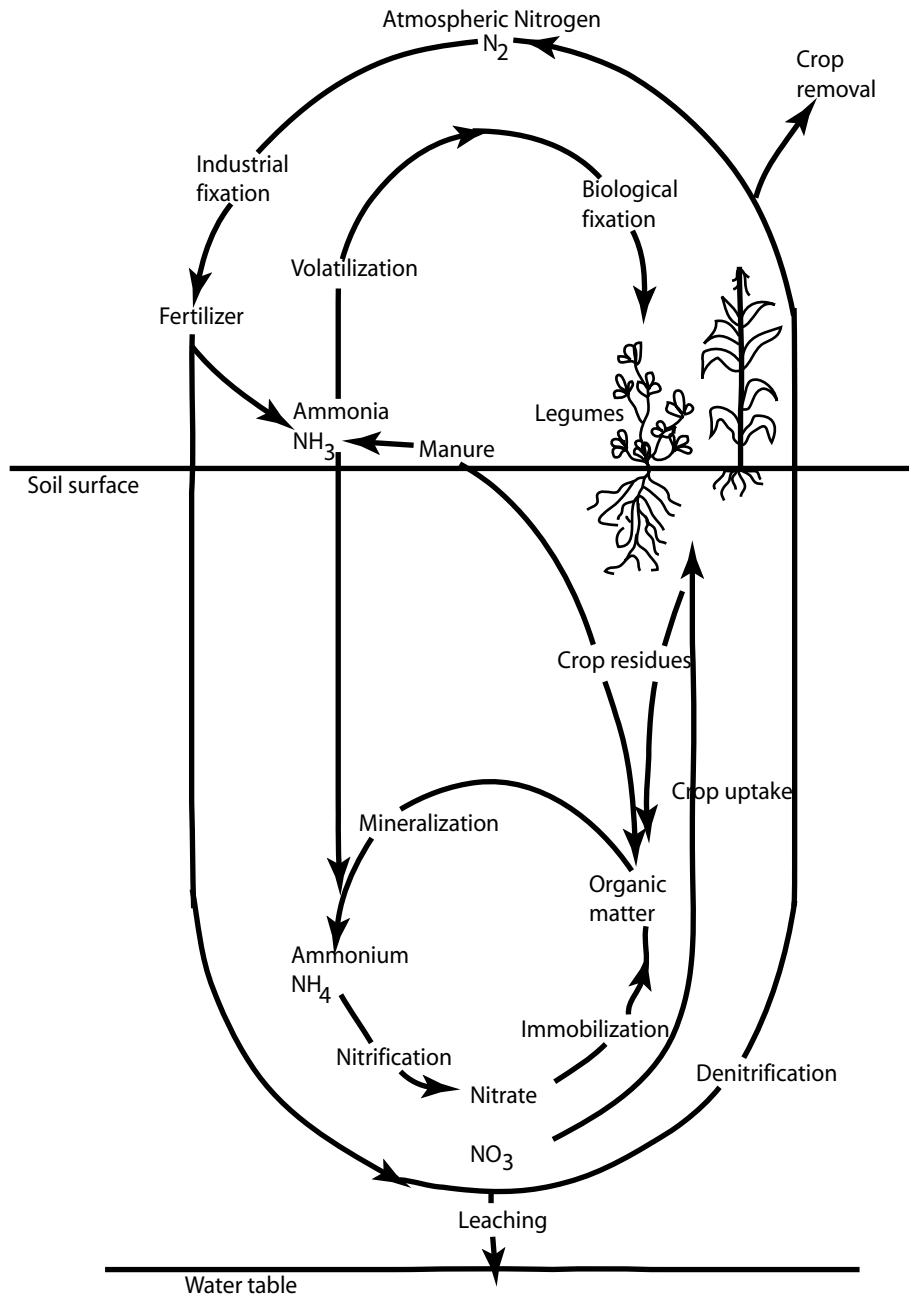


Figure 2. Nitrogen gains, losses, and transformations occurring in agricultural soils.

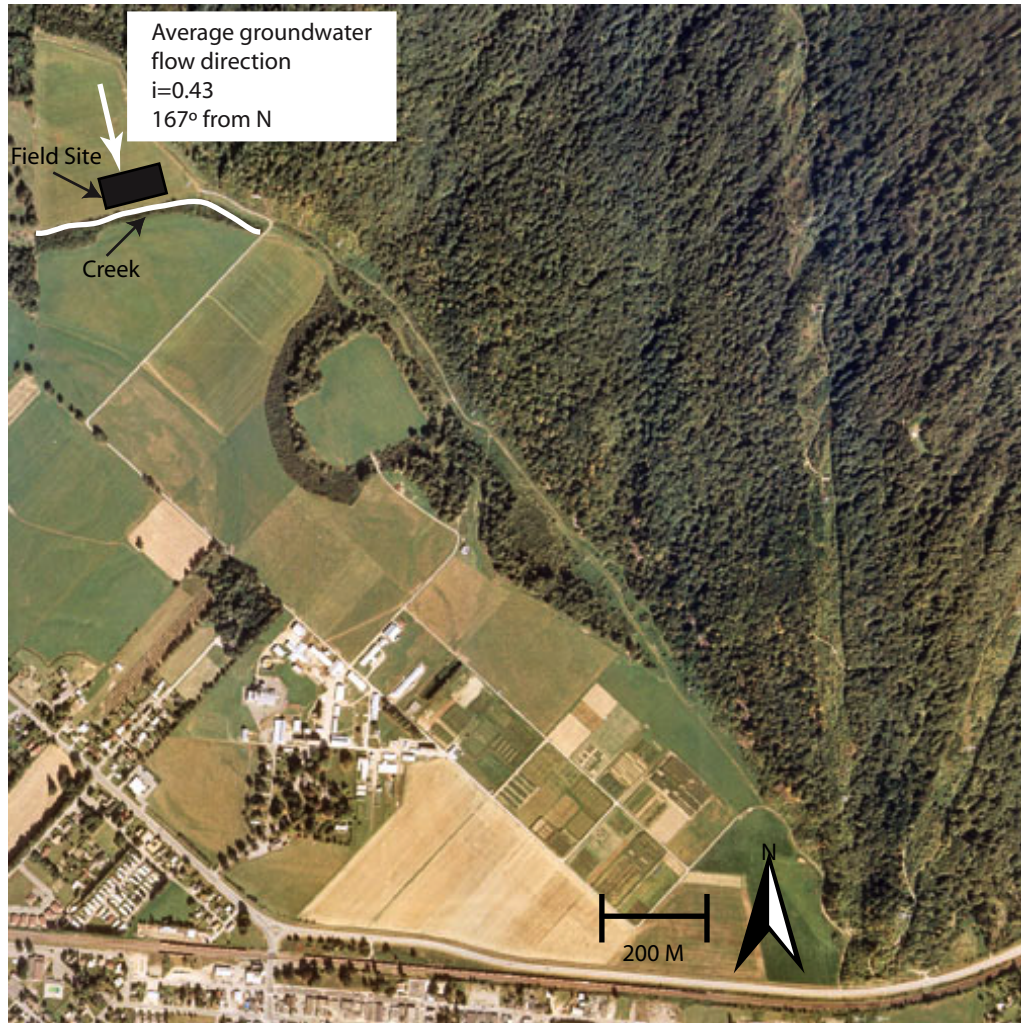


Figure 3. Aerial photo (1995) of the Pacific Agri-Foods Research Centre, Agassiz BC (i is the groundwater flow gradient).

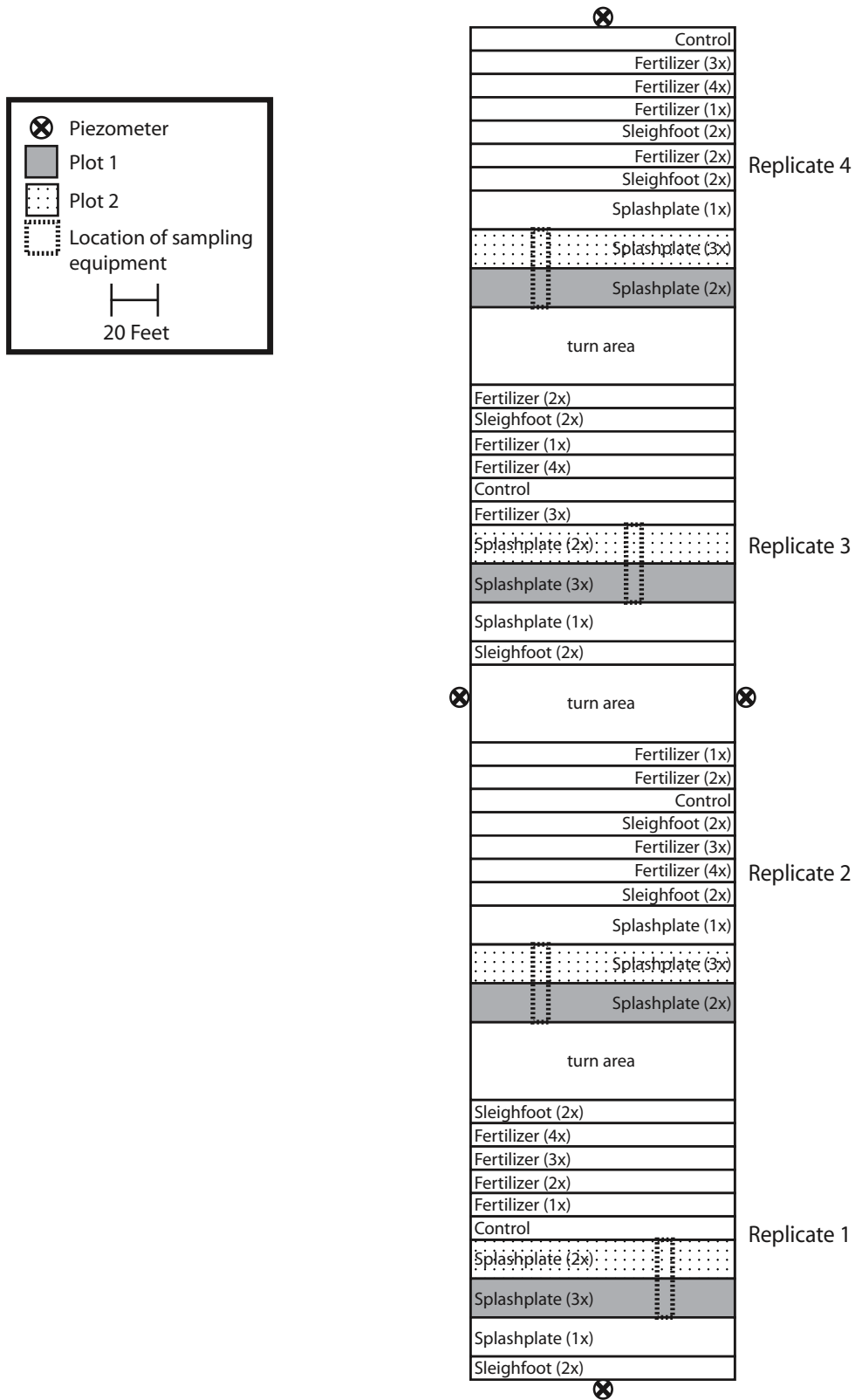


Figure 4. Field layout used for the swine manure study conducted on the study site from 1998-2001.

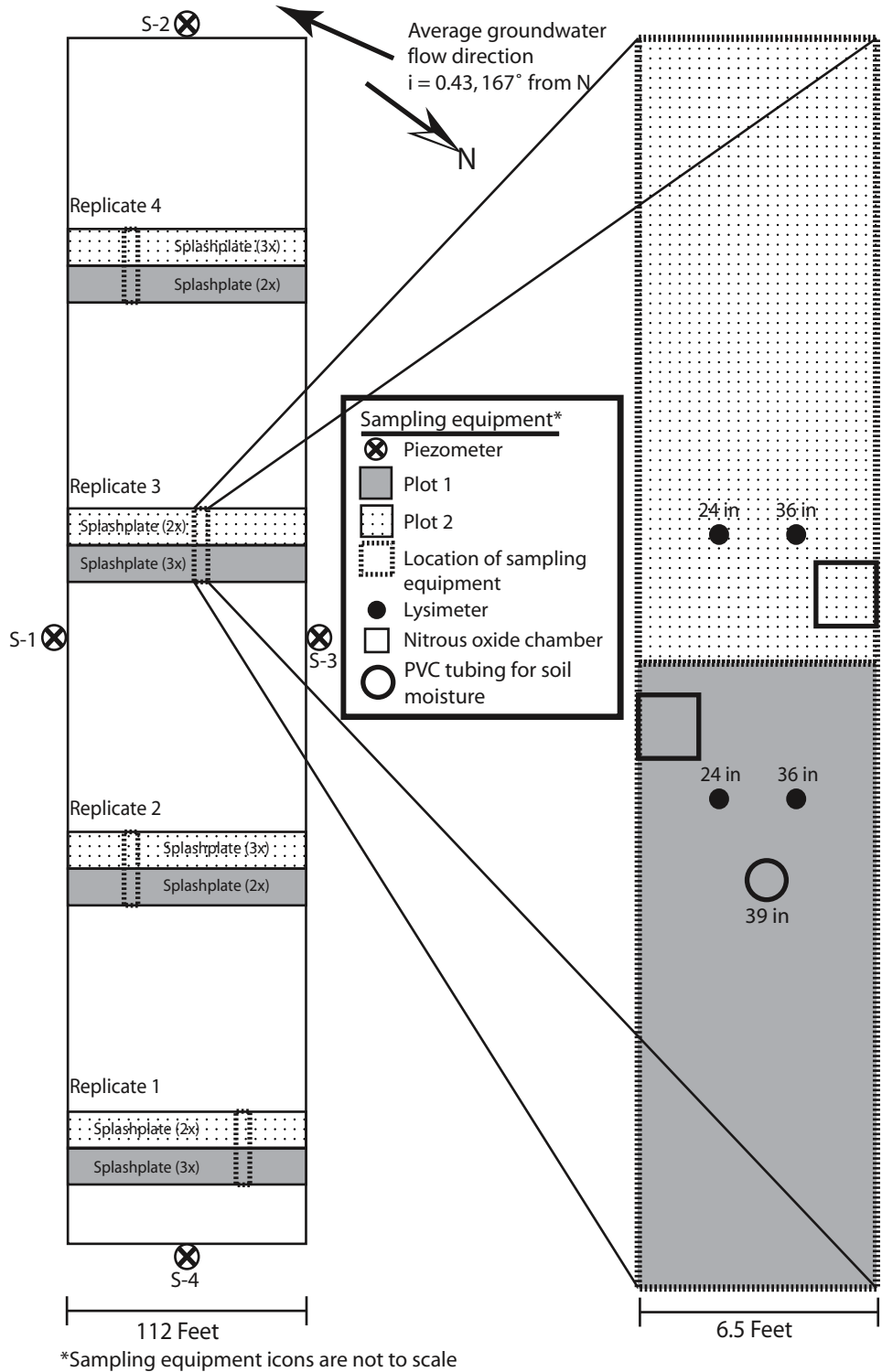


Figure 5. Field site set-up.



Figure 6. A push-probe soil core sampler used in this study.

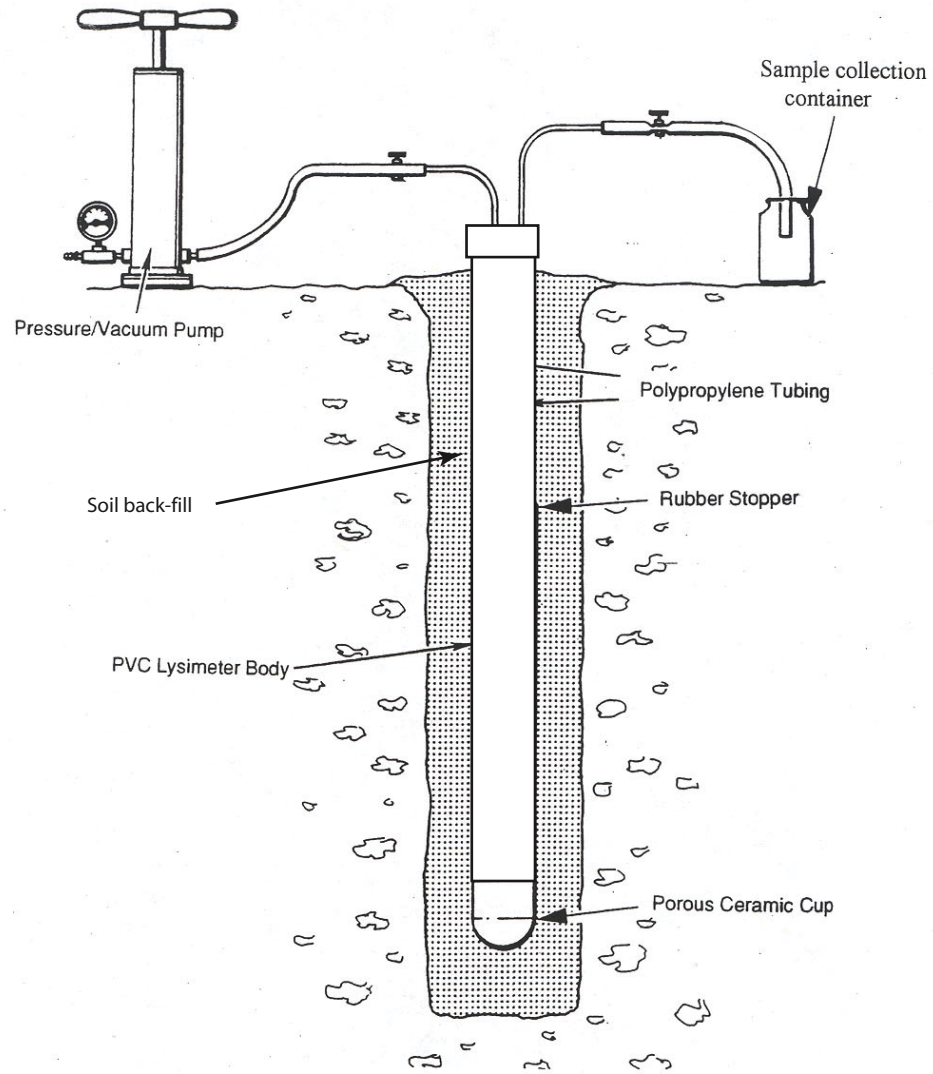


Figure 7. Ceramic cup lysimeter set-up.

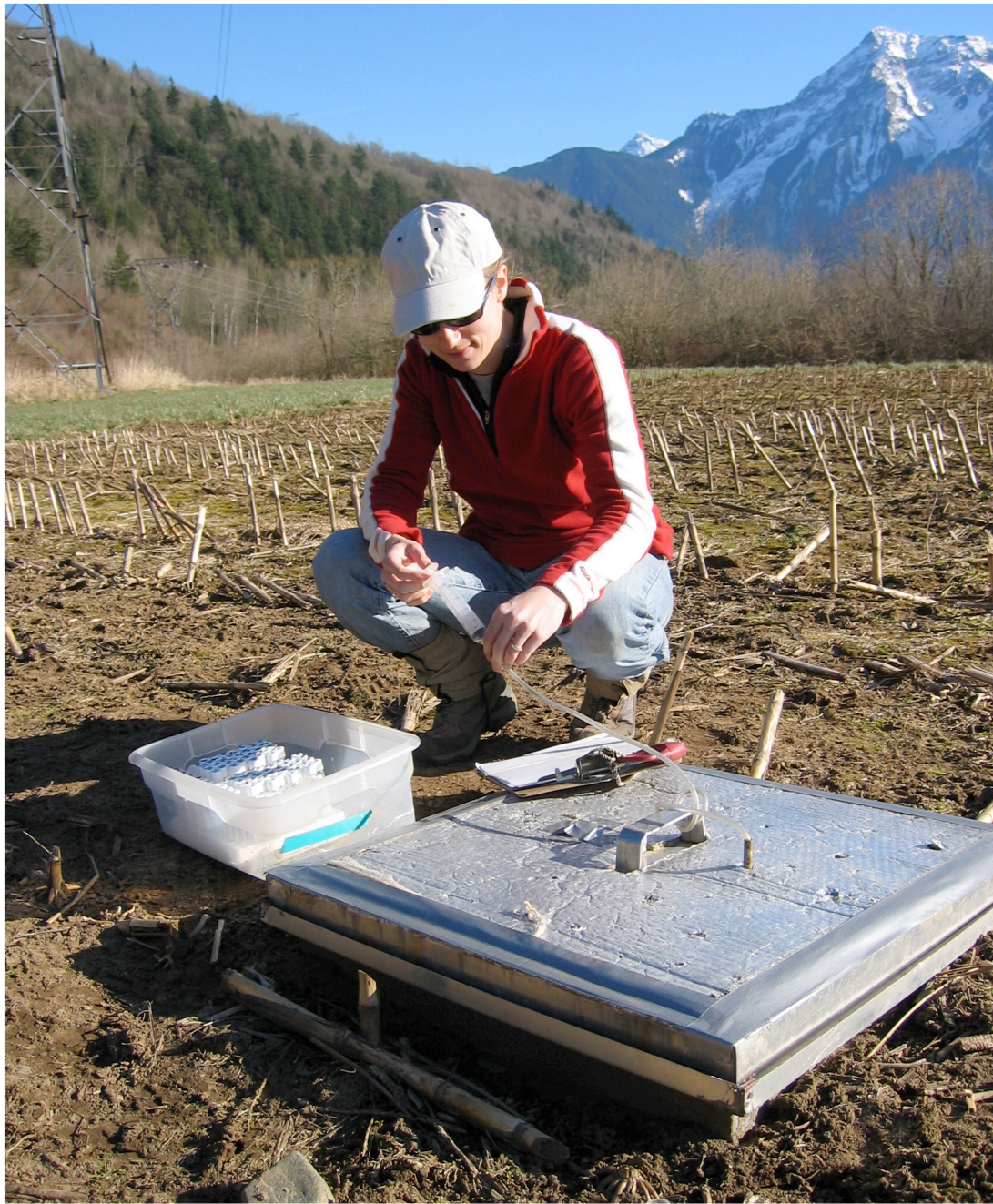


Figure 8. A non-flow-through chamber for nitrous oxide sample collection.

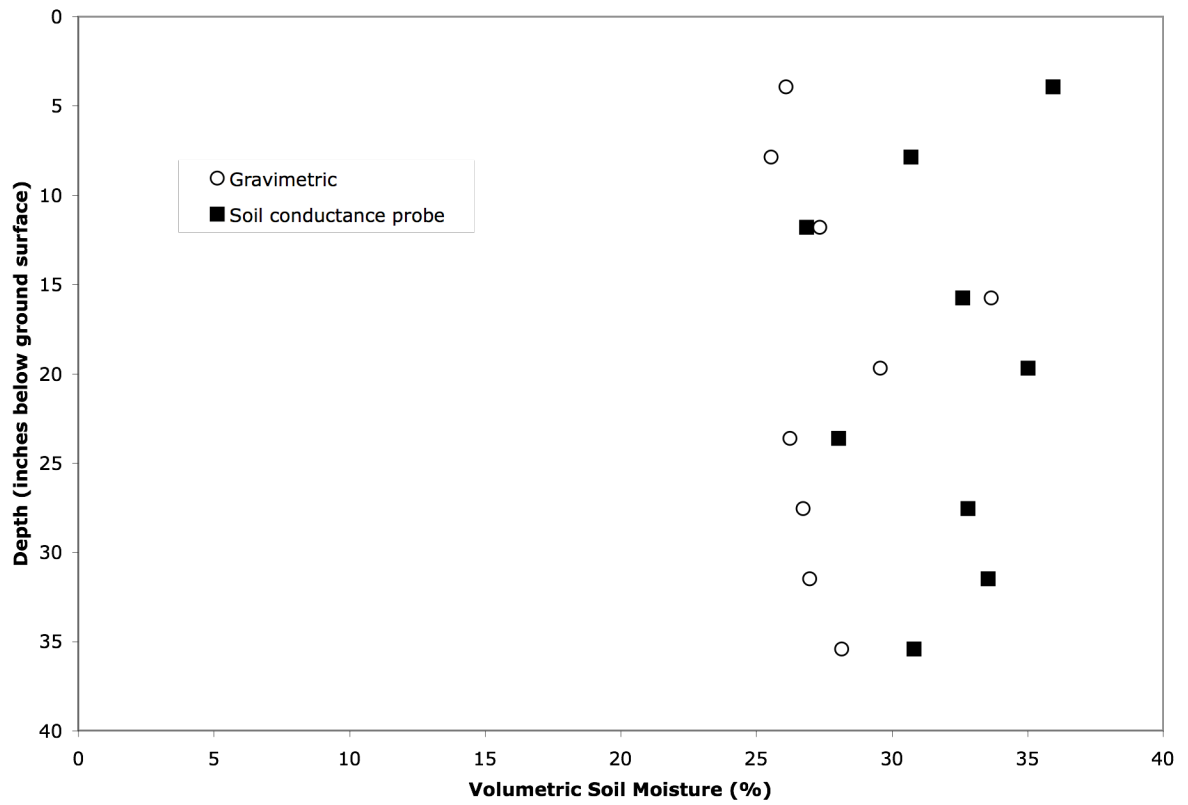


Figure 9. Gravimetric soil moisture vs. Diviner 2000 soil conductance probe soil moisture measurements.

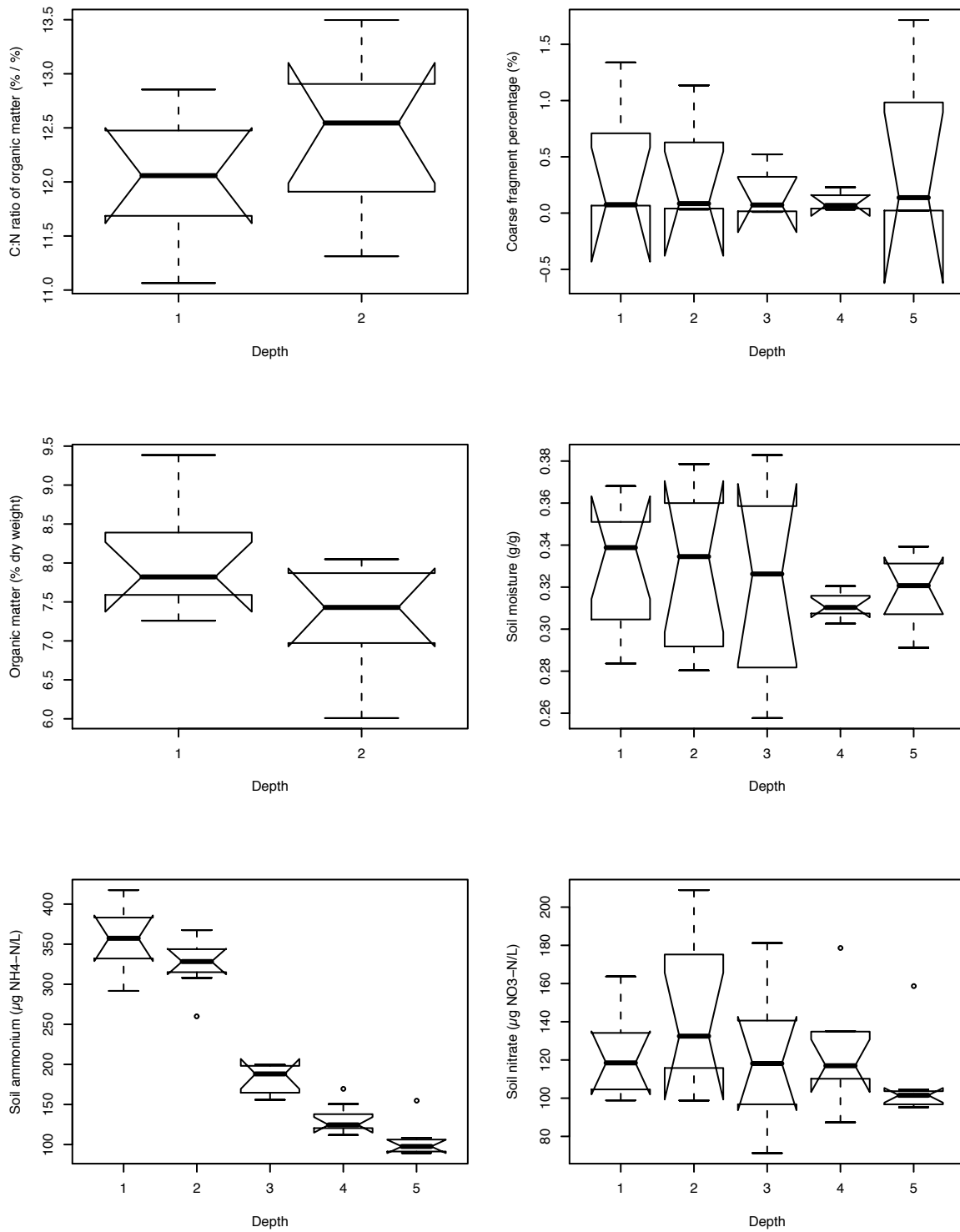


Figure 10. Notched boxplots of initial soil data collected on March 24, 2004 by depth. Soil nitrate and ammonium are presented as the concentration in soil extract solution ($\mu\text{g N/L}$).

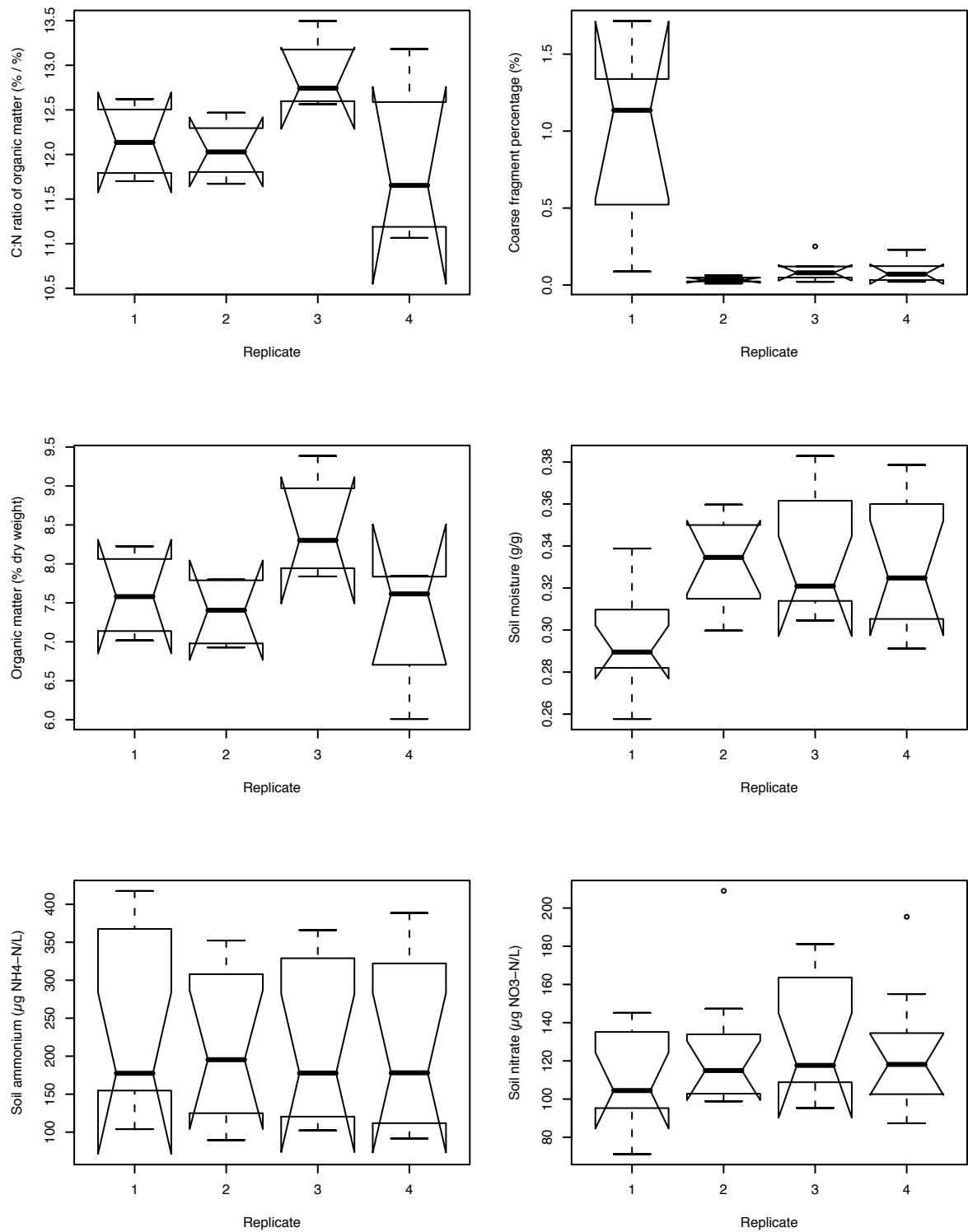


Figure 11. Notched boxplots of initial soil data collected on March 24, 2004 by replicate. Soil nitrate and ammonium are presented as the concentration in soil extract solution ($\mu\text{g N/L}$).

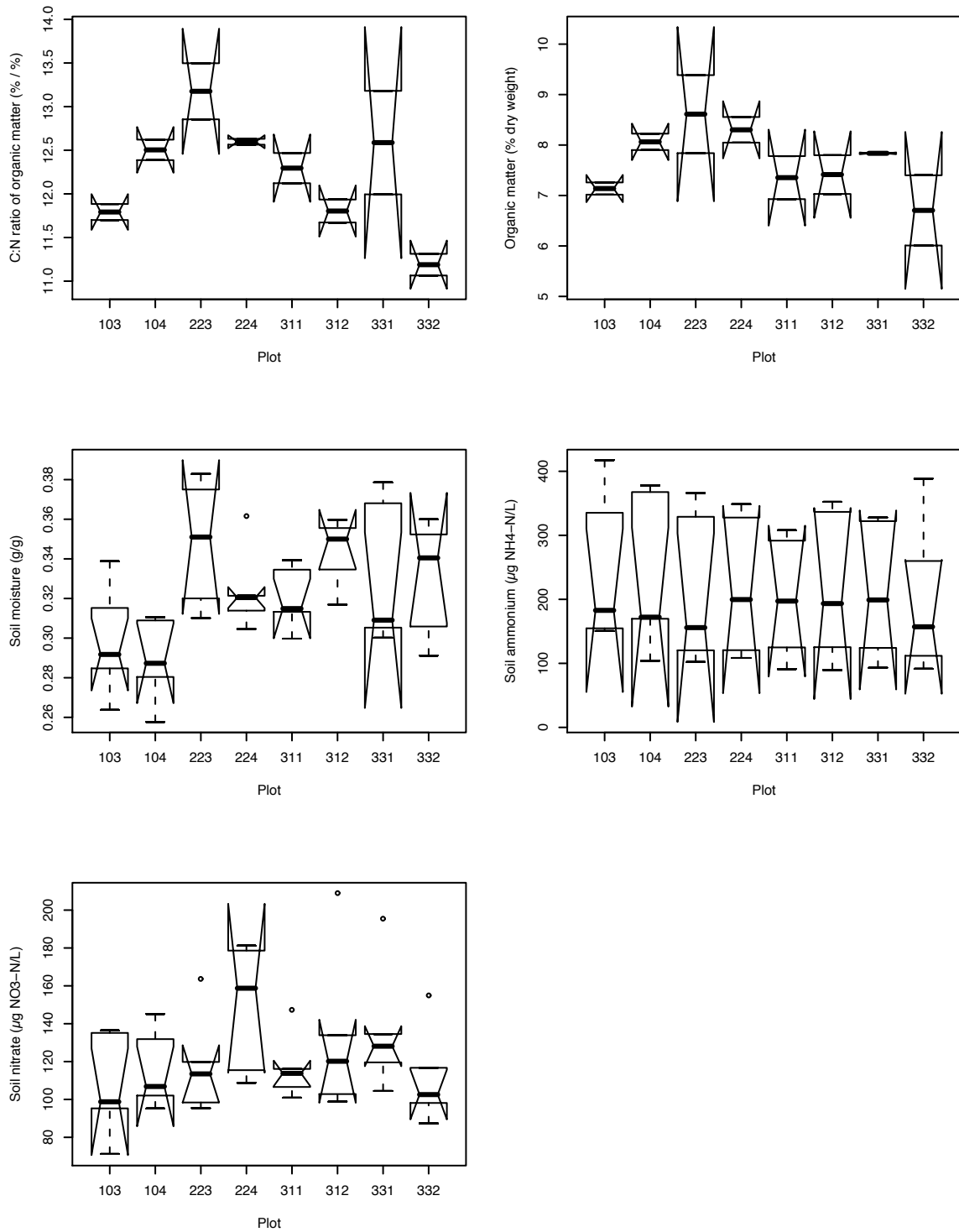


Figure 12. Notched boxplots of initial soil data collected on March 24, 2004 by plot. Soil nitrate and ammonium are presented as the concentration in soil extract solution ($\mu\text{g N/L}$).

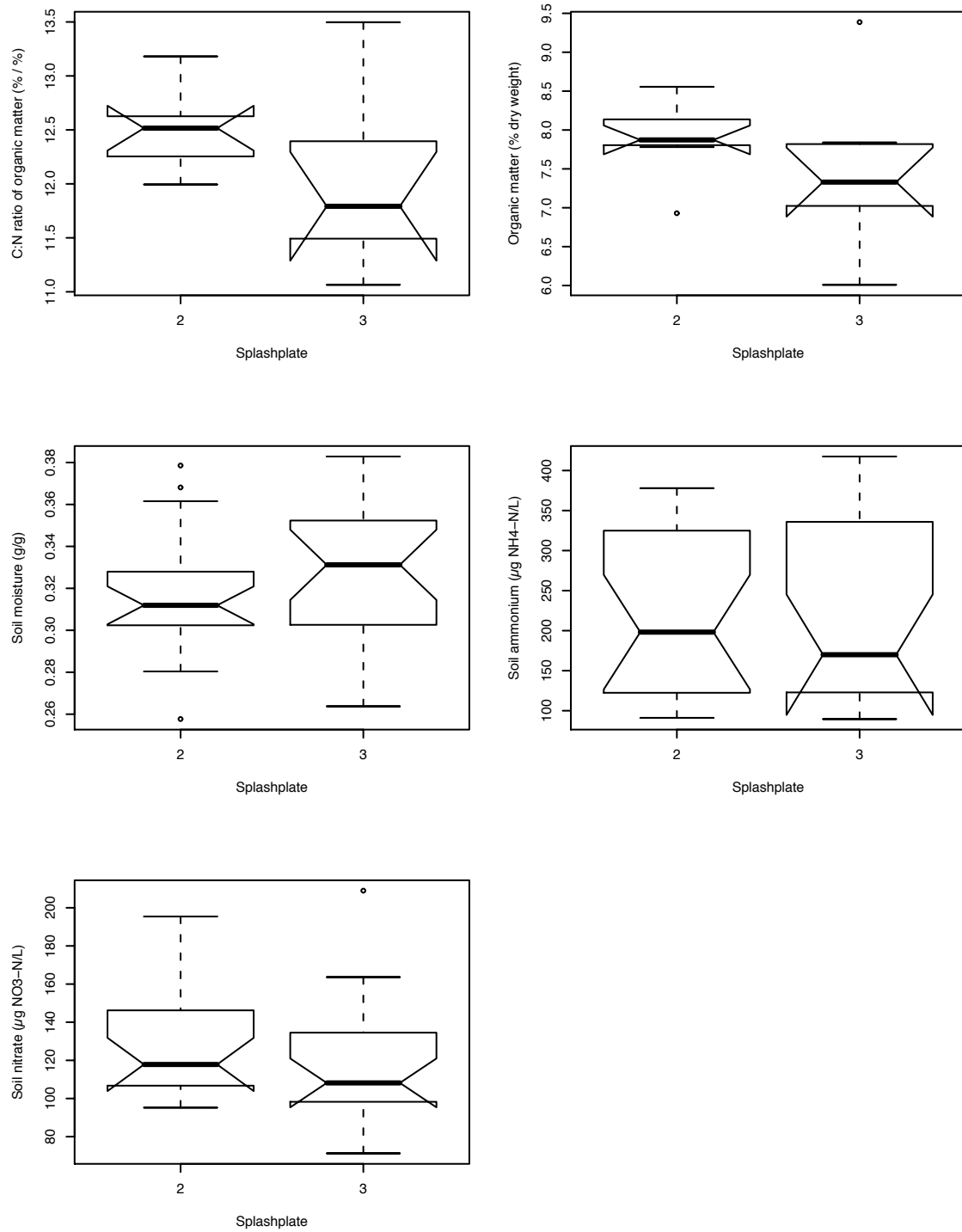


Figure 13. Notched boxplots of initial soil data collected on March 24, 2004 by splashplate. Soil nitrate and ammonium are presented as the concentration in soil extract solution ($\mu\text{g N/L}$).

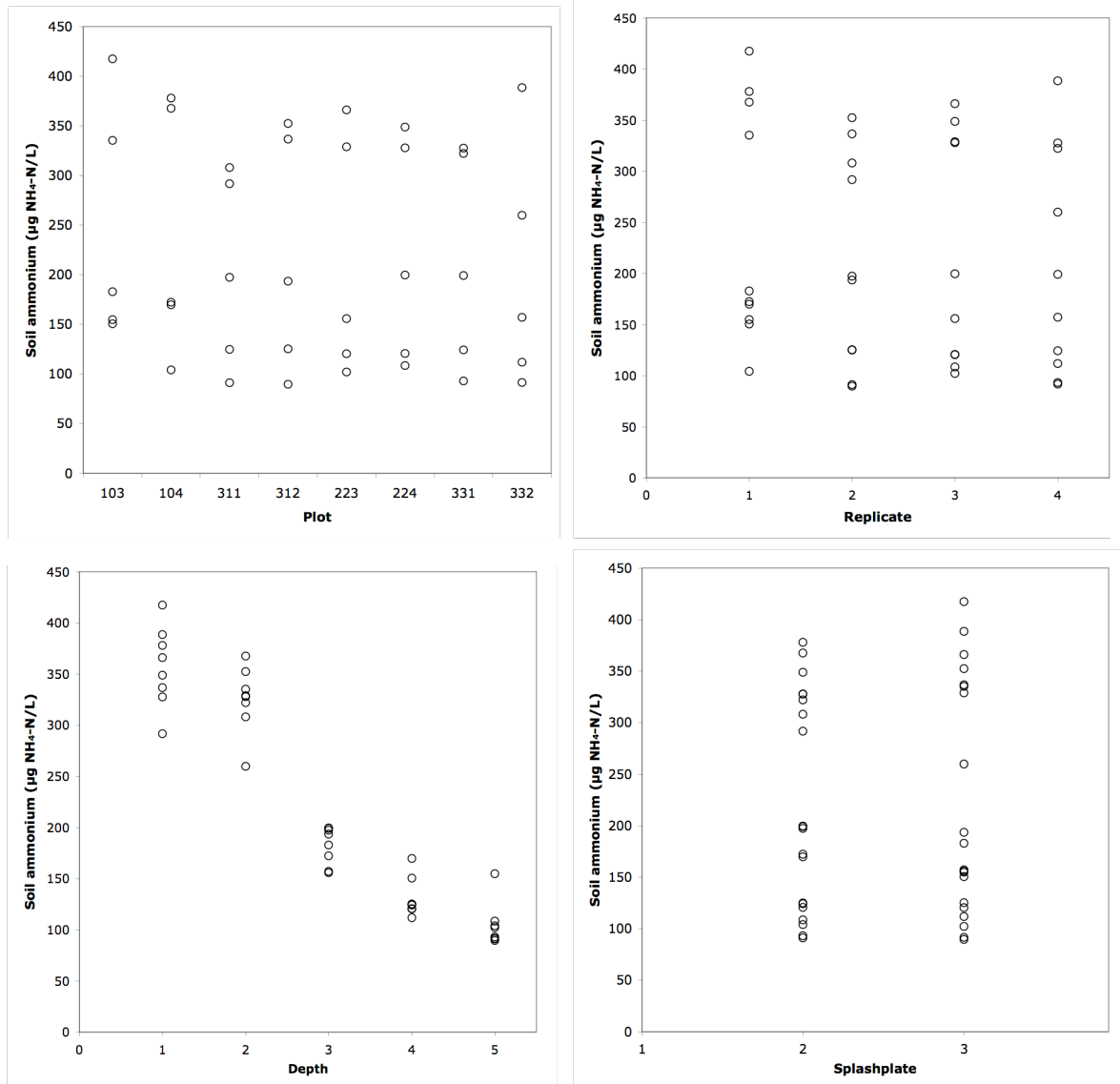


Figure 14. Scatterplots of initial soil ammonium data collected on March 24, 2004 by plot, replicate, depth and splashplate. Soil ammonium is presented as the concentration in soil extract solution ($\mu\text{g N/L}$).

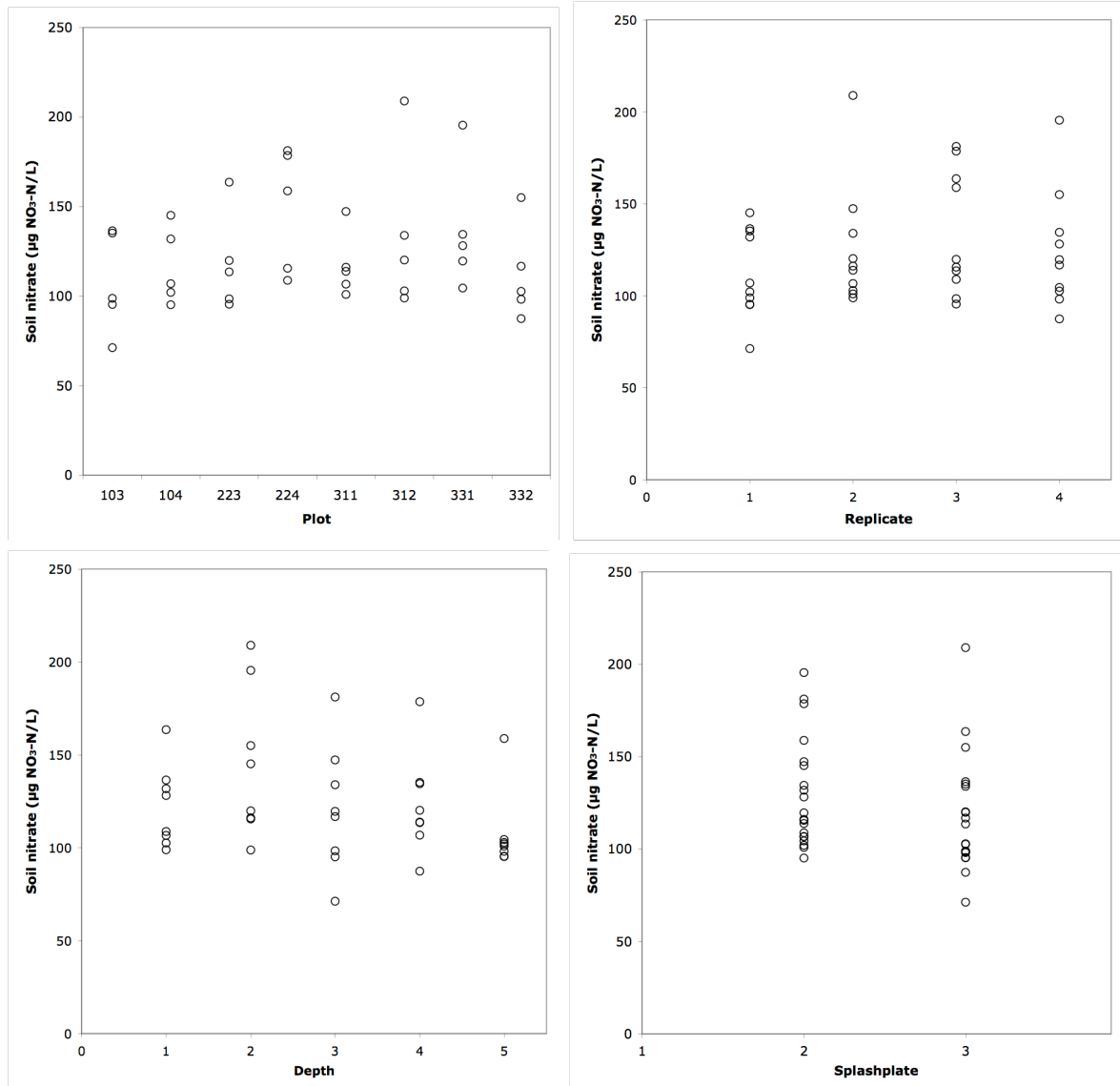


Figure 15. Scatterplots of initial soil nitrate data collected on March 24, 2004 by plot, replicate, depth and splashplate. Soil nitrate is presented as the concentration in soil extract solution ($\mu\text{g N/L}$).

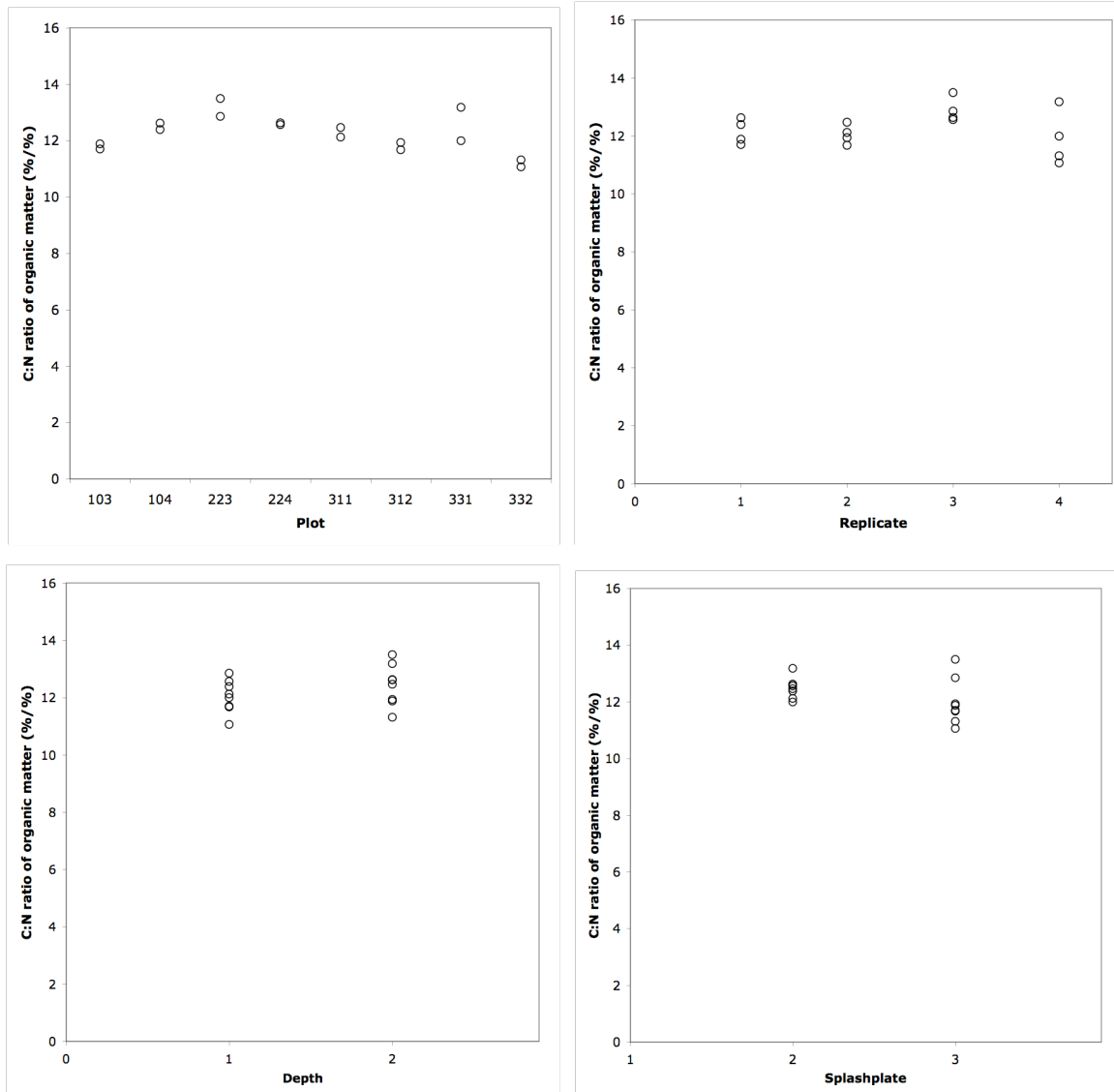


Figure 16. Scatterplots of initial soil carbon to nitrogen ratio (C:N) data collected on March 24, 2004 by plot, replicate, depth and splashplate.

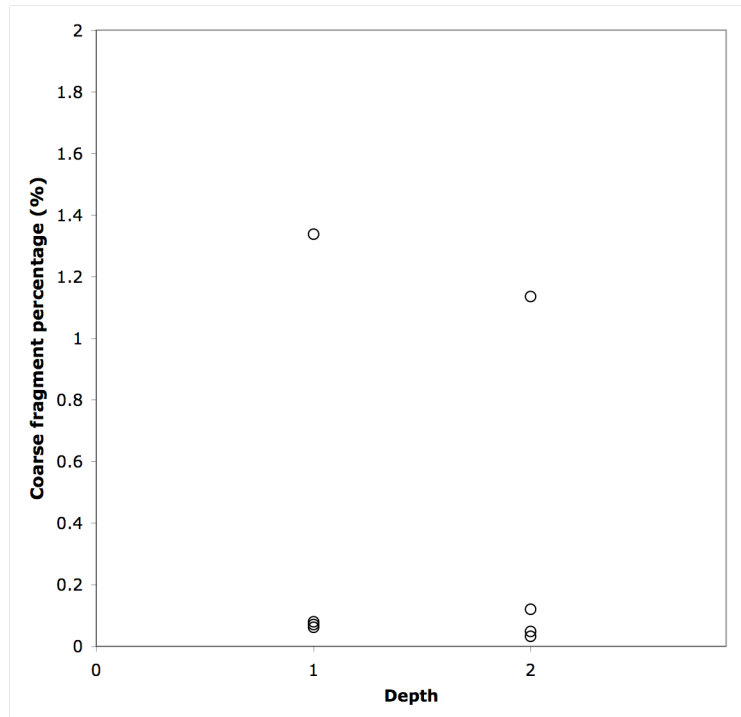
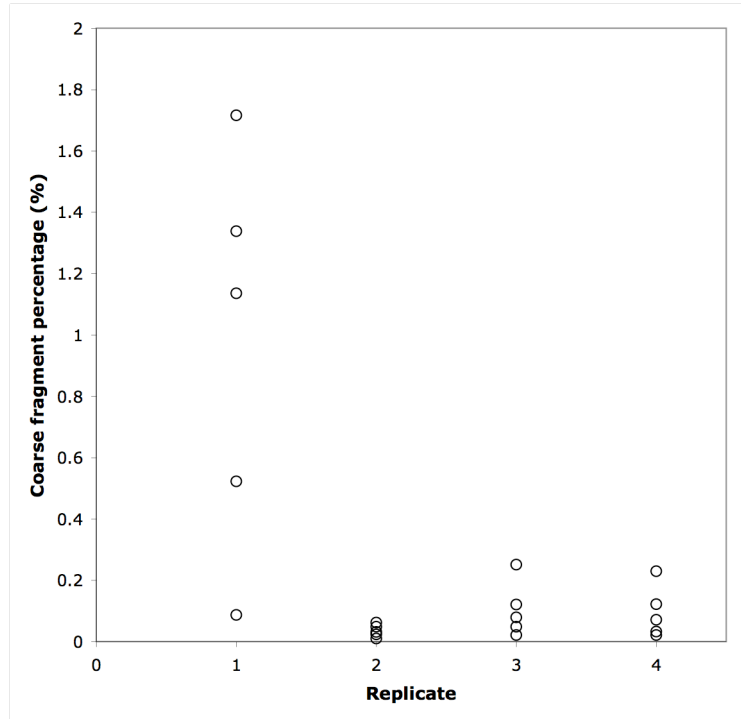


Figure 17. Scatterplots of initial soil coarse fragment percentage data collected on March 24, 2004 by replicate and depth.

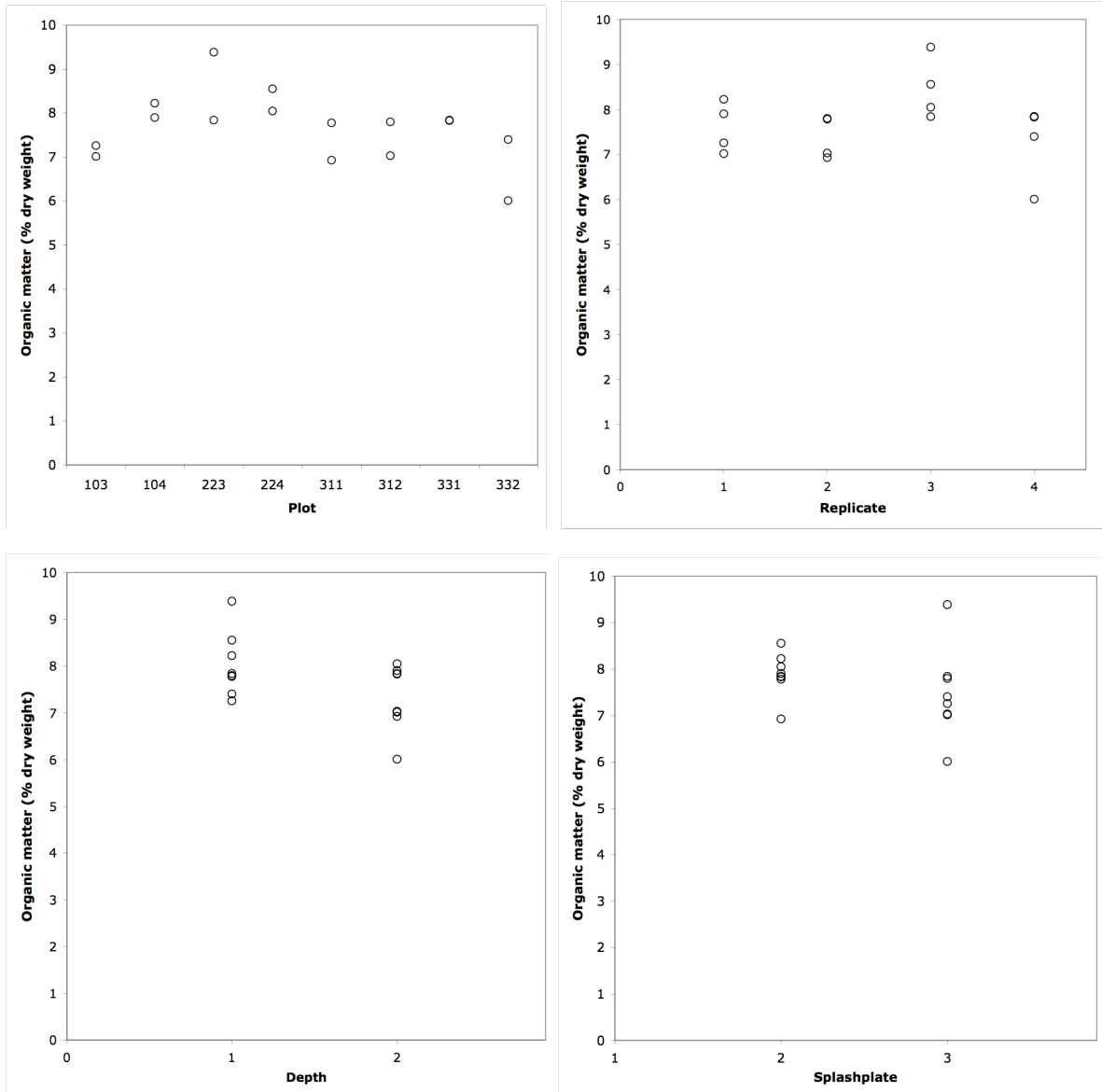


Figure 18. Scatterplots of initial soil organic matter content data collected on March 24, 2004 by plot, replicate, depth and splashplate.

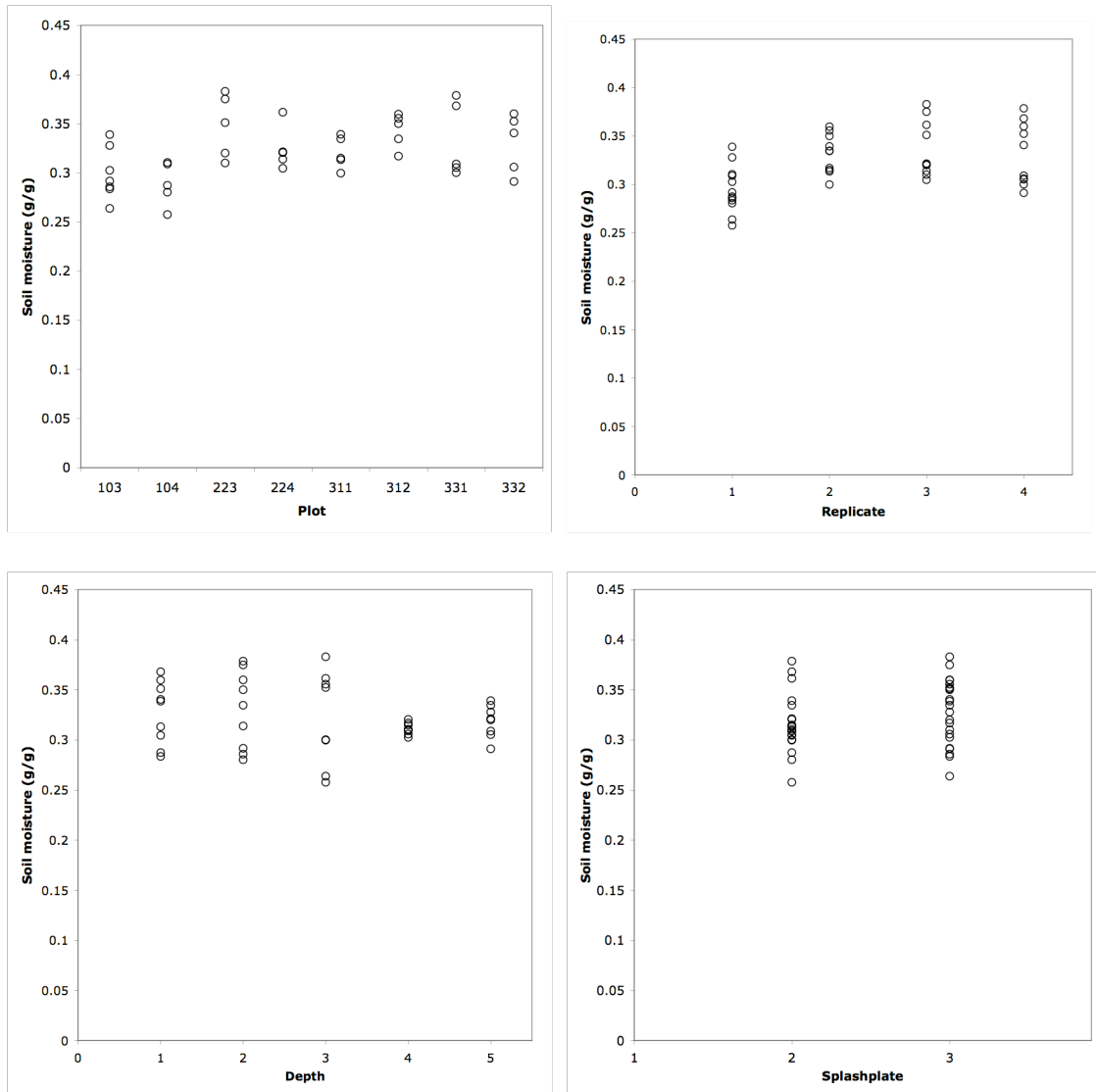


Figure 19. Scatterplots of initial soil moisture data collected on March 24, 2004 by plot, replicate, depth and splashplate.

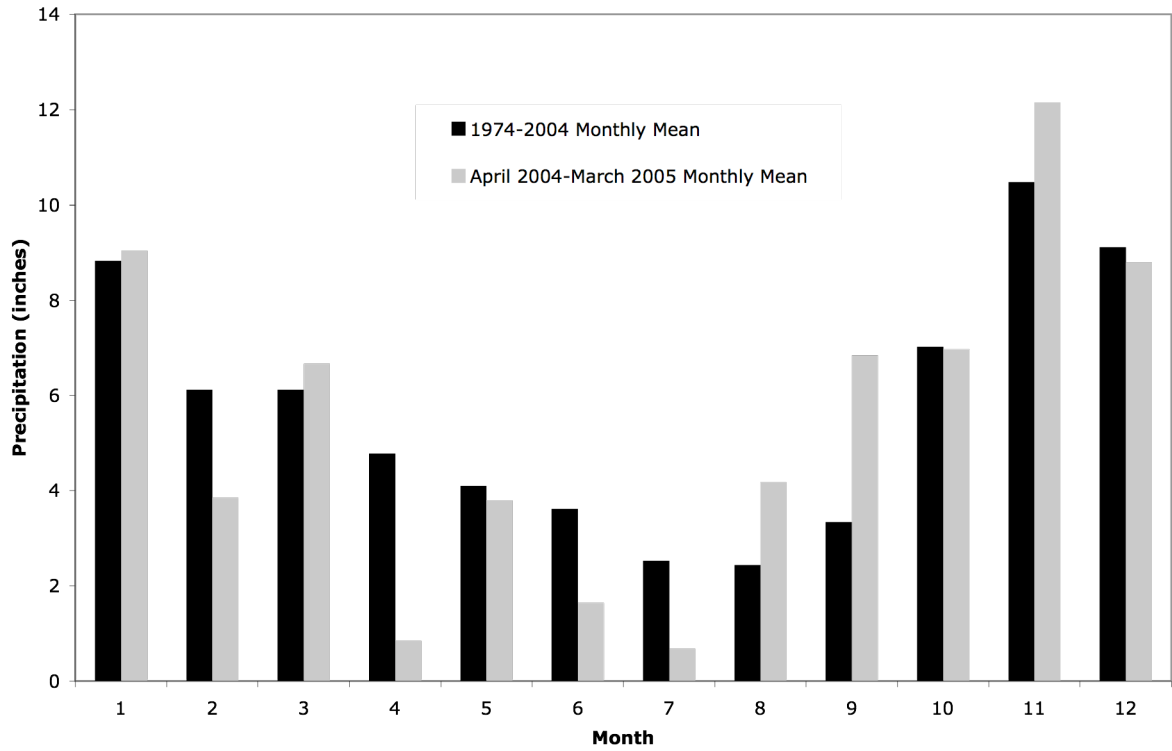


Figure 20. Mean monthly precipitation totals for the study period (April 2004 – March 2005) vs. the 30-year average mean monthly totals (1974 – 2004).

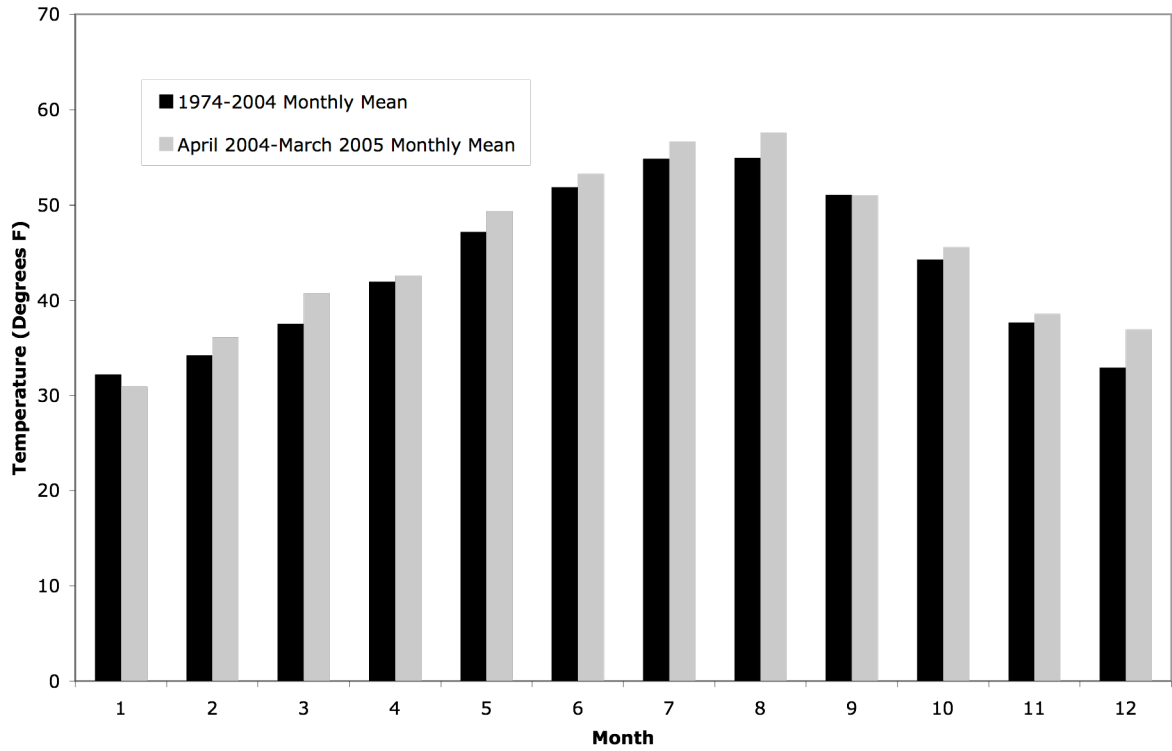


Figure 21. Mean monthly minimum temperature for the study period (April 2004 – March 2005) vs. the 30-year average (1974 – 2004).

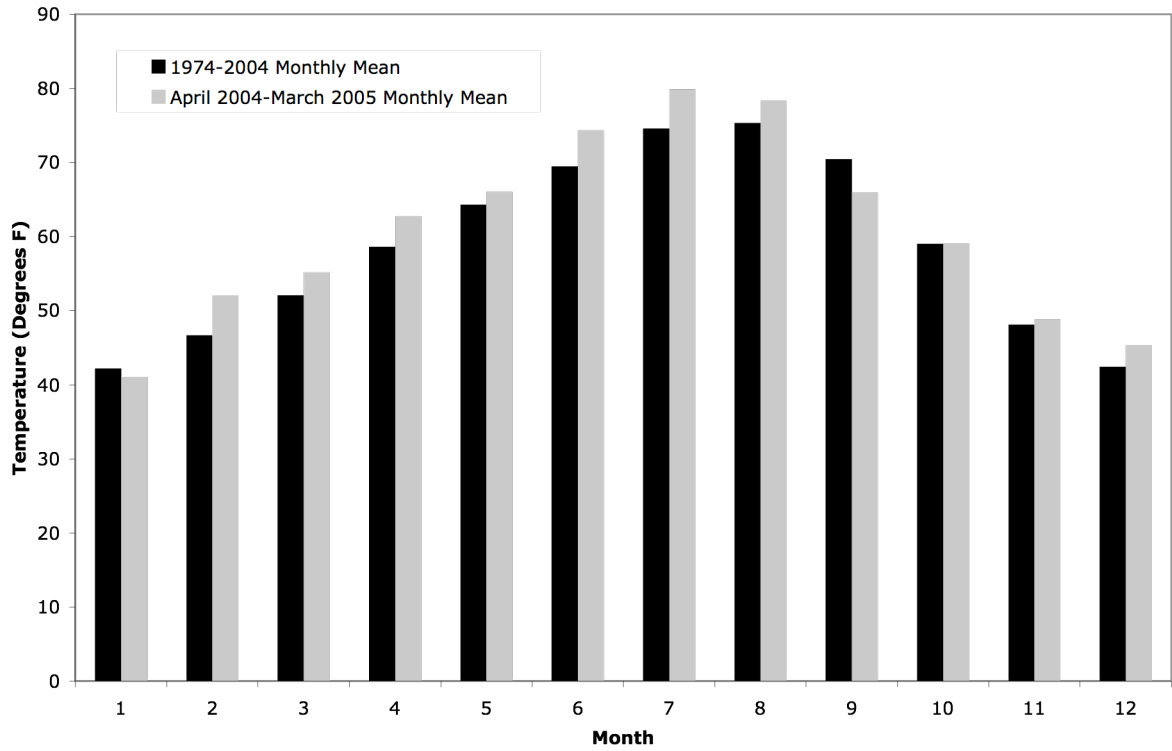


Figure 22. Mean monthly maximum temperature for the study period (April 2004 – March 2005) vs. the 30-year average (1974 – 2004).

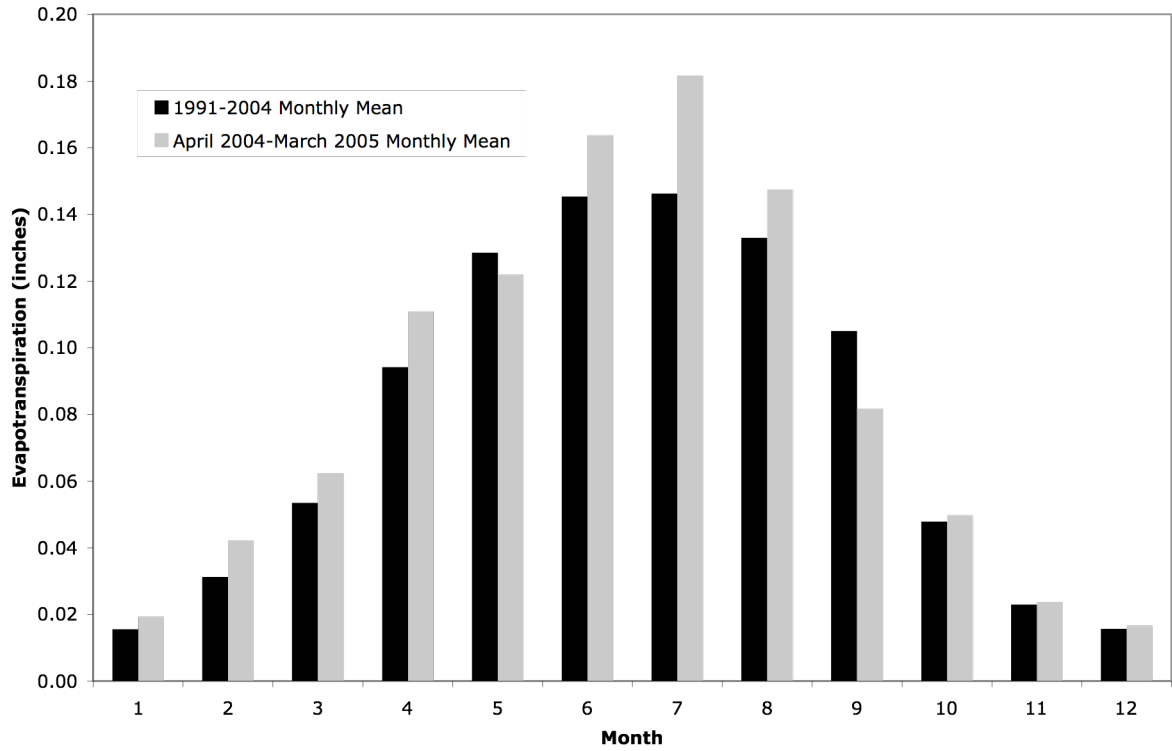


Figure 23. Mean daily values of evapotranspiration by month for the study period (April 2004 – March 2005) vs. the long-term mean monthly values (1991 – 2004).

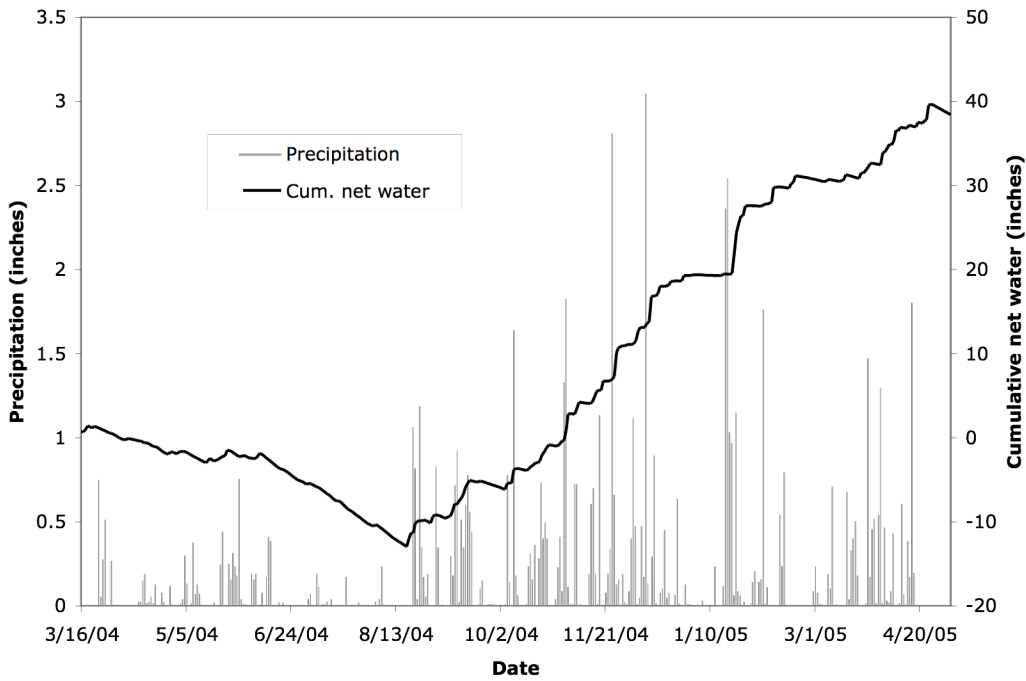
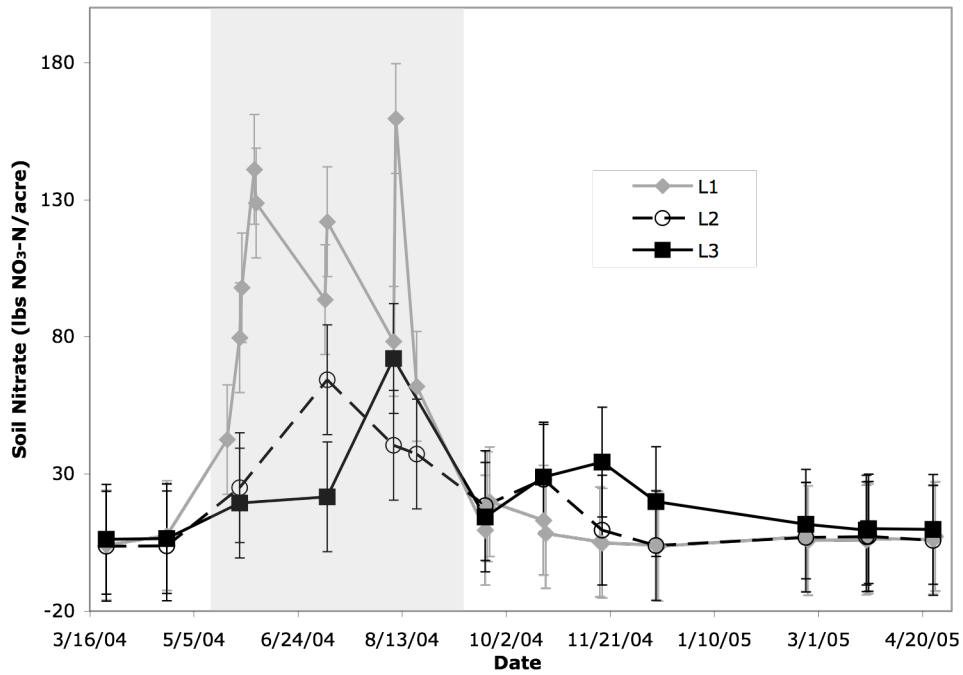


Figure 24. Observed soil nitrate for soil layers 1 to 3 (L1 – L3), cumulative net water (precipitation – evapotranspiration), and precipitation. The light grey region represents the time span from crop planting and fertilization to crop harvesting.

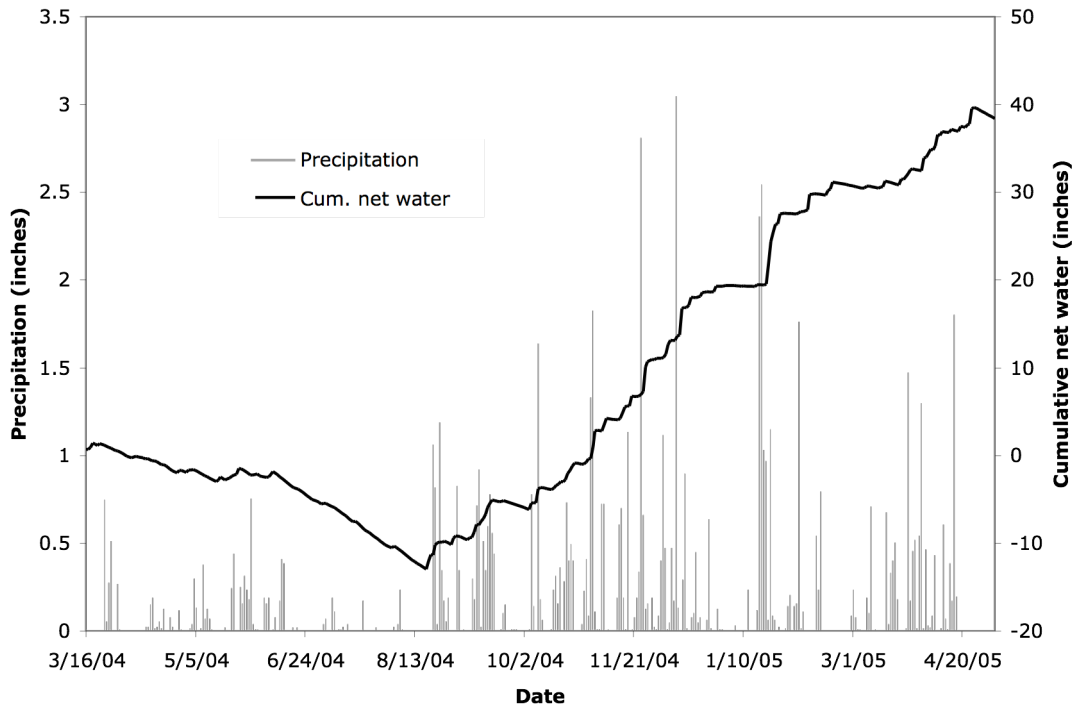
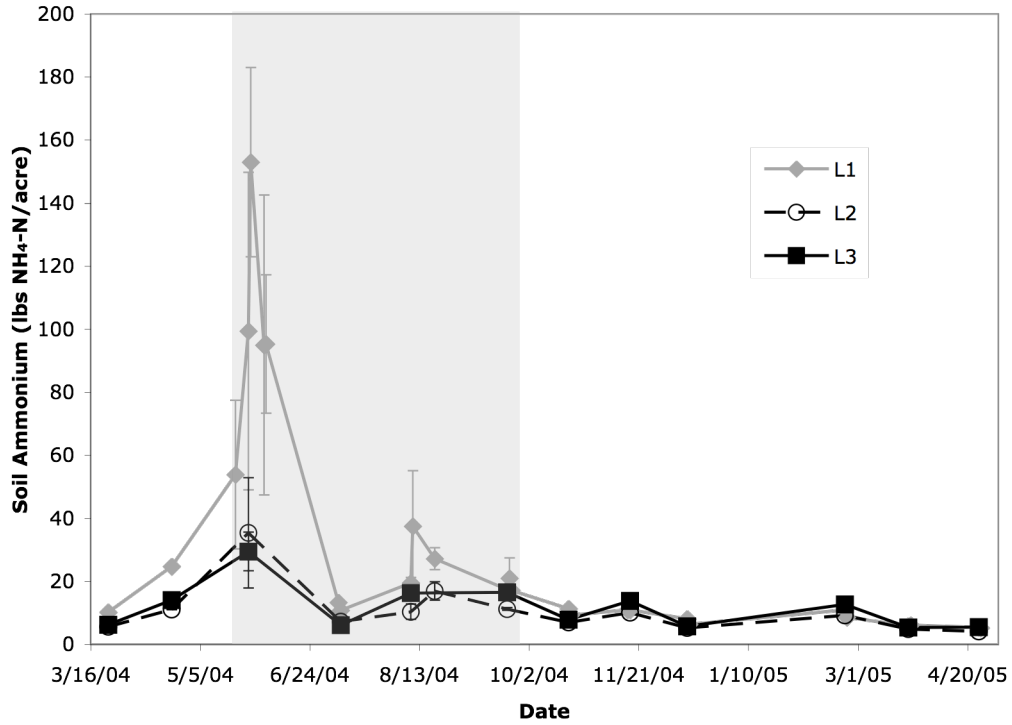


Figure 25. Observed soil ammonium for soil layers 1 to 3 (L1 – L3), cumulative net water (precipitation – evapotranspiration), and precipitation. The light grey region represents the time span from crop planting and fertilization to crop harvesting.

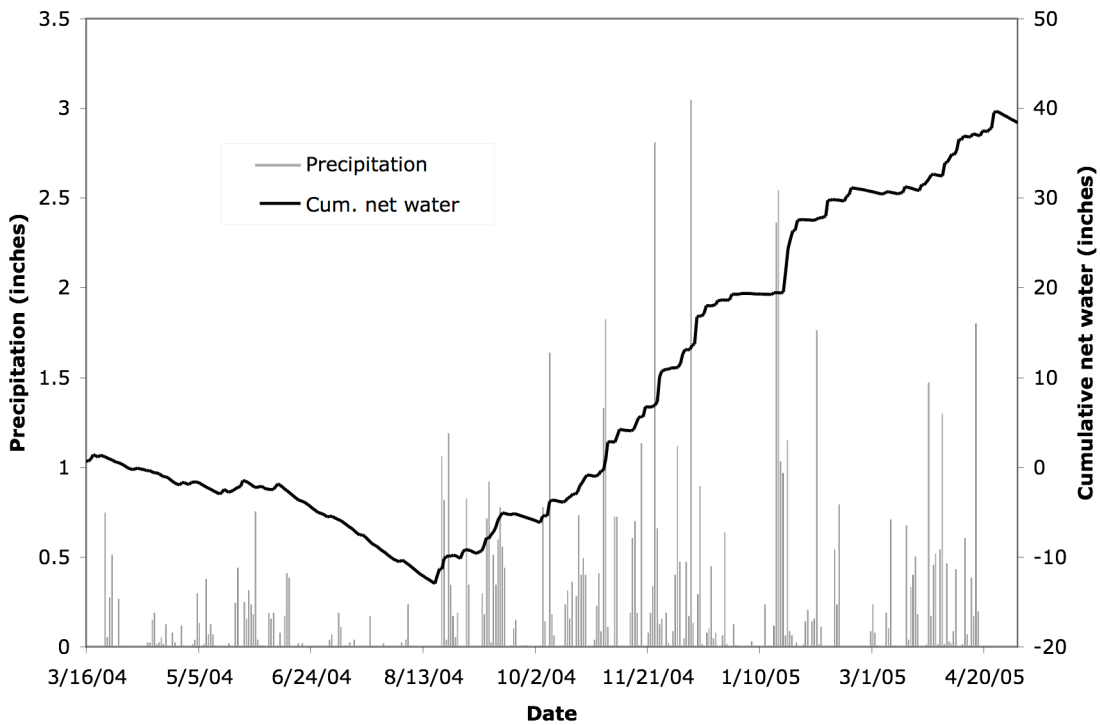
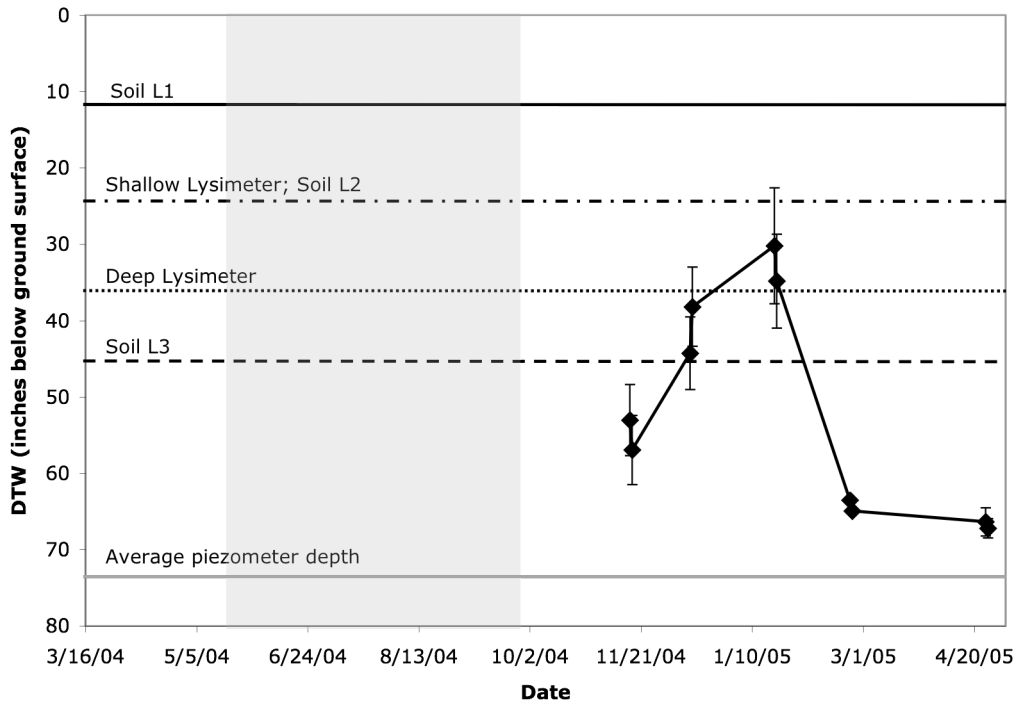


Figure 26. Observed depth to water (DTW) in relation to the sampling depths, cumulative net water (precipitation – evapotranspiration), and precipitation. The light grey region represents the time span from crop planting and fertilization to crop harvesting.

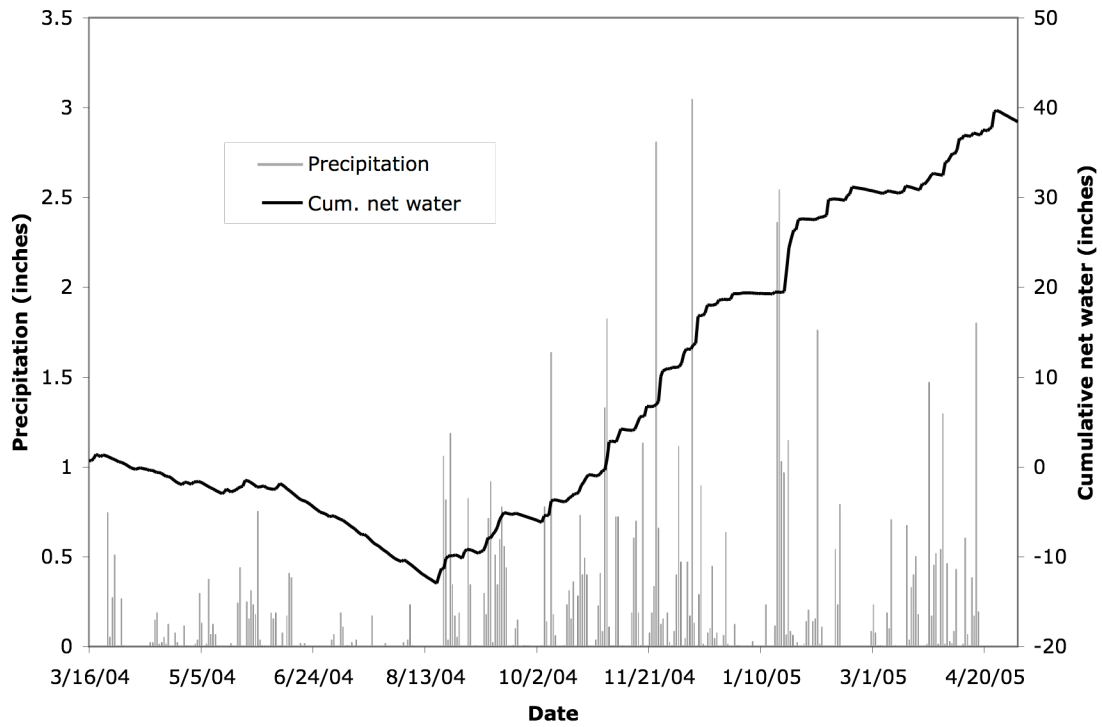
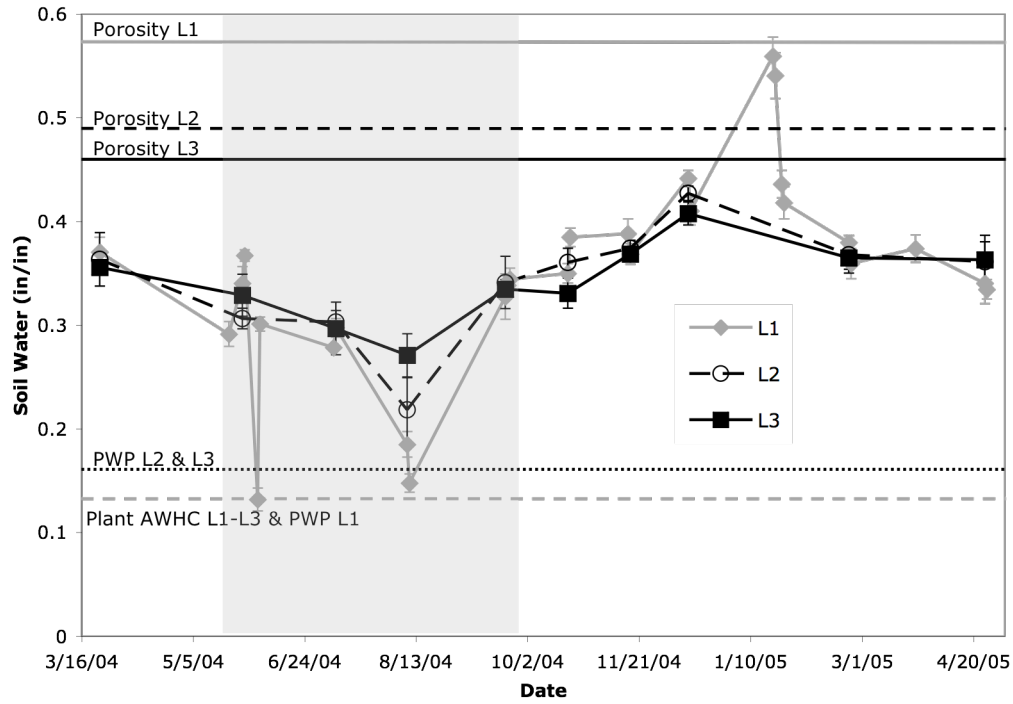


Figure 27. Observed soil water for soil layers 1 -3 (L1 – L3), cumulative net water (precipitation – evapotranspiration), and precipitation. The light grey region represents the time span from crop planting and fertilization to crop harvesting.

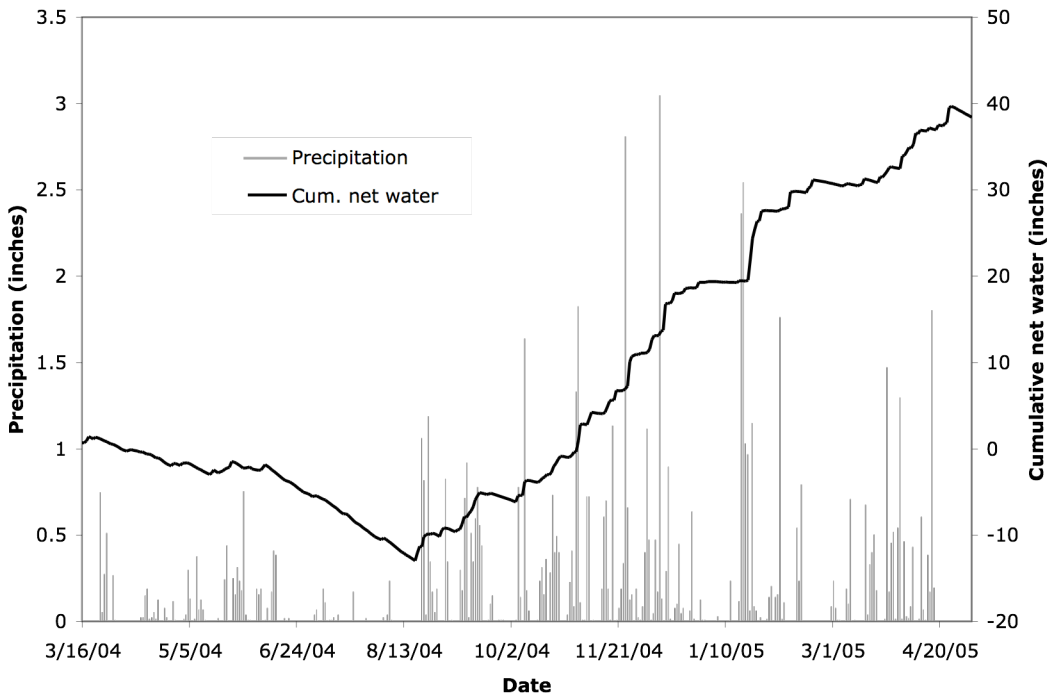
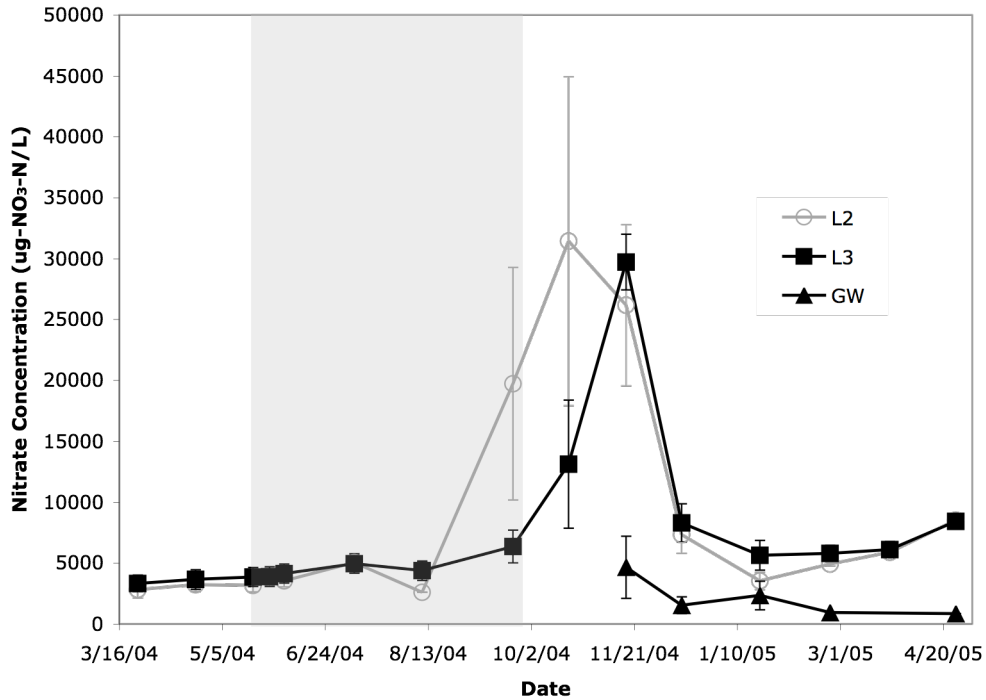


Figure 28. Observed nitrate concentration in soil water, as measured in the shallow (L2) and deep (L3) lysimeters, and groundwater (GW), cumulative net water (precipitation – evapotranspiration), and precipitation. The light grey region represents the time span from crop planting and fertilization to crop harvesting.

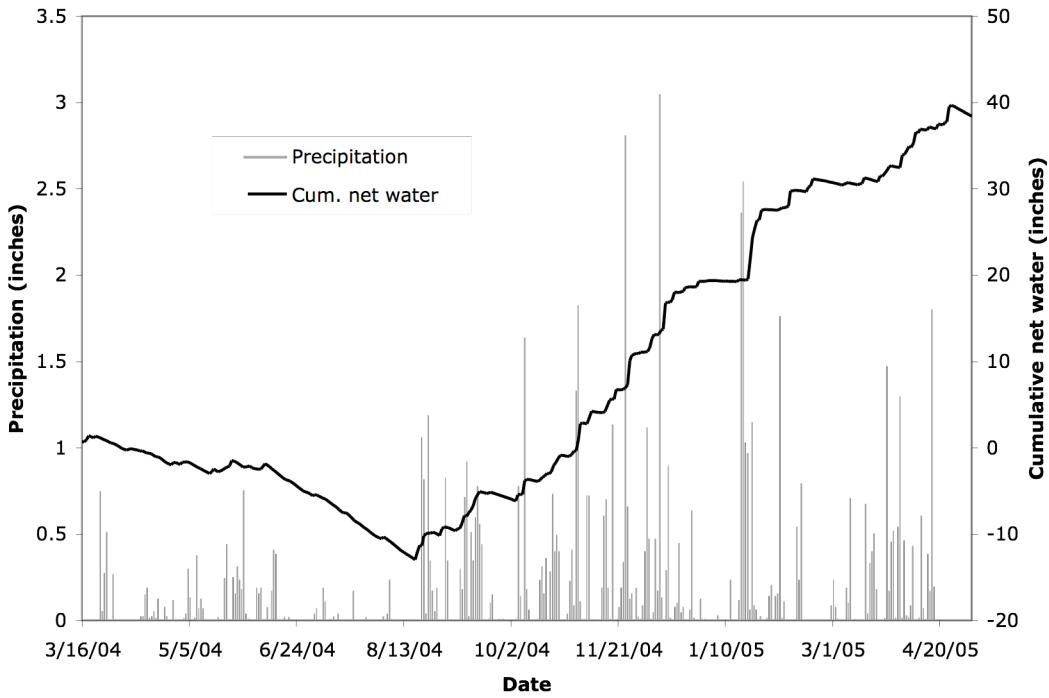
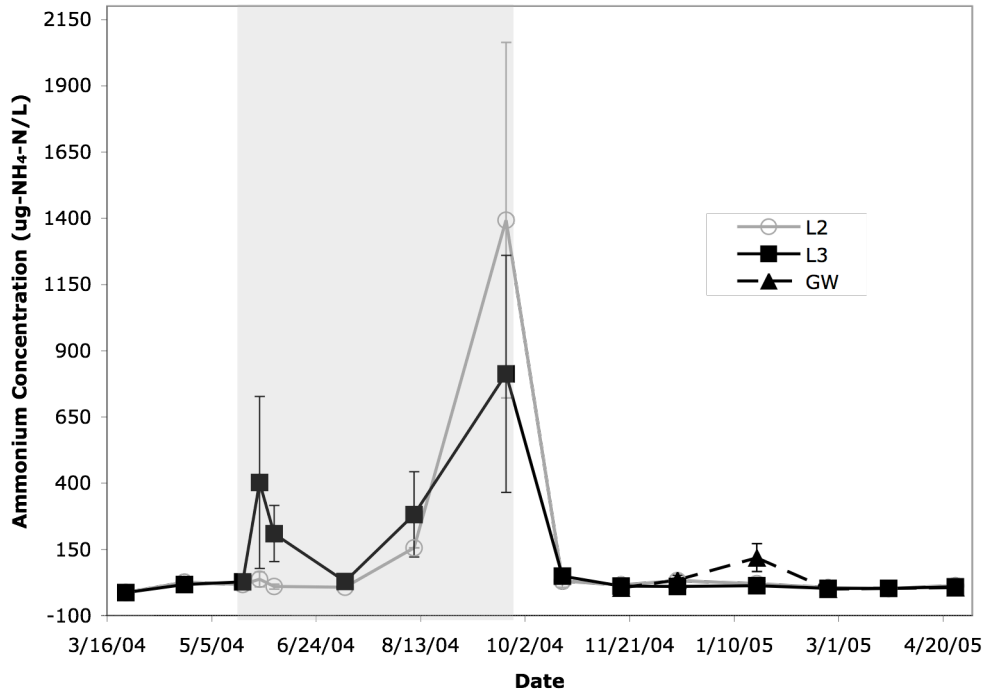


Figure 29. Observed ammonium concentration in soil water, as measured in the shallow (L2) and deep (L3) lysimeters, and groundwater (GW), cumulative net water (precipitation – evapotranspiration), and precipitation. The light grey region represents the time span from crop planting and fertilization to crop harvesting.

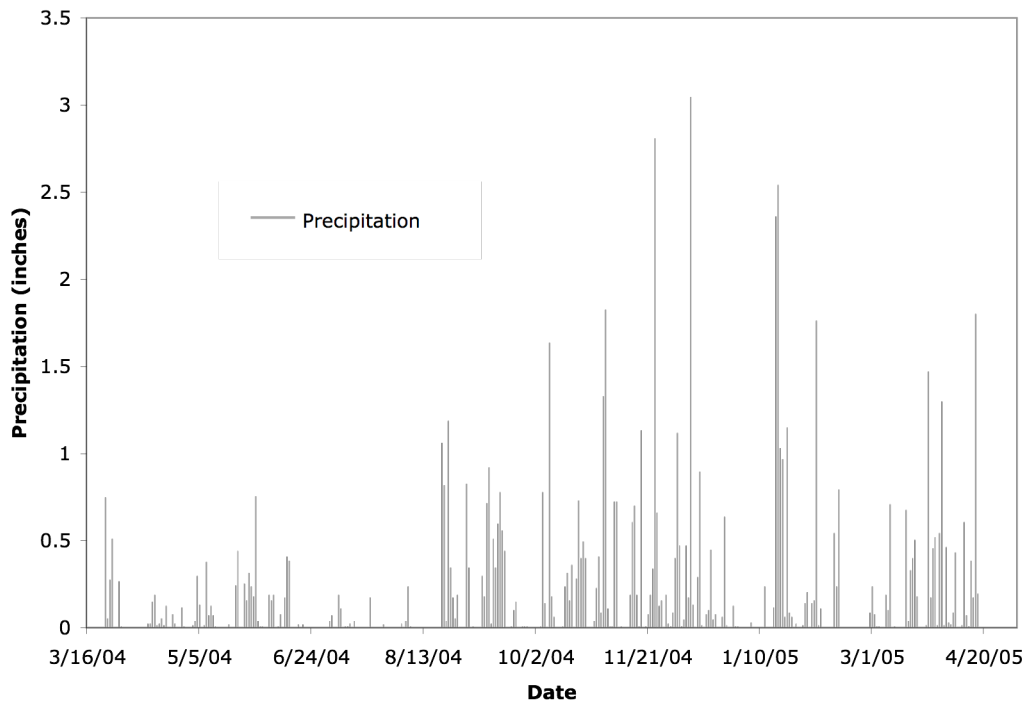
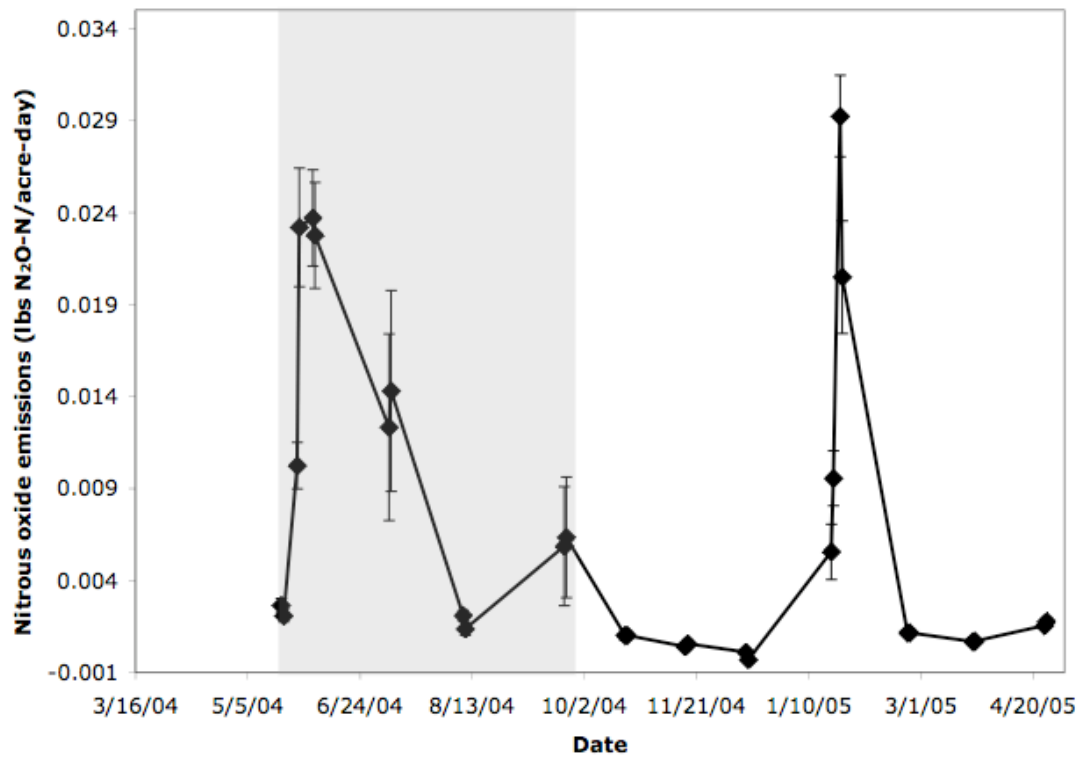


Figure 30. Observed daily nitrous oxide emissions and precipitation. The light grey region represents the time span from crop planting and fertilization to crop harvesting.

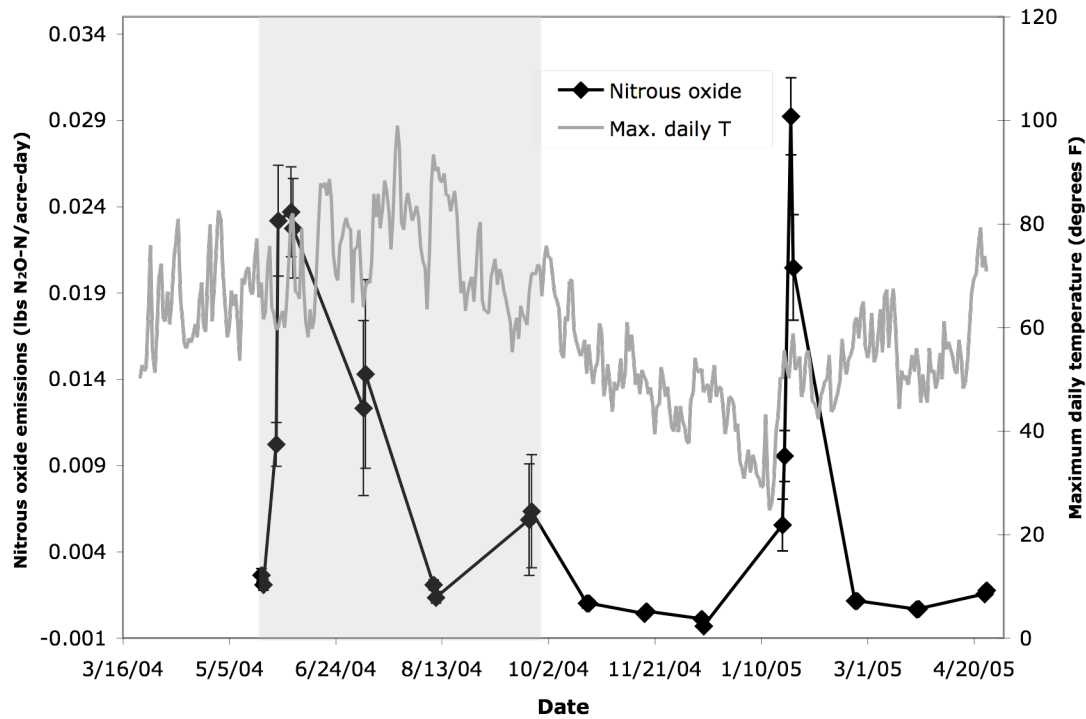
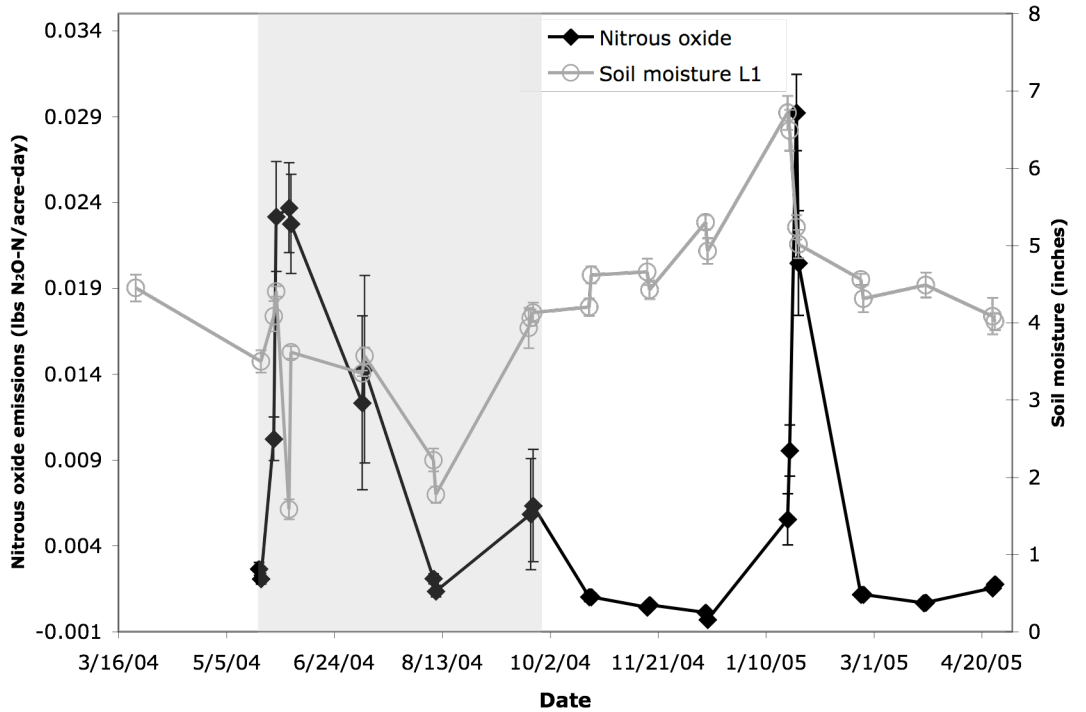


Figure 31. Observed daily nitrous oxide emissions, soil moisture in soil layer 1 (L1), and maximum daily air temperature (T). The light grey region represents the time span from crop planting and fertilization to crop harvesting.

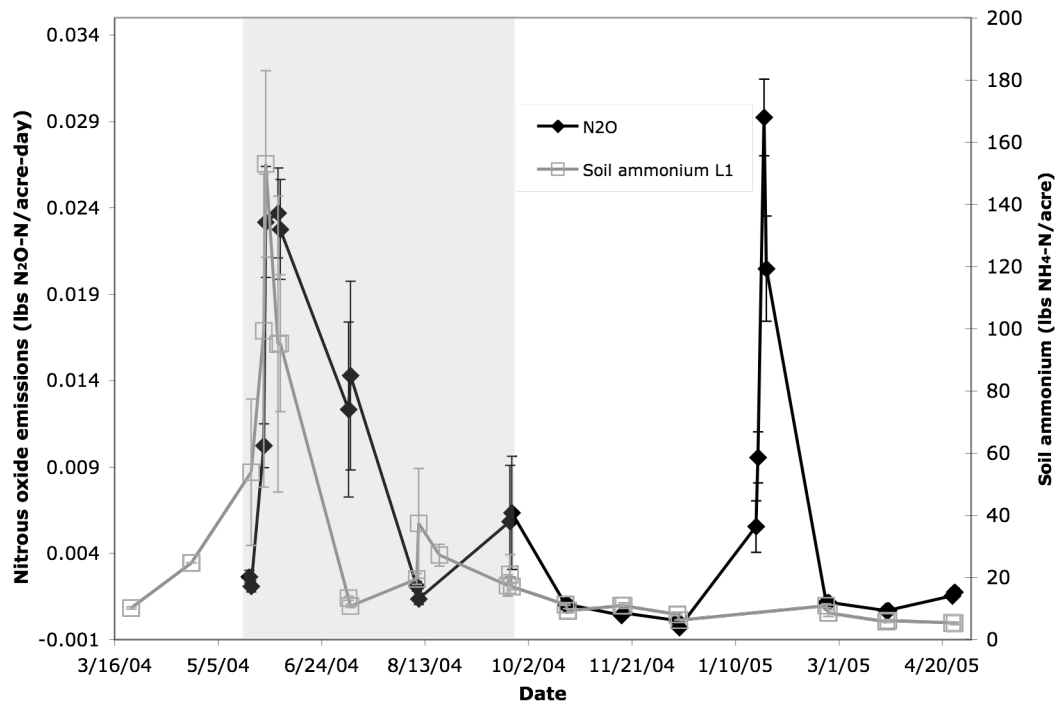
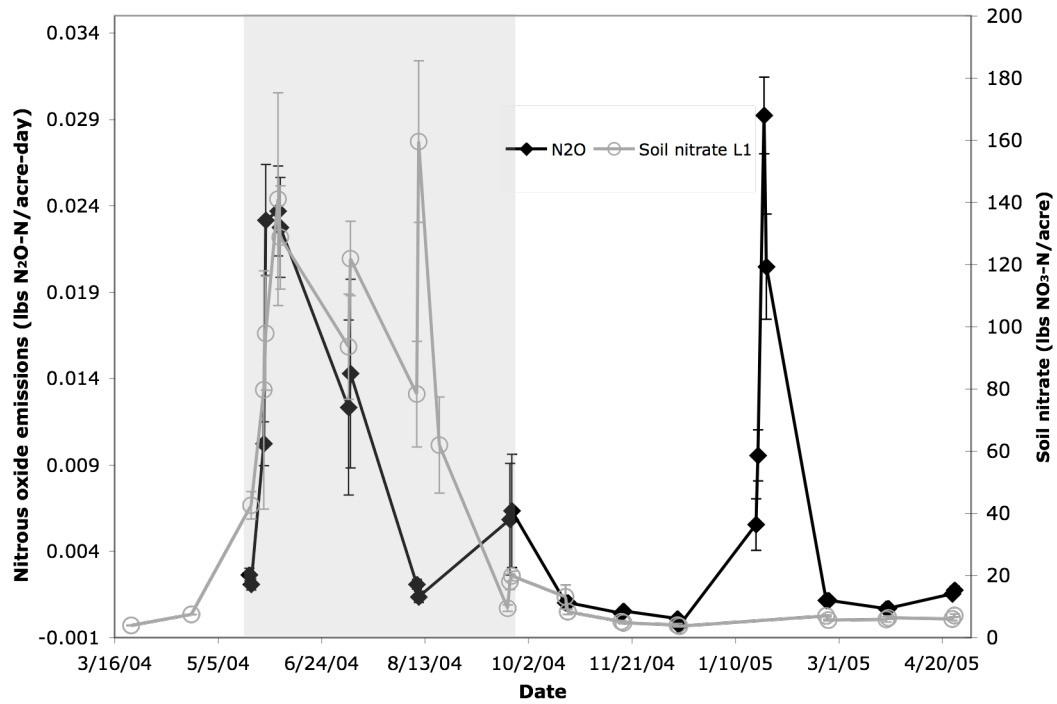


Figure 32. Observed daily nitrous oxide emissions and soil nitrate and ammonium in soil layer 1 (L1). The light grey region represents the time span from crop planting and fertilization to crop harvesting.

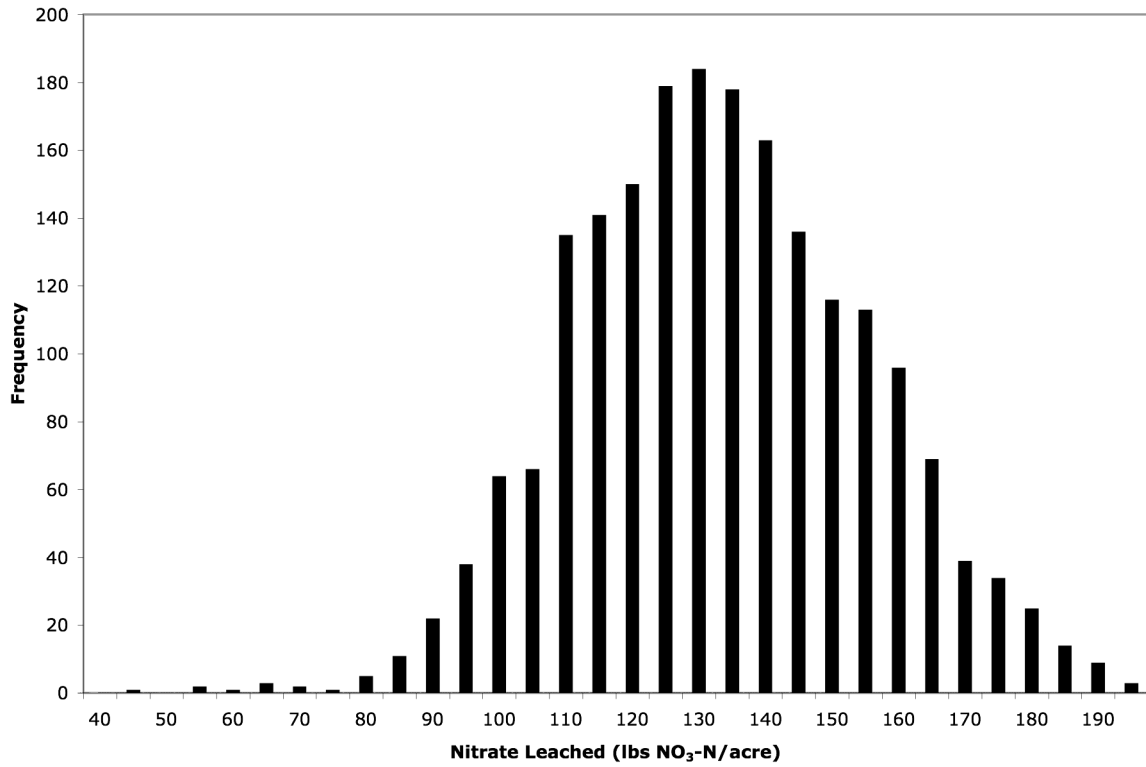


Figure 33. Histogram of the 2,000 simulated values of nitrate leached from the uncertainty analysis.

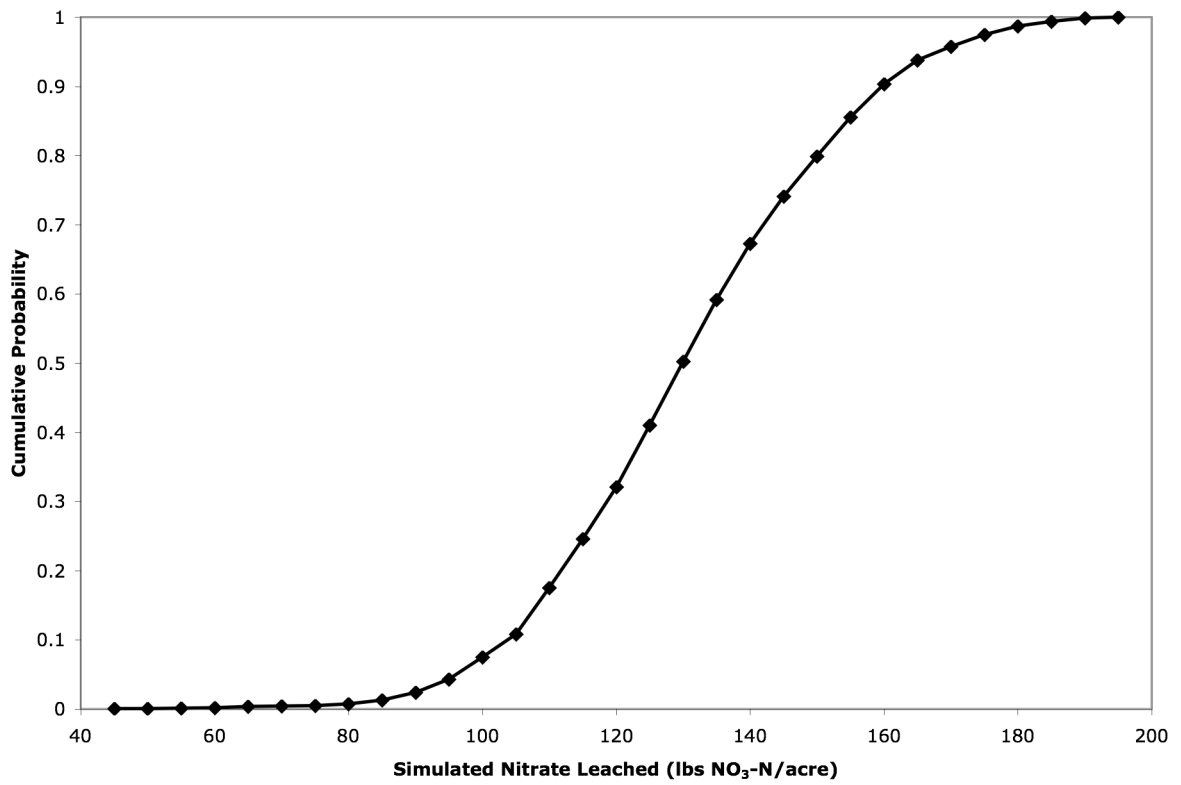


Figure 34. Cumulative probability of obtaining the simulated values of nitrate leached generated during the uncertainty analysis.

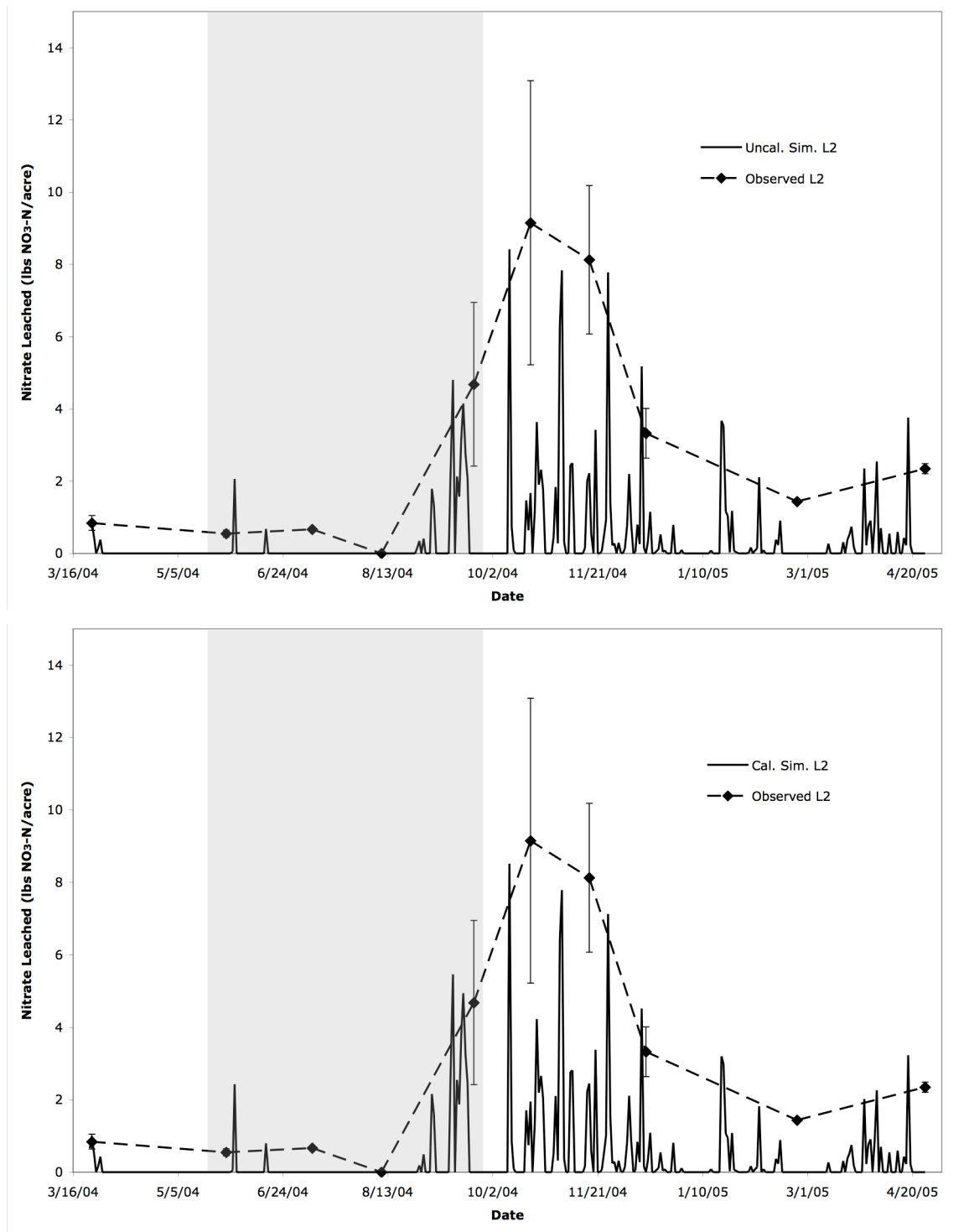


Figure 35. Observed values of nitrate leached, as measured in the shallow lysimeter, vs. the uncalibrated and calibrated simulations of nitrate leached from soil layer 2 (L2). The light grey region represents the time span from crop planting and fertilization to crop harvesting.

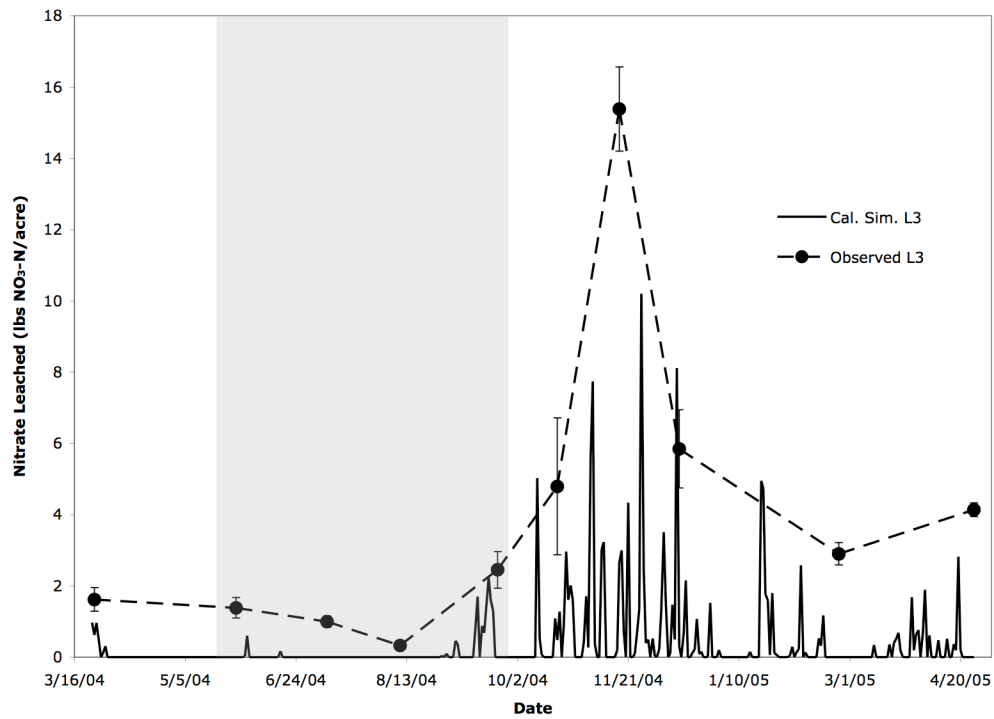
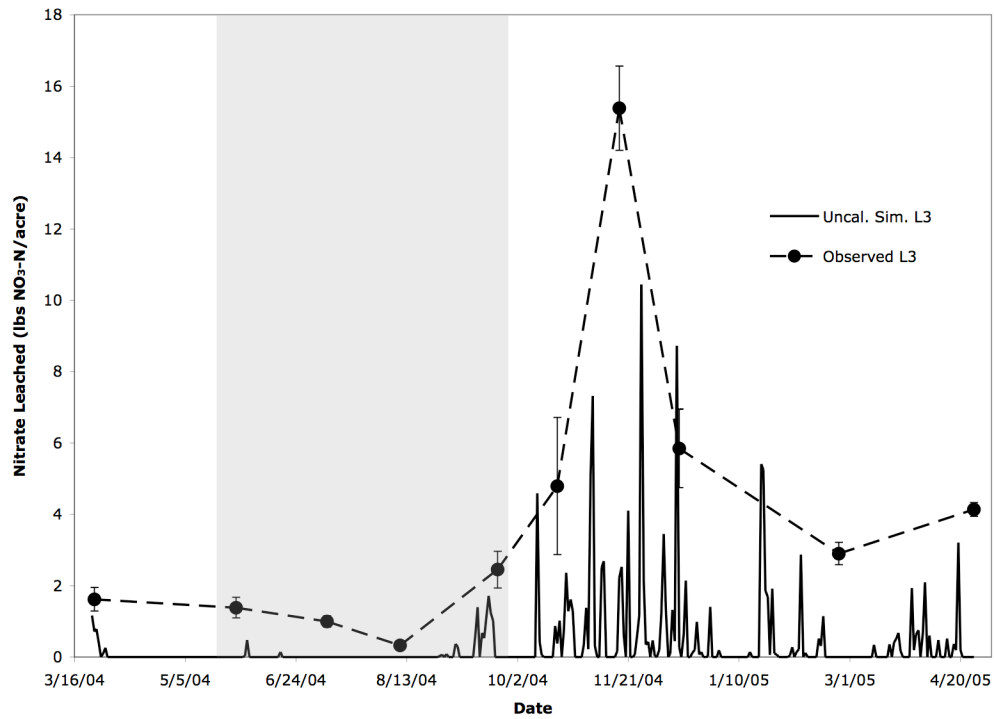


Figure 36. Observed values of nitrate leached, as measured in the deep lysimeter, vs. the uncalibrated and calibrated simulations of nitrate leached from soil layer 3 (L3). The light grey region represents the time span from crop planting and fertilization to crop harvesting.

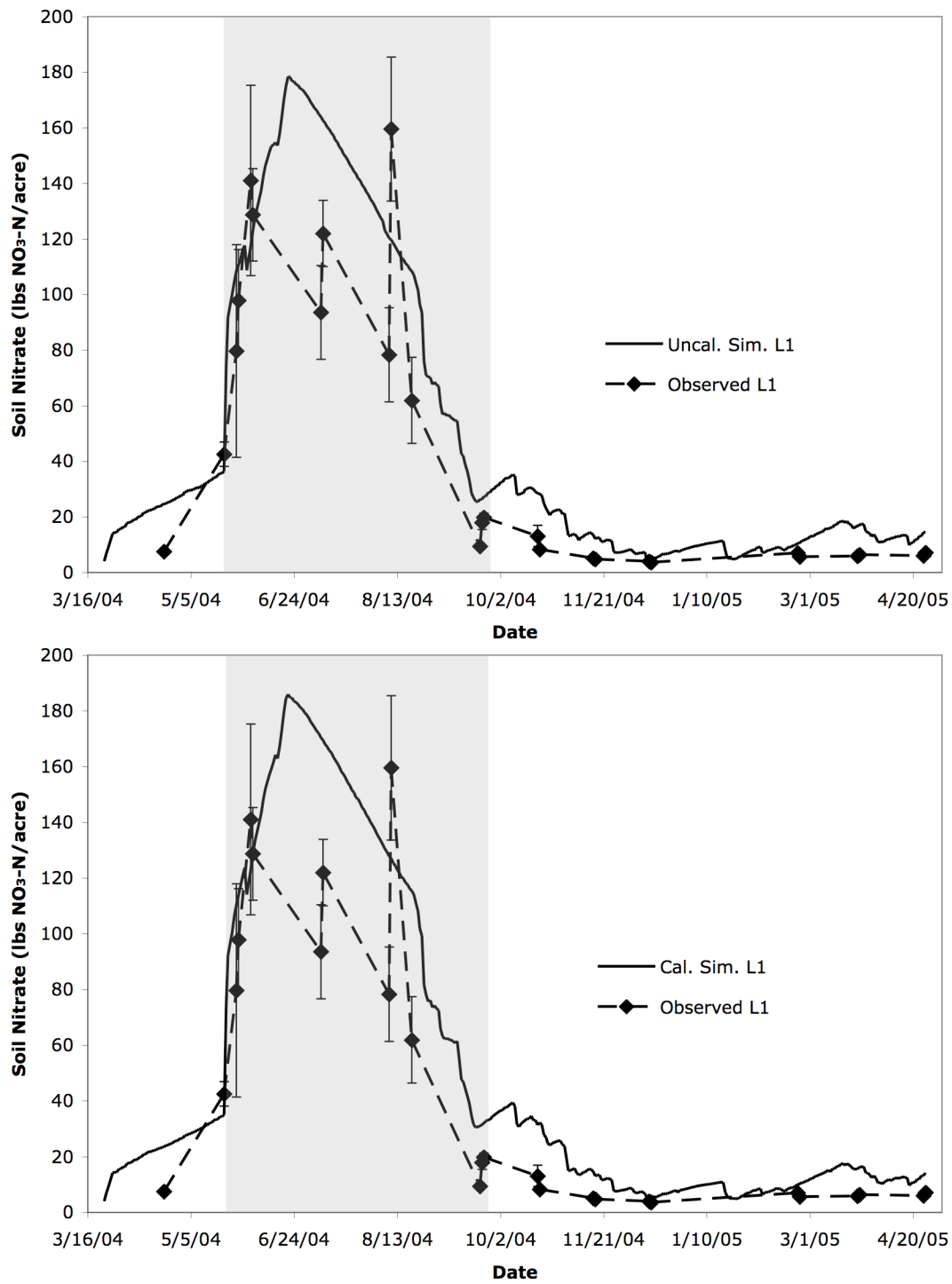


Figure 37. Observed vs. the uncalibrated and calibrated simulations of soil nitrate in layer 1 (L1). The light grey region represents the time span from crop planting and fertilization to crop harvesting.

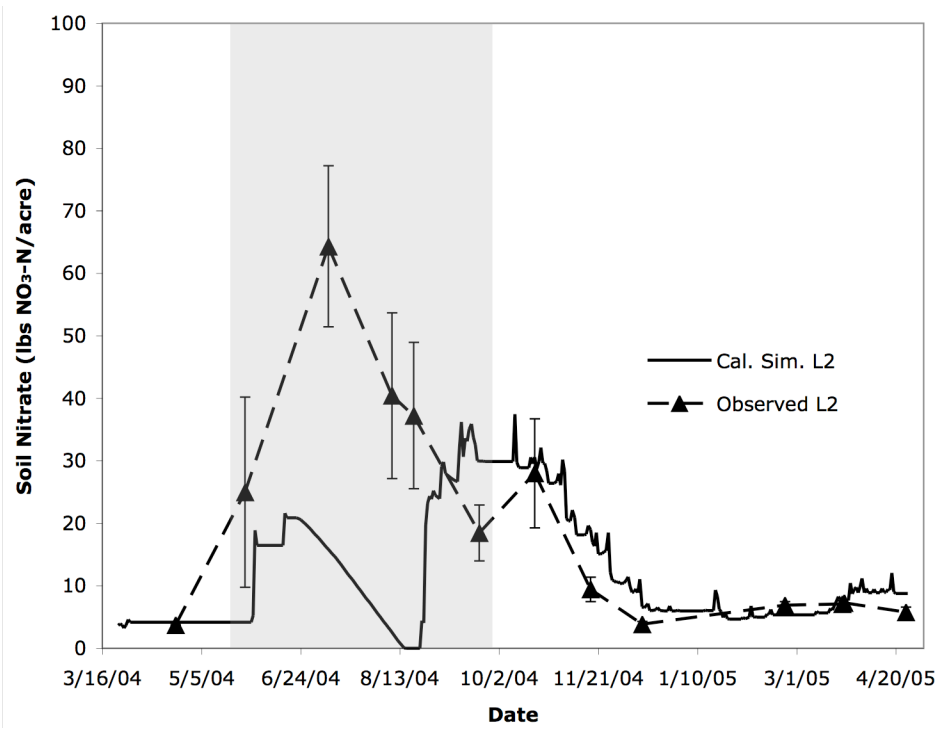
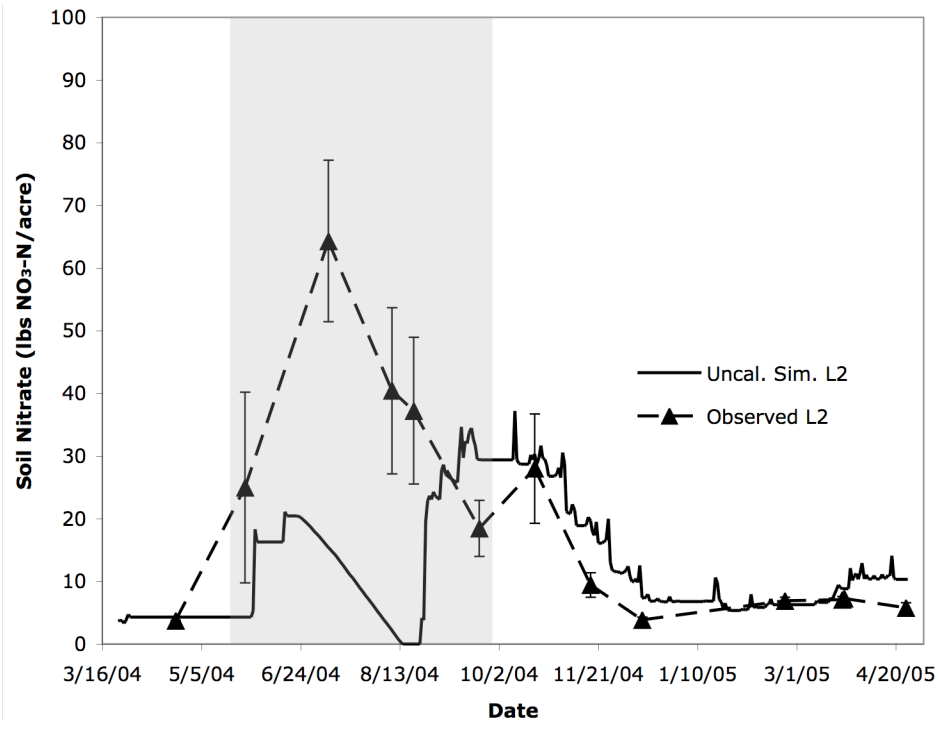


Figure 38. Observed vs. the uncalibrated and calibrated simulations of soil nitrate in layer 2 (L2). The light grey region represents the time span from crop planting and fertilization to crop harvesting.

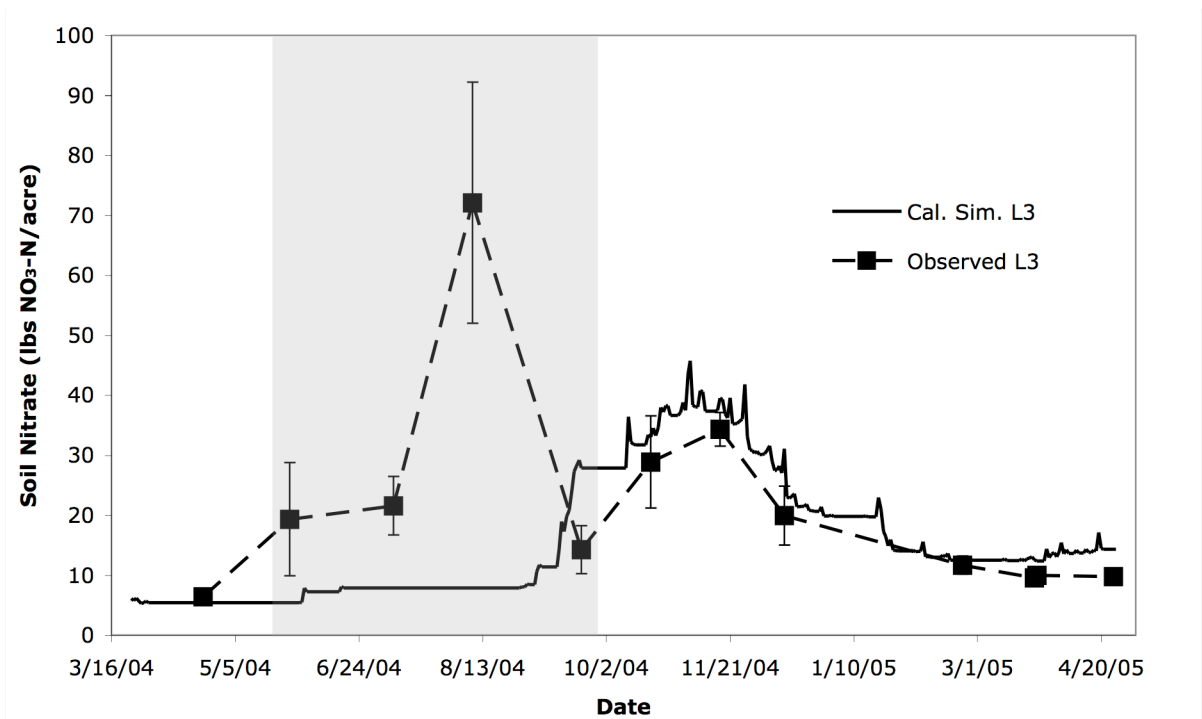
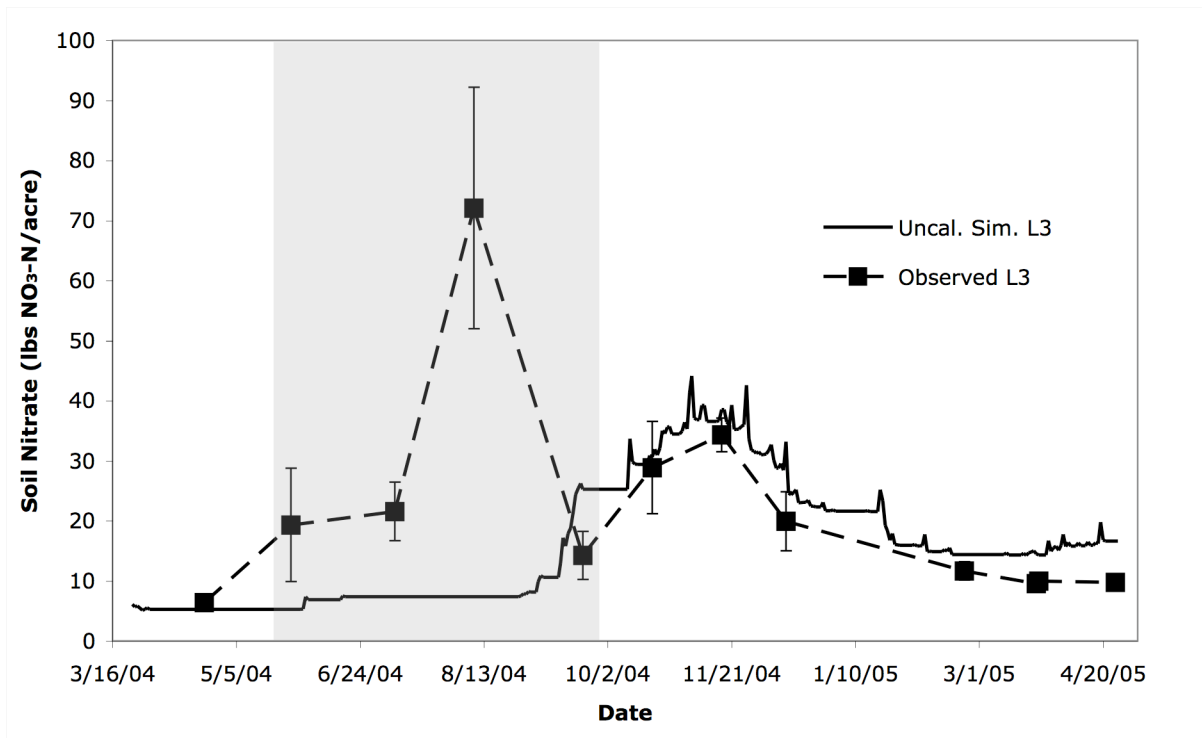


Figure 39. Observed vs. the uncalibrated and calibrated simulations of soil nitrate in layer 3 (L3). The light grey region represents the time span from crop planting and fertilization to crop harvesting.

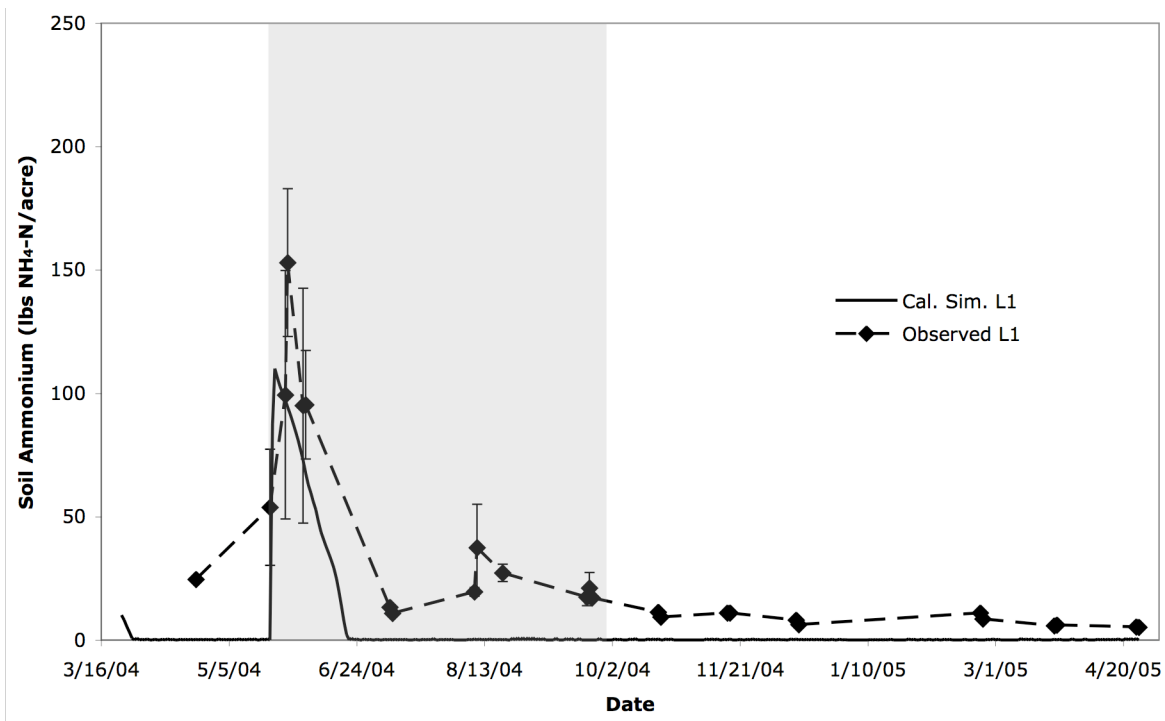
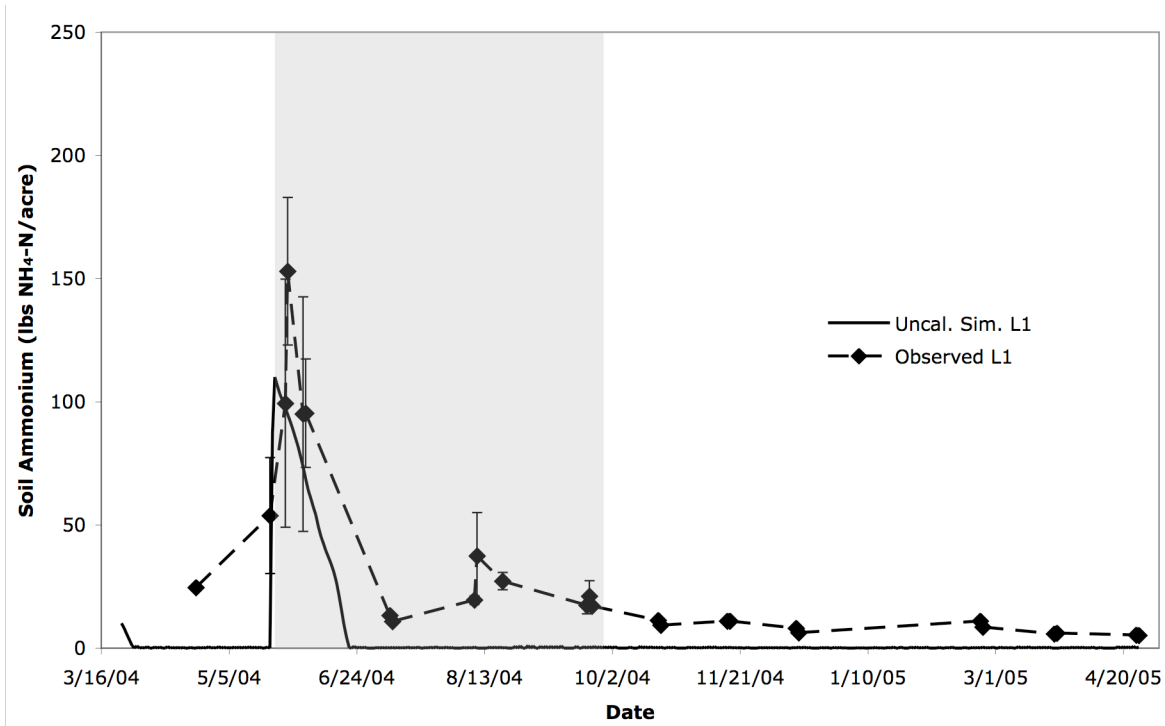


Figure 40. Observed vs. the uncalibrated and calibrated simulations of soil ammonium in layer 1. The light grey region represents the time span from crop planting and fertilization to crop harvesting.

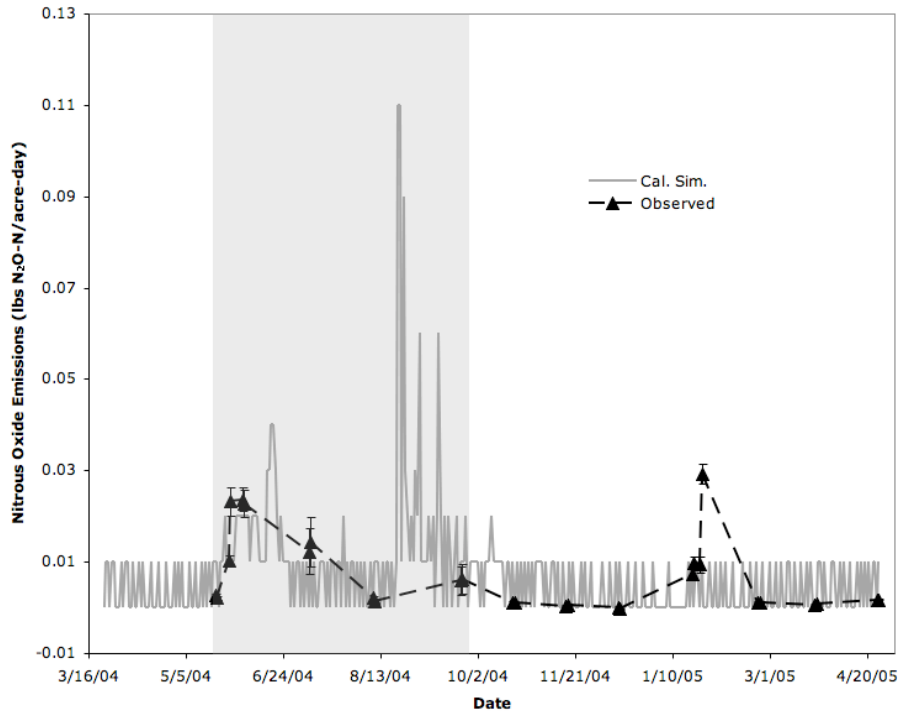
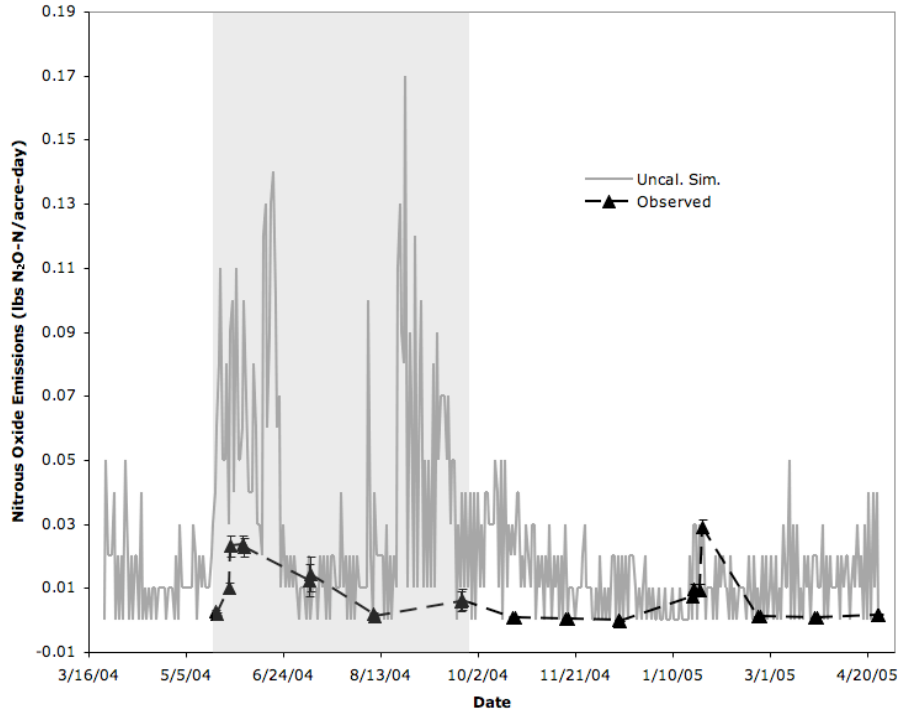


Figure 41. Observed vs. the uncalibrated and calibrated simulations of nitrous oxide emissions. The light grey region represents the time span from crop planting and fertilization to crop harvesting.

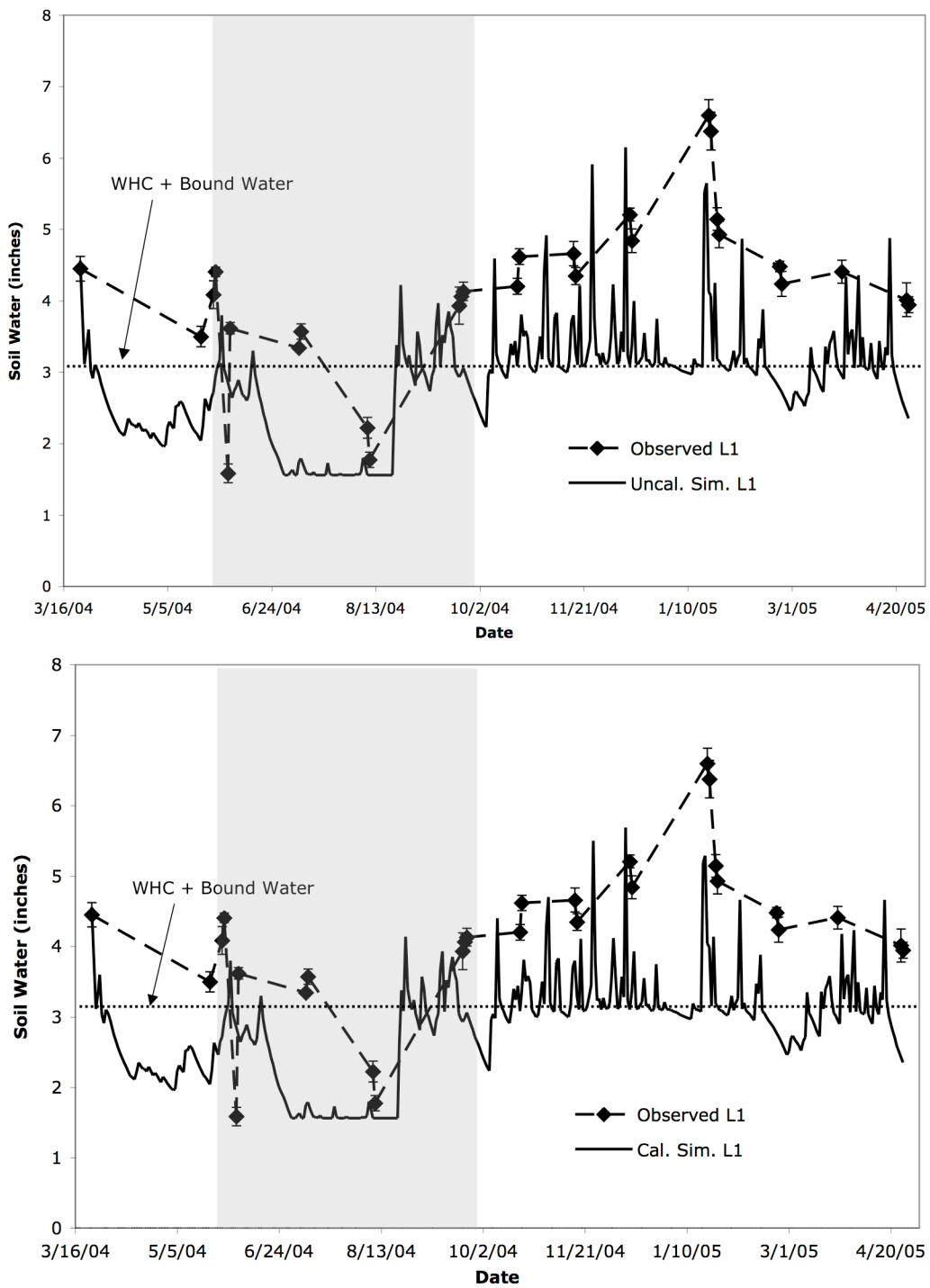


Figure 42. Observed vs. the uncalibrated and calibrated simulations of soil water in layer 1 (L1). The light grey region represents the time span from crop planting and fertilization to crop harvesting.

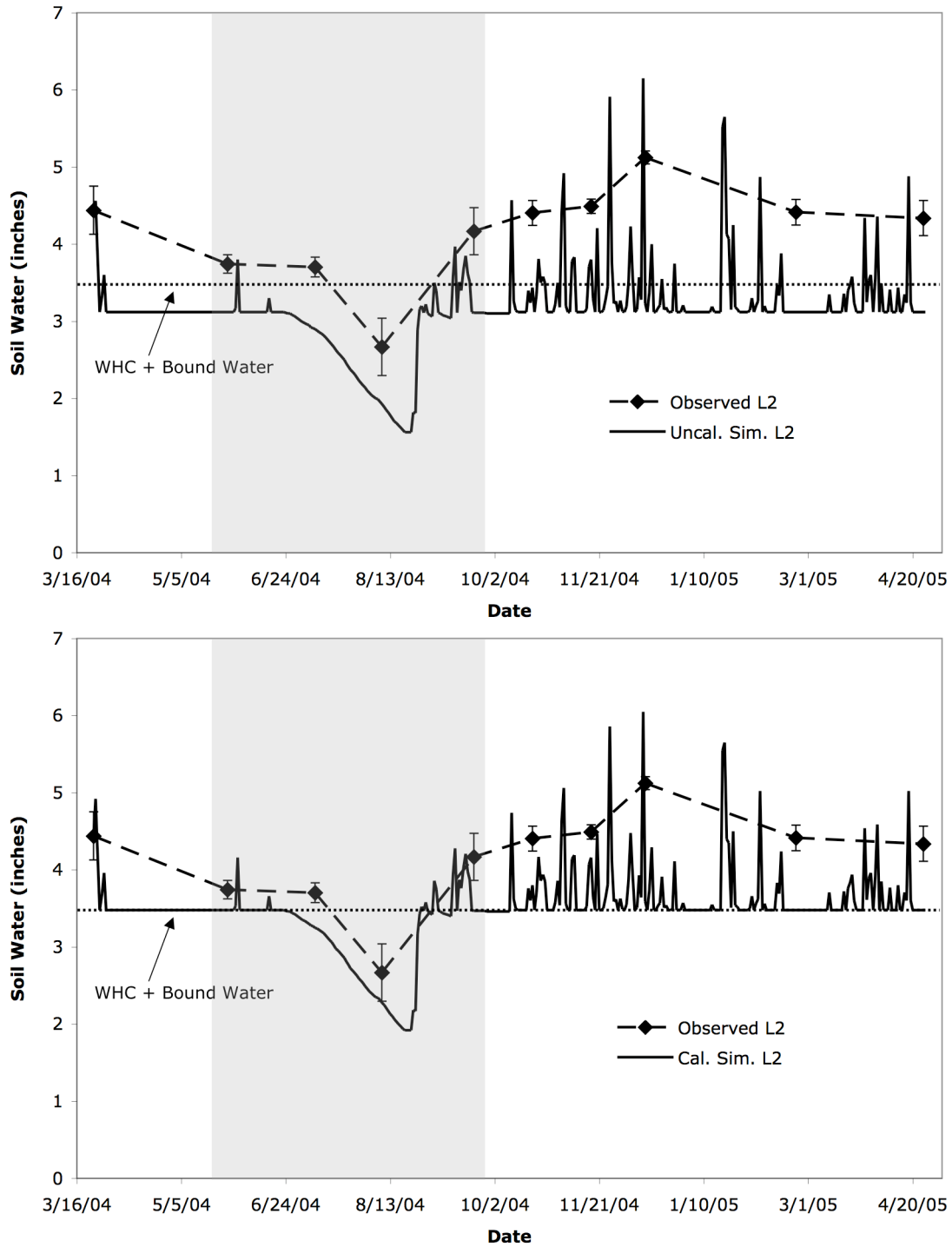


Figure 43. Observed vs. the uncalibrated and calibrated simulations of soil water in layer 2 (L2). The light grey region represents the time span from crop planting and fertilization to crop harvesting.

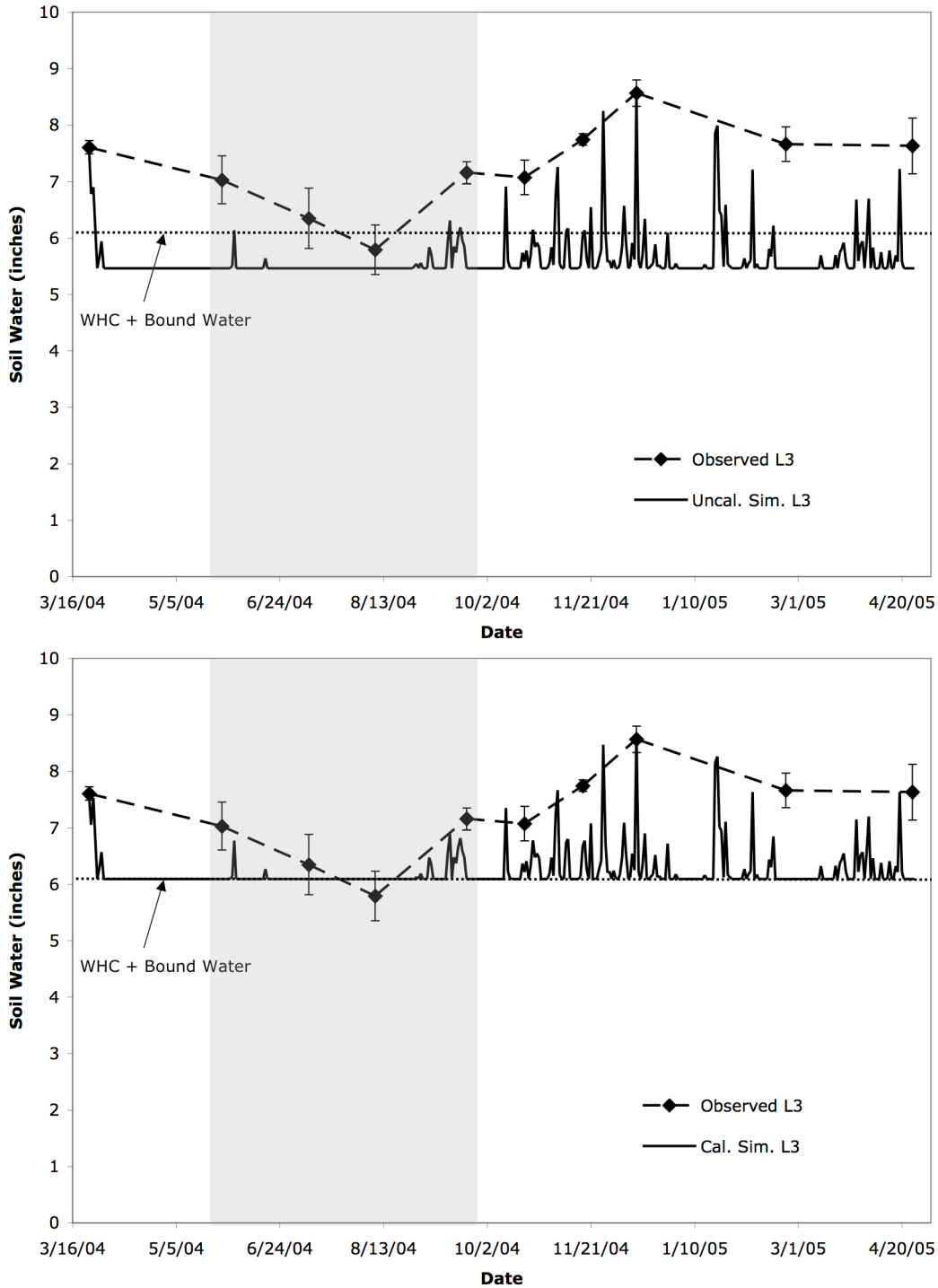


Figure 44. Observed vs. the uncalibrated and calibrated simulations of soil water in layer 3 (L3). The light grey region represents the time span from crop planting and fertilization to crop harvesting.

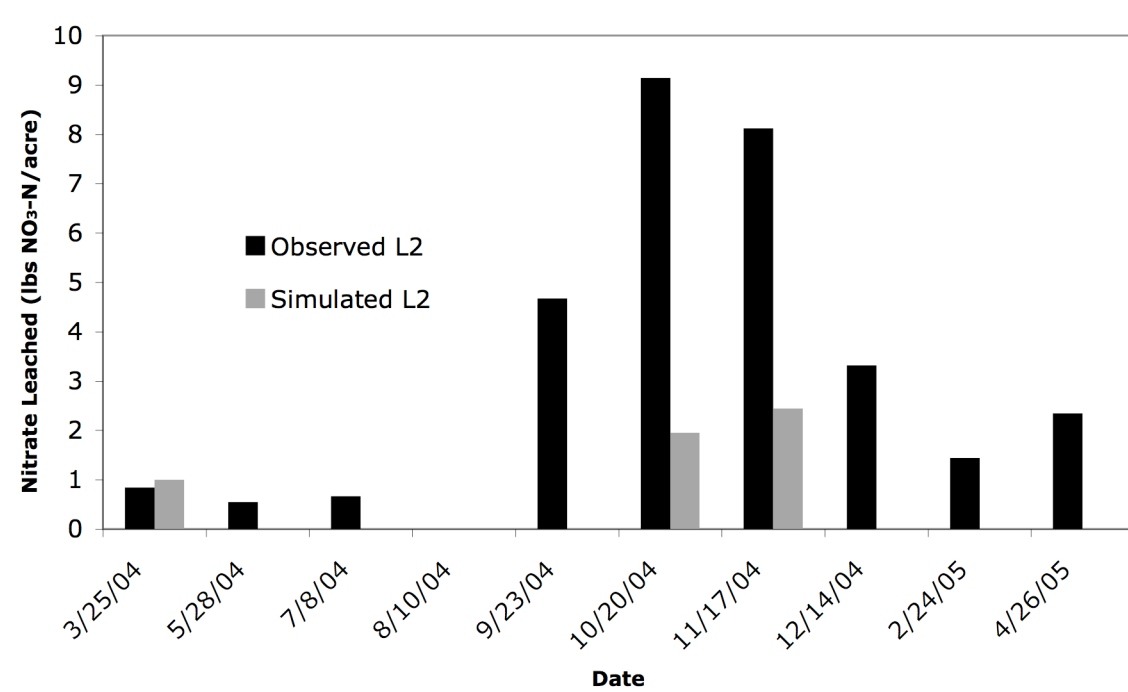
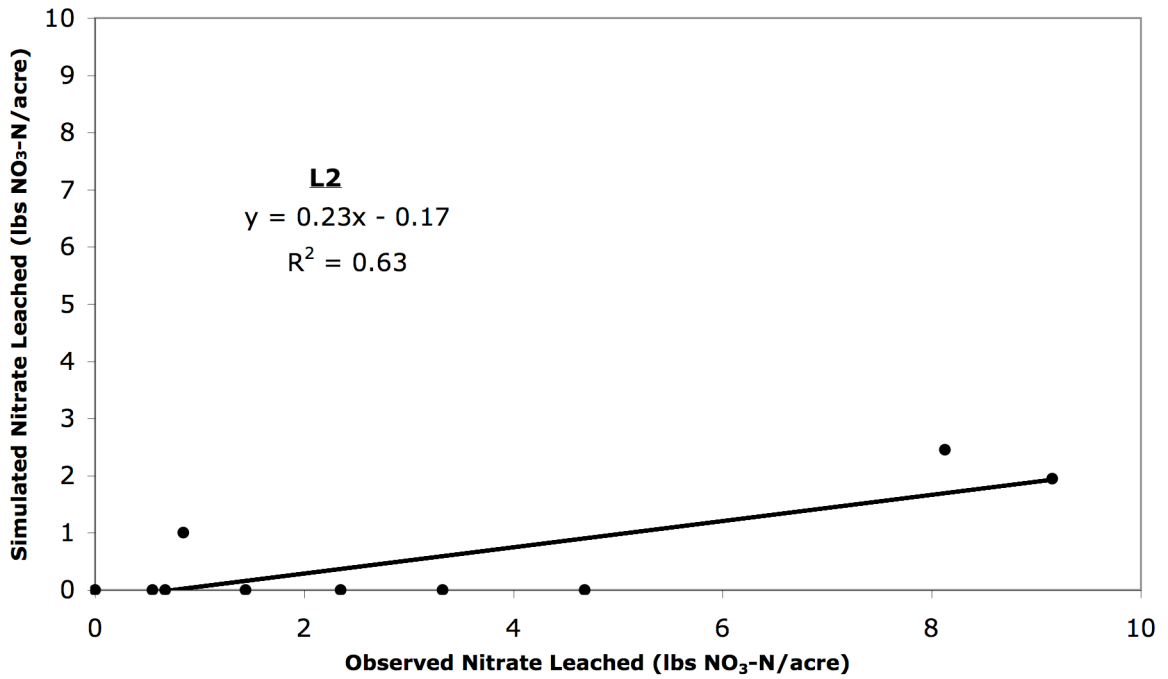


Figure 45. Observed values of nitrate leached, as measured in the shallow lysimeter, vs. the calibrated simulation of nitrate leached from soil layer 2 (L2) (where no bar is shown, the observed or simulated value was equal to zero).

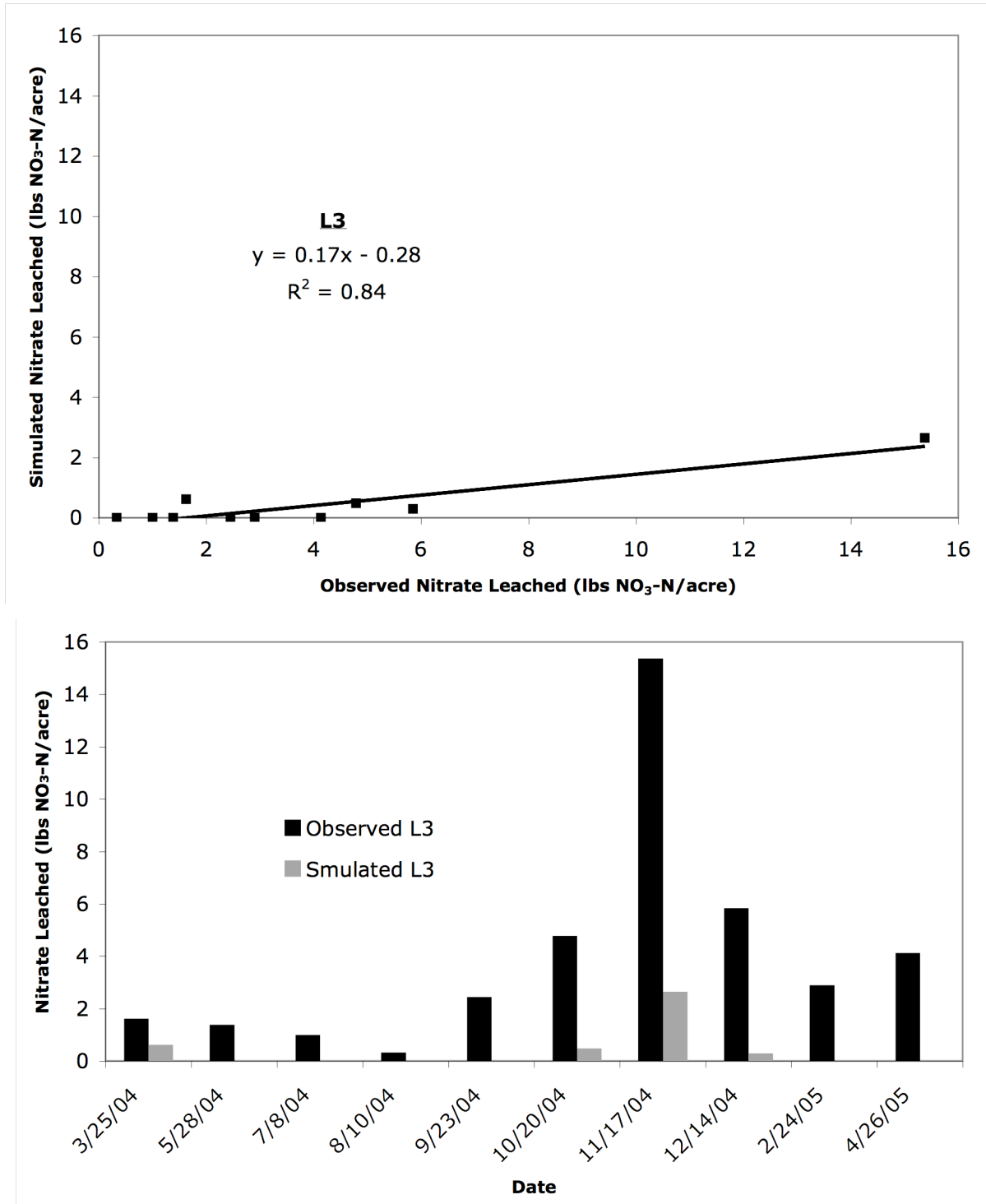


Figure 46. Observed values of nitrate leached, as measured in the deep lysimeter, vs. the calibrated simulation of nitrate leached from soil layer 3 (L3) (where no bar is shown, the observed or simulated value was equal to zero).

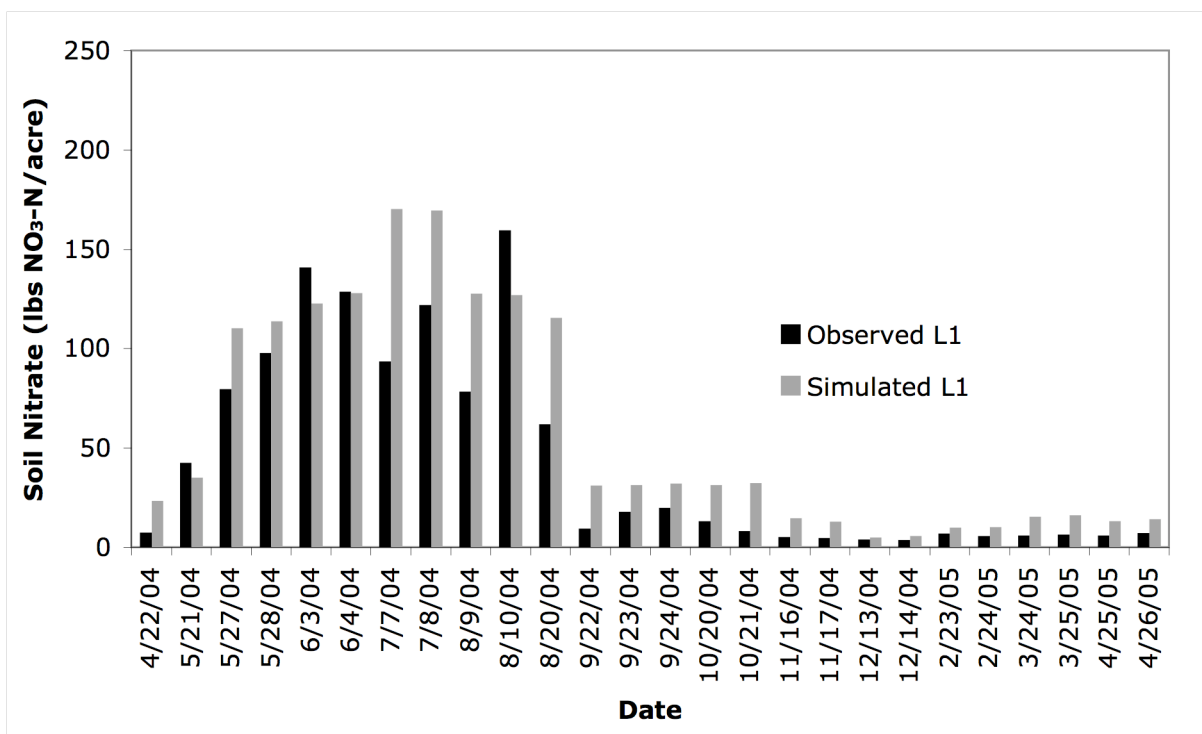
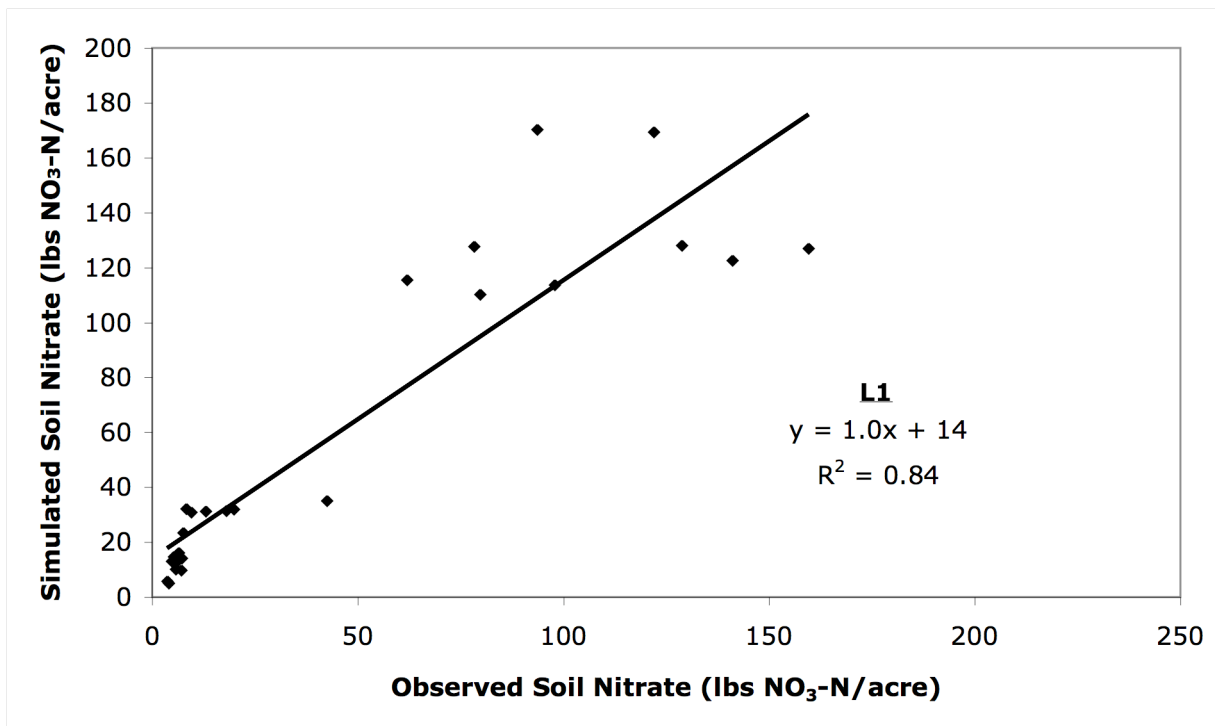


Figure 47. Observed vs. the calibrated simulation of soil nitrate in layer 1 (L1) (where no bar is shown, the observed or simulated value was equal to zero).

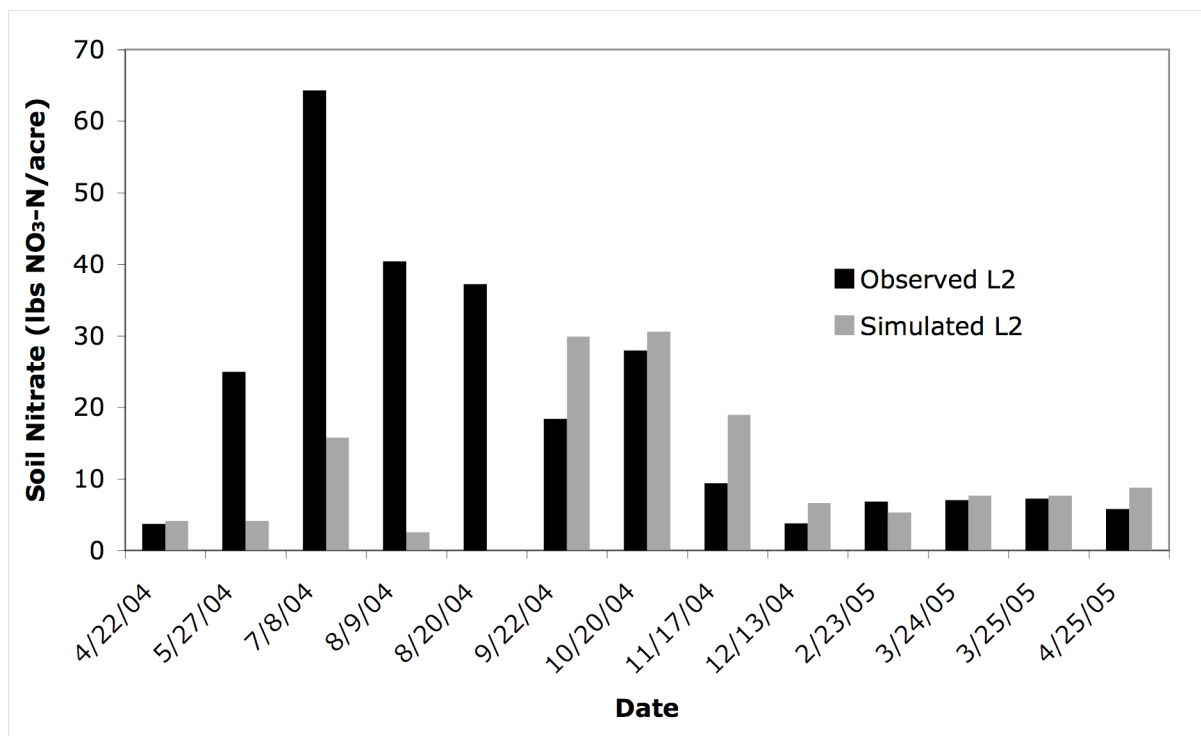
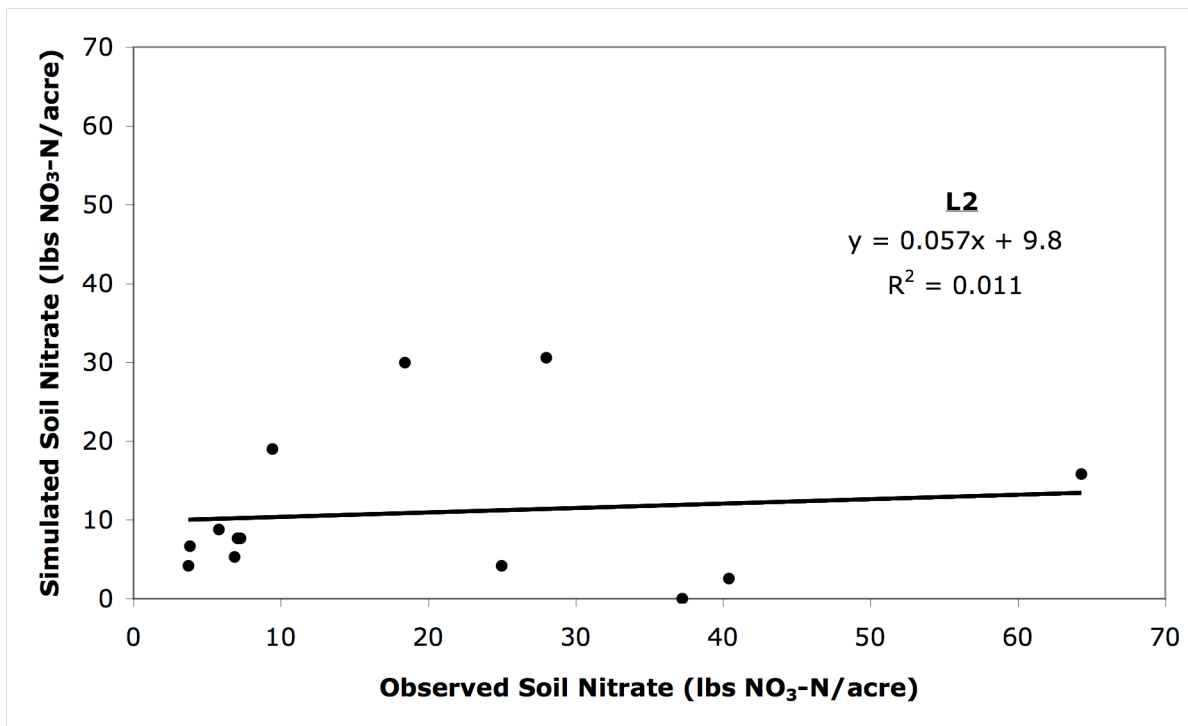


Figure 48. Observed vs. the calibrated simulation of soil nitrate in layer 2 (L2) (where no bar is shown, the observed or simulated value was equal to zero).

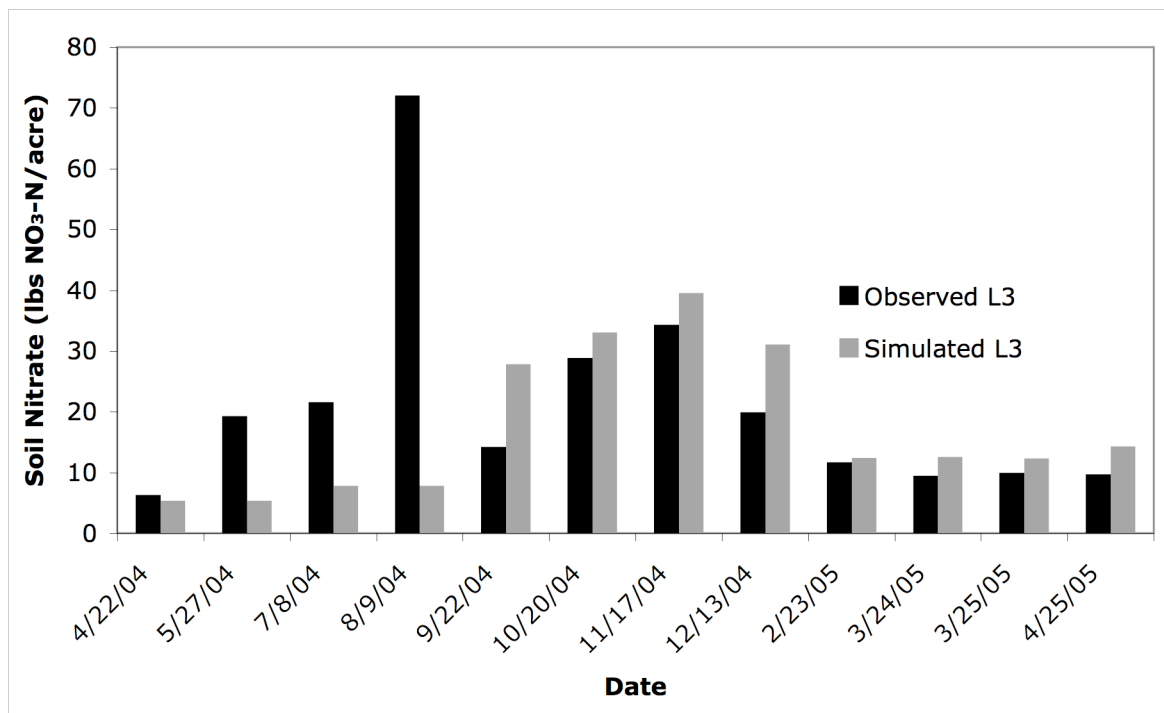
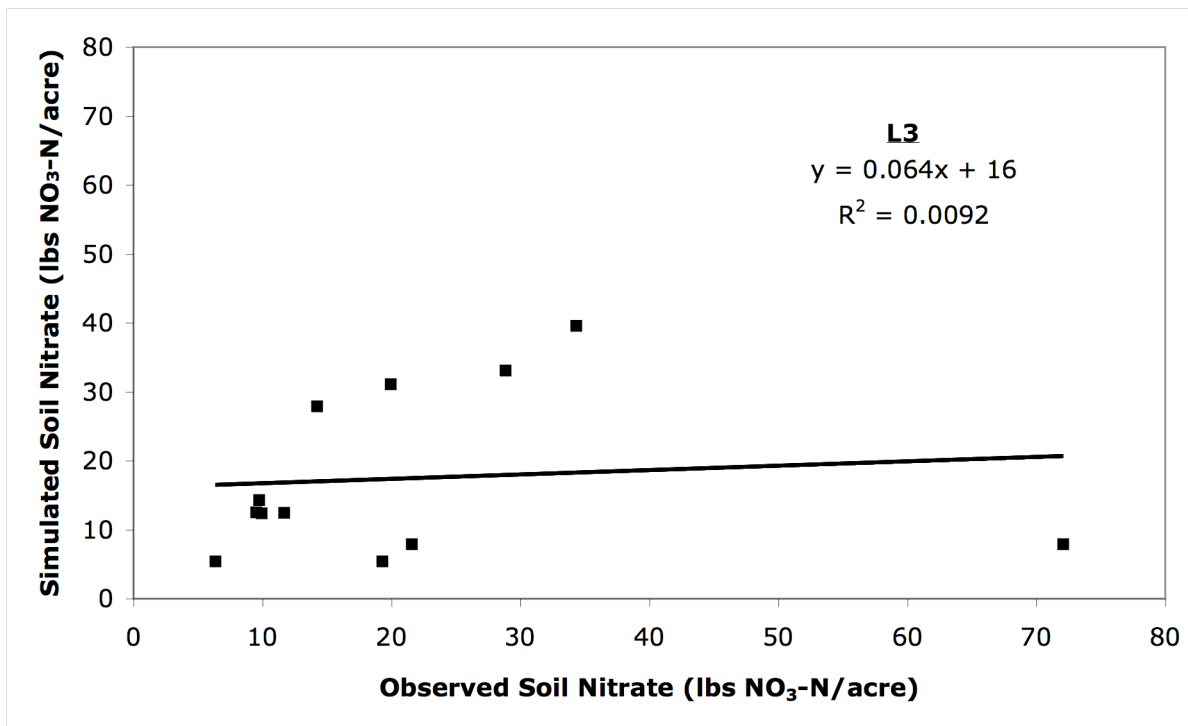


Figure 49. Observed vs. the calibrated simulation of soil nitrate in layer 3 (L3) (where no bar is shown, the observed or simulated value was equal to zero).

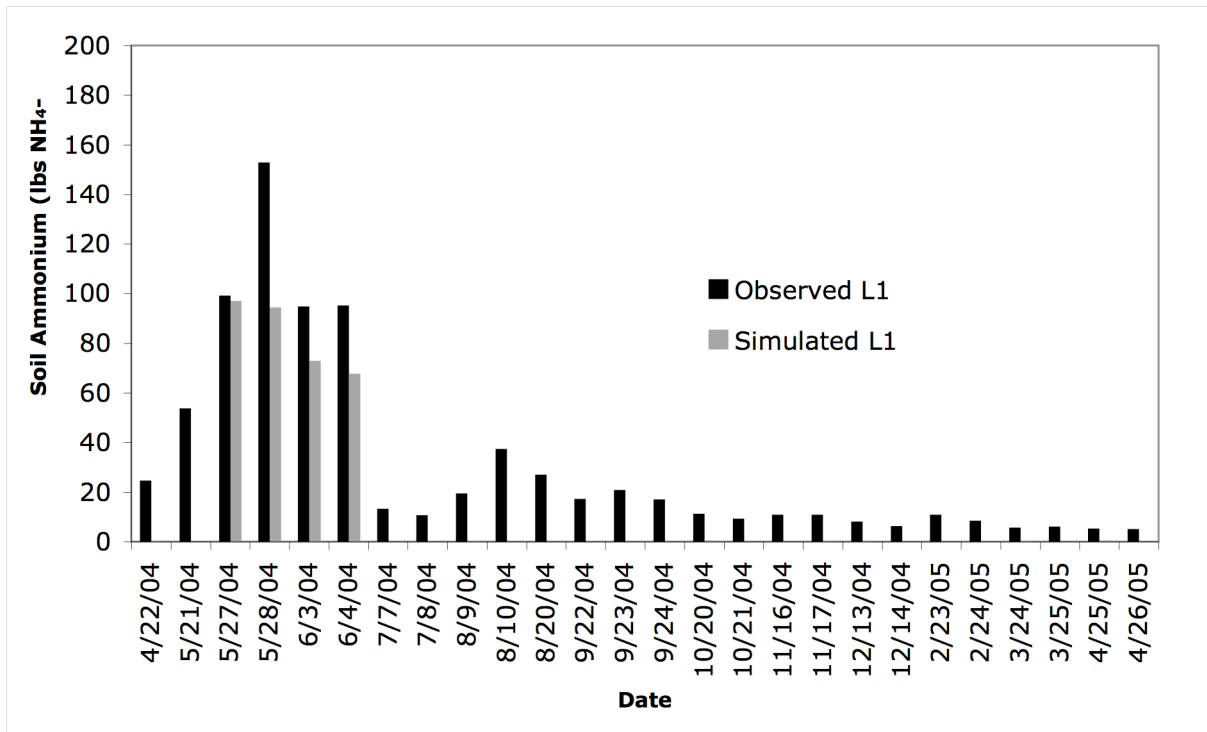
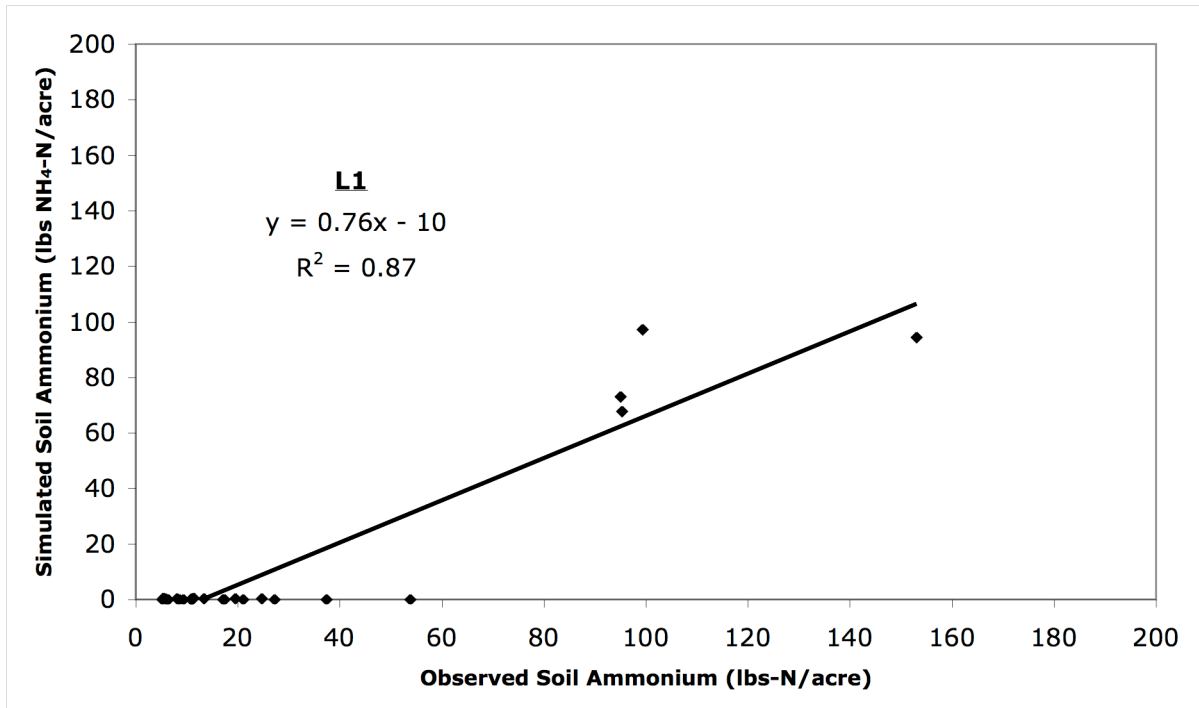


Figure 50. Observed vs. the calibrated simulation of soil ammonium in layer 1 (L1) (where no bar is shown, the observed or simulated value was equal to zero).

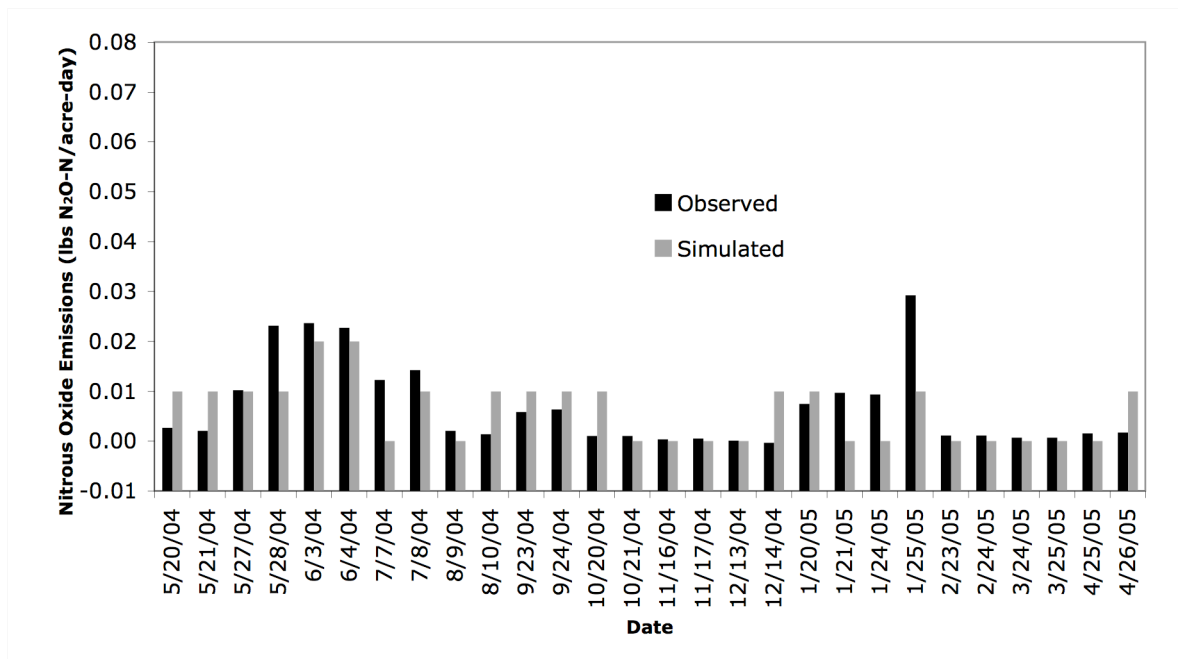
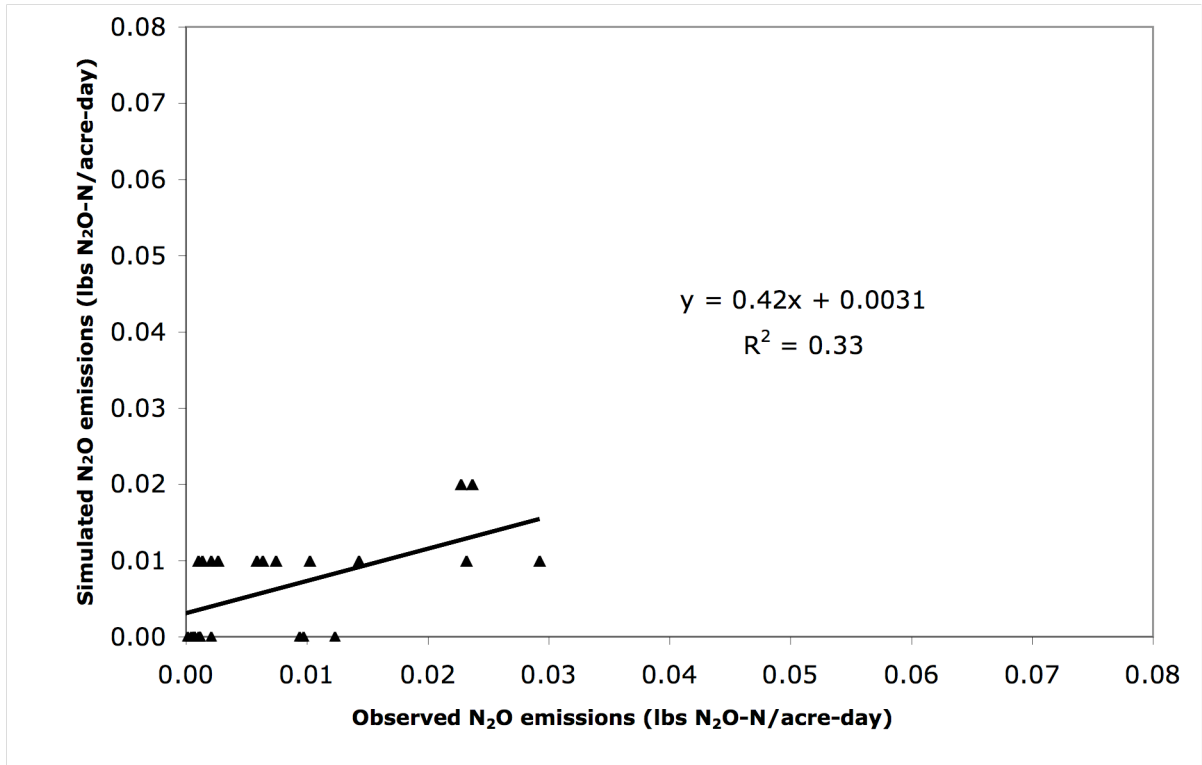


Figure 51. Observed vs. the calibrated simulation of nitrous oxide emissions (where no bar is shown, the observed or simulated value was equal to zero).

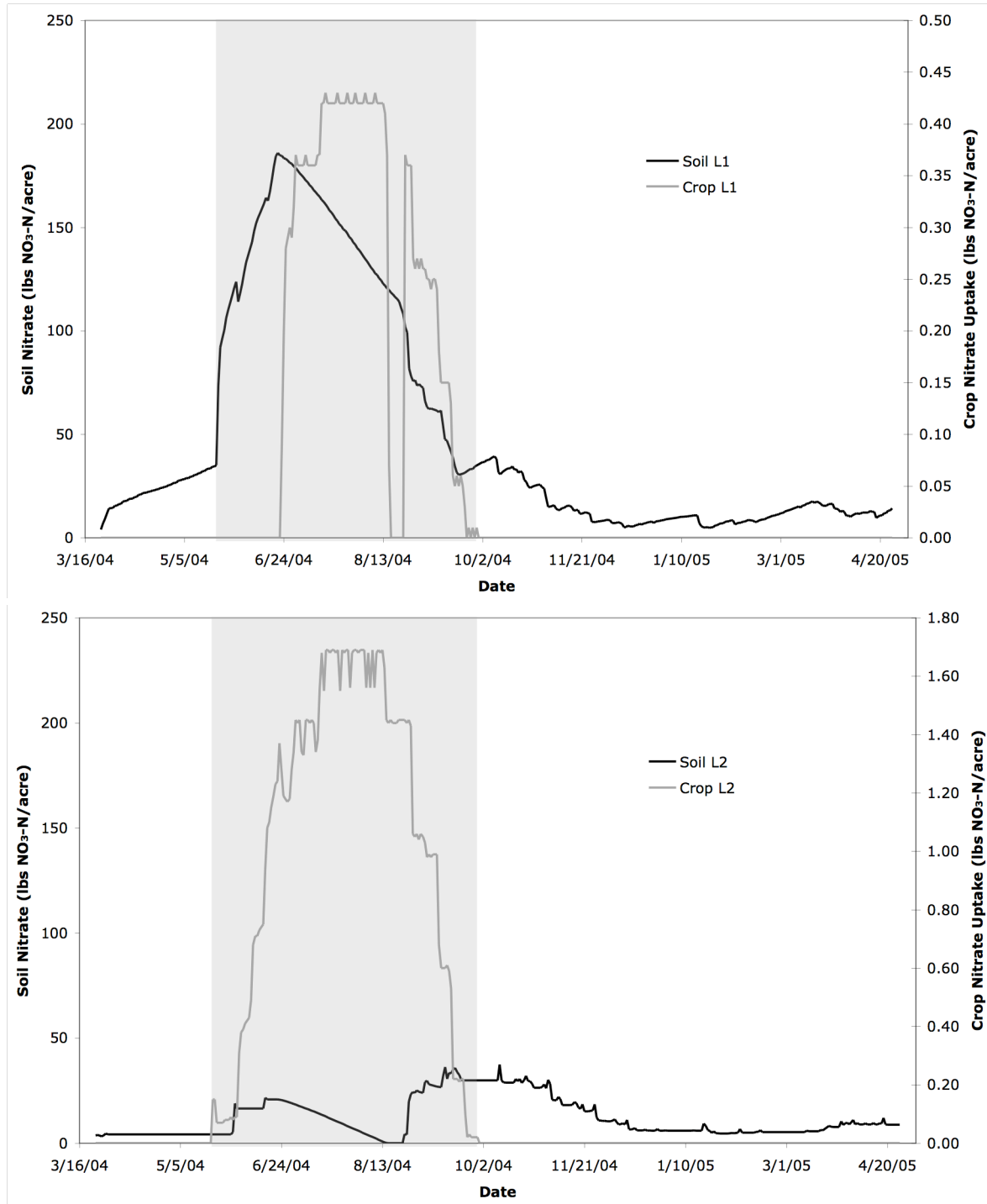


Figure 52. Simulated soil nitrate for layers 1 and 2 (Soil L1 & L2) and crop nitrate uptake (Crop L1 & L2). The light grey region represents the time span from crop planting and fertilization to crop harvesting.

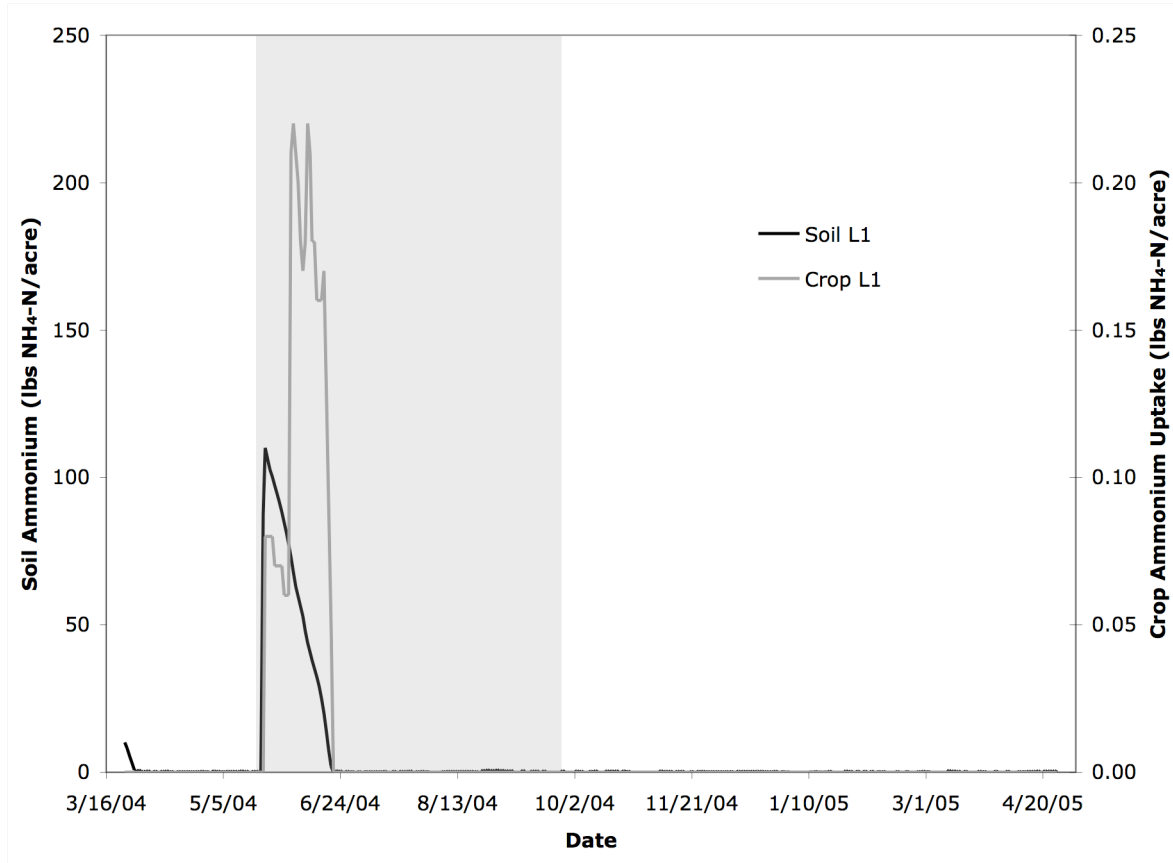


Figure 53. Simulated soil ammonium for layer 1 (Soil L1) and crop ammonium uptake (Crop L1). The light grey region represents the time span from crop planting and fertilization to crop harvesting.

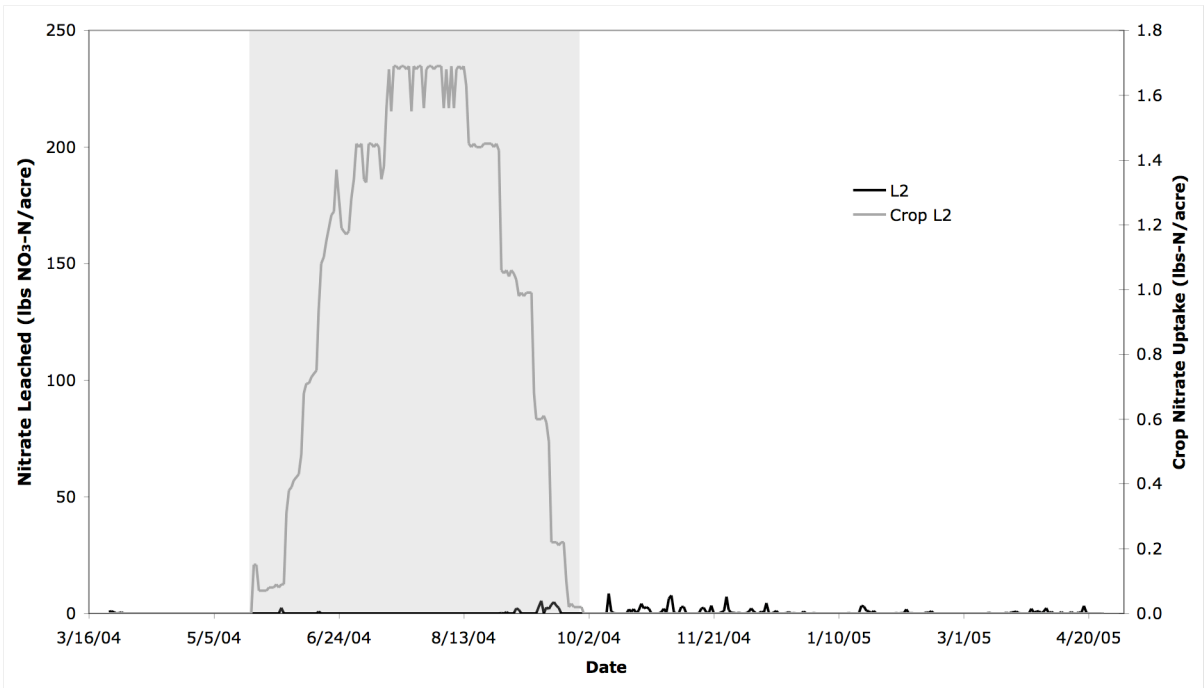
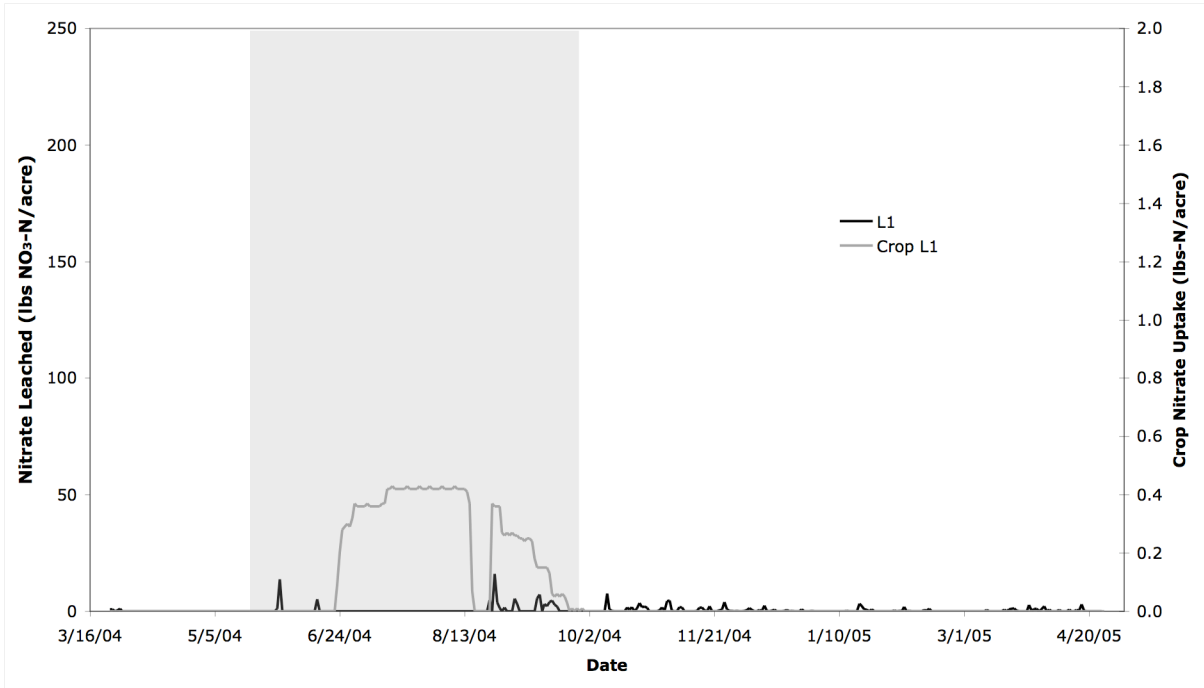


Figure 54. Simulated nitrate leached from soil layers 1 and 2 (L1 & L2) and crop nitrate uptake (Crop L1 & L2). The light grey region represents the time span from crop planting and fertilization to crop harvesting.

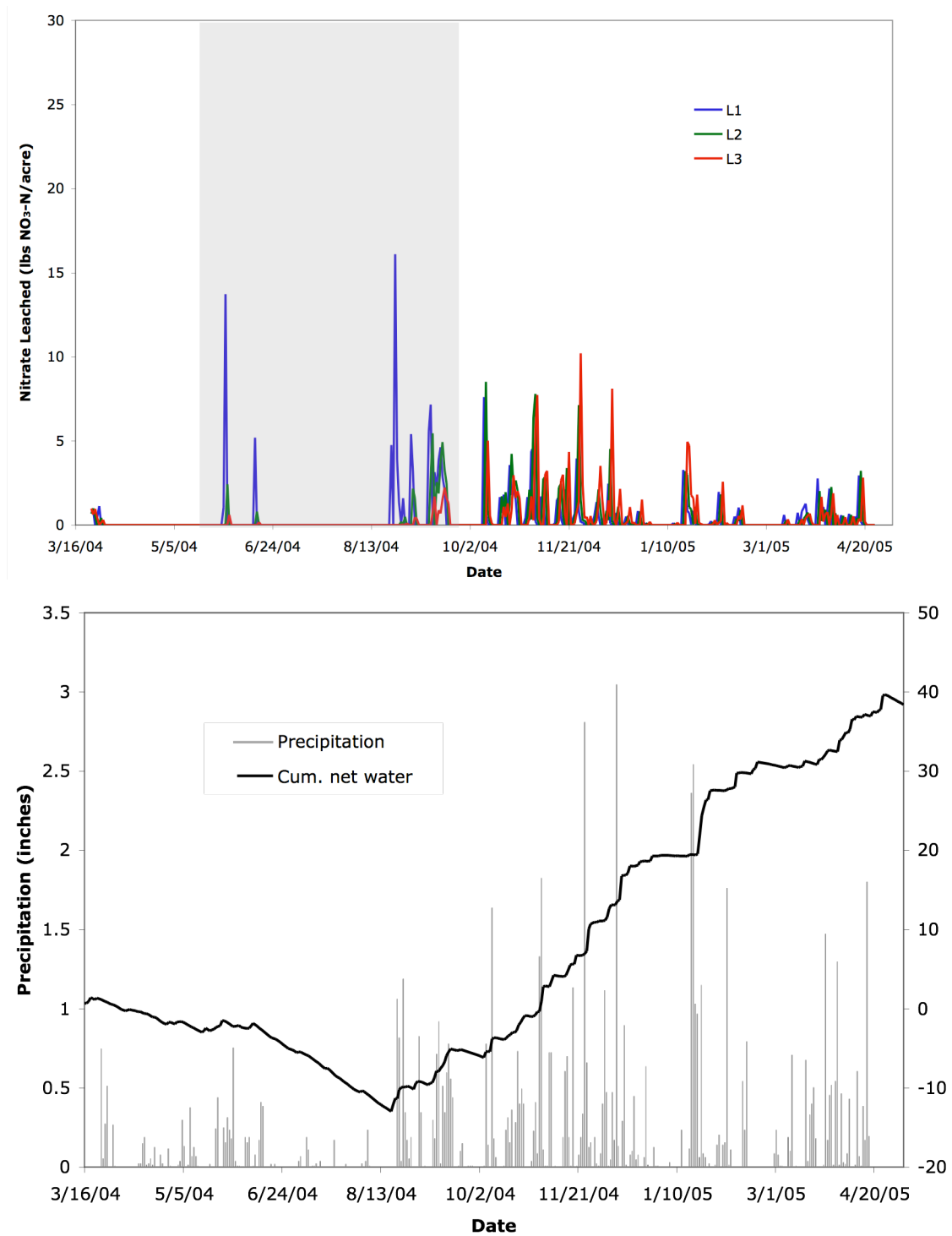


Figure 55. Simulated nitrate leached from soil layers 1 - 3 (L1 – L3), cumulative net water (precipitation – evapotranspiration), and precipitation. The light grey region represents the time span from crop planting and fertilization to crop harvesting.

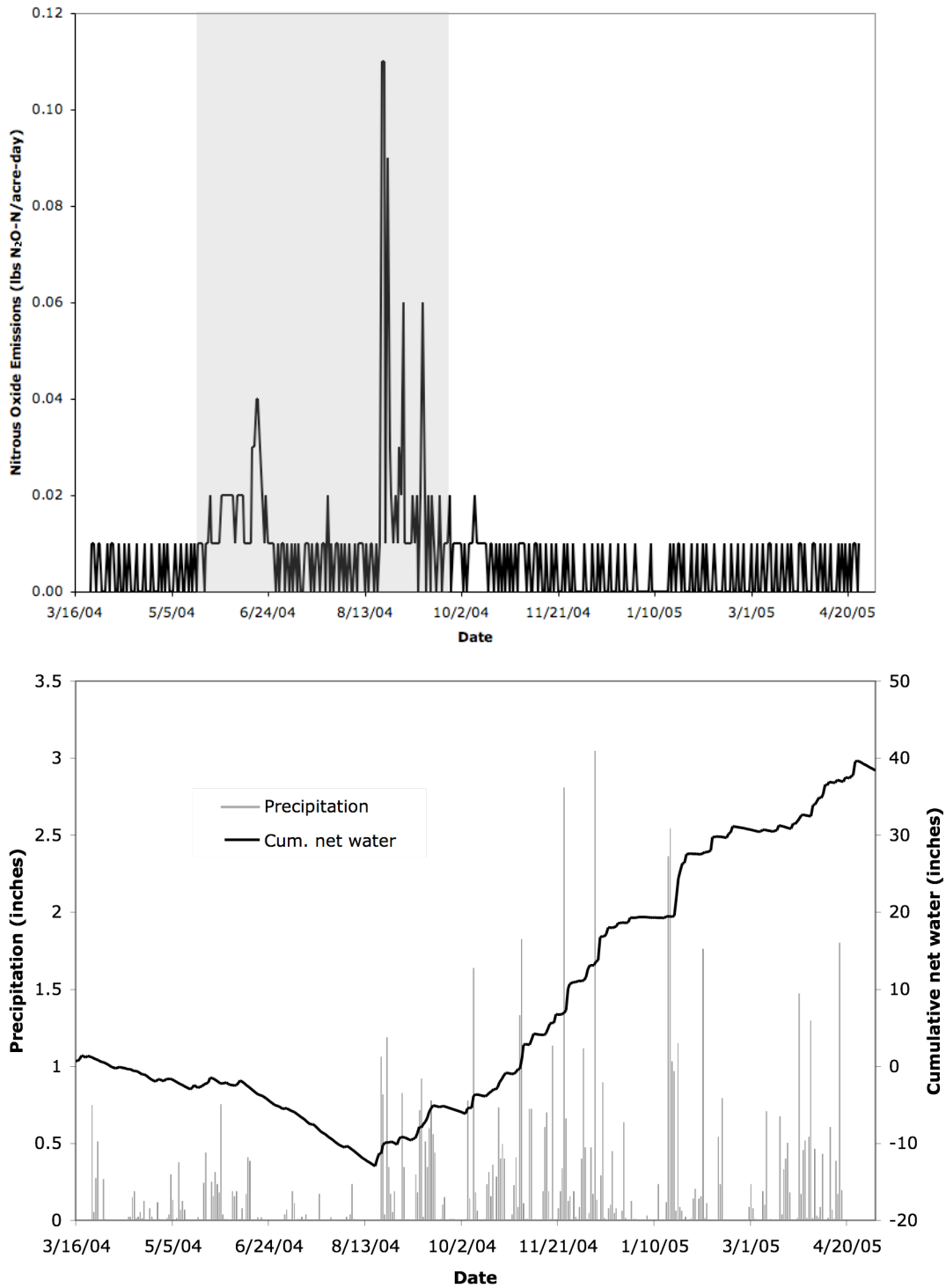


Figure 56. Simulated nitrous oxide emissions, cumulative net water (precipitation – evapotranspiration), and precipitation. The light grey region represents the time span from crop planting and fertilization to crop harvesting.

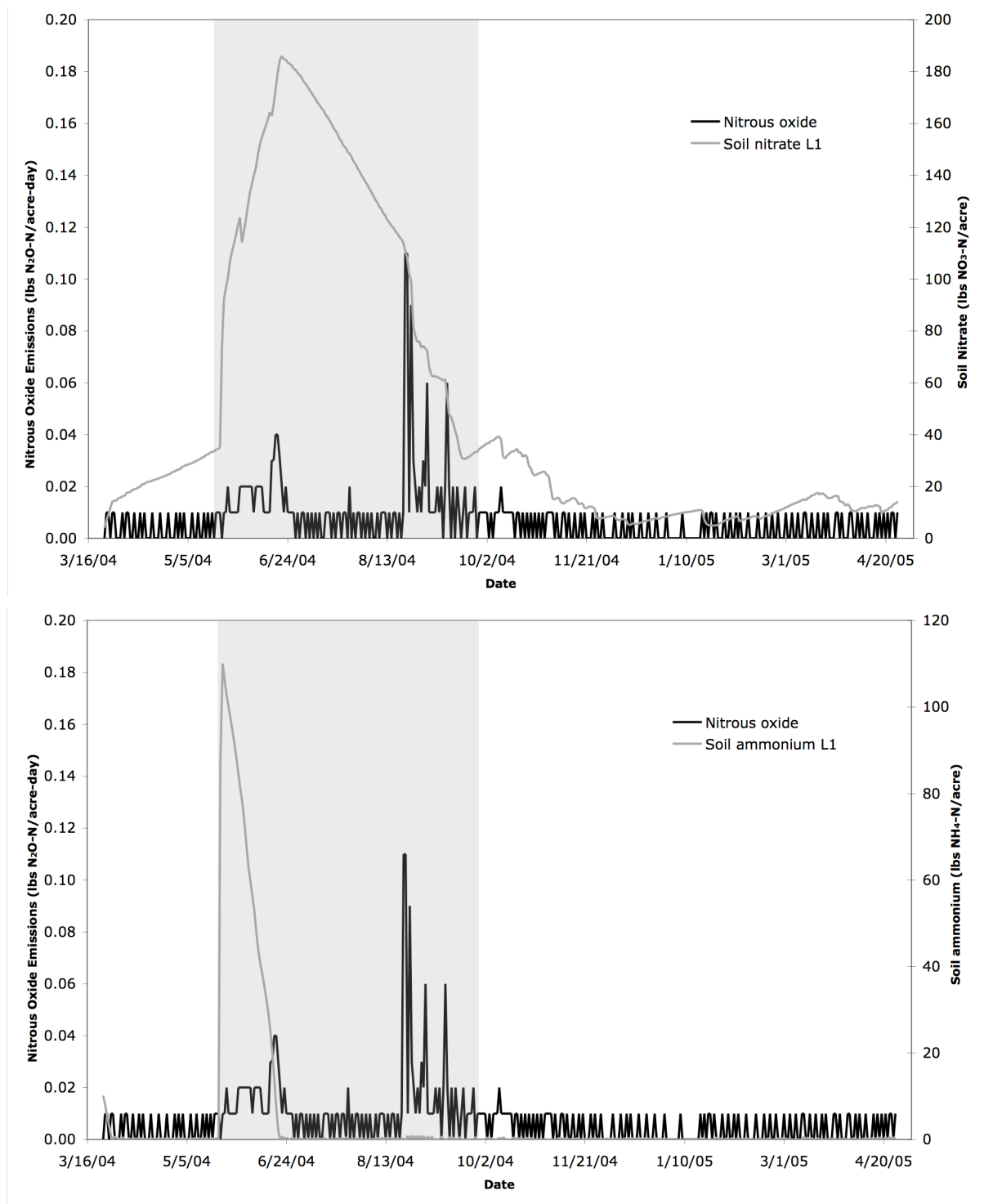


Figure 57. Simulated nitrous oxide emissions and soil nitrate and ammonium in layer 1 (L1). The light grey region represents the time span from crop planting and fertilization to crop harvesting.

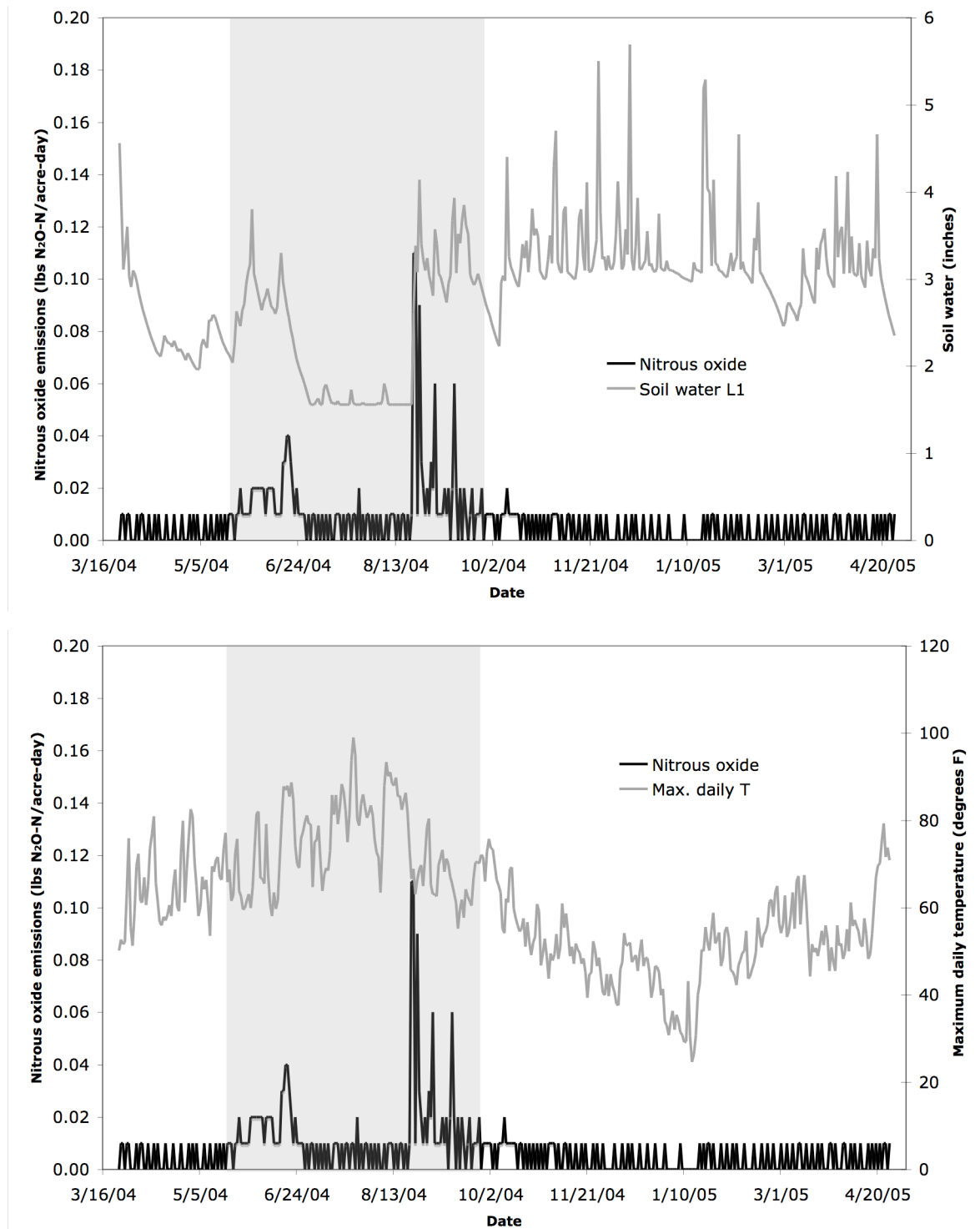


Figure 58. Simulated nitrous oxide emissions, soil water in layer 1 (L1), and maximum daily air temperature (T). The light grey region represents the time span from crop planting and fertilization to crop harvesting.

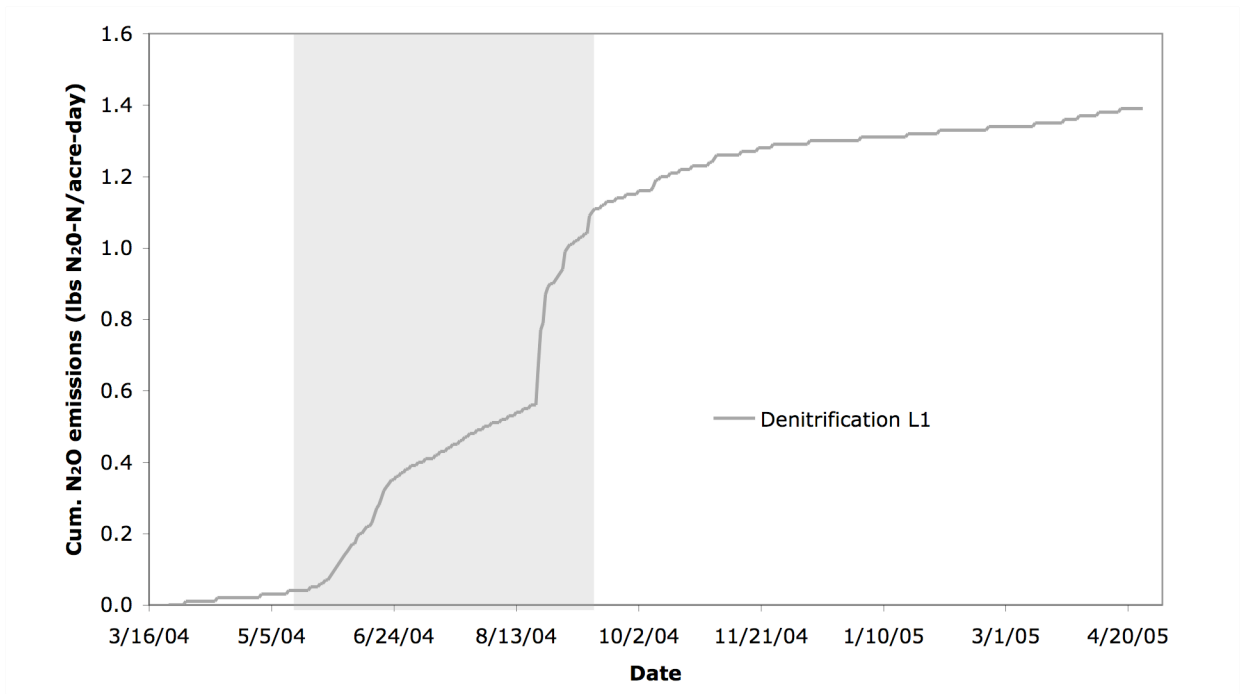
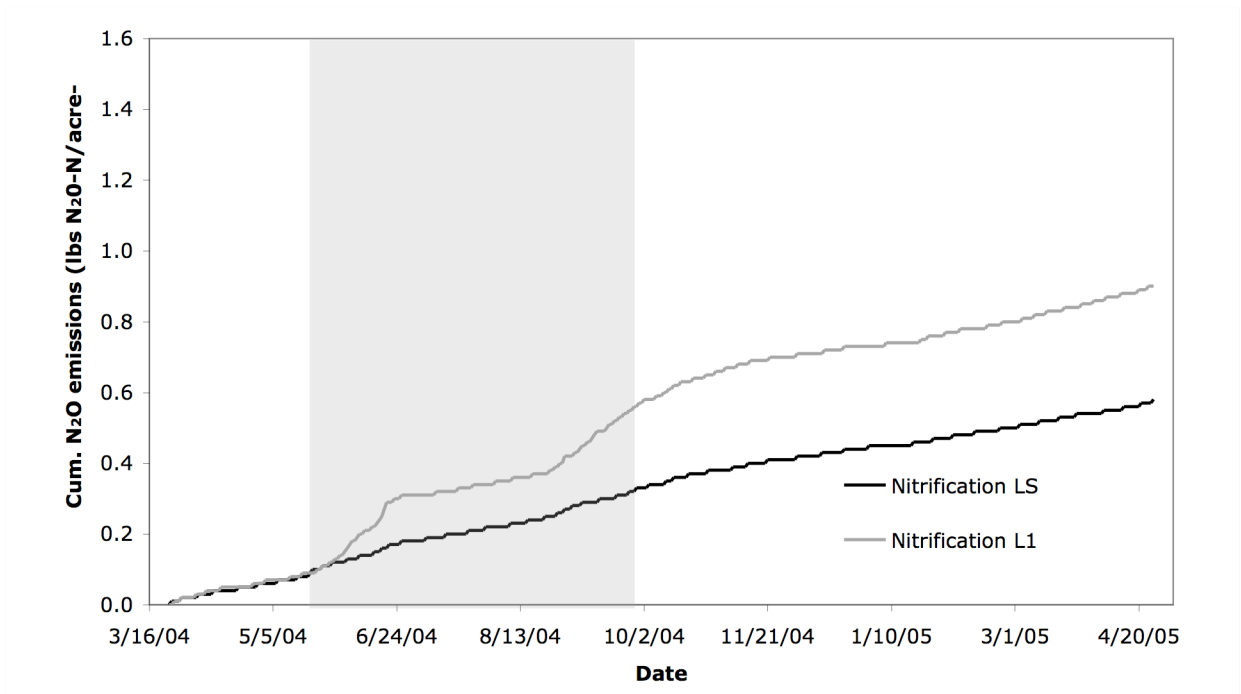


Figure 59. Simulated cumulative nitrous oxide (N₂O) emissions from nitrification and denitrification in the surface layer (LS) and soil layer 1 (L1). The light grey region represents the time span from crop planting and fertilization to crop harvesting.

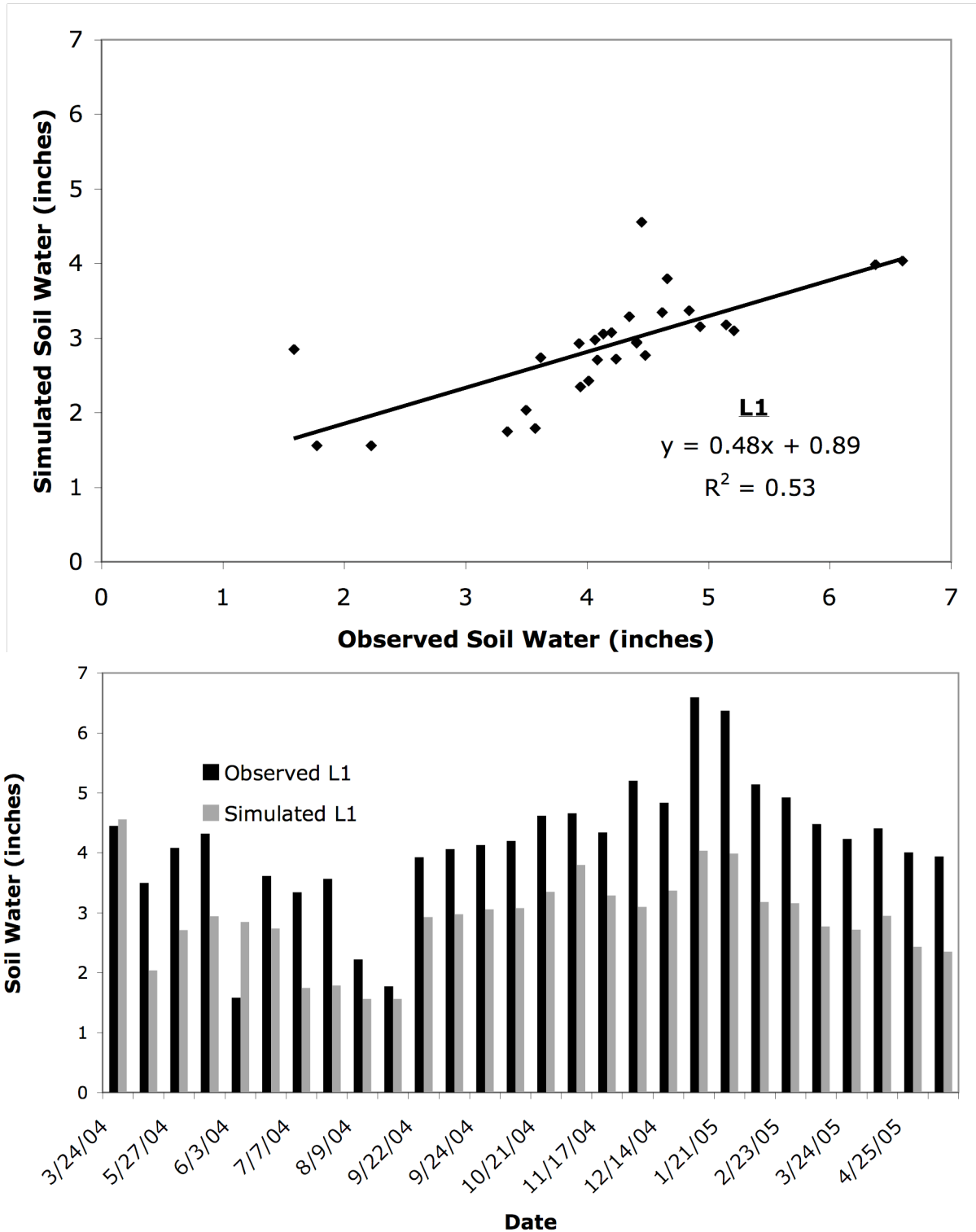


Figure 60. Observed vs. the calibrated simulation of soil water in layer 1 (L1) (where no bar is shown, the observed or simulated value was equal to zero).

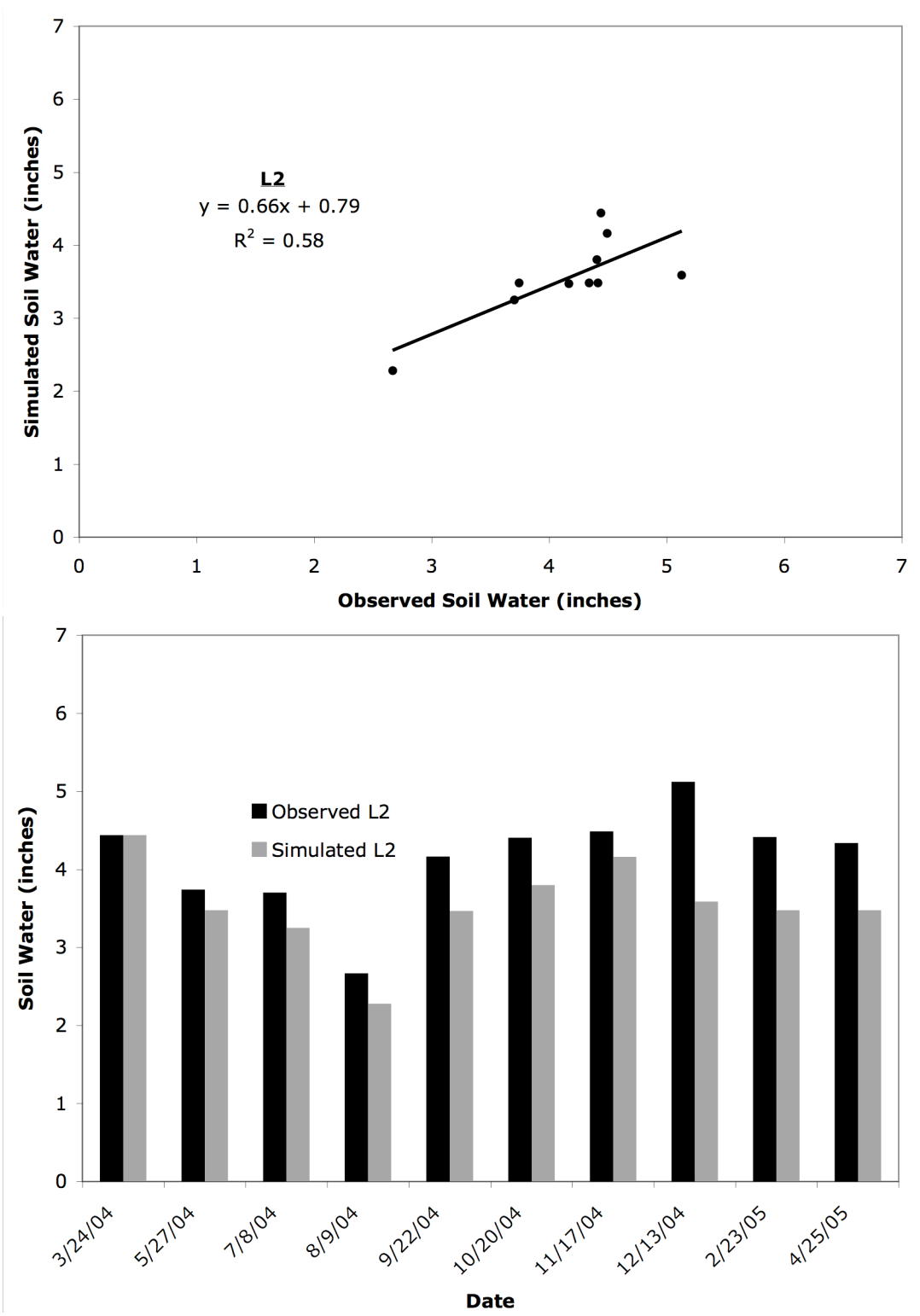


Figure 61. Observed vs. the calibrated simulation values of soil water in layer 2 (L2) (where no bar is shown, the observed or simulated value was equal to zero).

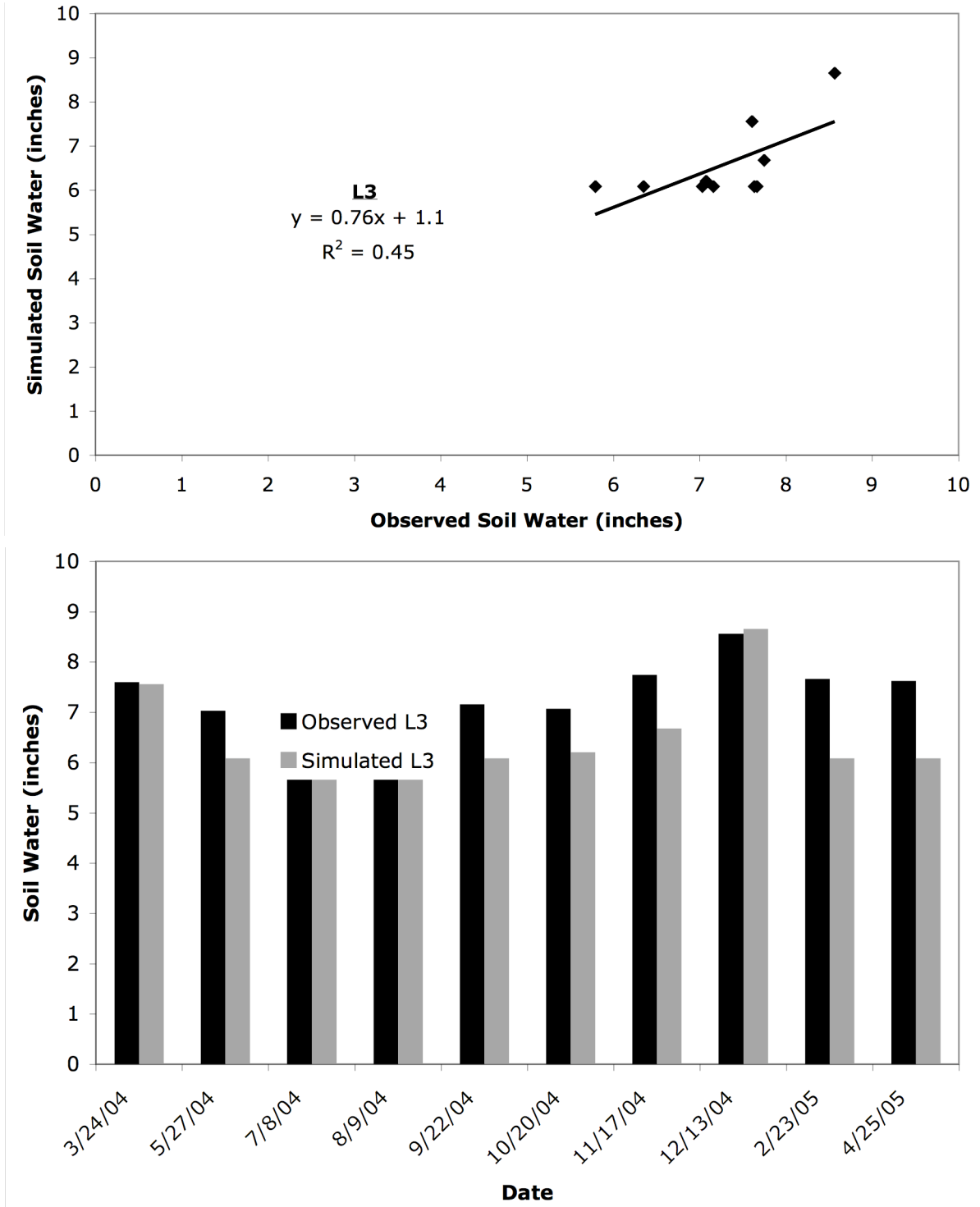


Figure 62. Observed vs. the calibrated simulation values of soil water in layer 3 (L3) (where no bar is shown, the observed or simulated value was equal to zero).

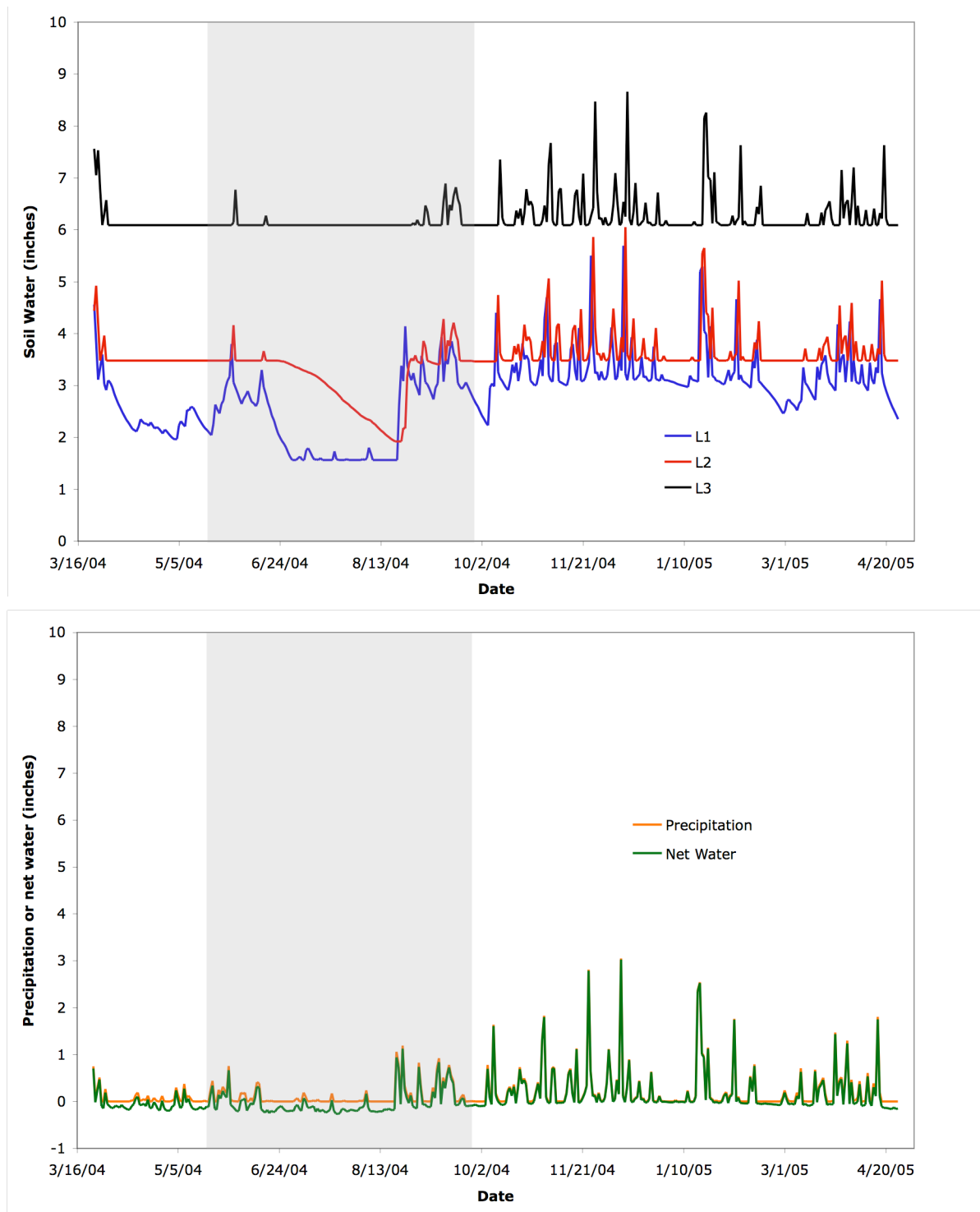


Figure 63. Simulated soil water in layers 1-3 (L1-L3), precipitation, and net water (precipitation – evapotranspiration). The light grey region represents the time span from crop planting and fertilization to crop harvesting.

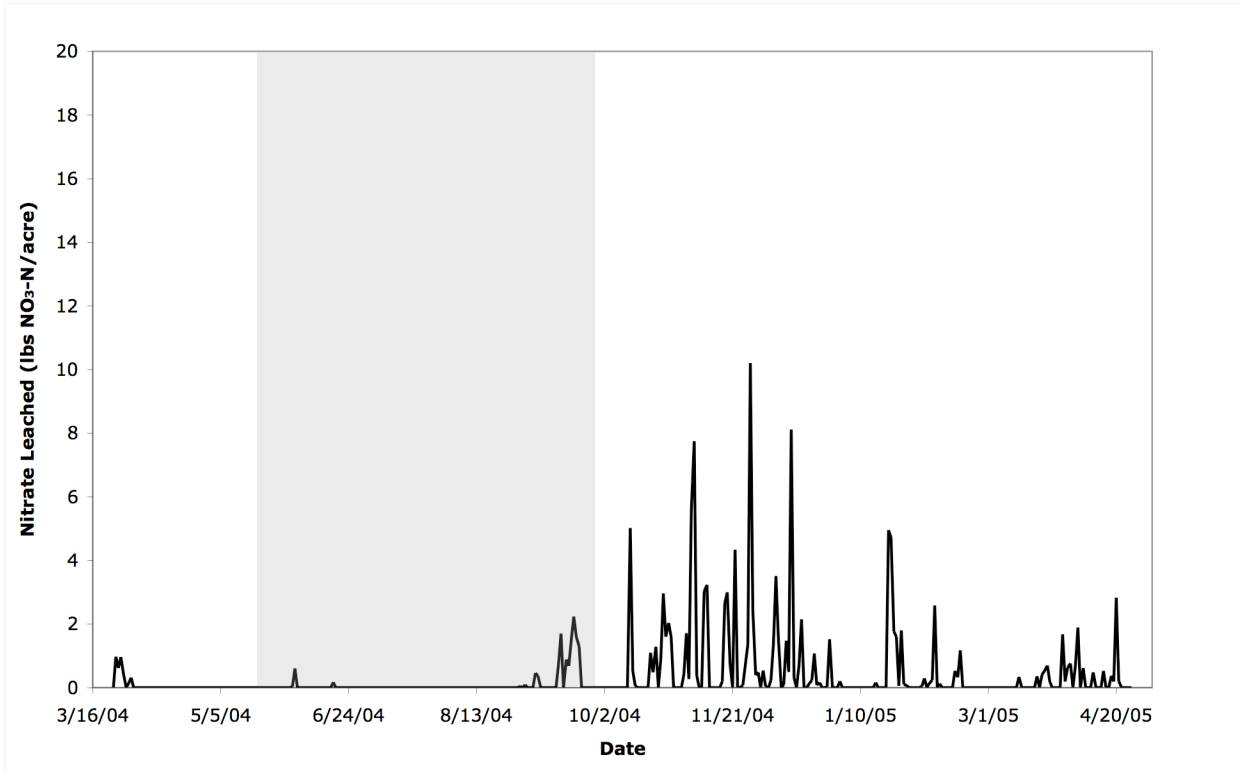


Figure 64. Simulated nitrate leached from the bottom of the soil profile (i.e. from the bottom of soil layer 3). The light grey region represents the time span from crop planting and fertilization to crop harvesting.

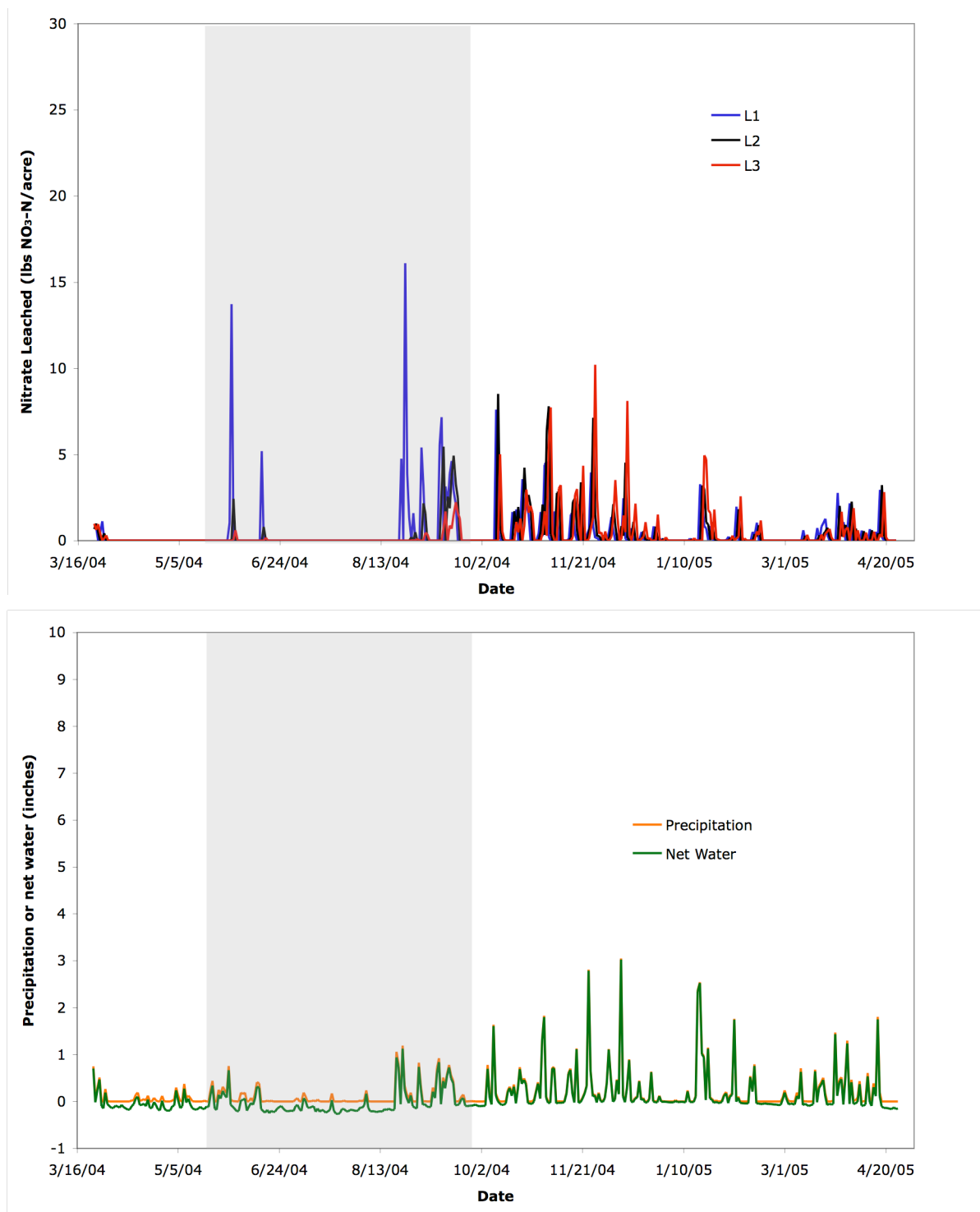


Figure 65. Simulated nitrate leached from soil layers 1-3 (L1-L3), precipitation, and net water (precipitation – evapotranspiration). The light grey region represents the time span from crop planting and fertilization to crop harvesting.

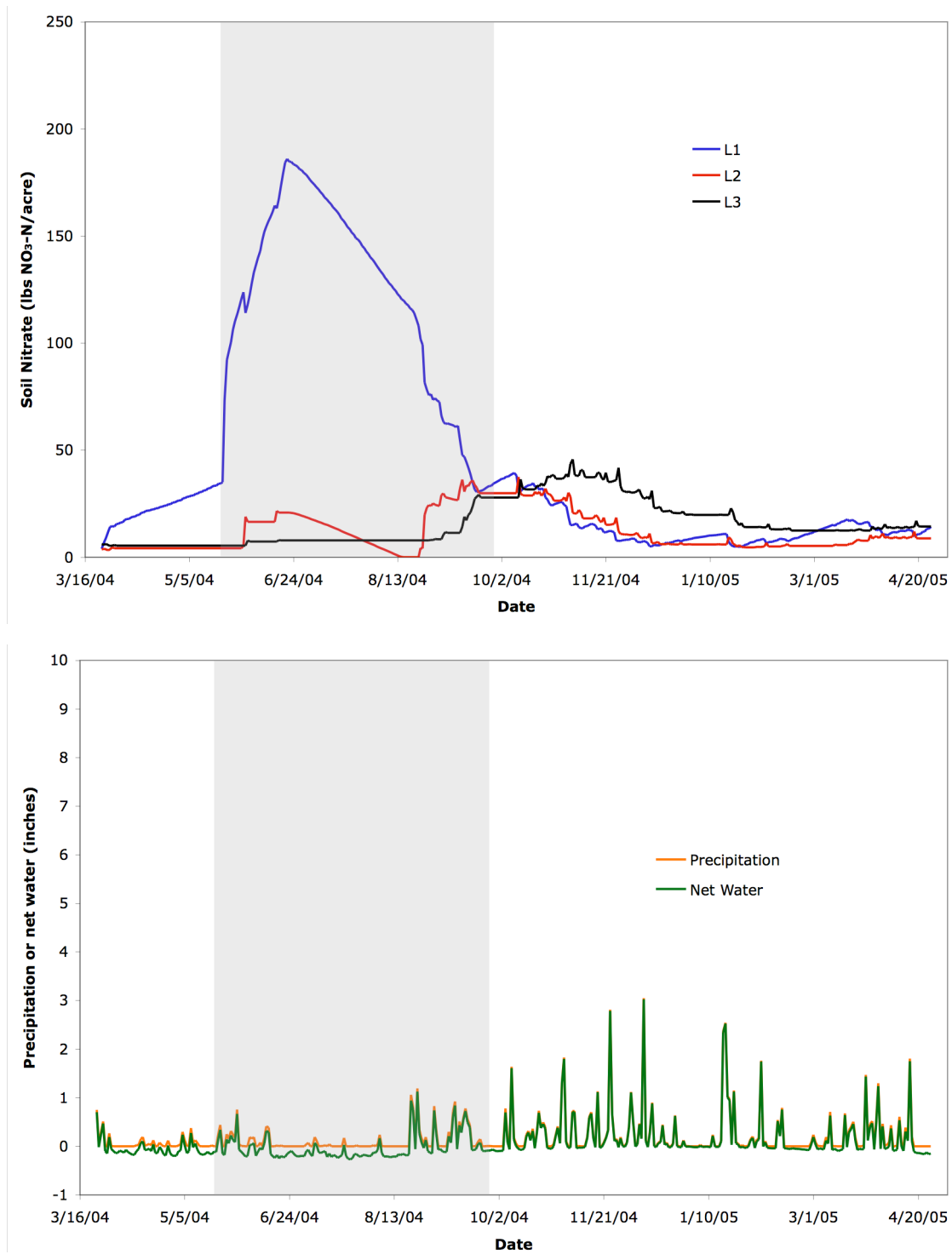


Figure 66. Simulated soil nitrate in layers 1-3 (L1-L3), precipitation, and net water (precipitation – evapotranspiration). The light grey region represents the time span from crop planting and fertilization to crop harvesting.

Appendix A. Quality Control

Data quality control measures closely follow the procedures used by the IWS as detailed in the Abbotsford-Sumas Final Monitoring Report 2002/2004 (Mitchell et al., 2005). The control measures applicable to this project are explained here using quality control data collected during analysis of the laboratory data. Analytical methods, detection limits, and analytical precision are listed in Table A2. Sample container, storage, and holding time protocol (following IWS standard operating procedures) are listed in Table A1.

The following quality control measures were used for all analyses conducted at the IWS laboratory. Note that the data used to generate the statistics are uncensored for values below the detection limits. Some ammonium values are negative due to errors in the assignment of the location of the zero value for the calibration curve. Note that the quality control chart labels state ammonia when it is ammonium that was actually measured. The control charts were created with a program called QCCharts, which communicates with the statistical software R. QCCharts, created by Geoffrey Matthews, a WWU computer science professor, was designed to work mainly with surface water data; therefore, ammonia is typically the measured variable. The preset ammonia plot titles could not be changed for this study.

Laboratory duplicates

Laboratory duplicates are a second portion of the original sample analyzed at the same time as the original. Duplicate samples were analyzed for at least 10% of nitrate and ammonium samples for each sample run. They were used to assess analytical precision over the time period of this project (March 2004 through April 2005) using control charts (Figures A1 & A2). Upper and lower warning limits (± 2 standard deviations) and upper and lower control

limits (± 3 standard deviations) were developed using training data from the Abbotsford-Sumas Groundwater Monitoring Project (July 2002 through June 2004). These limits were then used to assess the performance of the results from this project.

The control charts indicated that there was a slight improvement in analytical precision for nitrate during the period of this project with no values falling outside the warning or control limits, whereas, there were a few out of control values recorded in the training data set. The control charts for ammonium indicated there was little change in analytical precision during this project. Two values fall just outside the lower control limit for ammonium, but these are not a concern since they are below the detection limit and also since the nature of the samples analyzed in the two projects was slightly different: the Abbotsford-Sumas samples were all from groundwater wells whereas the samples for this project were either from vadose zone lysimeters or soil extractions.

Field duplicates

Field duplicates are a second field sample collected at the same place and at the same time as the original sample. One field duplicate was collected for each sampling event for all water samples. Field duplicates are used to assess variability in field sampling. The absolute mean difference and detection limits are shown on the charts comparing the field duplicate concentration to the original sample concentration (Figures A3 & A4). Since the data are uncensored, there are some negative ammonium values.

There is a linear (1:1) trend to the original samples and the field duplicates for nitrate and ammonium. The absolute mean difference for ammonium is below the detection value suggesting there is no significant variability in the field sampling method as it pertains to ammonium sample collection. The absolute mean difference for nitrate (245 $\mu\text{g-N/L}$) is

almost one magnitude greater than the analytical detection limit (27.4 $\mu\text{g-N/L}$), but greater than one magnitude less than the average field duplicate sample concentration (8073 $\mu\text{g-N/L}$). This suggests that there is some variability in the lysimeter and/or piezometer sampling method as it pertains to nitrate sample collection. Some possibilities include natural field variation between the collection of samples or possible contamination between the collecting of each individual sample or in the sample containers. This variability will constrain the reporting confidence of nitrate in water values to $\pm 0.245 \text{ mg NO}_3\text{-N/L}$.

Field blanks

Field blanks are bottles of ultra-pure water filled in the laboratory and then taken into the field and subjected to the same field and laboratory analysis conditions as all the field samples. Field blanks are used to identify contamination from sample bottles, sample handling, or sample preparation in the laboratory.

Field blanks for nitrate were all below laboratory detection limits. For ammonium, 27% of field blanks were above laboratory detection limits with the greatest measured concentration in an ammonium field blank equal to 0.14 $\text{mg NH}_4^+\text{-N/L}$. This variability will constrain the reporting confidence of ammonium in water values to $\pm 0.14 \text{ mg NH}_4^+\text{-N/L}$. The median ammonium field blank was below detection, although, the mean field blank concentration was slightly above detection. If the one outlier is removed, the mean is well below the detection limit.

Laboratory check standards

Laboratory check standards are samples of ultra-pure water to which a known concentration of the analyte of interest has been added. They are used to evaluate laboratory performance

and analyte recovery in a blank matrix (APHA, 1998). Two check standards of 20% and 80% of the calibration standard range were included with each analytical run.

Control charts were used to assess analytical accuracy and precision using training data from the Abbotsford-Sumas Groundwater Monitoring Project (Figures A5 & A6). The control charts show that laboratory performance and analyte recovery was acceptable during this project. There were no values outside of control limits and only a few values outside the warning limits. The values outside the warning limits were deemed acceptable due to the different nature of the samples used to develop the control limits and the test data (groundwater versus vadose zone water or soil extract).

Laboratory spike recoveries

A laboratory spike is an additional portion of the original sample to which a known concentration of the analyte of interest is added. They are used to evaluate analyte recovery in a sample matrix (APHA, 1998). Laboratory spikes were analyzed at least once a run and every 30 samples thereafter.

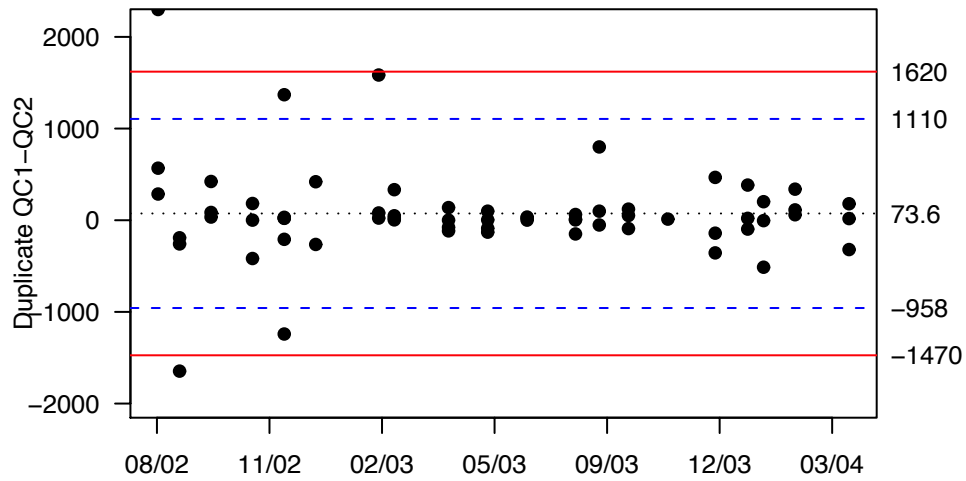
Control charts were used to assess analyte recovery using training data from the Abbotsford-Sumas Groundwater Monitoring Project (Figures A7 & A8). The control charts show acceptable analyte recovery for this project with only a few values falling outside the warning and control limits. The values outside the limits were deemed acceptable due to the different nature of the samples used to develop the control limits and the test data (groundwater versus vadose zone water or soil extract). Also, a common objective is $\pm 20\%$ recovery and all values fell within that range.

Table A1. Sample container, storage, and holding times.

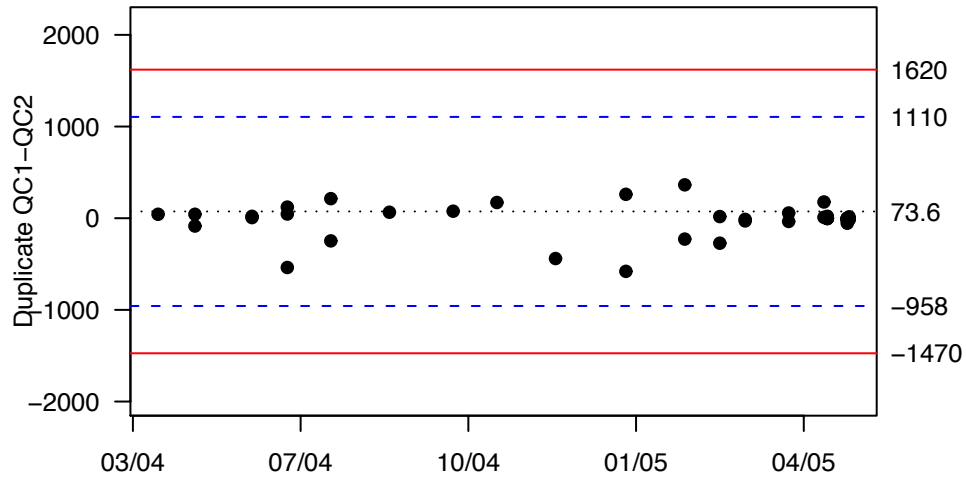
<u>Parameter</u>	<u>APHA Storage/ Max Holding Time</u>	<u>Container</u>	<u>IWS Storage/ Holding Time</u>
Ammonia	Filter, cool 4°C, H ₂ SO ₄ to pH<2, 28 days	Nalgene	Filter, digest within 8 hrs and hold up to 28 days
Nitrate	Filter, cool 4°C, H ₂ SO ₄ to pH<2, 1-2 days	Nalgene	Filter, digest within 8 hrs and hold up to 60 days

Table A2. Analytical methods, detection limits, and precision.

<u>Parameter</u>	<u>Method</u>	<u>Description</u>	<u>Precision</u>	<u>Detection Limit</u>
Ammonia (ug-N/L)	APHA 4500-NH3 G (1998)	Automated phenate	+17.6	11.8
Nitrate+nitrite (ug-N/L)	APHA 4500-NO3 I (1998)	Automated Cd reduction	+30.2	27.4

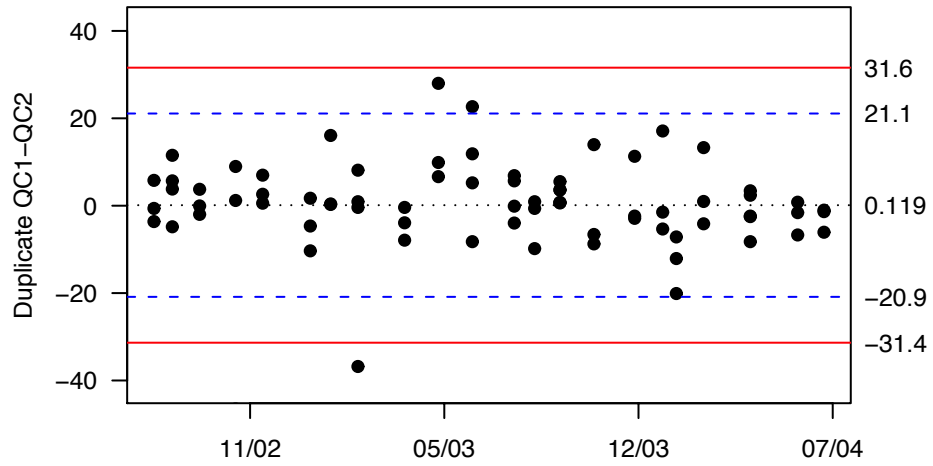


Nitrate+Nitrite Laboratory Duplicates, Training Data

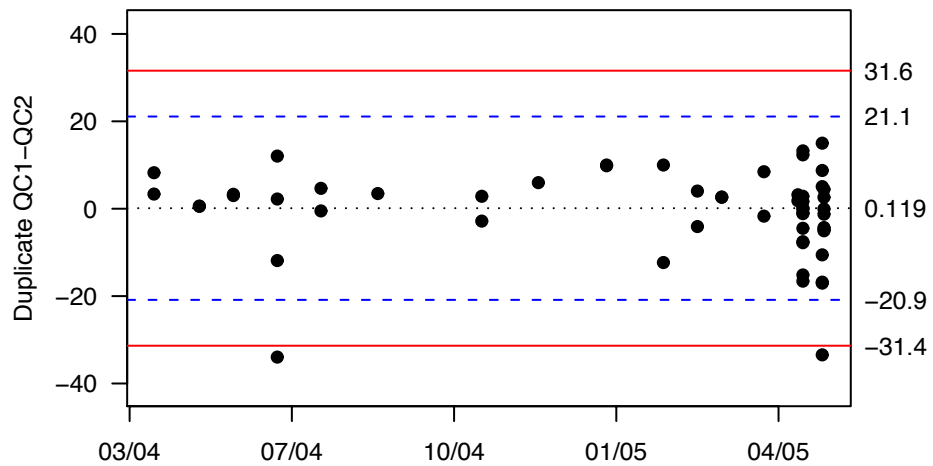


Nitrate+Nitrite Laboratory Duplicates, Test Data

Figure A1. Control chart for nitrate laboratory duplicates. Upper/lower acceptance limits (± 2 std. dev. from mean pair difference) and upper/lower warning limits (± 3 std. dev. from mean pair difference) were calculated using data from the Abbotsford-Sumas Water Quality Monitoring Project.



Ammonia Laboratory Duplicates, Training Data



Ammonia Laboratory Duplicates, Test Data

Figure A2. Control chart for ammonium laboratory duplicates. Upper/lower acceptance limits (± 2 std. dev. from mean pair difference) and upper/lower warning limits (± 3 std. dev. from mean pair difference) were calculated using data from the Abbotsford-Sumas Water Quality Monitoring Project.

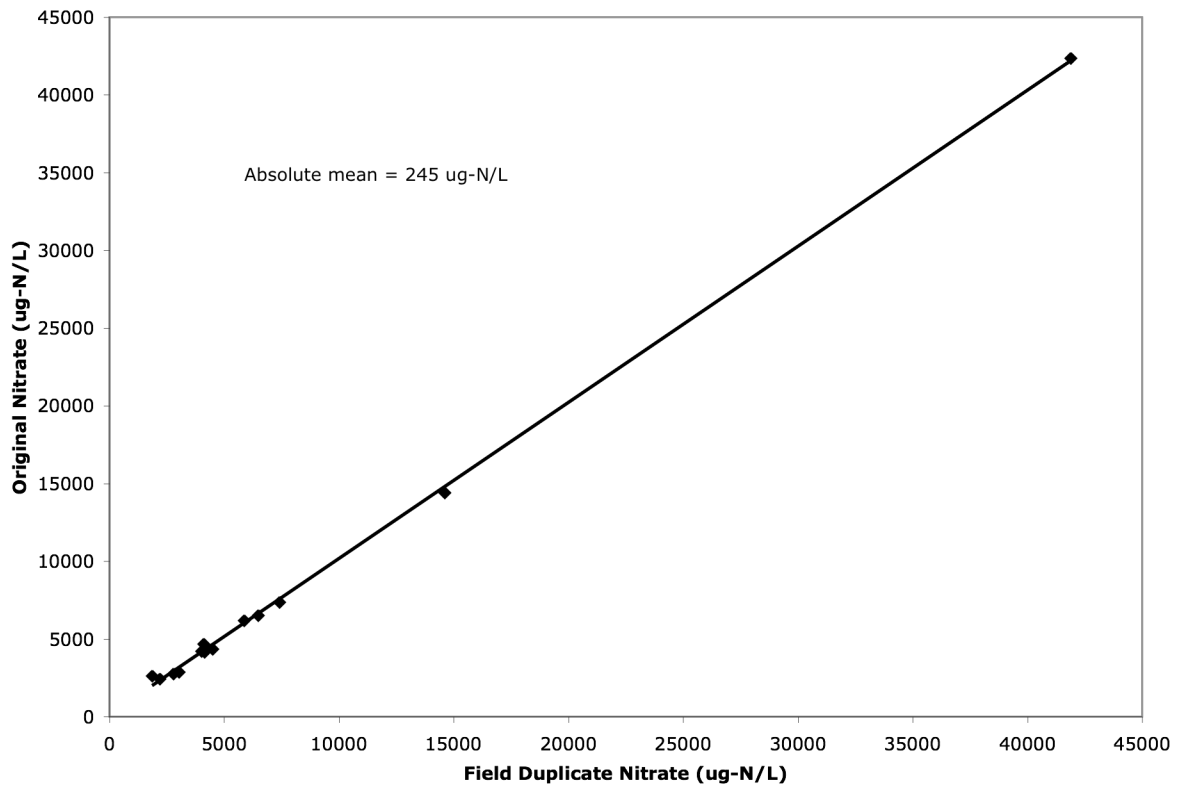


Figure A3. Nitrate field duplicates. Diagonal reference line shows a 1:1 relationship. The absolute mean is the absolute difference between the original and field duplicate sample concentrations divided by the number of observations. The detection limit of 27.4 $\mu\text{g-N/L}$ is not shown.

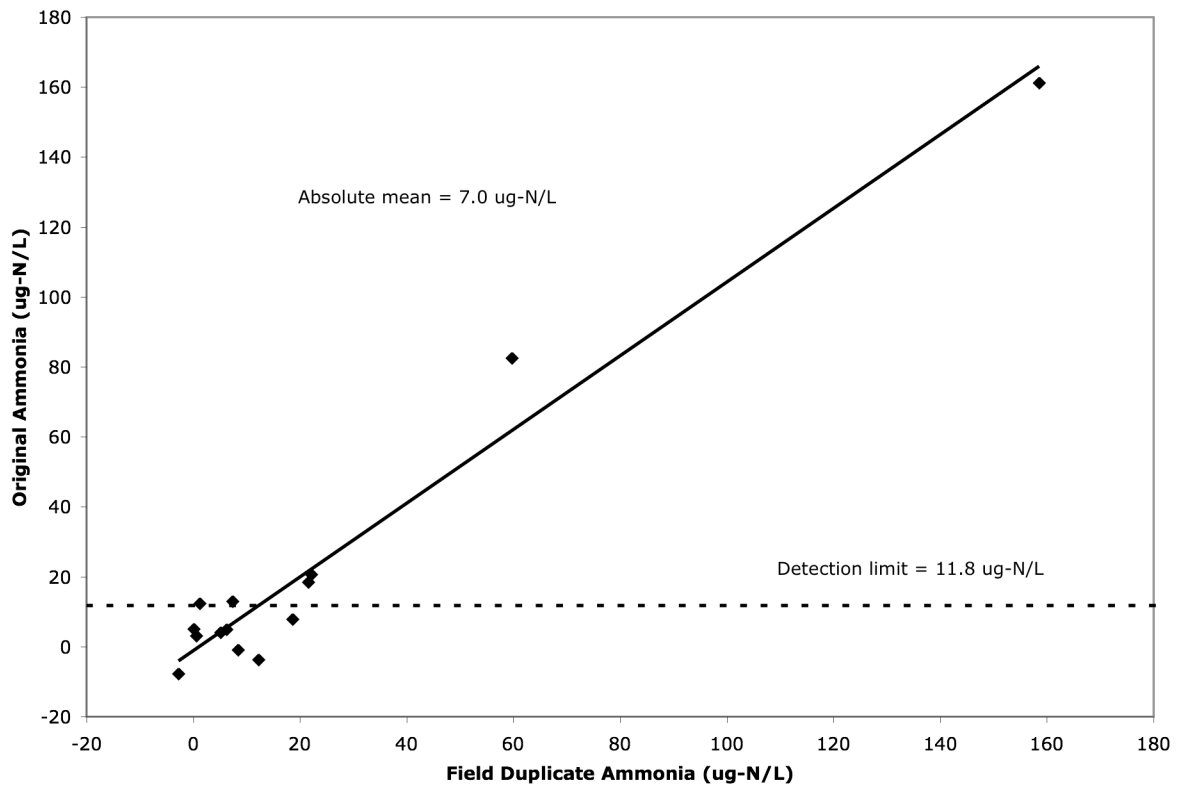


Figure A4. Ammonium field duplicates. Diagonal reference line shows a 1:1 relationship. The absolute mean is the absolute difference between the original and field duplicate sample concentrations divided by the number of observations.

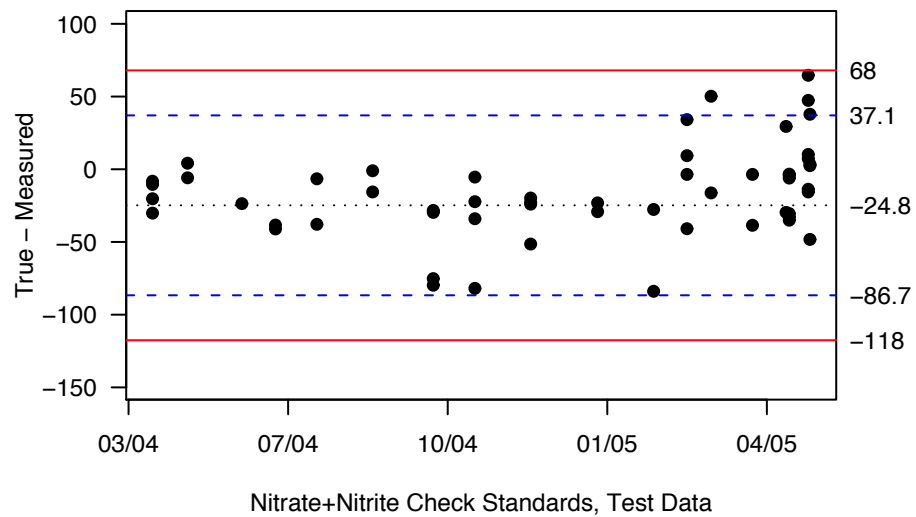
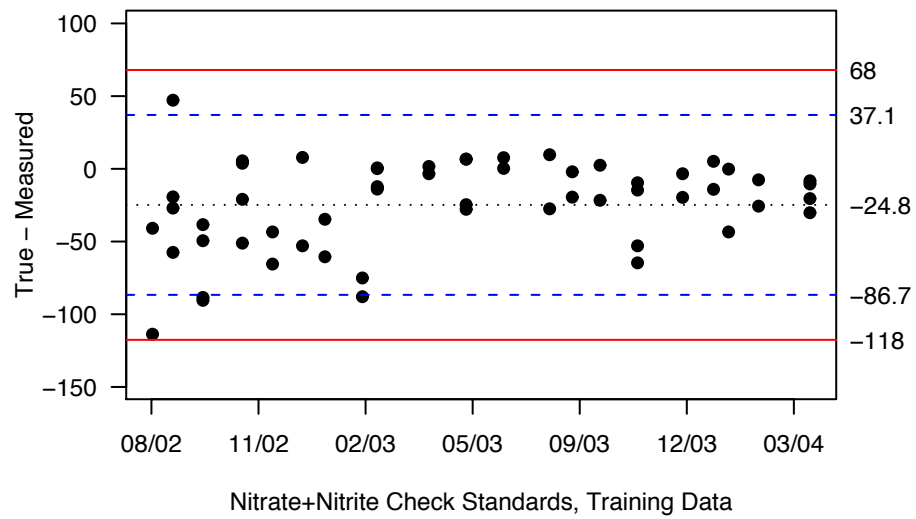
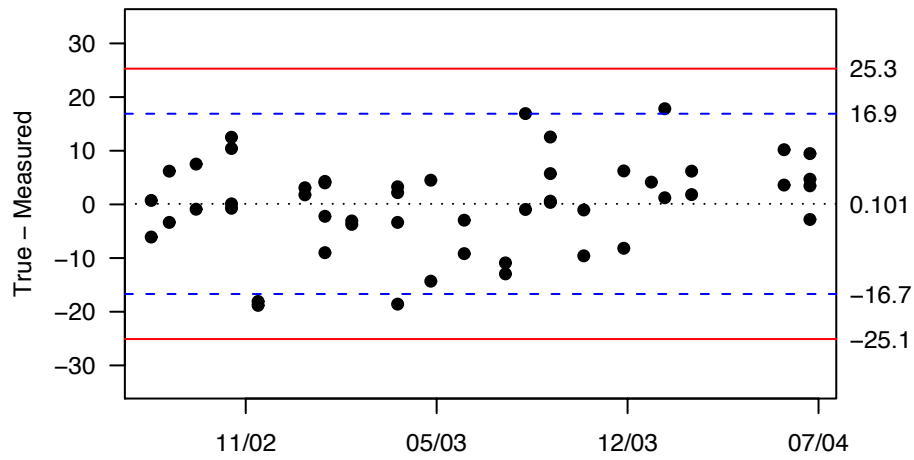
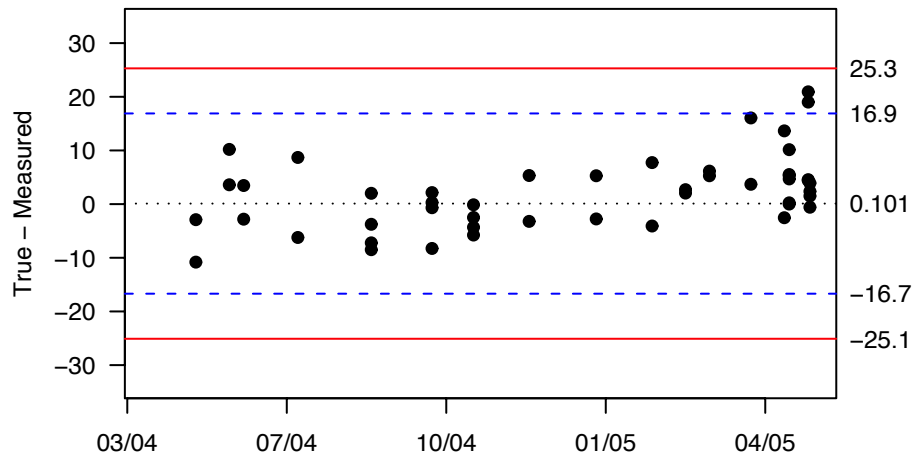


Figure A5. Control chart for nitrate check standards. Upper/lower acceptance limits (± 2 std. dev. from mean pair difference) and upper/lower warning limits (± 3 std. dev. from mean pair difference) were calculated using data from the Abbotsford-Sumas Water Quality Monitoring Project.



Ammonia Check Standards, Training Data



Ammonia Check Standards, Test Data

Figure A6. Control chart for ammonium check standards. Upper/lower acceptance limits (± 2 std. dev. from mean pair difference) and upper/lower warning limits (± 3 std. dev. from mean pair difference) were calculated using data from the Abbotsford-Sumas Water Quality Monitoring Project.

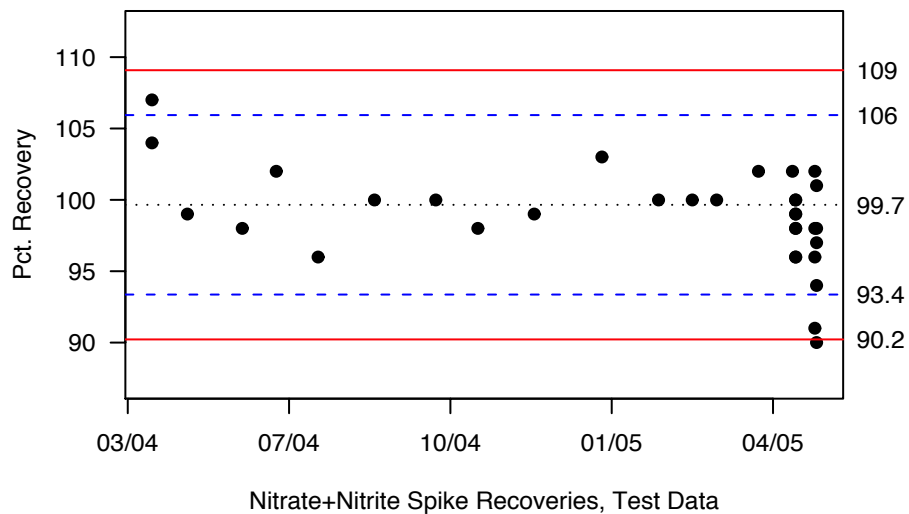
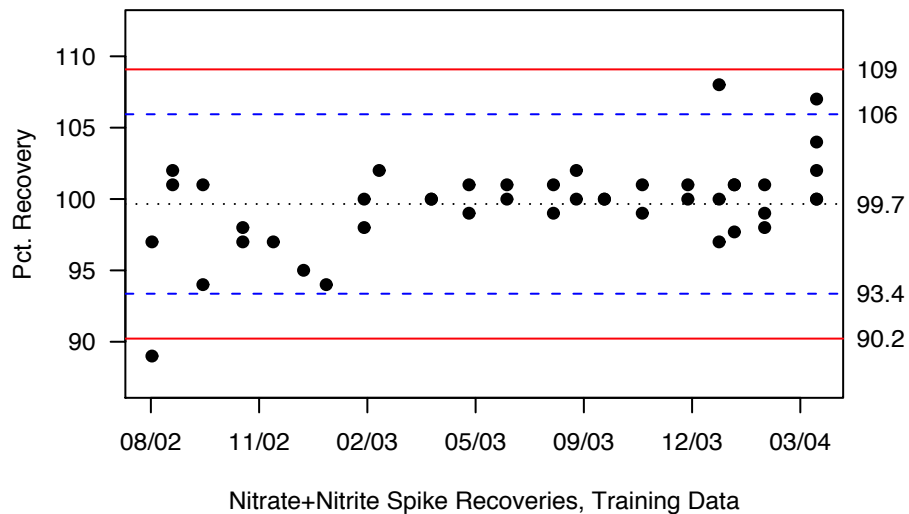


Figure A7. Control chart for nitrate spike recoveries. Upper/lower acceptance limits (± 2 std. dev. from mean pair difference) and upper/lower warning limits (± 3 std. dev. from mean pair difference) were calculated using data from the Abbotsford-Sumas Water Quality Monitoring Project.

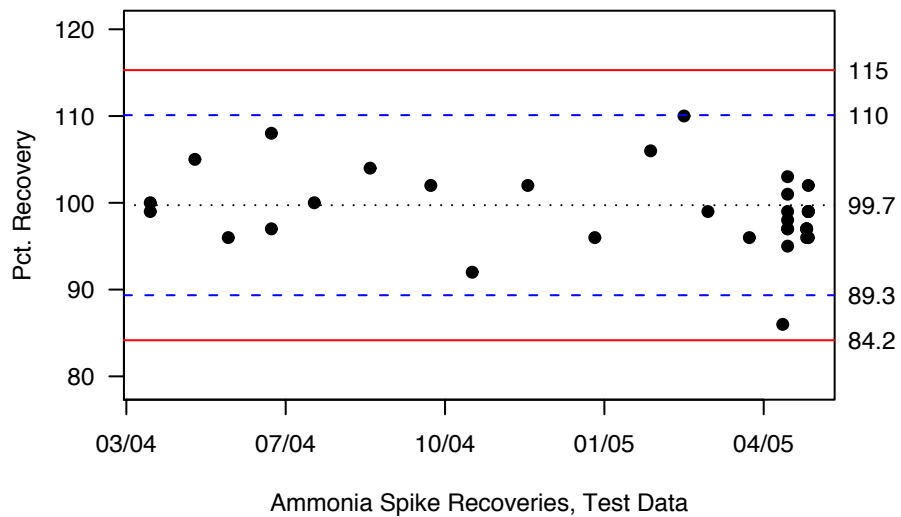
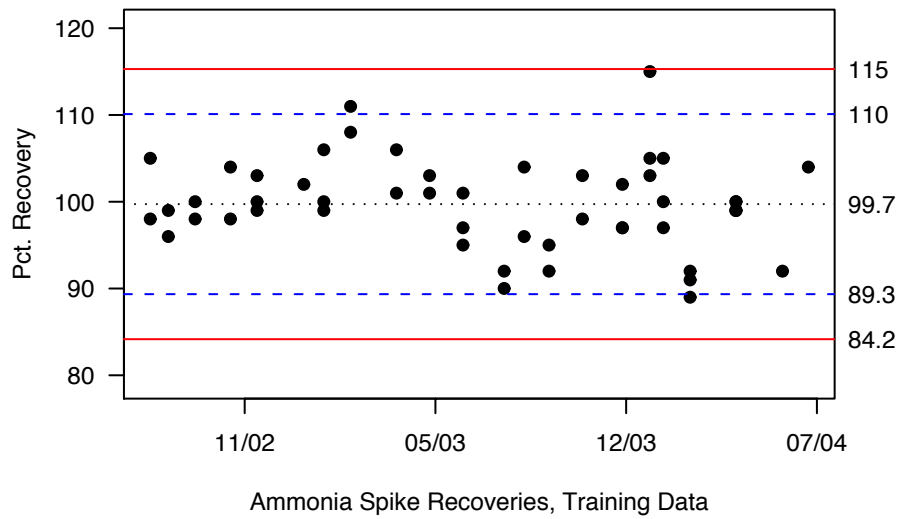


Figure A8. Control chart for ammonium spike recoveries. Upper/lower acceptance limits (± 2 std. dev. from mean pair difference) and upper/lower warning limits (± 3 std. dev. from mean pair difference) were calculated using data from the Abbotsford-Sumas Water Quality Monitoring Project.

Appendix B. Changes Made to NLOS

The following updates, improvements, or additions were made to NLOS10 and saved as model version NLOS11:

- Max/min allowable inputs were changed for various soil characteristic input tables in order to allow the input of field data for this project. Min/max for variables used in the Monte Carlo simulations were set to those min/max;
- The model run stats were set to run from day 84 to 482;
- The default (original) input values were reset to use the input data for this study;
- Tables and counters were added to track the parameters involved in the water and N budgets;
- The algorithms for tracking ACCUM FERT APPLIC NH4/NO3 LS/L1 were updated to include the new method of allowing multiple fertilizer applications on the same day (as described below);
- Changed the name of “Crop moisture fraction (%)” list input device to “Crop moisture fraction”;
- Removed inputs from their respective list input devices that will be used in Monte Carlo simulation. Created new list input devices for Monte Carlo variables;
- Created a Monte Carlo algorithm;
- Changed CN Before, During, and After from their defaults of 87, 79, and 79, respectively to 86, 78, and 86, which were determined to be the best-case values for the field conditions.

Updates to allow multiple fertilizer applications on the same day.

The basic problem was that the Fert_type_applic_date is an array over FANumber (fertilizer application number, currently ranges up to 15), and FTcharAD is an array over Fertilizer_Type (the set of possible fertilizer types, currently ranges up to 15, with the last 5 being user-defined). In the previous model, fert_type_applied was a scalar sum of the Fert_type_applic_date array (thus combining all applications for the current date). In the revision, fert_type_applied is removed, and a new “converter” 2-D array is created to allow transfer of the values into a Fertilizer_Type-based array, FTcharAD.

EXAMPLE

Need to apply 3 fertilizers on a given day (140), Ammonium Nitrate (4), Urea (1), and Monoammonium Phosphate (7).

Select_fert_date:

FANumber:

1	2	3	4	5	6	7	8	9	10	11	12	13	14	15
140	140	140	0	0	0	0	0	0	0	0	0	0	0	0

Select_fert_type:

FANumber:

1	2	3	4	5	6	7	8	9	10	11	12	13	14	15
4	1	7	0	0	0	0	0	0	0	0	0	0	0	0

Fert_NH4_applic_date (on day 140, zeros otherwise):

Fertilizer_Type:

1	2	3	4	5	6	7	8	9	10	11	12	13	14	15
0.46	0	0	0.17	0	0	0.11	0	0	0	0	0	0	0	0

Fert_type_applic_date (on day 140, zeros otherwise):

FANumber:

1	2	3	4	5	6	7	8	9	10	11	12	13	14	15
4	1	7	0	0	0	0	0	0	0	0	0	0	0	0

FTcharAD needs to look like this on day 140 (and zeros otherwise):

Fertilizer_Type:

1	2	3	4	5	6	7	8	9	10	11	12	13	14	15
1	0	0	1	0	0	1	0	0	0	0	0	0	0	0

The original algorithm would sum the Fert_Type_applic_date array (giving 12), and produce this on day 140:

Fertilizer_Type:

1	2	3	4	5	6	7	8	9	10	11	12	13	14	15
0	0	0	0	0	0	0	0	0	0	0	1	0	0	0

The new algorithm uses a temporary 2-D array, **fert_type_converter**, to convert from

FANumber to Fertilizer_Type:

		FANumber:														
		1	2	3	4	5	6	7	8	9	10	11	12	13	14	15
Fertilizer_Type:	1	0	1	0	0	0	0	0	0	0	0	0	0	0	0	0
	2	0	0	0	0	0	0	0	0	0	0	0	0	0	0	0
	3	0	0	0	0	0	0	0	0	0	0	0	0	0	0	0
	4	1	0	0	0	0	0	0	0	0	0	0	0	0	0	0
	5	0	0	0	0	0	0	0	0	0	0	0	0	0	0	0
	6	0	0	0	0	0	0	0	0	0	0	0	0	0	0	0
	7	0	0	1	0	0	0	0	0	0	0	0	0	0	0	0
	8	0	0	0	0	0	0	0	0	0	0	0	0	0	0	0
	9	0	0	0	0	0	0	0	0	0	0	0	0	0	0	0
	10	0	0	0	0	0	0	0	0	0	0	0	0	0	0	0
	11	0	0	0	0	0	0	0	0	0	0	0	0	0	0	0
	12	0	0	0	0	0	0	0	0	0	0	0	0	0	0	0
	13	0	0	0	0	0	0	0	0	0	0	0	0	0	0	0
	14	0	0	0	0	0	0	0	0	0	0	0	0	0	0	0
	15	0	0	0	0	0	0	0	0	0	0	0	0	0	0	0

This is summed for each row to achieve the correct FTcharAD array.

For actual application of the fertilizer onto a layer, Fertilizer_Type-based Fert_NH4_applic_date was converted into the FANumber-based Fert_NH4_applic_LS (as well as equivalent calculations for NO3, and Layer 1). Previously, this was accomplished by doing an array sum over the values in Fert_NH4_applic_date, which produces incorrect values. The revision uses the converter above, in combination with Fert_NH4_applic_date to produce a new 2-D converter array:

		FANumber:														
		1	2	3	4	5	6	7	8	9	10	11	12	13	14	15
Fertilizer_Type:	1	0	.46	0	0	0	0	0	0	0	0	0	0	0	0	0
	2	0	0	0	0	0	0	0	0	0	0	0	0	0	0	0
	3	0	0	0	0	0	0	0	0	0	0	0	0	0	0	0
	4	.17	0	0	0	0	0	0	0	0	0	0	0	0	0	0
	5	0	0	0	0	0	0	0	0	0	0	0	0	0	0	0
	6	0	0	0	0	0	0	0	0	0	0	0	0	0	0	0
	7	0	0	.11	0	0	0	0	0	0	0	0	0	0	0	0
	8	0	0	0	0	0	0	0	0	0	0	0	0	0	0	0
	9	0	0	0	0	0	0	0	0	0	0	0	0	0	0	0
	10	0	0	0	0	0	0	0	0	0	0	0	0	0	0	0
	11	0	0	0	0	0	0	0	0	0	0	0	0	0	0	0
	12	0	0	0	0	0	0	0	0	0	0	0	0	0	0	0
	13	0	0	0	0	0	0	0	0	0	0	0	0	0	0	0
	14	0	0	0	0	0	0	0	0	0	0	0	0	0	0	0
	15	0	0	0	0	0	0	0	0	0	0	0	0	0	0	0

In the formula for Fert_NH4_applic_LS, this is summed for each FANumber, giving an array like this:

FANumber:															
1	2	3	4	5	6	7	8	9	10	11	12	13	14	15	
.17	.46	.11	0	0	0	0	0	0	0	0	0	0	0	0	

CHANGES MADE TO THE FERTILIZER APPLICATION SUB-MODEL

Sector = Fertilizer Application

Removed fert_type_applied

Original Algorithm:

(Variable type: scalar)

```
ARRAYSUM(Fert_type_applic_date[*])
```

Created **fert_type_converter** for use by FTcharAD in order to apply multiple fertilizers on one day.

Algorithm:

(Variable type: 2-D Array over FANumber and Fertilizer_Type)

```
fert_type_converter[FANumber, Fertilizer_Type] = IF
```

```
(Fert_type_applic_date [FANumber] =
```

```
Fertilizer_Code[Fertilizer_Type]) THEN 1 ELSE 0
```

Documentation:

This is a utility 2-D variable that is used to transform the fertilization information from the FANumber-based Fert_type_applic_date variable (one array element for each FANumber, with the value of the fertilizer type to be applied on the current day) into the Fertilizer_Type-based FTcharAD variable (one array element for each Fertilizer_Type, with a value of 1 if that fertilizer type is to be applied on the current day, and 0 if not).

The structure of this variable is a 2-D array, with FANumber columns and Fertilizer-Type rows, with a 1 in the element if that FANumber consists of that Fertilizer_Type on the current day, and zero if not. This allows FTcharAD to be calculated correctly.

This replaces an array sum over the values in Fert_type_applic_date .

Changed how **FTcharAD** is calculated so that multiple fertilizer applications may be made on one day.

Original algorithm:

(Variable type: 1-D Array over Fertilizer_Type)

```
FTcharAD[fertilizer_Type] = IF Fert_type_applied = 0 THEN 0 ELSE  
IF Fert_type_applied =Fertilizer_Code[Fertilizer_Type] THEN 1  
ELSE 0
```

Updated algorithm:

(Variable type: 1-D Array over Fertilizer_Type)

```
FTcharAD[fertilizer_Type] = ARRAYSUM(fert_type_converter[*,  
Fertilizer_Type])
```

Documentation (unchanged):

FTcharAD creates an array with a value of 1 in the position for which type of fertilizer is applied on that date. This is then used to calculate either NH4-N and/or NO3-N that is applied on that date by using the NO3 and NH4 characteristics of each fertilizer type. Unitless switch of either 0 or 1. dh Jan 2001.

Sector = Fertilizer Mineral N

Created **fert_NH4_applic_date_converter** for use by Fert_NH4_applic_LS

Algorithm:

(Variable type: 2-D Array over FANumber and Fertilizer_Type)

```
fert_NH4_applic_date_converter[FANumber, Fertilizer_Type] =  
fert_type_converter[FANumber, Fertilizer_Type]*Fert_NH4_applic_da  
te[Fertilizer_Type]
```

Documentation:

This takes the 2-D array in fert_type_converter, multiplies the values by the fraction of product that is NH4 so that the array can be rolled up into an FANumber-based array of NH4 fractions in the Fert_NH4_applic_LS formula. In other words, we need to make a 1-D array of FANumber elements, each of which is the NH4 fraction for that fertilizer application on the current date.

Updated **Fert_NH4_applic_LS** to roll up the NH4 converter array by Fertilizer_Type

Original Algorithm:

(Variable type: 1-D array over FANumber)

```
Fert_NH4_applic_LS[FANumber] = IF  
Select_fert_applic_method[FANumber] < 5 THEN  
Fert_amount_applic_date[FANumber] *  
ARRAYSUM(Fert_NH4_applic_date[*]) ELSE 0
```

Original Documentation:

Fert_NH4_applic_LS is application of fertilizer NH4 applied to the soil surface. Method of fertilizer application (Fert_method_applic_date) is tested to see if the fertilizer is applied to the surface or soil layer 1. If the method of fertilizer application is 1 (none applied) or fertilizer is applied to the surface, that is method < 5 (2=surface broadcast, 3=surface banded, 4=surface dribbled) then the application to the surface is calculated from the product of the total quantity of fertilizer applied (Fert_amount_applic_date) and the NH4-N content of that applied fertilizer (Fert_NH4_applic_date), otherwise the value is 0 since

either the application is 0 or fertilizer is applied directly to soil layer 1. Units lbs N / acre / day. dh Jan 2001.

Updated Algorithm:

(Variable type: 1-D array over FANumber)

```
IF Select_fert_applic_method[FANumber] < 5 THEN  
    Fert_amount_applic_date[FANumber] *  
    ARRAYSUM(Fert_NH4_applic_date_converter[FANumber,*]) ELSE  
    0
```

Updated Documentation:

Removed original ARRAYSUM and replaced with updated ARRAYSUM to get a FANumber-based 1-D array of NH4 fractions.